ЖУРНАЛ
ЭКСПЕРИМЕНТАЛЬНОЙ И ТЕОРЕТИЧЕСКОЙ
ФИЗИКИ
Zhurnal Eksperimental'noi i Teoreticheskoi Fiziki

468

PROPERTY OF MELPAR, INC.

SOVIET PHYSICS
JETP

VOL. 12, No. 1 ~~JANUARY, 1961~~

A Translation
of the
Journal of Experimental and Theoretical Physics
of the
Academy of Sciences of the USSR

(Russian Original Vol. 39, No. 1 (7), July, 1960)

Published by the
AMERICAN INSTITUTE OF PHYSICS
INCORPORATED

PROPERTY OF MELPAR, INC.

SOVIET PHYSICS
JETP

A translation of the Journal of Experimental and Theoretical Physics of the USSR.

A publication of the

AMERICAN INSTITUTE OF PHYSICS

Governing Board

RALPH A. SAWYER, *Chairman*
J. G. BAKER
R. H. BOLT
WALLACE R. BRODE
HARVEY BROOKS
DIRK BROUWER
J. W. BUCHTA
VERNET E. EATON
J. H. ELLIOTT
HERBERT A. ERF
S. A. GOUDSMIT
W. W. HAVENS, JR.
WINSTON E. KOCK
R. BRUCE LINDSAY
H. V. NEHER
C. J. OVERBECK
GEORGE E. PAKE
RAY PEPINSKY
FRANCIS W. SEARS
FREDERICK SEITZ
JOHN STRONG
GEORGE E. UHLENBECK
MARY E. WARGA
VICTOR F. WEISSKOPF
WILLIAM R. WILLETS

Administration

ELMER HUTCHISSON
Director
WALLACE WATERFALL
Secretary and Treasurer
HENRY A. BARTON
Administrative Consultant
W. C. KELLY
Director of Education
EUGENE H. KONE
Director of Public Relations
HUGH C. WOLFE
Director of Publications
KATHRYN SETZE
Assistant Treasurer
NORMA FRANKEL
Publications Editor
SISTINA GRECO
Circulation Manager
EDWARD TOBER
Manager, Production and Distribution
THEODORE VORBURGER
Advertising Manager
EMILY WOLF
Manager, Special Services

American Institute of Physics Advisory Board on Russian Translations

ROBERT T. BEYER, *Chairman*
J. GEORGE ADASHKO, FREEMAN DYSON, DWIGHT GRAY, MORTON HAMERMESH, DAVID HARKER, HAROLD F. WEAVER

Editor of SOVIET PHYSICS—JETP

J. GEORGE ADASHKO, 25 WEST 81ST ST., NEW YORK 24, NEW YORK

SOVIET PHYSICS—JETP is a monthly journal published by the American Institute of Physics and contains a complete translation of the JOURNAL OF EXPERIMENTAL AND THEORETICAL PHYSICS of the U.S.S.R. Academy of Sciences.

This translating and publishing project was undertaken by the institute in the conviction that dissemination of the results of researches everywhere in the world is invaluable to the advancement of science. The NATIONAL SCIENCE FOUNDATION of the United States has encouraged the project initially and is supporting it in large part by a grant.

The American Institute of Physics and its translators propose to translate faithfully all the material appearing in the original articles. The views expressed in the translations are therefore those of the original authors, and not those of the translators nor of the American Institute of Physics.

Volume 1 of SOVIET PHYSICS—JETP corresponds to Russian Volume 28 (1955). Two volumes are published annually, each of six issues. Each volume contains the translation of one volume of the JOURNAL OF EXPERIMENTAL AND THEORETICAL PHYSICS.

Beginning with Vol. 9 (36), the transliteration of the names of Russian authors follows British Standard 2979, which is being adopted by a large number of scientific journals in the United States. The Library of Congress transliteration is followed in the earlier volumes.

Subscription Prices

Per Year (12 issues)	
General:	
United States and Canada	$75.00
Elsewhere	79.00
Libraries of non-profit degree-granting Institutions:	
United States and Canada	$35.00
Elsewhere	39.00
Single Copies	$ 8.00

Subscriptions should be addressed to the American Institute of Physics, 335 East 45th Street, New York 17, New York.

SOVIET PHYSICS, JETP is published monthly by the American Institute of Physics, Inc. Second Class postage paid at Ann Arbor, Michigan.

Copyright by American Institute of Physics 1961

SOVIET PHYSICS

JETP

A translation of Zhurnal Éksperimental'noĭ i Teoreticheskoĭ Fiziki.

Vol. 12, No. 1 pp. 1-161 (Russ. orig. Vol. 39, No. 1, pp 1-223, July, 1960) January, 1961

ANGULAR DISTRIBUTION OF PROTONS FROM THE $C^{12}(dp)C^{13}$ *REACTION WITH 5 – 13 Mev DEUTERONS*

N. I. ZAIKA, O. F. NEMETS, and M. A. TSERINEO*

Submitted to JETP editor December 11, 1959

J. Exptl. Theoret. Phys. (U.S.S.R.) 39, 3-6 (July 1960)

Angular distributions of protons corresponding to the ground state of C^{13} have been measured for five deuteron energies in the interval 5 – 13 Mev, and for protons corresponding to the three lowest excited states for deuteron energies of 13.3 and 12.1 Mev. The parities and possible spin values of these states were determined. It is shown that, with decreasing energy, reactions other than stripping become more important.

THE deviation of experimental angular distributions of protons and neutrons from (dp) and (dn) reactions from those predicted by the simple stripping theory[1] are known to indicate the occurrence in the reaction of other mechanisms[2,4] and of interaction of the incident deuteron and the outgoing particle with the nucleus.[5] The magnitude of this interaction and the relative importance of the various mechanisms depend both on the properties of the nucleus and on the energy of the bombarding deuterons. It was therefore of interest to make corresponding measurements over a wide range of deuteron energies.

We have measured angular distributions of protons corresponding to the ground state of C^{13}, for deuteron energies of 13.3 ± 0.2, 12.1 ± 0.2, 9.55 ± 0.2, 7.15 ± 0.2, and 4.65 ± 0.2 Mev (Fig. 1), and of the protons corresponding to the three lowest excited states of C^{13} for deuteron energies of 13.3 ± 0.2 and 12.1 ± 0.2 Mev (Figs. 2, 3).

For the measurements we used the external beam of deuterons from the cyclotron of the Institute of Physics of the Academy of Sciences of the Ukrainian S.S.R., with a deuteron energy of 13.6 Mev. The proton detector and the experimental geometry were the same as described in reference 6; to reduce the load on the amplifier, an absorber was placed at the entrance to the chamber to cut off the deuterons. Unfortunately the experimental geometry limited the maximum angle at which measurements could be made to values ~ 140°

The deuteron energy was changed by using a set of aluminum foils placed at the entrance to the reaction chamber; the beam of deuterons was collimated further beyond the absorbers. The reduction in energy of the deuterons was accompanied by a considerable decrease in beam intensity and by the appearance of a noticeable spread in angle and energy, which made measurements at large angles for low energies unsatisfactory. The results of these measurements are not given here.

A comparison of the experimental angular distributions with theory enables one to assign values of spins to the ground state and the three lowest excited states of C^{13} with values of $1/2^- - 3/2^-$, $1/2^+$, $1/2^- - 3/2^-$ and $3/2^+ - 5/2^+$, respectively.

The angular distribution of protons corresponding to the excited states of C^{13} is in good agreement with the predition of the Butler theory[1] for $r_0 = 4.6$f. At the same time, there are various peculiar features in the proton distribution corresponding to the ground state of C^{13} which we feel should be pointed out.

First of all, the distributions obtained for deuteron energies of 4.65 and 7.15 Mev differ from the distributions for energies of 9.55, 12.1 and 13.3

---

*Institute Rudjer Boscovic, Zagreb, Yugoslavia.

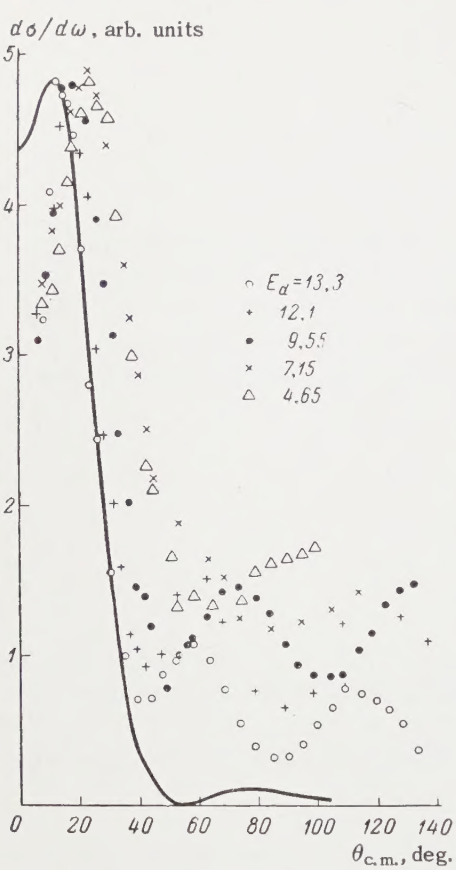

FIG. 1. Angular distributions of protons from the $C^{12}(dp)C^{13}$ reaction corresponding to the ground state of C^{13}, for various values of E_d in Mev. The solid curve is calculated from the Butler theory for $E_d = 13.3$ Mev, $l_n = 1$ and $r_0 = 4.6 \times 10^{-13}$ cm.

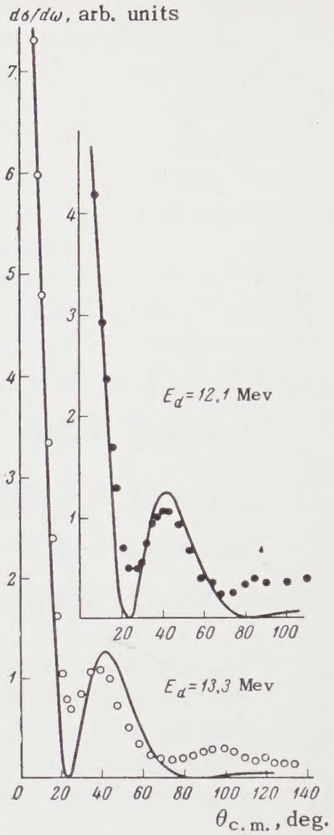

FIG. 2. Angular distributions of protons corresponding to the excited state of C^{13} at 3.09 Mev, for two values of E_d. The solid curves are calculated from the Butler theory for these energies; $l_n = 0$, $r_0 = 4.6 \times 10^{-13}$ cm.

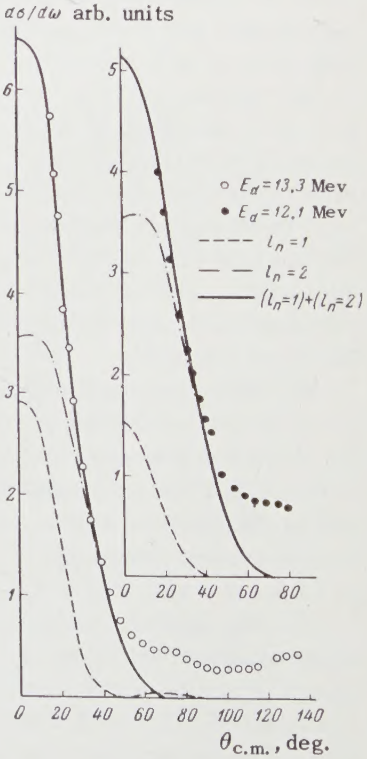

FIG. 3. Angular distribution of protons corresponding to the first (3.68 Mev) and the second (3.86 Mev) excited states of C^{13}. The curves are calculated from the Butler theory for the corresponding energies and for various values of l_n (the ratio of the curves for $l_n = 1$ and $l_n = 2$ was selected by calculating the best fit of the curve ($l_n = 1$) + ($l_n = 2$) with the experimental data); $r_0 = 4.6 \times 10^{-13}$ cm.

Mev. While the first distributions are characterized by a distribution peak wider than theoretical and an indication of a rise at large angles, in the second distributions the peak appears to be the theoretical value, but instead of the rise at large angles there are two additional maxima which recall a diffraction distribution. A similar picture has been observed by other authors for deuteron energies exceeding[7,8] and less than[9] the energies used by us.

The change in character of the angular distribution occurring in the energy interval 7 — 9 Mev may be related to a change in the contributions of the various mechanisms in the reaction and to a changing relative importance of nuclear and Coulomb interactions. The presence of nuclear interaction in the $C^{12}(dp)C^{13}$ reaction is indicated by a narrowing of the peak which occurs for $E_d \geq 9$ Mev.[5] For energies $E_d \leq 7.15$ Mev one should assume increasing importance of compound nucleus formation[4] and stripping of heavy particles,[2] which give an increase in cross section at large angles as well as a broadening of the peak. The work of other authors[9,10] shows that for $E_d = 2.7 - 3.3$ Mev agreement with theory is attained for $r_0 = 6.5$f. and a distribution at the peak which is broader than the theoretical. Similarly, for agreement with theory of our data for an energy of $E_d = 4.65$ Mev we had to increase the value of the radius up to 5.5 f.

We also measured the differential cross section of the reaction $C^{12}(dp)C^{13}_{gr}$ for angles corresponding to the maximum in the distribution and energies of 7.15, 9.55, 12.1, and 13.3 Mev. The cross section values were equal respectively to 24, 18, 14 and 13 mb/sr. The error in the measurement of the absolute value of the cross section was ±30% To measure the cross section we used the current integrator[11] with Faraday cup developed earlier.

In conclusion, the authors take this opportunity to express their gratitude to Prof. M. V. Pasechnik for his interest in the work; to A. M. Korolev and Yu. V. Tsekhmistrenko for participating in discussion of the results, and to the personnel of the cyclotron for assuring uninterrupted operation.

---

[1] S. T. Butler, Proc. Roy. Soc. (London) A208, 559 (1951). Bhatia, Huang, Huby, and Newns, Phil. Mag. **43**, 485 (1952).

[2] L. Madansky and G. E. Owen, Phys. Rev. 99, 1608 (1955).

[3] J. E. Bowcock, Phys. Rev. **112**, 923 (1958).

[4] L. Wolfenstein, Phys. Rev. **82**, 690 (1951).

[5] W. Tobocman and M. H. Kalos, Phys. Rev. **97**, 132 (1955).

[6] N. I. Zaika and O. F. Nemets, Izv. Akad. Nauk SSSR, Ser. Fiz. **23**, 1460 (1959), Columbia Tech. Transl., in press.

[7] H. E. Gove, Phys. Rev. **81**, 364 (1951).

[8] Freemantle, Gibson, and Rotblat, Phil, Mag. **45**, 1200 (1954).

[9] Benenson, Jones, and McEllistrem, Phys. Rev. **101**, 308 (1956).

[10] Holmgren, Blair, Simmons, Stratton, and Stuart, Phys. Rev. **95**, 1544 (1954).

[11] Dobrikov, Zaika, and Nemets, Приборы и техника эксперимента (Instr. and Meas. Techniques) **4**, 23 (1958).

Translated by M. Hamermesh
1

SOVIET PHYSICS JETP VOLUME 12, NUMBER 1 JANUARY, 1961

INVESTIGATION OF THE ANISOTROPY OF THE ENERGY GAP IN SUPERCONDUCTING TIN

P. A. BEZUGLYĬ, A. A. GALKIN, and A. P. KOROLYUK

Physico-Technical Institute, Academy of Sciences, Ukrainian S.S.R.

Submitted to JETP editor January 12, 1960

J. Exptl. Theoret. Phys. (U.S.S.R.) **39**, 7-12 (July, 1960)

The methods and the results of measuring the temperature dependence of the attenuation coefficient of 70-Mcs ultrasound along various directions in a superconducting single crystal of tin are presented. From the difference in the temperature variation of the ratio α_s/α_n for sound propagating along the binary C_2 and tetragonal C_4 axes of the crystal it is concluded that the energy gap in tin is anisotropic. The width of the gap at the absolute zero along the C_2 direction is $(3.5 \pm 0.2)kT_c$, and along the C_4 direction it is $(3.1 \pm 0.1)kT_c$.

THE present microscopic theory of superconductivity[1] is in good agreement with a considerable amount of experimental data. It should, however, be noted that for a number of superconductors which have quite a pronounced lattice anisotropy the experimental results on the variation of the specific heat,[2] the thermal conductivity,[3] and the jump in the specific heat at the transition from the normal to the superconducting state, differ from the theoretical values.

This discrepancy can be explained by the fact that an isotropic model of the superconductor is considered in the theory of superconductivity, and the effect of the lattice anisotropy on the width of the energy gap is not taken into account. At the same time it is known that the transition temperature, and therefore also the width of the gap, is affected by the isotopic composition of the sample,[4,5] and by the homogeneous lattice deformation.[6] It is natural to expect that the anisotropy of the crystal lattice should manifest itself to an even larger extent in the width of the energy gap. Actually, as has been shown in the theoretical work of Khalatnikov,[7] account of superconductor anisotropy leads to values of the coefficient of thermal conductivity which vary with the crystallographic direction. It should, however, be noted that from the measurements of the thermal characteristics of the superconductor, the specific heat and the coefficient of thermal conductivity, one can only obtain indirect information on the anisotropy of the gap.

One of the simplest and most direct methods of observing the effect of the lattice anisotropy on the width of the energy gap is the attenuation coefficient of ultrasound propagating along various directions of the superconducting single crystal. Actually, one can determine from studies of the attenuation of a longitudinal ultrasound wave in superconductors[8] both the width of the energy gap at the absolute zero, and also its temperature dependence. For this purpose account must be taken of the following relation between the value of α_s/α_n (α_s and α_n are the coefficients of ultrasound attenuation in the superconducting and normal states respectively), and the width $2\epsilon_0$ of the energy gap:[8]

$$\alpha_s/\alpha_n = 2/(e^{\varepsilon_0/kT} + 1). \qquad (1)$$

This formula, obtained for the isotropic case, means that α_s/α_n should be a function of the temperature only. In other words, for an arbitrary direction of propagation of the ultrasound wave in the crystal the temperature dependence of the ratio α_s/α_n should in the event of the validity of the isotropic model be identical.

With a view to clarifying the effect of the lattice anisotropy on the electron energy spectrum in a superconductor, we undertook to measure the temperature dependence of the attenuation coefficient of a longitudinal ultrasound wave along various directions of a single crystal of tin. A short communication of our results has previously been published.[9] In the present article we present a more complete account both of the methods of measurement and of the results obtained.

Figure 1 shows the block diagram of the measuring setup employed in the described experiments. Pulses $(1 \text{ to } 1.5) \times 10^{-6}$ sec long were fed at a repetition rate of 2500 to 3000 sec^{-1} to the radiating quartz crystals from the high-frequency generator, 2, operating at 70 Mcs. The pulsed operation of the generator was realized by connecting to the anode circuit of the generator a modulator fed by a 26-I rectangular-pulse generator. The quartz

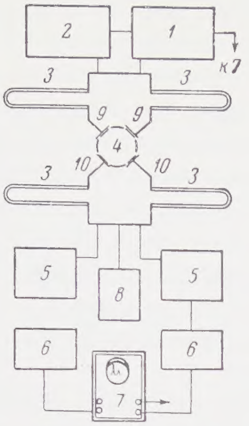

FIG. 1

crystals were connected to the high-frequency generator by ordinary flexible coaxial cables outside the Dewar and by an argentan coaxial line inside it. Between these lines was placed a coaxial cable 3 of variable length with the aid of which the generator was matched to the load. Similar components were used in the coaxial line connecting the receiving quartz crystals 10 to the calibrated attenuators 5.

Sample 4 was a spherically shaped single crystal of tin with a diameter of 13 to 15 mm on which planes perpendicular to the crystallographic axis with a diameter of 5 to 6 mm were etched by the electroerosion method. The radiating and receiving quartz crystals were glued to these planes with vacuum putty. The same putty was used to glue to the quartz crystals brass disks with a diameter of 5 to 6 mm and a thickness of 0.2 to 0.3 mm, to which the central conductors of the coaxial lines were connected. The sample was attached to a special holder, and the external conductors of the coaxial lines were grounded.

The tin samples used in the described experiments were very pure* with $R(4.2°K)/R(300°K) = (1.8 \text{ to } 2.5) \times 10^{-5}$. For such samples at helium temperatures and at 70 Mcs, the condition $l \gg \lambda$ is fulfilled (l is the mean free path of the electrons and λ is the wavelength of the longitudinal sound wave); the estimated value of $2\pi l/\lambda$ is in excess of 70.

The temperature dependence of the attenuation coefficient of the longitudinal sound wave was simultaneously recorded for two directions in the crystal. For this purpose, high-frequency pulses, giving rise to the propagation of ultrasound waves in two mutually perpendicular directions, were fed to one pair of mutually perpendicular radiating quartz crystals 9. The other pair of receiving crystals 10, placed opposite the radiating crystals, transformed the pulses transmitted by the crystal into electromagnetic signals which after passing the attenuators 5 were amplified by the amplifiers 6, and were then recorded with the aid of an oscillograph 7. The synchronization of the oscillograph beam was carried out with the aid of the same rectangular pulse generator 1 which controlled the operation of the high-frequency generator 2 through the modulator.

Having at our disposal attenuators which were calibrated with the standard signal generator 8, we could find the attenuation due to the conduction electrons for every temperature of the sample. For this purpose the curve of the temperature dependence of the attenuation coefficient was extrapolated to absolute zero, for which the ultrasound attenuation due to the electrons is zero.[8]

We used the device shown on Fig. 2 to record the temperature dependence of the ratio α_s/α_n down to 1°K. In an ordinary helium Dewar 3 we placed another small glass Dewar 2, inside which we placed the sample 1 attached to a special holder. The small Dewar was welded to a section of a kovar cylinder 5 whose upper portion was soldered to the external ground sleeve section 6. The ground sleeve was placed on vacuum putty which made the inner Dewar air tight both at room and at low temperatures.

High-frequency pulses from a high-frequency generator were fed to the crystal, and then from the crystal to the recording portion of the setup in the Dewar by means of coaxial argentan lines 4

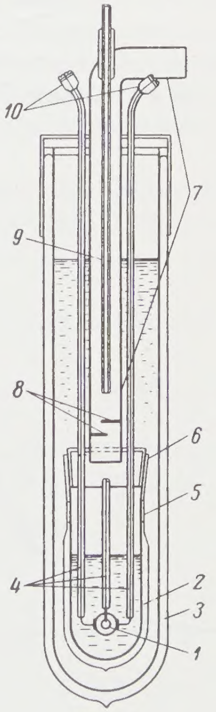

FIG. 2

---

*We take the opportunity to thank B. N. Aleksandrov for supplying the pure tin for the samples.

terminated at the external portion of the instrument by vacuum-sealed inserts 10. Coaxial cables of variable length were connected to these inserts (cf. Fig. 1).

In performing the experiments, liquid helium was first poured into the outer Dewar, and then through tube 9 into the inner small Dewar; during the measurements the crystal was in direct contact with the liquid helium.

The temperature was reduced by pumping out the helium vapor, initially by a common pump simultaneously from the inner and outer Dewar, and then, after a temperature of about 2°K had been reached, from each vessel independently. To screen the liquid helium in the inner small Dewar from infrared radiation coming from the sealed end of the device, small blackened copper-foil screens 8 were placed in the lower portion of the argentan tube 7, through which the helium vapor from the small Dewar 2 was being pumped out.

The temperature of the sample was determined from the pressure of the saturated helium vapor using the T_L55 scale.[10]

To check out the procedure and to establish the possibility of reaching conclusions on the anisotropy of the energy gap from the nature of the temperature dependence of α_s/α_n for various crystallographic directions, we measured the temperature variation of the coefficient of attenuation of longitudinal ultrasound under conditions in which the ultrasound was propagated along two mutually perpendicular binary C_2 axes (the black and white points on Fig. 3). It can be seen from Fig. 3 that in this case the experimental points fit the same curve excellently, thus proving that the physical properties of the superconductor are identical along two different C_2 axes.

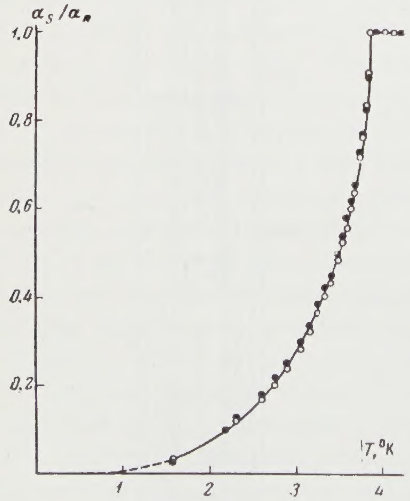

FIG. 3

Figure 4 illustrates the temperature variation of α_s/α_n when the ultrasound is propagated along the tetragonal C_4 and the binary C_2 axis. Unlike the preceding case, the temperature dependence of α_s/α_n is different in the C_4 direction than in the C_2 direction, which indicates a pronounced anisotropy of the energy gap in tin. The cited results were obtained from measurements on two samples; the experimental points obtained from each sample for the propagation of ultrasound along the same directions in the crystal fit the same curve well.

The following are typical absolute values of the electron part of the attenuation coefficient in a metal in the normal state near T_c:

$\alpha_n = (47.6 \pm 0.2)$ db/cm for the C_2 direction,

$\alpha = (21.4 \pm 0.2)$ db/cm for the C_4 direction.

It is of interest to estimate the width of the energy gap in superconducting tin along the C_2 and C_4 axes at absolute zero. Such an estimate is most simply obtained from the graphs of the dependence of $\log(\alpha_s/\alpha_n)$ on T_c/T. Actually, for $T \ll T_c$, as is easily seen from Eq. (1), the above dependence is expressed by a straight line whose slope yields the value of the width of the gap at 0°K.

The dependence of α_s/α_n on T_c/T for the C_2 and C_4 directions is shown in Fig. 5 on a logarithmic scale. The difference of the gap widths at the absolute zero follows directly from the various slopes of the linear portions of these graphs: $(3.5 \pm 0.2)kT_c$ along the C_2 axis, and $(3.1 \pm 0.1)kT_c$ along the C_4 axis.

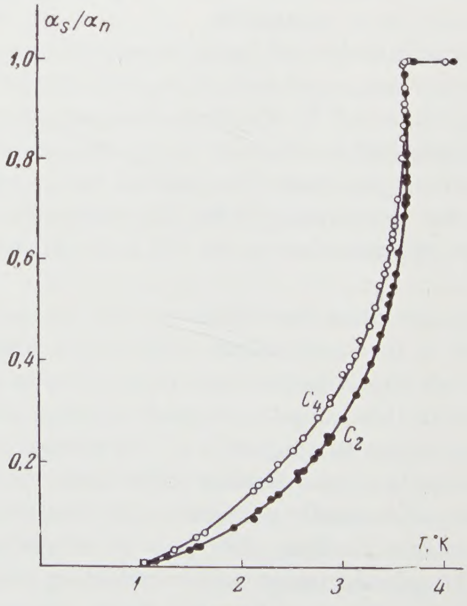

FIG. 4

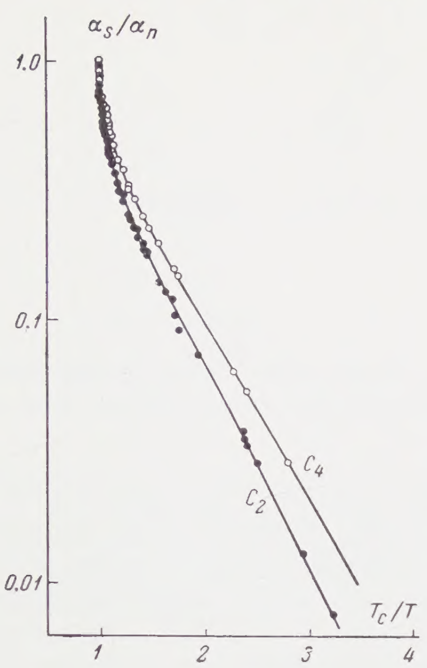

FIG. 5

The width of the gap at 0°K found for the C_4 axis agrees with the value obtained for this direction in analogous experiments of Morse et al.[11] whose results were published slightly later than our preliminary note.[9] The results of our experiments and the data of the above authors are in complete agreement, now that Morse et al. published a correction[12] in which they concede the error in their previous value of the gap width along the C_2 axis, and in which they cite the new value $(3.5 \pm 0.1)\,kT_c$.

The energy-gap anisotropy established in these experiments is due to the shape of the Fermi surface. Therefore, for those directions of the crystal for which anomalous behavior is observed in investigating the oscillations of the attenuation coefficient of the longitudinal ultrasound wave in a magnetic field,[13] one should apparently also expect a particularly strong deviation of the gap width from the values given by the present microscopic superconductivity theory.

It must be noted that along with the anisotropy of the temperature dependence of the attenuation coefficient, an anisotropy in the transition temperature T_c was also observed in our experiments. The temperature of the transition of the sample from the normal to the superconducting state for the C_2 direction exceeded the transition temperature for the C_4 direction in all the measurements by 0.004°K.

It is still impossible to say with all certainty that this is not caused by some side effects. However, it is clear that this phenomenon cannot be explained by unequal heat elimination from the sample by the helium bath during the propagation of the sound along different directions in the crystal. Actually, the simultaneous recording of the temperature variation of the attenuation coefficient in one and the same experiment excludes an effect of the above on the transition temperature. On the other hand, the difference of T_c for the C_2 and C_4 axes cannot be explained by the influence of the terrestrial magnetic field, since compensating for it did not lead to a disappearance of the difference in the transition temperatures.

In conclusion, we express our gratitude to A. I. Berdovskiĭ and É. I. Ponomarenko for help in the measurements, and also to V. L. Korpachevskiĭ for the exceptionally careful electroerosion cutting of the samples.

---

[1] Bardeen, Cooper, and Schrieffer, Phys. Rev. **108**, 1175 (1957).

[2] H. A. Boorse, Phys. Rev. Lett. **2**, 391 (1959).

[3] N. V. Zavaritskiĭ, JETP **37**, 1506 (1959), Soviet Phys. JETP **10**, 1096 (1960).

[4] Reynolds, Serin, Wright, and Nesbitt, Phys. Rev. **78**, 487 (1950).

[5] Lock, Pippard, and Shoenberg, Proc. Cambr. Phil. Soc. **47**, 811 (1957).

[6] V. G. Lazarev and L. S. Kan, JETP **14**, 463 (1944).

[7] I. M. Khalatnikov, JETP **36**, 1818 (1959), Soviet Phys. JETP **9**, 1296 (1959).

[8] R. W. Morse and H. V. Bohm, Phys. Rev. **108**, 1094 (1957).

[9] Bezuglyĭ, Galkin, and Korolyuk, JETP **36**, 1951 (1959), Soviet Phys. JETP **9**, 1388 (1959).

[10] H. van Dijk and M. Durieux, Physica **24**, 920 (1958).

[11] Morse, Olsen, and Gavenda, Phys. Rev. Lett. **3**, 15 (1959).

[12] Morse, Olsen, and Gavenda, Phys. Rev. Lett. **3**, 193 (1959).

[13] A. A. Galkin and A. P. Korolyuk, JETP **37**, 310 (1959), Soviet Phys. JETP **10**, 219 (1960).

Translated by Z. Barnea
2

SOVIET PHYSICS JETP VOLUME 12, NUMBER 1 JANUARY, 1961

DECAY OF Er^{161}

I. S. DNEPROVSKIĬ, L. NÉMET, and L. K. PEKER

Institute of Geochemistry and Analytic Chemistry, Academy of Sciences, U.S.S.R.

Submitted to JETP Editor, January 14, 1960

J. Exptl. Theoret. Phys. (U.S.S.R.) **39**, 13-15 (July, 1960)

The radiation accompanying the decay of Er^{161} was studied using a scintillation spectrometer and a double-focusing β spectrometer. On the basis of these and previously obtained data, a decay scheme is proposed for this isotope.

ACCORDING to the data of Handley and Olson,[1] the decay of Er^{161} established by them is accompanied by the emission of γ radiation which includes quanta of the following energies: 65, 195, 824 and 1125 kev. The mass number of this isotope was measured by time of flight on a mass spectrometer.[2] The best value for the half-life is 183 min.[3]

In investigating the spectrum of conversion electrons from the decay of this isotope,[4] an E3 transition with an energy of (210.6 ± 0.7) kev was discovered in the daughter nucleus Ho. It was assumed that this transition takes place between the levels $\frac{1}{2}^+[411]$ and $\frac{7}{2}^-[523]$. The occurrence of this isomeric transition and its location were confirmed in the work of Harmatz et al.,[5] carried out on a permanent-magnet spectrometer. However, other transitions listed in papers 1 and 4, in particular the intense γ transition at 826 kev, occurring in the Ho^{161} nucleus, were not found by these authors.

To clarify the nature of the transition with $h\nu = 826$ kev, we investigated the erbium fraction formed by bombardment of tantalum with 660 Mev protons from the synchrocyclotron of the Joint Institute for Nuclear Research. The measurements were done with a double-focusing β spectrometer[6] and a scintillation spectrometer whose efficiency was calibrated against standards.

A value of (190 ± 10) min was obtained for the half-life of this transition; the energy is (826.5 ± 1.5) kev.

The conversion coefficient for this transition was determined by making measurements of the ratio of the heights of the electron conversion lines and the ratio of the heights of the photopeaks from the γ spectra of this transition and the 661.6 kev transition in Ba^{137}.

It was necessary to take account of the radiation from decay products of other isotopes of erbium which were present in our sample: Er^{160} ($T_{1/2} = 30$ hr) and Er^{158} ($T_{1/2} = 2.5$ hr). It is easy to make corrections for the presence of Er^{160} because of the large difference in the half lives.

A more important correction is the taking account of the fractions of γ radiations at 848 and 851 kev from the decay of Ho^{158} (reference 7) in the photopeak measured by us at 826 kev, since the resolving power of the crystal, which is 9%, does not allow us to see the photopeaks of these radiations separately. From our earlier data[7] the transitions at 848 and 851 kev, which occur between the levels of the second and first rotational bands, should be E2. This determines the conversion coefficient so that from the ratios of the heights of the conversion lines we were able to find the ratio of the intensities of the γ radiations:

$$I_{\gamma 826}/I_{\gamma 848,851} = 4.0 \pm 0.2.$$

The value obtained for the conversion coefficient of the 826-kev transition in the K shell, including all corrections, is

$$\alpha_K = 0.008 \pm 0.002.$$

According to the tables of Sliv and Band[8] this value allows us to assign this γ transition as M1 or E3. We can use the K/L ratio as an additional argument for choosing the type of transition. The theoretical values of this ratio for different types of transition are the following:

*E*1	*E*2	*E*3	*M*1	*M*2	*M*3
5.72	5.63	4.91	6.41	6.25	5.51

The experimental value of the ratio, K/L = 7.0 ± 0.8, clearly allows us to exclude E3.

The complexity of the γ spectrum obtained with the scintillation spectrometer does not permit us to make an estimate of the ratio of the intensities of the 211- and 826-kev γ transitions directly from the photopeaks. The ratio of the intensities of these transitions calculated from their conversion lines is

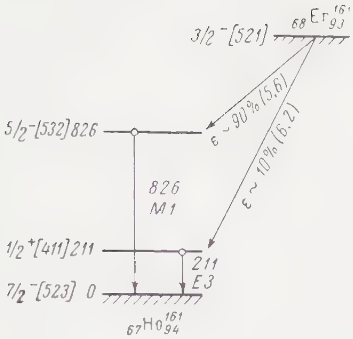

$$I_{\gamma 826}/I_{\gamma 211} = 8.0 \pm 1.5.$$

The large intensity of the 826-kev γ transition shows that there is a level at 826 kev in Ho^{161}, which is populated in 90% of the decays of Er^{161}.

The multipolarity of the transition and the spin $7/2^-$ of the ground state of Ho^{161} determine the spin and parity of this level to be $5/2^-$, which corresponds to the single particle level $5/2^-[532]$ in the Nilsson diagram. Since the ground state of Er^{161} is most probably $3/2^-[521]$, such an interpretation of the levels enables us to explain the relative intensity of the electron transitions. The electron transition to the 826 kev level of Ho^{161} is allowed by the selection rules on spin and parity while the transition to the isomeric level at 211 kev is first forbidden.

In the figure we show the decay scheme of Er^{161} constructed on the basis of the above considerations. The asymptotic Nilsson quantum numbers N, n_Z, and Λ are given in square brackets. The data on intensities of the electron transitions are indicated next to the sloping lines. The ft values, calculated on the assumption that the decay energy of Er^{161} is 2 or 2.5 Mev (according to Cameron[9] it is 2033 kev), are given in parentheses.

It is a pleasant duty to thank I. A. Yutlandov and S. Khaĭnatskiĭ for carrying out the chemistry for this work.

---

[1] T. H. Handley and B. L. Olson, Phys. Rev. **93**, 524 (1954).

[2] M. C. Michel and D. H. Templeton, Phys. Rev. **93**, 1422 (1954).

[3] W. B. Nervik and G. T. Seaborg, Phys. Rev. **97**, 1092 (1955).

[4] I. S. Dneprovskiĭ and G. M. Kolesov, Izv. Akad. Nauk SSSR, Ser. Fiz. **22**, 935 (1958), Columbia Tech. Transl. p. 927.

[5] Harmatz, Handley, and Mihelich, Phys. Rev. **114**, 1082 (1959).

[6] Bekkerman, Gumenyuk, and Dneprovskiĭ, Бета-спектрометр типа БПП (Beta-Spectrometer Type BPP) VINITI, Moscow (1959).

[7] I. S. Dneprovskiĭ. Investigation of the Erbium Fraction on the Type BPP Beta-Spectrometer. (Papers of the Conference on Nuclear Spectroscopy of Rare-Earth Elements, Dubna, 1959).

[8] L. A. Sliv and N. I. Band. Таблицы коэффициентов внутренней конверсии (Tables of Internal Conversion Coefficients), Acad. Sci. U.S.S.R., Moscow, 1956.

[9] A. G. W. Cameron. A Revised Semi-Empirical Atomic Mass Formula, Chalk River, Ontario, CRP-690, 1957.

Translated by M. Hamermesh
3

SOVIET PHYSICS JETP VOLUME 12, NUMBER 1 JANUARY, 1961

THE DYNAMIC COMPRESSIBILITY, EQUATION OF STATE, AND ELECTRICAL CONDUCTIVITY OF SODIUM CHLORIDE AT HIGH PRESSURES

L. V. AL'TSHULER, L. V. KULESHOVA, and M. N. PAVLOVSKIĬ

Submitted to JETP editor January 25, 1960

J. Exptl. Theoret. Phys. (U.S.S.R.) **39**, 16-24 (July, 1960)

Results are presented of an experimental investigation of the compressibility and electrical conductivity of shock-compressed single crystals of sodium chloride in the pressure range from 50 to 800 thousand atmospheres. The equation of state for sodium chloride in the high pressure region is deduced from these data. It is shown that in the compression range investigated, the interaction potential between ions can be satisfactorily described by a formula with an exponential term for the repulsive forces. The method for measuring the electrical conductivity is described. The dependence of electrical conductivity on temperature under shock compression conditions is derived and the activation energy is deduced. It is shown that a sharp increase in conductivity takes place behind the shock wave front. Just as under normal conditions, the conductivity is of an ionic nature.

INTRODUCTION

THE classical theory of ionic lattices was developed by Born and Madelung, who expressed the repulsive forces potential by a power term of the form br^{-n}. Later investigators tried to bring the classical theory into as close agreement as possible with the laws of quantum mechanics, representing[1] the repulsive potential as an exponential $Be^{-r/\rho}$. The parameters n and ρ in these expressions are determined from the experimental values of the compressibility. The validity of the formulae is usually established by comparing the calculated and experimental values for the lattice energy. However, this criterion is not unambiguous since the binding energy is weakly dependent on these parameters under normal conditions.

The most direct evidence about the law of ionic interaction can be obtained by measuring the pressure obtaining when the interatomic distance is reduced. Bridgman's measurements of the isothermal compressibility of rock salt[2] are of special interest in this respect. At a pressure of 100×10^3 atm the density was found to increase 1.27 times.

In the present work the compressibility and the equation of state of sodium chloride were investigated over a considerably greater range of pressure and density, obtained by using intense shock waves.

We also carried out a series of determinations of the electrical conductivity of sodium chloride. A sharp increase in conductivity for a number of solid dielectrics during the passage of shock waves was first found by Brish, Tarasov and Tsukerman[3] in 1950. A short note was published by Alder and Christian[4] in 1956 concerning the electrical conductivity of ionic and molecular crystals under dynamic loading. Unfortunately, the quantitative characteristics of the shock waves were not given and the relation between conductivity and the pressure and temperature was not determined.

We give below the results of a complex determination of the dynamic and electrical properties of sodium chloride, from which the conductivity can be related to the parameters of the shock compression and the equation of state derived for pressures up to 800×10^3 atm.

1. THE DYNAMIC COMPRESSIBILITY AND EQUATION OF STATE OF SODIUM CHLORIDE

Pure single crystals of sodium chloride, with density 2.16 gm/cm^3 were used for the investigations. The reflection method[5] was applied for measuring the dynamic compressibility behind the front of a plane shock wave. Several series of experiments were made, differing in the power of the explosive charge and also in the thickness of the copper, aluminium and iron barrier plates. The wave velocities were measured over reference bases of 4 — 8 mm. Time intervals were determined by the electrical contact method,[5] using high speed oscillographs of the OK-21 type. The time intervals were measured to an accuracy of 5×10^{-9} sec, and the wave velocities were accurate to ± 1.0%.

TABLE I

Point No.	D, km/sec	U, km/sec	P_H 10^{10} bars	v_0/v	δ	Plate material	U_p, km/sec
1	4.16	0.59	5.3	1.16	1.14	Copper	0.37
2	4.73	0.98	10.0	1.26	1.24	Aluminum	0.70
3	5.29	1.33	15.2	1.34	1.32	Aluminum	1.10
4	5.41	1.55	18.2	1.39	1.36	Iron	1.03
5	5.59	1.59	19.3	1.40	1.37	Aluminum	1.32
6	5.66	1.71	20.9	1.43	1.40	Aluminum	1,42
7	5.96	1.85	23.6	1.45	1.42	Aluminum	1.54
8	6.18	2.07	27.6	1.50	1.47	Aluminum	1.74
9	7.85	3.24	54.7	1.70	1.67	Aluminum	2.80
10	8.91	4.10	79.0	1.85	1.82	Iron	2.80

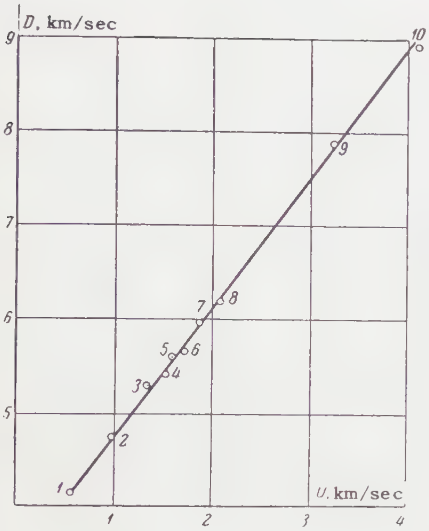

FIG. 1. D–U diagram of the shock adiabat of sodium chloride (the points are numbered to correspond to Table I).

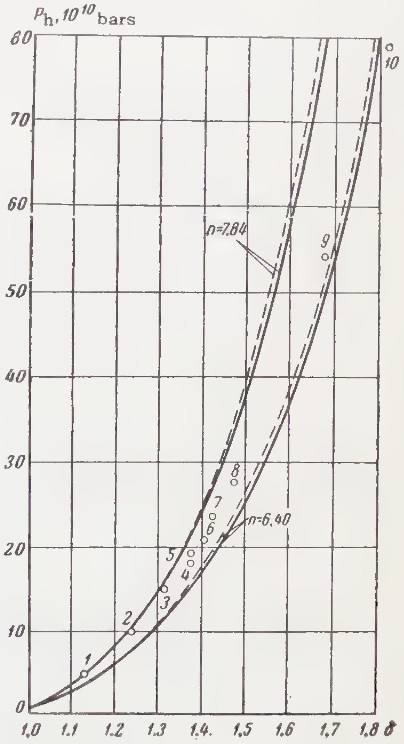

FIG. 2. Experimental data and calculated shock adiabats (with a power law for the repulsive forces): dashed curve is calculated according to Eq. (7a), the continuous curve according to (7b).

Table I shows the parameters for the experimental points for the shock adiabats of sodium chloride. The wave, D, and mass, U, velocities of the shock waves are given for each point and also the shock compression pressure P_H, the relative compression v_0/v and $\delta = v_{0K}/v$ (where v, v_0 and v_{0K} are the corresponding specific volumes behind the shock front, in the initial state and for P = 0, T = 0°K). The mass velocities in the plates, U_p, are given in the last column. The parameters of the points were determined by using a P–U diagram. The D–U relation for copper, aluminum and iron, given previously[6] was used. In the first eight series of experiments the pressure in the specimens was produced by reflection of the detonation wave from the barrier plate, and in the final two by impact from aluminum and iron discs, driven by the explosion products.[6] The measurements cover the pressure range from 50×10^3 to 790×10^3 atm. At the highest pressure the density of the crystal is increased 1.85 times. The dynamic adiabatics of sodium chloride are shown graphically in D–U coordinates in Fig. 1 and in P–δ coordinates in Figs. 2 and 3.

We express the equation of state of sodium chloride by the Debye formula:

$$P = P_c + (\gamma/v)E_t, \tag{1}$$

where P is the pressure, P_c the pressure at absolute zero, v the specific volume, γ the Grüneisen constant, determining the ratio of thermal pressure to the thermal energy density and E_t is the thermal energy of the lattice.

On the assumption that the atoms of the lattice undergo harmonic oscillations, Slater[7] and Landau[8] derived the following relation for γ(v)

$$\gamma = -\frac{2}{3} - \frac{v}{2}\frac{d^2P_c/dv^2}{dP_c/dv}. \tag{2a}$$

There is another expression for γ(v), derived by Dugdale and MacDonald[9] from the theory of finite deformations:

$$\gamma = -\frac{1}{3} - \frac{v}{2}\frac{d^2(P_c v^{2/3})/dv^2}{d(P_c v^{2/3})/dv}. \tag{2b}$$

The system (1), (2a) and (2b) is usually used to

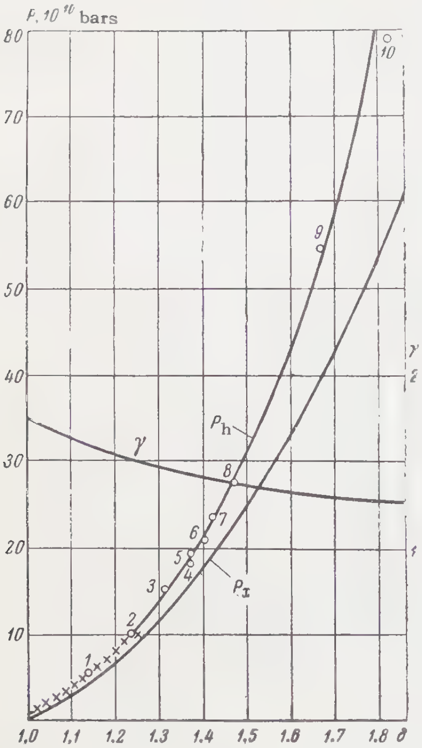

FIG. 3. The shock adiabat, the "cold" compression curve $P_c(\delta)$ and the function $\gamma(\delta)$ for sodium chloride, with ρ = 0.318 A. γ is calculated from equation (9b). o – experimental data, x – Bridgman's data on isothermal compression.

obtain the unknown functions $P_c(v)$ and $\gamma(v)$ from the data of dynamic experiments. For this purpose the pressure P_H and the internal energy

$$E_t = E_0 + \frac{1}{2} P_\Gamma (v_0 - v) - \int_v^{v_{0K}} P_c\, dv$$

of the states on the shock adiabat are substituted into (1) (E_0 is the energy of the initial state for $v = v_0$ and $T = 300°$ K). The equation then obtained

$$P_H = \left[P_c + \frac{\gamma}{v} E_0 - \frac{\gamma}{v} \int_v^{v_{0K}} P_c\, dv\right]\left[1 - \frac{\gamma}{2}\left(\frac{v_0}{v} - 1\right)\right]^{-1} \quad (3)$$

is solved together with (2a) or (2b). The value of v_{0K} can be determined easily from (3), since for $v = v_{0K}$

$$P_c = 0, \quad \gamma \approx \gamma_0 = \frac{\beta v_0}{K c_v}, \quad P_H \approx \frac{1}{K}\left(\frac{v_0}{v_{0K}} - 1\right).$$

β is the coefficient of volume expansion, K is the compressibility, and c is the specific heat. The values of the various parameters used in the calculations below are as follows:

$$K = (4.24 \text{ to } 4.16)\cdot 10^{-12}\ \text{cm}^2/\text{dyne}, \quad \beta = 1.15\cdot 10^{-4}\ \text{deg}^{-1},$$
$$\gamma_0 = 1.51, \quad v_0 = 0.463\ \text{cm}^3/\text{g}, \quad v_{0K} = 0.455\ \text{cm}^3/\text{g}.$$

The unknown functions $P_c(v)$ and $\gamma(v)$ can also be determined by another method. We can use the analogous expression for $P_c(v)$ given by ionic lattice theory, which contains the undetermined parameter n or ρ. The system (2) and (3) is solved for P_H and γ with various values for the undetermined parameters which enter into the expression for P_c, and the variant is chosen which gives the best agreement with the experimental data on the dynamic compressibility.

As has been pointed out, there is no unique way of representing the repulsive force potential in an ionic crystal. We shall examine two expressions for the interaction energy:

$$E = -A[r_{0K}/r - n^{-1}(r_{0K}/r)^n], \quad (4)$$

$$E = -A[r_{0K}/r - (\rho/r_{0K}) \exp\{(r_{0K} - r)/\rho\}], \quad (5)$$
$$A = N\alpha e^2/r_{0K}\mu.$$

N is Avogadro's number, μ the molecular weight, α the Madelung constant, e the electronic charge, r the interatomic distance and r_{0K} is the interatomic distance for P = 0 and T = 0° K; with v_{0K} = 0.455 cm³/g, r_{0K} = 2.797 A.

We will first consider the representation of the potential in the form (4). The pressure is then

$$P_c = -\frac{dE}{dv} = \frac{A}{3v_{0K}}(\delta^{n/3+1} - \delta^{4/3}), \qquad \delta = \frac{v_{0K}}{v} = \left(\frac{r_{0K}}{r}\right)^3. \quad (6)$$

Substituting $P_c(v)$ in (2a) and (2b) leads to the following expressions for the Grüneisen constant:

$$\gamma = \frac{1}{6}\,\frac{(n-2)(n+3)\delta^{(n-1)/3} - 12}{(n+3)\delta^{(n-1)/3} - 4}, \quad (7a)$$

$$\gamma = \frac{1}{6}\,\frac{(n+1)(n+2)\delta^{(n-1)/3} - 6}{(n+1)\delta^{(n-1)/3} - 2}. \quad (7b)$$

The pressure on the Hugoniot adiabat is found from Eq. (3) using expression (7a) or (7b) for γ and (6) for P_c.

Different authors[10,11] give values between 7.84 and 9.1 for n. Figure 2 shows the dynamic adiabats calculated for two values of n for the two values of γ obtained from (7a) and (7b). The curves for n = 7.84 fit the initial part of the experimental adiabat satisfactorily and the curves for n = 6.4 fit the final part. The repulsive forces cannot be fitted throughout by using a power expression.

We now look at the representation of the lattice energy in the form (5). As before, we obtain an expression for the pressure

$$P_c = (A/3v_{0K})\{\delta^{2/3} \exp[(r_{0K}/\rho)(1 - \delta^{-1/3})] - \delta^{4/3}\} \quad (8)$$

and the two corresponding expressions for the Grüneisen constant:

$$\gamma = \frac{1}{6}\,\frac{[2\delta^{-2/3} + 2r_{0K}/\rho\delta + (r_{0K}/\rho)^2\delta^{-4/3}]\exp[(r_{0K}/\rho)(1 - \delta^{-1/3})] - 12}{[2\delta^{-2/3} + r_{0K}/\rho\delta]\exp[(r_{0K}/\rho)(1 - \delta^{-1/3})] - 4}, \quad (9a)$$

$$\gamma = \frac{1}{6}\,\frac{(r_{0K}/\rho)^2\delta^{-4/3}\exp[(r_{0K}/\rho)(1 - \delta^{-1/3})] - 6}{(r_{0K}/\delta\rho)\exp[(r_{0K}/\rho)(1 - \delta^{-1/3})] - 2}. \quad (9b)$$

The dynamic pressure is calculated by substituting (8) and (9) into (3).

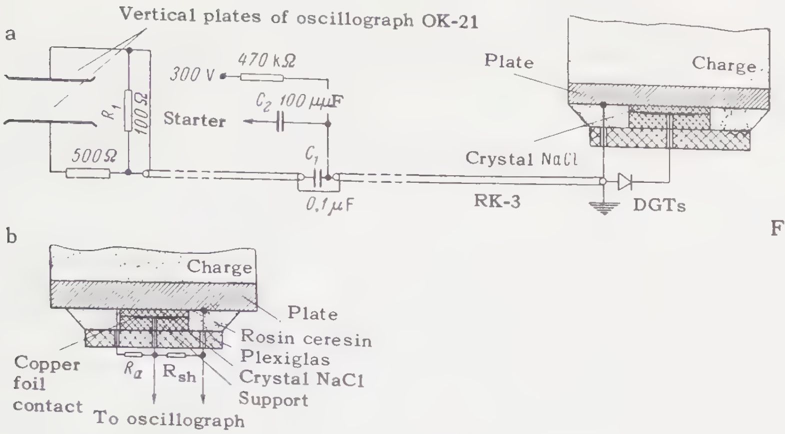

FIG. 4. Apparatus for measuring electrical conductivity.

The parameter ρ was determined earlier from the compressibility. With the value $\rho = 0.328$ A given by Born and Huang,[12] the calculated adiabat lies somewhat lower than the experimental. Davydov[13] previously used Eq. (8) with $\rho = 0.287$ A ($r_{0K}/\rho = 9.69$) to extrapolate Bridgman's data to a pressure of 2×10^6 atm. The value of ρ chosen by Davydov differs from the true in the opposite direction, in so far as the corresponding shock adiabat lies above the experimental.

We tried to obtain the best agreement between calculation and experiment by changing the parameter ρ. The closest agreement was reached with $\rho = 0.318$ A when γ is calculated according to Dugdale's formula (9b) (see Fig. 3). The calculated adiabat then agrees satisfactority with the experimental data over the whole pressure range from 50×10^3 to 800×10^3 atm. Slater's formula (9a) with $\rho = 0.324$ A gives only a slightly worse result, but preference must be given to Dugdale's formula since it gives for $v = v_0$ better agreement with the experimental values, as follows:

	γ_0	$K(v_0)$
Experimental data	1.51	$(4.24-4.16)\times 10^{-12}$ bar^{-1}
Calculated from formulae:		
Dugdale	1.75	4.32×10^{-12} bar^{-1}
Slater	2.02	4.45×10^{-12} bar^{-1}

The values of P_C, $E_C = \int_V^{V_{0K}} P_C dv$; γ, P_H and T are given as functions of δ in table 2.

The temperatures on the Hugoniot adiabat are calculated from the equation

$$T, ^\circ K = 300^\circ + [\tfrac{1}{2} P_H (v_0 - v) - E_c]/c_v.$$

The analysis carried out shows that in the density range studied the repulsive forces can be represented as $Be^{-r/\rho}$ with the constant $\rho = 0.318$ A. In the same range the Grüneisen constant changes from 1.75 to 1.27.

TABLE II

δ	P_c 10^{10} bars	E_c 10^{10} ergs	γ	P_H 10^{10} bars	T, °K
1.0	0	0	1.75	0.5	300
1.1	2.9	0.04	1.64	3.5	320
1.2	6.8	0.21	1.55	7.8	380
1.3	11.8	0.46	1.48	13.4	550
1.4	17.7	0.82	1.43	20.8	920
1.5	25.1	1.29	1.38	31.1	1500
1.6	33.2	1.81	1.34	43.0	2400
1.7	42.7	2.44	1.30	59.2	3850
1.8	53.7	3.13	1.27	80.7	6150

2. THE ELECTRICAL CONDUCTIVITY OF SODIUM CHLORIDE AT HIGH PRESSURES.

For measuring the electrical conductivity, sodium chloride crystals were attached to plates of aluminum or iron (see Figs. 4, a and b), through which the shock waves passed, produced by the explosive charge or by impact of a plate. The distance between the face of the charge and the center of the crystal being studied was made the same in the conductivity measurements as in the corresponding experiments on the compressibility. The support of crystalline sodium chloride, placed under the 0.02-mm copper foil contact, prevented unloading of the working part of the crystal over the free surface. The crystals were sealed at the sides with ceresin rosin to prevent shorting of the contacts through the air. The crystals were about 3 mm thick and the support 4 — 9 mm.

Special apparatus was required to measure the conductivity behind the shock wave front because of the short duration of the process. We used two arrangements with different measuring ranges.

The first apparatus is shown diagramatically in Fig. 4a.* The principle on which it works is as follows: due to the passage of the shock wave

---

*The arrangement was suggested by A. V. Reĭmers.

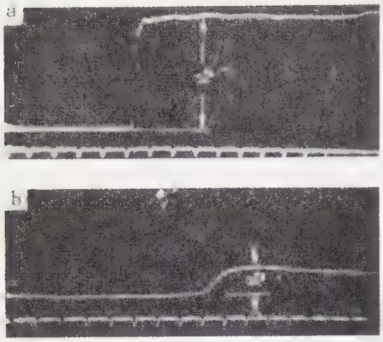

FIG. 5. Oscillograms obtained in experiments by the method of Fig. 4a: a – control, b – working oscillogram. Frequency scale 5 Mcs.

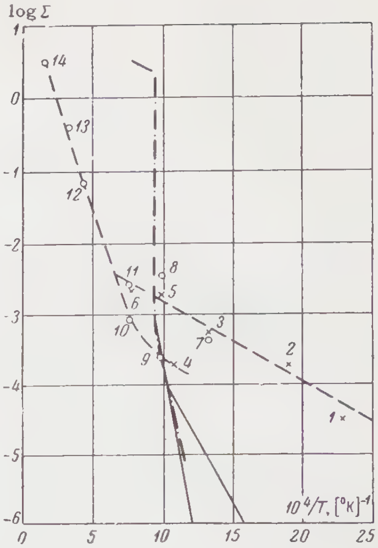

FIG. 6. The dependence of the electrical conductivity of sodium chloride on temperature: dashed curve shows data of the present work (see Table III for the parameters of the experimental points), continuous curve represents Lehfeldt's[15] data and the dashed and fotted curve that of Arndt.[16]

through the crystal there is a sharp reduction in its resistivity, and as a result the capacitors C_1 and C_2 discharge through the crystal. The discharge of capacitor C_2 activates the starter for the whole measuring apparatus. Capacitor C_1 discharges through the resistance $R_1 = 100$ ohms and R_x the resistance of the shock compressed crystal. The value of R_x is determined from the formula

$$R_x = (V_0/V_x - 1)R_1,$$

where V_0 is the deflection on the oscilloscope for shortcircuiting through zero resistance ($R_x \approx 0$) and V_x is the deflection on the picture taken under working conditions. Figure 5 shows oscillograms taken in one of the experiments using this apparatus.

The second arrangement (see Fig. 4b) was similar to that used earlier[14] for measuring the electrical conductivity of explosion products.

The resistance R_{sh} varied in different experiments between 0.8 and 6 ohms and the resistance $R_a = 50\ R_{sh}$ was used to obtain time markers on the oscillogram corresponding to the instant when the shock wave reaches the specimen surface. Measurements showed that the greatest deflection indicating the reduction in resistivity of the crystal, occurred at the moment when the shock wave reached the copper foil contact. The resistance of the crystal R_x was derived from the relation

$$R_x = V_{xsh}\,[(V_{sh} - V_{xsh})\,(1/R_{sh} + 1/R_a)]^{-1},$$

where V_{sh} and V_{xsh} are the electrode voltages before and after the passage of the shock wave through the crystal.

The specific conductivity, Σ, of the crystal was calculated from the formula

$$\Sigma = L/R_x S,$$

where R_x is the measured resistance of the shock compressed crystal, S is the area of the copper foil contact (which varied between 0.2 and 7 cm^2) and L is the thickness of the crystal (between the plate and the metal contact). Several series of experiments were made with various shock wave parameters, just as in the measurements of dynamic compressibility.

The experimental results are collected in Table III, which gives the relative compression v_0/v, the pressure P_H, the temperature in the crystal behind the shock wave front, T, and the specific conductivity of the crystal, Σ. The apparatus shown in Fig. 4a was used for the first six experiments (these points are marked by crosses in Fig. 6), and the previously described apparatus[14] was used for series 7 — 14.

The results of the present experiments are shown in Fig. 6 as log Σ vs. $10^4 T^{-1}$, together with the data of Lehfeldt[15] who measured the conductivity at atmospheric pressure, and of Arndt[16] who measured the conductivity of fused sodium chloride. It can be seen that for relatively low pressures and temperatures there is considerable scatter in the

TABLE III

Point No.	v_0/v	T, °K	P_H, 10^{10} bars	Σ, $\Omega^{-1}\cdot$cm^{-1}	Point No.	v_0/v	T, °K	P_H, 10^{10} bars	Σ, $\Omega^{-1}\cdot$cm^{-1}
1	1.26	440	10.0	$2.0\cdot10^{-5}$	8	1.45	1020	23.6	$3.5\cdot10^{-3}$
2	1.31	530	13.7	$1.9\cdot10^{-4}$	9	1.45	1020	23.6	$2.6\cdot10^{-4}$
3	1.39	760	18.2	$5.7\cdot10^{-4}$	10	1.50	1320	27.6	$8.6\cdot10^{-4}$
4	1.43	940	20.9	$2.0\cdot10^{-4}$	11	1.50	1320	27.6	$2.5\cdot10^{-3}$
5	1.45	1020	23.6	$1.9\cdot10^{-3}$	12	1.62	2280	43.3	$6.8\cdot10^{-2}$
6	1.50	1320	27.6	$2.5\cdot10^{-3}$	13	1.68	3030	54.5	$4.1\cdot10^{-1}$
7	1.39	760	18.2	$4.4\cdot10^{-4}$	14	1.85	6150	79.0	3.26

magnitude of the conductivity, especially in experiments with crystals taken from different sources.

The experimental results obtained show that the electrical conductivity of a crystal compressed by intense shock waves increases by several orders of magnitude. We found a similar effect earlier in Plexiglas and in caesium iodide.

In the high temperature region the $\log \Sigma\ (T^{-1})$ curve has a constant slope, corresponding to an activation energy of 1.2 ev. This leads us to presume that the main factor determining the increase in conductivity is temperature. Judging by the activation energy, the conductivity of sodium chloride is of an ionic nature, just as under normal conditions.

The $\log \Sigma\ (T^{-1})$ dependence does not show the rapid changes in conductivity or activation energy, characteristic for the melting process.

The authors consider it a pleasant duty to express their thanks to academician Ya. B. Zel'dovich for his interest and advice in the work and to V. P. Drakin for help with the experiments.

---

[1] F. Seitz, The Modern Theory of Solids. (Russ. Transl.), GITTL, 1949.

[2] P. W. Bridgman, Proc. Amer. Acad. **76**, 1 (1945).

[3] Brish, Tarasov, and Tsukerman, JETP **38**, 22 (1960), Soviet Phys. JETP **11**, 15 (1960).

[4] B. J. Alder and R. H. Christian, Phys. Rev. **104**, 550 (1956).

[5] Al'tshuler, Krupnikov, and Brazhnik, JETP **34**, 886 (1958), Soviet Phys. JETP **7**, 614 (1958).

[6] Al'tshuler, Kormer, Bakanova, and Trunin, JETP **38**, 790 (1960), Soviet Phys. JETP **11**, 573 (1960).

[7] J. C. Slater, Introduction to Chemical Physics, McGraw-Hill, New York, 1939.

[8] L. D. Landau and K. P. Stanyukovich, Dokl. Akad. Nauk SSSR **46**, 399 (1945).

[9] J. S. Dugdale and D. K. C. MacDonald, Phys. Rev. **89**, 832 (1953).

[10] E. Grüneisen, Handbuch der Physik, 1926, Vol. 10, p. 15.

[11] J. C. Slater, Phys. Rev. **23**, 488 (1924).

[12] M. Born and Kun Huang, The Dynamical Theory of Crystal Lattices (Russ. Transl.), IIL, 1958.

[13] B. N. Davydov, Izv. Akad. Nauk SSSR, Ser. Geofiz. **12**, 1411 (1956).

[14] Brish, Tarasov, and Tsukerman, JETP **37**, 1543 (1959), Soviet Phys. JETP **10**, 1095 (1960).

[15] W. Lehfeldt, Z. Phys. **85**, 717 (1933).

[16] K. Arndt, Z. Electroch. **12**, 337 (1906); **13**, 509 (1907); see also Handbook of Chemistry, Goskhimizdat, 1951-2.

Translated by R. Berman
4

SOVIET PHYSICS JETP VOLUME 12, NUMBER 1 JANUARY, 1961

ON THE LEVEL SCHEME OF Ta^{181}

G. A. VARTAPETYAN and A. G. KHUDAVERDYAN

Physics Institute, Academy of Sciences, Armenian S.S.R.

Submitted to JETP editor February 4, 1960

J. Exptl. Theoret. Phys. (U.S.S.R.) **39**, 25-26 (July, 1960)

It is shown by the $\beta\gamma$-coincidence technique that a 137-kev transition between the 619- and 482-kev levels ($T_{1/2} = 10^{-8}$ sec) does not exist, whereas some new γ transitions at 619, 480, and 345 kev have been detected. The period of the 619-kev level is less than 10^{-9} sec.

THE decay of Hf^{181}, which has a half-life of 46 days, has been investigated by many authors (see reference 1). Measurements carried out on β and γ spectrometers lead to the decay scheme shown in the work of Boehm and Marmier[2] and Snyder and Frankel.[3]

We measured the decay scheme of Hf^{181} by the $\beta\gamma$-coincidence technique, in order to determine the lifetime of the 619-kev level, which has been previously found to be smaller than 10^{-8} sec.[3]

The β radiation was detected by anthracene of thickness 2 mm and the γ quanta by a NaI(Tl) crystal of size 30 × 25 mm. The fast — slow coincidence circuit consisted of (2 or 3) energy-discrimination channels a slow-coincidence circuit (2×10^{-6} sec), and a fast-coincidence circuit with a resolving time of 5×10^{-9} to 2×10^{-8} sec.[4]

Without the absorber in the β channel (according to the cited decay scheme[2,3]) the curve of the delayed coincidences of β particles and 482-kev γ rays should show a half-life of 10^{-8} sec for the 482 kev level. Curve a in Fig. 1 shows that we have coincidences with a period less than 10^{-8} sec. In order to explain this, we examined, by means of an aluminum absorber (30 mg/cm^2), conversion electrons from the K and L shells due to the 133-kev γ transition (which contributes to the 10^{-8} period of the 482 kev level). We thus obtained curve b of Fig. 1. Repetition of the same experiment with 345-kev γ quanta gave analogous curves; β radiation with an upper cut-off of 404 kev is in coincidence with 480- and 345-kev γ rays. It thus follows that, in contrast to the Ta^{181} decay scheme, there is no 137-kev γ transition from the 619-kev level to the 482-kev level.

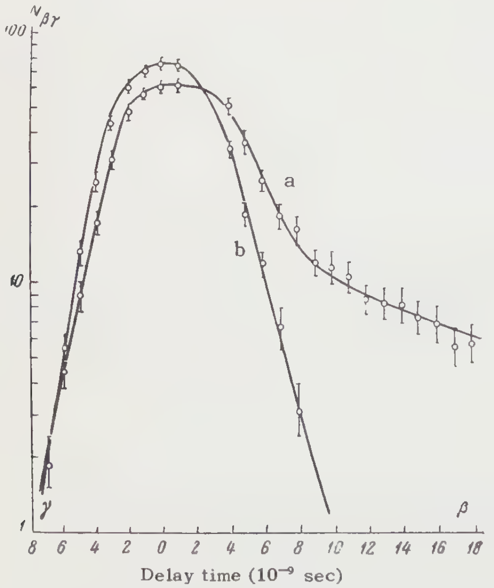

FIG. 1. a – curve of coincidences $e^-_{133} + \beta - \gamma$, 480 kev; b – curve of $\beta\gamma$ coincidences, 480 kev.

Moreover, the measurements show that there still exists a 619-kev γ transition in coincidence with 404-kev β radiation. From a study of the slope of the delayed-coincidence curve we find that the period of this transition is less than 10^{-9} sec.

In its intensity, the spectrum of γ rays in coincidence with conversion electrons from the 133-kev γ transition (the γ-spectrum coincidences were obtained introducing a delay of 1.7×10^{-8} sec in the β channel) corresponds to the direct γ spectrum of Hf^{181}, which is obtained from the β transition with an upper cut-off of 408 kev (93.5%).

The curve of Fig. 2 shows the γ spectrum in coincidence with β rays for which $E_{\max} = 404$ kev. [An aluminum filter (30 mg/cm^2) which absorbs the conversion electrons from the 133-kev γ rays was placed in the β channel.] In this case we obtained a new ratio for the intensities of the 480-kev and 345-kev γ quanta. These new photons of energy close to 480 and 345 kev are in coincidence with 136-kev photons. This confirms the results of the triple coincidences $\beta_{404}-\gamma_{136}-\gamma_{480}$ and $\beta_{404}-\gamma_{136}-\gamma_{345}$.

Thus, the measurements lead to the following conclusions:

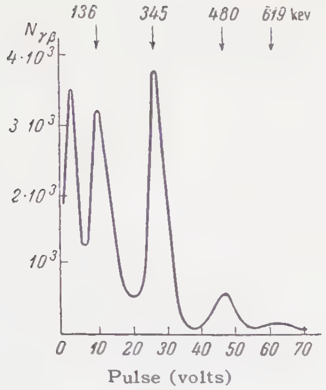

FIG. 2

1) There is no 137-kev γ transition from the 619-kev level to the 482-kev level ($T_{1/2} = 10^{-8}$ sec).

2) There exists a 619-kev γ transition, in agreement with reference 5, and two new γ transitions of energy close to 480 and 345 kev; the latter two transitions are in coincidence with 136-kev γ rays.

3) The period of the 619-kev level is less than 10^{-9} sec. On the basis of the preliminary data, it can be concluded that the 619-kev level is not the first rotational level of the family which belongs to the 615-kev level ($K = \frac{1}{2}^{+}[411]$).

We express our deep gratitude to A. I. Alikhanyan for his constant interest in this work. We thank Z. Petrosyan for help in the experiment.

---

[1] B. S. Dzhelepov and L. K. Peker, Схемы распада радиоактивных ядер (Decay Schemes of Radioactive Nuclei), Izv. Akad. Nauk. SSSR, 1958.

[2] F. Boehm and P. Marmier, Phys. Rev. 103, 342 (1956).

[3] E. Snyder and S. Frankel, Phys. Rev. 106, 755 (1957).

[4] H. Vartapetian, Ann. phys. 3, 569 (1958).

[5] Borovikov, Gvozdev, Kondurov, and Khazov, Izv. Akad. Nauk SSSR, Ser. Fiz. 23, 1448 (1959), Columbia Tech. Transl. (in press).

Translated by E. Marquit
5

WEAK FERROMAGNETISM IN AN ANTIFERROMAGNETIC $CoCO_3$ SINGLE CRYSTAL

A. S. BOROVIK-ROMANOV and V. I. OZHOGIN

Institute for Physical Problems, Academy of Sciences, U.S.S.R.

Submitted to JETP editor February 13, 1960

J. Exptl. Theoret. Phys. (U.S.S.R.) **39**, 27-36 (July, 1960)

The magnetic properties of a $CoCO_3$ single crystal were studied at temperatures from 1.3 to to 300°K by means of a magnetic balance. In agreement with earlier results,[1] antiferromagnetic ordering with weak ferromagnetism is established in $CoCO_3$ below $T_N = 18.1$°K. Some properties differing from the data for $MnCO_3$[4] are the very large anisotropy of the paramagnetic susceptibility, the large spontaneous ferromagnetic moment ($\sigma_0 = 1440$ cgs emu/mole) and the sharp peak of $\chi_\perp$ near T_N. It is shown that the latter feature, can be explained within the thermodynamic theory of weak ferromagnetism,[3] and is associated with the fact that a magnetic field imposed on a disordered substance induces antiferromagnetic ordering.

The anomaly observed in the temperature dependence of the spontaneous moment at low temperatures can be explained within the framework of the spin-wave theory as a transition from the excitation of a single branch to the excitation of both branches of the spin-wave spectrum. As in the case of $MnCO_3$,[4] no quantitative agreement with the spin-wave theory is observed.

1. INTRODUCTION

WEAK ferromagnetism has been observed in polycrystalline samples of manganese and cobalt carbonates.[1] The antiferromagnetism of $MnCO_3$ has been confirmed directly by means of neutron diffraction.[2] A detailed theoretical investigation by Dzyaloshinskiĭ[3] and the study of the magnetic properties of $MnCO_3$ single crystals[4] have revealed several interesting properties of antiferromagnets possessing weak ferromagnetism.

The character of the orbital level splitting of the cobalt ion in the crystalline field results in a large value for the anisotropy energy that is due to spin-orbit interaction. A detailed investigation of weak ferromagnetism in a $CoCO_3$ single crystal was therefore of interest, since the spin-orbit interaction is responsible for this weak ferromagnetism[5,6] and larger effects could be expected together with the appearance of finer details. It was also important to verify an earlier conclusion[4] that the existing theory of spin waves requires correction.

2. APPARATUS AND SAMPLES

The magnetic moments of the samples were measured by the Faraday technique using the magnetic balance that is described in reference 7. The apparatus was improved in two ways.* Oil damping of the balance was replaced by an electronic technique. In order to correct for the torsion of the sample, which was attached to the balance arm by means of a quartz fiber, a device for measuring the angle of rotation was positioned around the vertical axis. This is very important for corrections in measuring the magnetic susceptibility of $CoCO_3$ along the trigonal axis, since the very large anisotropy of magnetic properties in this case results in rotations up to 3°.

Measurements were performed on single crystals grown hydrothermally by N. Yu. Ikornikova of the Institute of Crystallography, Academy of Sciences U.S.S.R. Cobalt carbonate is isomorphic with $MnCO_3$ and possesses a rhombohedral structure with two ions in its unit cell. Each crystal was a smooth hexagonal plate with its plane perpendicular to the trigonal z axis (all notation agrees with reference 4). It was therefore not difficult to orient the crystal with respect to its axis of suspension.

3. RESULTS

The principal measurements were performed on a 0.47-mg crystal distinguished by good uni-

---

*The final form of the magnetic balance is described in detail in reference 6.

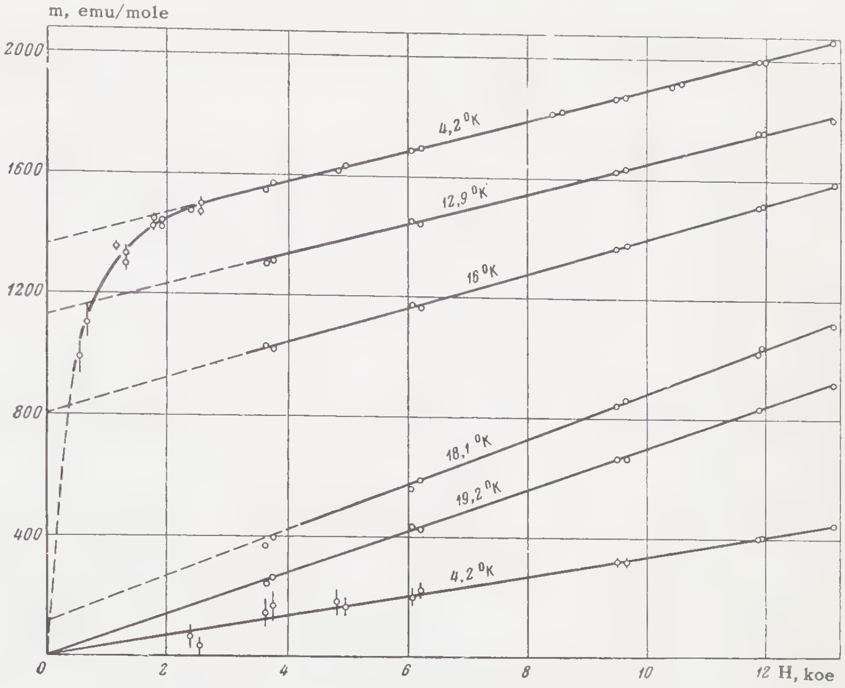

FIG. 1. The molar magnetic moment m as a function of magnetic field strength H for several temperatures: the five upper curves for $H \perp z$, the lowest curve for $H \parallel z$.

formity, while another crystal weighing 0.61 mg was used for a few control measurements. The absolute molar magnetic properties of the two crystals differed by 9%, which is included in the estimate of absolute experimental accuracy. All graphs shown below pertain to the 0.47-mg crystal, while the absolute values of constants in the text are averages for the two crystals.

As in the case of $MnCO_3$, measurements performed with the z axis of the samples parallel to the direction of suspension revealed no magnetic anisotropy in the basal plane. We therefore conclude, as in reference 4, that the anisotropy field for directions lying in the basal plane does not exceed 200 oe. Magnetic properties in a plane passing through the trigonal axis are shown in Figs. 1—4.

Figure 1 shows the measurements of the magnetic moment m as a function of the applied field H at several temperatures. It should be noted that when $m_\perp$ was measured (with the field in the basal plane) the demagnetizing factor was zero, since the crystal plate was quite thin. The correction resulting from the demagnetizing factor ($\sim 4\pi$) in measurements of $m_\parallel$ (with the field perpendicular to the plate) amounts to ~1% of the measured moment at T = 1.3°K and decreases with decreasing $\chi_\parallel$. The torsion correction of $m_\parallel(H)$ was obtained from measurements of $\sigma_\perp$, $\chi_\perp$, H and the torsion angle. Figure 1 shows that for $H > 2$ koe the field dependence of the magnetic moments when $T < T_N = 18.1$°K may be represented by

$$m_\perp(H, T) = \sigma(T) + \chi_\perp(T) H_\perp; \qquad (1)$$

$$m_\parallel(H, T) = \chi_\parallel(T) H_\parallel. \qquad (2)$$

Figure 2 shows how the projection m_H of the moment on the magnetic field direction depends on the angle between the field and the z axis. The solid curve, which was plotted assuming (1) and (2) to be valid for all field directions, is in good agreement with experiment; this indicates that the spontaneous moment σ always remains in the basal plane.

It must be mentioned that balance readings along the z axis in weak and moderate fields at $T \leq 16$°K were very unsteady and that reproducibility was much less satisfactory than for measurements in the basal plane. We can therefore not arrive at a decision regarding the existence of

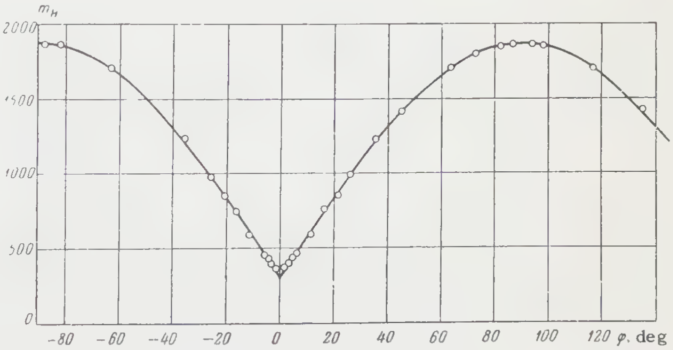

FIG. 2. Angular dependence of the projection of the moment on the magnetic field direction in the yz plane for H = 9480 oe and T = 4.2°K. φ is the angle between the field and the z axis. The solid curve is a plot of $m(\varphi) = \chi_\parallel H + \sigma|\sin\varphi| + (\chi_\perp \chi_\parallel) H \sin^2\varphi$.

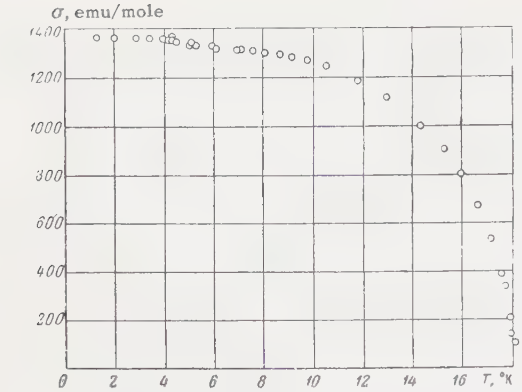

FIG. 3. Temperature dependence of the spontaneous ferromagnetic moment σ: $T_N = (18.1 \pm 0.1)$°K; $\sigma_0 = (1440 \pm 75)$ cgs electromagnetic units per mole (average for the two crystals).

any anomaly of $m_{||}(H)$ such as was detected for $MnCO_3$.[4]

Our experimental accuracy permits the statement that the spontaneous moment in the z direction does not exceed 25 cgs electromagnetic units per mole.

Curves similar to those in Fig. 1 were obtained for a considerable number of temperatures between 1.3 and 19°K and were treated graphically in order to yield values of $\sigma(T)$, $\chi_\perp(T)$ and $\chi_{||}(T)$. In the 1.3–8°K region, $\sigma(T)$ and $\chi_\perp(T)$ were calculated from experimental data by least squares. The accuracy of $\sigma(T)$ values was ±0.6%. Anomalous behavior of $\sigma(T)$ was observed below 6°K (Fig.3). In order to verify whether the relatively sharp change of $\sigma(T)$ near 4.2°K is associated with the change in the methods of maintaining temperatures above and below the helium boiling point, we performed a control experiment in which heating began in a bath at 2.8°K. The anomalous region of $\sigma(T)$ was not affected.

Figure 4 shows values of $\chi_\perp(T)$ and $\chi_{||}(T)$, relative measurements of which below 100°K were obtained with about 0.4% accuracy. At room temperature this was reduced to 1 and 1.5%, respectively, because of lower susceptibility. Fig. 4b shows that in the 50-300°K region $\chi_\perp$ obeys the Curie-Weiss law

$$\chi_\perp = C_\perp/(T-\Theta_\perp), \qquad (3)$$

where $C_\perp = 3.80 \pm 0.18$* and $\Theta_\perp = -48 \pm 1°$. The behavior of $\chi_{||}(T)$ above 100°K can be described by the same law with $C_{||} = 4.00 \pm 0.25$ and $\Theta_{||} = -215 \pm 5°$. The behavior of the principal susceptibilities at the transition point (Fig. 4a) exhibits a pronounced peak of $\chi_\perp(T)$ and relatively little change of $\chi_{||}(T)$.

We are aware of two previous studies of the magnetic properties of $CoCO_3$ at low temperatures,[1,8] in which polycrystalline samples were used. For a comparison with their results, above T_N we calculated $\chi_p = \frac{2}{3}\chi_\perp + \frac{1}{3}\chi_{||}$ from our data. Because of small $\chi_{||}$ it appears that χ_p is also satisfactorily described by the Curie-Weiss law (3) with $C_p = 3.6$ and $\Theta_p = -63$°K. C_p is ~10% greater in reference 1 and ~15% smaller in reference 8 than in the present work. The agreement with reference 1 may be considered satisfactory if we take into account the authors' statement that their absolute values for χ may have been reduced by ~10% because of nonmagnetic impurities. It is difficult to make a quantitative comparison with the results obtained by Bizette,[8] who does not state the experimental values nor estimate the experimental error and sample purity. However, there is clear qualitative agreement.

Bizette gives data only for temperatures above T_N. As already mentioned, the transition of $CoCO_3$ to an antiferromagnetic state with weak ferromagnetism was first observed by one of the present authors and Orlova.[1] A small discrepancy in determining T_N (~0.5°) may be associated with insufficient accuracy of thermocouple temperatures in reference 1, where measurements were confined to a very small temperature interval below T_N, so that values of σ cannot be compared.

4. DISCUSSION OF RESULTS. DEVELOPMENT OF THE THERMODYNAMIC THEORY OF WEAK FERROMAGNETISM

1. In agreement with preliminary results obtained using polycrystalline samples[1] and with thermodynamic theory,[3] our results have established that a $CoCO_3$ single crystal becomes antiferromagnetic with weak ferromagnetism below $T_N = 18.1$°K. As in the case of $MnCO_3$,[4] the ferromagnetic moment σ always remains in the basal plane but is almost 10 times larger than in $MnCO_3$. For $T \to 0$ we have $\sigma \to 1440$ cgs emu/mole. Differences in the behavior of the two crystals will be discussed in detail below.

2. In the paramagnetic region ($T \gg T_0$) the susceptibility of $CoCO_3$ exhibits very large anisotropy (~30% at T = 300°K). Anomalously large anisotropy has also been observed in other cobalt compounds, both in the case of a strong exchange interaction (CoF_2, $CoSO_4$) and in the case of dilute salts with weak interaction. In a number of theoretical papers (such as reference 9) this anisotropy has been attributed to the anomalous splitting of the orbital septet in the ground state

---

*Values are given here and hereafter in cgs electromagnetic units per mole.

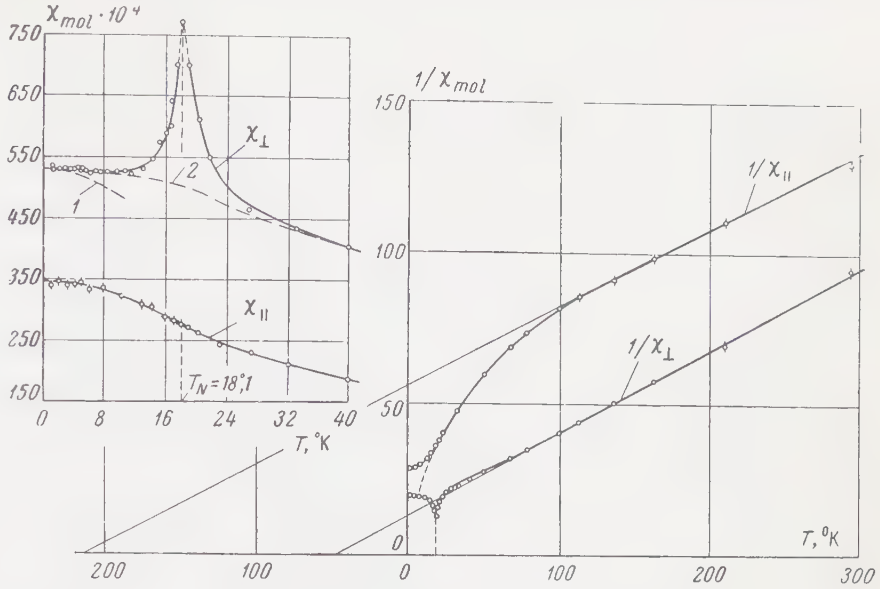

FIG. 4. Temperature dependence of the magnetic susceptibility of $CoCO_3$ in the paramagnetic and antiferromagnetic states. Curve 1 – from spin-wave theory; curve 2 – smooth interpolation through the transition region.

($^4F_{9/2}$) of a free cobalt ion in the crystalline field. It was assumed that, in contrast with other ions of the iron group, in first approximation (a cubic field) when splitting into a singlet and two triplets occurs, a triplet level is split by the axially approximation this level is split by the axially symmetric crystalline field and spin-orbit interaction into six Kramers doublets. The specific scheme of these doublets should account for the following experimental features which we observed in the behavior of $\chi_\perp$ and $\chi_{\|}$: the large difference between $\Theta_{\|}$ and $\Theta_\perp$, the approximate equality of $C_{\|}$ and $C_\perp$ above 100°K and the sharp departure of $\chi_{\|}$ from the Curie-Weiss law below 100°K. However, these experimental facts are insufficient for determining the level scheme uniquely. In any event it is evident that the orbital moment makes a large anisotropic contribution to the magnetic properties of $CoCO_3$.

3. At very low temperatures ($T \ll T_N$) it is interesting to compare our results with spin-wave theory. The phenomenological theory of spin waves as applied to rhombohedral antiferromagnetics with weak ferromagnetism [4,10] yields the following conclusions. In this case the spin-wave spectrum consists of two branches, one of which exhibits the energy gap $kT_{AE} = \mu\sqrt{2H_AH_E}$ (H_A and H_E are the effective fields of anisotropy and spatial interaction, respectively). The other branch contains no gap and in the absence of an external field is of the phonon type. When $T \ll T_{AE}$ only the latter branch is excited. For the temperature dependence of σ and $\chi_\perp$ we then obtain

$$\sigma = \sigma_0\{1-\eta(T/T_N)^2\}, \qquad \chi_\perp = \chi^0_\perp\{1-2\eta(T/T_N)^2\}. \quad (4)$$

When $T \gg T_{AE}$ both branches are excited. The law for the variation of $\chi_\perp$ then remains unchanged, but σ begins to decrease twice as rapidly:

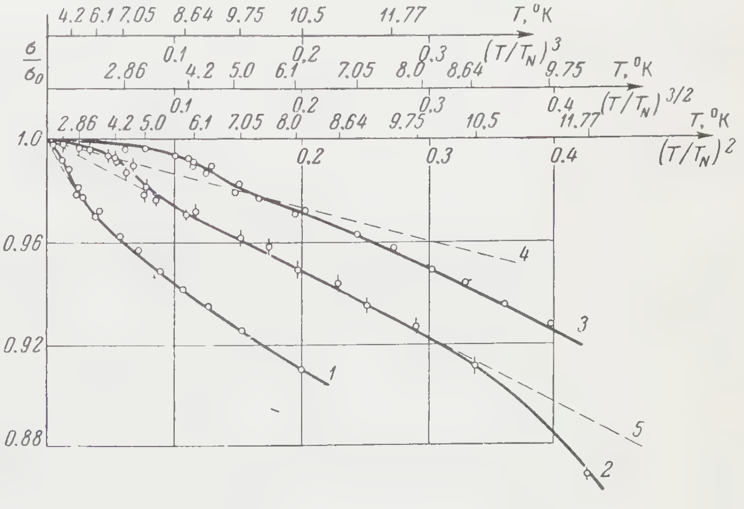

FIG. 5. Dependence of the relative ferromagnetic moment σ/σ_0 on the reduced temperature T/T_N. Curve 1 – for the cubic scale; curves 2, 4, 5 – for the quadratic scale; curve 3 – for the 3/2 scale. Curves 4 and 5 are theoretical spin-wave plots [see (4) and (5)].

$$\sigma = \sigma_0 \{1 - 2\eta (T/T_N)^2\} \text{ for } T_{AE} \ll T \ll T_N. \quad (5)$$

In the region of $T \sim T_{AE}$ an anomaly associated with the transition from (4) to (5) should appear in the behavior of $\sigma(T)$. In the case of $MnCO_3$ this region was below the investigated temperatures ($T_{AE} < 1.5°K$).[4] In the case of $CoCO_3$ the transition region was in the accessible temperature range, as is shown in Fig. 5, where the experimental behavior of σ/σ_0 is compared with (4) and (5). The values of σ/σ_0 are plotted for three temperature scales — cubic, quadratic and semicubic. For 5—10°K, in agreement with (5), the experimental points fit well on a straight line passing through the point (0;1) only for the quadratic scale. This was used to determine $2\eta = 0.26 \pm 0.2$ in (5). In the vicinity of 4.5°K the temperature dependence of σ/σ_0 exhibits the changed behavior that is predicted by theory for the T_{AE} region. Thus $T_{AE} \sim 4°K$ for $CoCO_3$. Our experiments were insufficiently accurate to confirm that at lower temperatures σ/σ_0 approaches unity in accordance with the first equation in (4) (curve 4 in Fig. 6). However, there is no experimental disagreement with this equation.

Figure 4a compares the experimental behavior of $\chi_\perp(T)$ with the second equation in (4) (curve 1). As in the case of $MnCO_3$, experimental values of $\chi_\perp$ do not fall off as rapidly as is required by the spin-wave theory. The results obtained for $CoCO_3$ confirm our earlier conclusion that the existing theory of spin waves is incomplete.[4]

4. Our most interesting result is the broad high peak of $\chi_\perp(T)$ in the vicinity of T_N, similar to that observed for $MnCO_3$,[4] although the latter peak was very small. As already stated, $CoCO_3$ is distinguished by an unusually large contribution of the spin-orbit interaction to the anisotropy energy. This is confirmed by the large ferromagnetic moment σ; it was shown in references 5 and 6 that the dipole interaction does not produce weak ferromagnetism in rhombohedral structures. The thermodynamic theory will be used below to show that the broad peak of the perpendicular susceptibility is also associated with large anisotropy energy.

5. According to the thermodynamic theory of antiferromagnetism,[3] the thermodynamic potential for rhombohedral crystals such as $MnCO_3$ and $CoCO_3$ (symmetry group D_{3d}^6) near the transition point is

$$\tilde{\Phi} = \tfrac{1}{2}(Al^2 + Bm^2 + al_z^2 + bm_z) + \beta(l_x m_y - l_y m_x) + \tfrac{1}{4}Cl^4 + \tfrac{1}{2}Dl^2m^2 - \mathbf{m}\mathbf{H}. \quad (6)$$

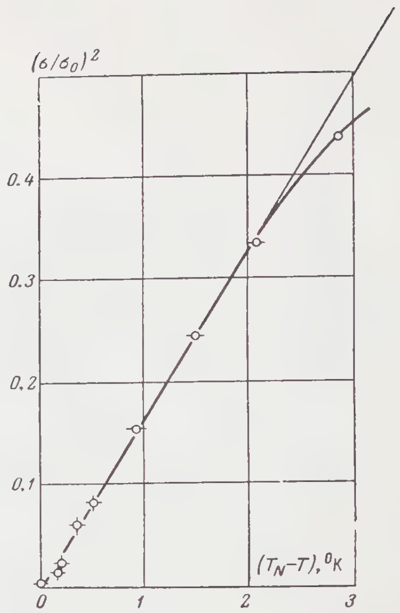

FIG. 6. Temperature dependence of the square of relative spontaneous magnetization near the transition point.

Here $\mathbf{l} = \mathbf{M}_1 - \mathbf{M}_2$ is the antiferromagnetic vector, $\mathbf{m} = \mathbf{M}_1 + \mathbf{M}_2$ is the magnetic moment of the crystal, and $\mathbf{M}_1$ and $\mathbf{M}_2$ are the magnetizations of the sublattices.

We shall hereinafter be interested only in the state with weak ferromagnetism where $\mathbf{l}$ lies in the basal plane ($a > 0$). Dzyaloshinskiĭ has shown[3] that when not too small magnetic fields $\mathbf{H}$ are applied to the basal plane* we always have $\mathbf{l} \perp \mathbf{m}$ and $\mathbf{m} \parallel \mathbf{H}$, so that the thermodynamic potential can be expressed, without affecting its generality, as

$$\tilde{\Phi} = \tfrac{1}{2}Al^2 + \tfrac{1}{4}Cl^4 + \tfrac{1}{2}Bm^2 - \beta m l - mH^{\dagger}. \quad (7)$$

We have here omitted the term $\frac{1}{2}Dl^2m^2$ which would change $\chi_\perp$ by only a few percent,[4] whereas the anomaly of interest amounts to some tens percent.

In the absence of a magnetic field ($H = 0$) the conditions for minimizing $\tilde{\Phi}$ are

$$\partial\tilde{\Phi}/\partial l = Al - \beta m + Cl^3 = 0,$$
$$\partial\tilde{\Phi}/\partial m = -\beta l + Bm = 0, \quad (8)$$

which show that the temperature for a transition to an ordered state ($l \neq 0$; $m \neq 0$) is determined by the condition that the determinant of equations which are homogeneous in l and m shall equal zero: $AB - \beta^2 = 0$. Near T_N we therefore have, as usual,

---

*For $\chi_\parallel$ our subsequent consideration of the anisotropy energy (β) leads to no new result; therefore the equations in references 3 and 4 for the temperature dependence of $\chi_\parallel$ remain valid.

†In a state of equilibrium the relative orientation of the vectors $\mathbf{l}$ and $\mathbf{m}$ is such that the term $-\beta\mathbf{m}\mathbf{l}$ is always less than zero.

$$A - \beta^2/B = \nu(T - T_N). \tag{9}$$

In Dzyaloshinskiĭ's calculations[3] the term βm in (8) was omitted and the condition for the transition to the antiferromagnetic state was $A = 0$. Inclusion of this term is seen to shift the transition point by the amount $\beta^2/\nu B$. In the case of $CoCO_3$ estimates of the coefficients (see below) show that this shift amounts to ~0.5°.

6. It is more important to include the same term in the presence of a magnetic field ($H \neq 0$), in which case the minimization of $\tilde{\Phi}$ is represented by

$$Al - \beta m + Cl^3 = 0, \qquad -\beta l + Bm = H. \tag{10}$$

When $T > T_N$ we have small l and the term Cl^3 may be neglected if T is not too close to T_N (the range of applicability of this approximation is given below). In view of (9) solutions of (10) then provide formulas for the temperature and field dependencies of l and m:

$$l = \beta H / B\nu(T - T_N), \tag{11}$$

$$m = [1/B + \beta^2/B^2\nu(T - T_N)]H. \tag{12}$$

(11) shows that in the given case antiferromagnetic ordering is induced by a magnetic field even above T_N. For antiferromagnets with weak ferromagnetism, as for exchange ferromagnets, T_N is therefore an isolated second-order transition point in the H—T plane.

(12) shows that the magnetic moment m varies linearly with the field, but $\chi_\perp$ must increase steeply as T_N is approached.

7. For $T < T_N$ antiferromagnetic ordering exists in the absence of a field, so that the term Cl^3 cannot be neglected. The second equation in (10) gives

$$m = (\beta l + H)/B, \tag{13}$$

and after substitution for m in the first equation we obtain the following cubic equation in l:

$$BCl^3 + B\nu(T - T_N)l - \beta H = 0. \tag{14}$$

The zeroth approximation in β, as in the absence of a field, gives

$$l_0^2 = (\nu/C)(T_N - T). \tag{15}$$

The first approximation for l will be sought in the form $l = l_0 + X\beta$. Assuming a weak field (see below) and dropping terms containing β^2 and β^3, after substitution in (14) we obtain

$$l = [(\nu/C)(T_N - T)]^{1/2} + \beta H/2B\nu(T_N - T). \tag{16}$$

Thus a field here also increases antiferromagnetic ordering.

With the dependence of l on H and T known, (13) gives for m the same formula containing the spontaneous moment as in reference 3:

$$m = \sigma + \chi_\perp H, \tag{17}$$

where

$$\sigma = \beta l_0/B = [\beta^2\nu(T_N - T)/B^2C]^{1/2}, \tag{18}$$

$$\chi_\perp = 1/B + \beta^2/2B^2\nu(T_N - T). \tag{19}$$

The temperature dependence of σ is the same as in reference 3. However, (12) and (19) show that magnetically induced ordering results in equations that predict a sharp rise of $\chi_\perp$ as T_N is approached from either direction.

8. As already indicated, the equations derived above are valid for not very strong fields and at temperatures that are close but not too close to the transition temperature [so that (8) and (9) will hold true]. The limitation on the closeness to T_N is associated with the necessity of observing the inequality $Cl^3 \ll \beta H/B$ (for $T > T_N$) and the possibility of dropping terms containing β^2 and β^3 in solving (14) (for $T < T_N$). The estimates of the interval ΔT near T_N where the derived equations cease to be satisfied almost coincide in both instances at the value

$$\Delta T \approx (\beta^2 CH^2/B^2\nu^3)^{1/3}.$$

Using the values of the expansion coefficients given below, we obtain $\Delta T \approx 0.5°$ for the maximum applied fields. For $|T - T_N| \lesssim \Delta T$ the expression for l contains terms which leave the derivative $\partial m/\partial H$ in T_N finite and lead to the field dependence of $\chi_\perp$.

9. Good qualitative agreement is found between the experimental temperature dependence of $\chi_\perp$ (Fig. 4a) and (12) and (19). For the purpose of a rough quantitative comparison we interpolated a curve which smooths out the peak at T_N (curve 2 in Fig. 4a), and plotted the temperature dependence of the reciprocal of $\Delta\chi = \chi_\perp - (\chi_\perp)_{\text{interp}}$. The resulting points could be satisfied by two straight lines intersecting at T_N, with slopes differing by a factor of about 2 in accordance with theory. This led to the estimate $(B^2/\beta^2)\nu = 40$.

The experimental temperature dependence of σ near T_N and a plot of (18) are shown in Fig. 6. $(\sigma/\sigma_0)^2$ is seen to depend linearly on $T_N - T$ up to ~2.5° from T_N and down to $\sigma/\sigma_0 \sim 0.6$. We thus determine $\xi = \beta^2\nu T_N/B^2 l\sigma_0^2 = 3.0$.

The foregoing experimental results enabled us

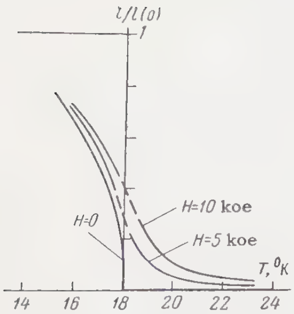

FIG. 7. Theoretical dependence of the antiferromagnetic vector l on T and H near T_N (the transition point in zero field).

to estimate the expansion coefficients of the thermodynamic potential (7): $B = 18$; $\beta = 1.5$; $\nu = 0.25$; $C = 4.5 \times 10^{-9}$. In calculating β we assumed that at $T = 0°K$ we have $l_0 = 16.75 \times 10^3$ (only the spin moment).

10. The values obtained for the coefficients permit a quantitative estimate of the antiferromagnetic ordering induced in $CoCO_3$ by an applied magnetic field. Figure 7 shows the temperature dependence of relative magnetization in antiferromagnetic sublattices for different fields as calculated according to (11) and (16). An effect of considerable magnitude should be exhibited by $CoCO_3$ in relatively weak fields and could presumably be detected directly by either the neutron diffraction or nuclear resonance technique for measuring antiferromagnetic ordering.

The authors are very grateful to Academician P. L. Kapitza for his continued interest, and also wish to thank I. E. Dzyaloshinskiĭ for valuable discussions, N. M. Kreĭnes for methodological discussions and N. Yu. Ikornikova for preparation of the single crystals. The experimental assistance of V. I. Kolokol'nikov is also gratefully acknowledged.

---

[1] A. S. Borovik-Romanov and M. P. Orlova, JETP **31**, 579 (1956), Soviet Phys. JETP **4**, 531 (1957).

[2] P. A. Alikhanov, JETP **36**, 1690 (1959), Soviet Phys. JETP **9**, 1204 (1959).

[3] I. E. Dzyaloshinskiĭ, JETP **32**, 1547 (1957), Soviet Phys. JETP **5**, 1259 (1957).

[4] A. S. Borovik-Romanov, JETP **36**, 766 (1959), Soviet Phys. JETP **9**, 539 (1959).

[5] F. Bertaut, Compt. rend. **246**, 335 (1958).

[6] A. S. Borovik-Romanov, Dissertation, Institute for Physical Problems, Acad. Sci. U.S.S.R., 1959.

[7] A. S. Borovik-Romanov and N. M. Kreĭnes, JETP **29**, 790 (1955), Soviet Phys. JETP **2**, 657 (1956).

[8] H. Bizette, Ann. phys. **1**, 233 (1946).

[9] A. Abragam and M. H. L. Pryce, Proc. Roy. Soc. (London) **A206**, 173 (1951).

[10] E. A. Turov, JETP **36**, 1254 (1959), Soviet Phys. JETP **9**, 890 (1959).

Translated by I. Emin
6

SOVIET PHYSICS JETP VOLUME 12, NUMBER 1 JANUARY, 1961

TEMPERATURE DEPENDENCE OF THE MAGNETIC SUSCEPTIBILITY OF INDIUM, LEAD, AND TIN CRYSTALS

B. N. ALEKSANDROV, B. I. VERKIN, and I. V. SVECHKAREV

Physico-Technical Institute, Academy of Sciences, Ukrainian S.S.R.

Submitted to JETP editor February 13, 1960

J. Exptl. Theoret. Phys. (U.S.S.R.) **39**, 37-43 (July, 1960)

A new version of the Faraday method is proposed for measuring the magnetic susceptibility of In, Pb, and Sn crystals in the range from room temperature to 20.4°K. The $\chi(T)$ curves thus obtained are characteristic of the whole group of elements which exhibit the long-period de Haas—van Alphen effect. This indicates the existence of small electron groups.

ATTEMPTS to classify magnetic substances by the sign of their experimentally-measured susceptibility have not been able to reveal sufficiently the connection between the magnetic properties and the nature of the solid state of the elements. The measured susceptibility is the sum of several terms

$$\chi_{\text{exp}} = \chi_{\text{ion}}^{\text{para}} + \chi_{\text{ion}}^{\text{dia}} + \chi_{\text{el}}^{\text{para}} + \chi_{\text{el}}^{\text{dia}} \qquad (1)$$

and its sign does not unambiguously determine which of the terms plays the largest part.

A systematic study of the de Haas—van Alphen effect,[1] and an investigation of the experimental data on the temperature dependence of the susceptibility of elements have made it possible to propose a new classification of magnetic substances,[2] based on the nature of the temperature dependence of their susceptibility. Such a classification also allows to determine the term which is mainly responsible for the magnetic properties, which turn out to be closely related to the place the element occupies in the periodic table. Thus, elements which exhibit the de Haas— van Alphen effect in normal fields form a single group in the long periodic system. The investigation of highly purified elements of this group to date — Bi (reference 3), Sb (reference 4), Zn (reference 5), Cd (reference 6), graphite (reference 7), and Ga (reference 8) — discloses (contrary to existing opinion), a considerable increase of diamagnetism with decreasing temperature, at least in certain directions.

The temperature dependence of the susceptibility of these elements is probably connected with the presence of small groups of electrons, and should consequently be characteristic of all elements exhibiting a long-period de Haas—van Alphen effect.[2] In order to check this assumption, we have investigated the temperature dependence of the magnetic susceptibility of three pure metals of cubic and tetragonal structure belonging to this group: Pb, I, and Sn.

PREPARATION OF THE SPECIMENS

Spherically shaped single crystals were grown in glass ampules by Bridgeman's method. The glass was removed by dipping in fluoric acid. The contaminated layer of the specimens was then removed with the aid of suitable pickling solutions, and the reflecting planes appeared. The orientation of the single crystal was determined with the aid of a two-dial Chapskiĭ goniometer.[10] A small quartz sleeve was attached to the specimen with Zapon lacquer on the goniometer stage, to make the shoulder produced by the center of gravity of the crystal relative to the length of the sleeve coincide with the chosen crystallographic direction. This was the direction along which the susceptibility of the specimen was measured.

The purity of the investigated metals was characterized by the ratio $\delta = R_{4.2°\text{K}}/R_{\text{room}}$, where $R_{4.2°\text{K}}$, is the electric resistance at a temperature of 4.2°K, and R_{room} is the resistance at room temperature.

We prepared and investigated: a) one tin specimen of high purity, obtained in the laboratory by repeated zone recrystallization and prolonged heating in vacuum;[11] the value of δ of this specimen was 1.8×10^{-5}; b) two lead specimens of the firm "Kalbaum" with $\delta = 5.4 \times 10^{-5}$; c) two indium specimens with $\delta = 1.2 \times 10^{-4}$. The mass of the specimens was 0.35 – 0.5 g.

EXPERIMENTAL METHOD AND APPARATUS

The principal values of the susceptibility were measured on a modified torsion balance by the

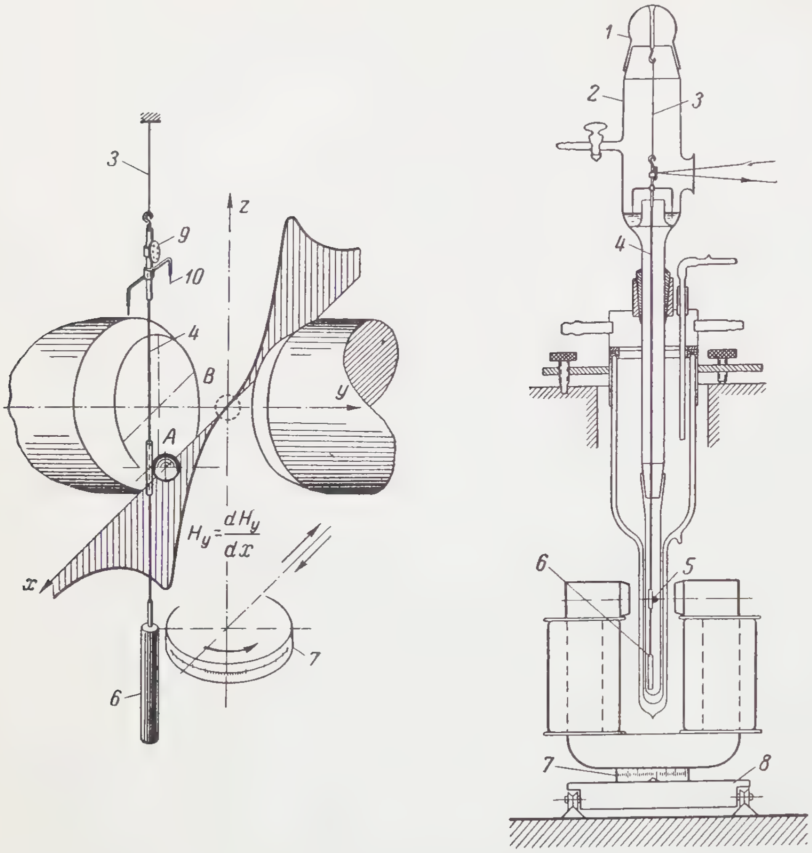

FIG. 1. Diagram of the apparatus and the position of the specimen in the magnetic field.

Faraday method (Fig. 1).

A system consisting of a small mirror 9, a damper 10, and a quartz rod 4, was suspended from the glass portion 2 of the apparatus by means of an elastic metal thread 3; a quartz sleeve with the specimen 5 was tightly fitted over the quartz rod. By displacing the electromagnet on the carriage 8, by a suitable pasting of the sleeve with the specimen, and by a rotation of the cap 1, the sample was placed level with the centers of the pole pieces and remained equidistant from them when the carriage with the magnet was displaced along the rails. The investigated crystallographic axis (and consequently also the "shoulder") were directed along the field. Thus, the specimen was only acted upon by the field gradient in the direction of the x axis. A cylindrical weight 6 fixed the quartz rod as the axis of rotation of the suspended system. The weight was prepared of extremely pure polycrystalline tin (so that it had a small susceptibility and anisotropy), and was placed in a very weak field; it practically introduced no distortion in the reading of the instrument. The force acting upon the specimen in an inhomogeneous field was applied to the shoulder 1 formed as a result of the eccentric position of the sample relative to the axis of rotation, and produced a twisting torque balanced by the elasticity of the metallic thread. The angle of rotation of the suspended system was determined with the aid of a mirror and a scale. In equilibrium

$$k\varphi = m\chi l H_y \, dH_y/dx, \tag{2}$$

where φ is the angle of rotation of the mirror, and k is the elastic modulus of the thread. The measurements were conducted by a relative method at the point A of the field where $H_y dH_y/dx$ had a maximum value; point A was found by displacing the electromagnet along the rails until a maximum deviation for a given magnet current was obtained.

In this case

$$\chi = \chi_0 (m_0 l_0 k / m l k_0)(\alpha/\alpha_0), \tag{3}$$

where the quantitites with the zero subscript refer to the standard substance, and those without a subscript to the investigated substance; the ratio α/α_0 is taken with an equal current flowing through the magnet. Twice-distilled water in a spherical glass ampule, whose dimensions differed little from those of the investigated specimens, served as the standard substance. The calibration consisted of recording the dependence of the deflection of the pointer along the scale on the current flowing through the magnet at points in which

$H_y dH_y/dx$ was a maximum, and averaging it over the following four positions of the ampule: a) on both sides of the pole pieces; b) in the same positions after the sleeve with the ampule has been turned through 180°. Such averaging allows to exclude the weak anisotropy of the suspended system, and the change in the magnitude of the "shoulder" due to a possible small bend of the quartz rod and also due to the possibility that the rod and the centering weight 6 do not have a common axis. The ampule was dried by evacuating the instrument, and an analogous dependence was recorded for the empty ampule. The true deflections for water were found by subtracting the curves. The specific susceptibility of water was taken to be 0.720 $cm^3/gauss$.

The measurements of the absolute values of the susceptibility of the samples and its temperature dependence were conducted in the same way as the calibration. The effect of the medium was excluded by evacuating the instrument and filling it with hydrogen at a low pressure.

The method which was used allowed to determine, in a single experiment, both one of the principal values of the susceptibility and its anisotropy in the xy plane, by bringing the crystal into a region of homogeneous field (point B). When the crystal was mounted so that the above plane contained its principal crystallographic axis, then the angle of rotation of the suspended system due to the orienting action of the field was

$$\varphi = (mH^2 \sin 2\theta / 2k)(\chi_\parallel - \chi_\perp), \tag{4}$$

where θ is the angle between the principal axis and the direction of the field (the magnet was free to rotate about the z axis, the angles of rotation were read on dial 7).

The mass of the crystal was determined by weighing, while the shoulder position relative to the axis of the sleeve was measured with a comparator; a correction was introduced for the commensurability of the mass of the crystal (0.5 g) and the fixing weight (4 g), because of which the axis of rotation did not coincide with the rod 4. Thin tungsten wires with diameters 0.05 and 0.03 mm and elastic moduli 6.44 and 0.844 dyne-cm/rad respectively were used as elastic threads.

In the course of the measurements we tried a quasi-elastic bifilar suspension; the idea is that during a rotation of a system suspended on two parallel threads there appears a weight component tending to return the system to its previous position. An elementary calculation shows that the elastic modulus of such a suspension (neglecting the elasticity of the threads) is

$$k = Pd^2/4L, \tag{5}$$

where P is the total weight of the suspended system, d the distance between the threads, and L their length.

The bifilar suspension is exceptionally convenient for similar apparatus, because of the simplicity of its construction (a loop of thin wire was freely slipped on two hooks, one attached to a section of the instrument and the other to the suspended system), the excellent time-stability of the modulus and of the "null," its noncritical nature with respect to large angles of twist and strong overloading, and the possibility of using two current conductors.

The magnetic field was produced by an electromagnet with which it was possible to obtain in a 25-mm gap a field of about 5000 oe using a maximum current of 20 amp. The diameter of the pole pieces was 50 mm, and the angle of taper ~40°. The field was calibrated by the usual ballistic method.

The measurement precision of the absolute values of the susceptibility was 7%, of the anisotropy ~1.5% (a little worse for tin); the precision of the relative measurements was not worse than 0.5 to 1%.

The specimens were cooled with liquid CH_4, O_2, N_2, and H_2; a temperature of 64°K was obtained by pumping out the vapor above liquid nitrogen.

EXPERIMENTAL RESULTS

We have investigated the principal values of the susceptibility tensor of single crystals of In, Pb, and Sn in the above-mentioned temperature range. The corresponding values at room temperature are listed in the Table along with data of other authors from the literature.

(a) Indium. The temperature dependence of the magnetic susceptibility of indium is most typical for the majority of the elements belonging to the group of interest. The measured values of $\chi_\perp(T)$ and $\Delta\chi(T)$ of two specimens were in full agreement. The values of $\chi_\perp(T)$ and the calculated $\chi_\parallel(T)$ are shown in Fig. 2. $\chi_\perp$ increases by 20% as the temperature decreases from room temperature to 80°K, then, after passing through a maximum, it decreases; at $T = 20.4$°K it exceeds the value at room temperature by 15%. $\chi_\parallel$ increases monotonically up to 20°K by almost a factor of 3, and has a point of inflection at $T \sim 100$°K.

(b) Lead. The $\chi(T)$ and the anisotropy in the (110) plane of two lead specimens which showed excellent agreement were investigated. The susceptibility increases almost linearly with de-

Metal	Author and year of measurement	$\chi_{\parallel} \cdot 10^6$	$\chi_{\perp} \cdot 10^6$	$\Delta\chi \cdot 10^6$	Remarks
In	Verhaeghe,[12] 1950	0.1215	0.0545	0.067	
	Verkin,[13] 1950	—	—	0.107	$\delta=1{,}6 \cdot 10^{-3}$
	Schoenberg,[14] 1952	—	—	0.096	Precision ~15%
	Present work	0.158	0.078	0.080	
Pb	deHaas and van Alphen,[15] 1933	0.111	—	—	
	Rao,[16] 1936	0.107	—	—	
	Present work	0.114	—	—	
Sn	Hoge,[17] 1935	0.0241	0.0270	0.0029	
	Itterbeek,[18] 1957	0.026	—	—	Polycrystal
	Present work	0.026	0.029	0.0029	

creasing temperature down to 20.4°K by 20% (cf. Fig. 2); there is no anisotropy.

(c) Tin. Tin is unusual in the investigated group in that it has a positive susceptibility, and it was therefore interesting to find out whether it obeys the basic rules characteristic of this group as a whole. The results of reference 18 indicating a decrease of the susceptibility of tin with decreasing temperature are only of qualitative nature, since they cannot be related to given crystallographic axes.

We have studied the values of $\chi_{\perp}(T)$ along the normal to the (010) plane and $\Delta\chi(T)$ in the (100) plane. The obtained curve, and the calculated $\chi_{\parallel}(T)$ curve for a tin crystal are shown on Fig. 2. Unlike other elements, the absolute value of the susceptibility of tin decreases with decreasing temperature. A linear decrease of $\chi_{\parallel}$ by 6% is observed down to 20.4°K, $\chi_{\perp}$ decreases by 15%, but has a deflection towards the temperature axis (this is better seen in the temperature dependence of the anisotropy).

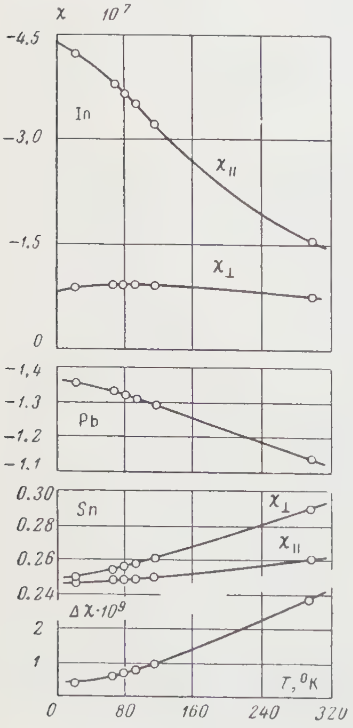

FIG. 2. Temperature dependence of the magnetic susceptibility of In, Pb, and Sn.

DISCUSSION OF THE RESULTS

The theory of the temperature dependence of the susceptibility which assumes that there exists one group of electrons with a quadratic dispersion law, yields the following expression for χ_{el}:[19,20]

$$\chi_{el} = \chi_0 f(T), \tag{6}$$

f(T) is a universal temperature function with the following asymptotic behavior:

$$T \ll E_0/k, \qquad f(T) = 1 - (\pi^2/12)(kT/E_0)^2,$$

$$T \gg E_0/k, \qquad f(T) = 2E_0/3kT. \tag{7}$$

χ_0 has the form:

$$\chi_0 = (\sqrt{2}\, e^2/6c^2 h\pi)\sqrt{E_0/m^*}\,[3(m^*/m)^2 - 1], \tag{8}$$

where E_0 is the limiting energy, m is the mass of the free electron, m* is its effective mass. The majority of the experimental $\chi(T)$ curves of the investigated elements (Figs. 2 and 3) can be described by the above formula if it is assumed that the limiting energies and effective masses of the electrons are anomalously small. The almost complete temperature independence of χ along some crystallographic directions in Cd, In, Sb, and C is apparently connected with the sharp anisotropy of the effective masses. These assumptions are in good agreement with the investigations of the de Haas—van Alphen effect.

Zil'berman and Itskovich[20] found the dependence $\chi(T)$ for cases where together with a small electron group there exists (a) a large electron group or (b) a large group of electrons and a large group of holes. The shapes of the curves are quite diverse; in particular, one can obtain a curve similar to the experimental curve obtained for Zn. However, near the temperature of degeneration of the small group, the form of the $\chi(T)$ curve is

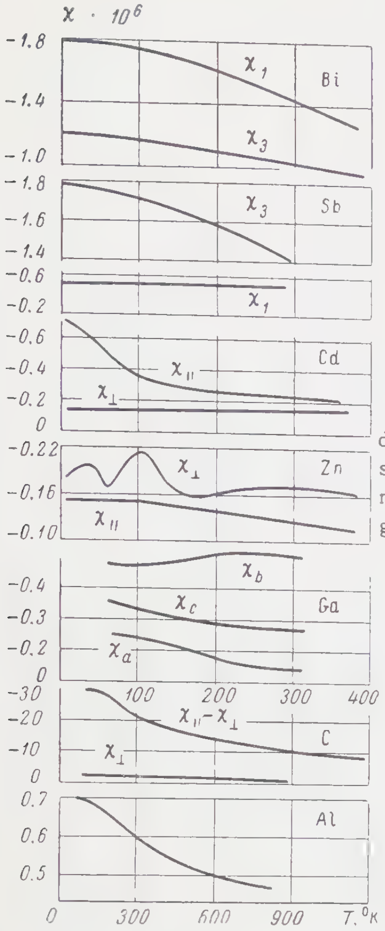

FIG. 3. The temperature dependence of the magnetic susceptibility of other elements in the investigated group (from the literature)

determined, as before, by the contribution due to this group.

The decrease of the absolute value of the susceptibility of tin with decreasing temperature can be explained either by the influence of the group of holes, or by the increase of the diamagnetism of the small electron group on a background of an anomalously large paramagnetic contribution of the main group, which is almost temperature independent in the investigated region. An unambiguous answer is possible on the basis of more complete information on the number and parameters of the groups of charge carriers, such as was obtained, for instance, from studies of the de Haas—van Alphen phenomenon. Making use of such data and of the corresponding theoretical relations, it was possible to plot $\chi(T)$ curves, and by comparing them with the experimental curves, to improve the precision of the zone structure and divide the groups into electrons and holes. However, the insufficient information makes a detailed quantitative comparison of theory and experiment difficult, and is one of the reasons of the discrepancy between them. Thus, the limiting energies of small groups of indium and cadmium found from the quantum oscillations of the values of χ (reference 14) exceed by more than a factor of 20 the values obtained from the $\chi_{\parallel}(T)$ curves (the limiting energy approximately corresponds to the point of inflection of the curve). The typical "electron" increase of paramagnetism with decreasing temperature in Al (reference 21) cannot be reconciled with the small effective mass of 0.08 m (reference 14), in spite of the fact that the agreement of the limiting energies (for the smaller groups) is good. Possibly the long-period oscillations of χ corresponding to these small groups have not been observed, and more careful studies of these elements are essential. The theory of the temperature dependence of the susceptibility is likewise in need of further development, since the quadratic dispersion law is in the majority of cases not even applicable to the small groups. Unfortunately, the possible peculiarities of the temperature dependence of χ, connected with the open Fermi surfaces of many metals of interest to us,[22] have as yet not been clarified.

Considering the nature of the anomalous groups, attention should be directed to the crystallochemical structure of the elements in the periodic table.[2,23] Here it is easy to follow the gradual transition from the purely metallic bonding forces on the left to the molecular forces in the crystals of the noble gases. Thus, the highly-compressible cubic structures of the so-called "ideal" (alkaline) metals are due to isotropic metallic bonds; the transition metals are characterized by an additional admixture of d-electron shells. The group of elements which exhibits the long-period de Haas—van Alphen effect is characterized by the largest diversity of simultaneously present types of bonding forces. These are mainly the layer-like (graphite, Bi, Sb, and As) and complex hexagonal (Be, Zn, and Cd) structures; metallic and covalent bonds are present within the layers, and van-der-Waals, metallic, and various intermediate bonds of a still unknown nature are active between the layers. The lattices, it can be seen, are extremely anisotropic with a small compressibility because of presence of forces which are highly sensitive to the spacing. Even the most symmetrical of these elements — lead, indium, and tin — have anomalously large lattice periods which indicate the presence of additional nonmetallic forces. A consistent account of the complex interactions in the lattices may possibly offer a natural explanation of the separation of the small charge-carrier groups.

The study of the temperature dependence of the susceptibility can serve as valuable supplementary information on the structure of the electron spectrum of the metals having such anomalous groups.

---

[1] Verkin, Lazarev, and Rudenko, JETP **20**, 93 (1950); JETP 21, 658 (1951); Dokl. Akad. Nauk SSSR 80, 45 (1951).

[2] B. I. Verkin, JETP 32, 156 (1957), Soviet Phys. JETP **5**, 117 (1957).

[3] D. Shoenberg and M. Z. Uddin, Proc. Roy. Soc. **A156**, 687, 701 (1936).

[4] D. Shoenberg and M. Z. Uddin, Proc. Cambr. Phil. Soc. 32, 499 (1936).

[5] J. A. Marcus, Phys. Rev. **76**, 413 (1949).

[6] J. A. Marcus, Phys. Rev. **76**, 621 (1949).

[7] K. S. Krishnan and N. Ganguli, Z.Krist. 100, 530 (1939).

[8] A. Marchand, Compt. rend. **241**, 468 (1955).

[9] Ya. G. Dorfman, Магнитные свойства и строение вещества (Magnetic Properties and the Structure of Matter) Gostekhizdat, 1955.

[10] B. I. Verkin and I. M. Dmitrenko, Izv. Akad. Nauk SSSR, Ser. Fiz. 19, 409 (1955), Columbia Tech. Transl. p. 365.

[11] B. N. Aleksandrov, Физика металлов и металловедение (Physics of Metals and Metallography) 9, 53 (1960).

[12] Verhaeghe, Vandermeersche, and LeCompte, Phys. Rev. 80, 758 (1950).

[13] Verkin, Lazarev, and Rudenko, JETP 20, 995 (1950).

[14] D. Shoenberg, Phil. Trans. Roy. Soc. **245**, 1, (1952).

[15] W. J. de Haas and P. M. van Alphen, Leid. Comm. 225b (1933).

[16] S. R. Rao and K. C. Subramaniam, Phil. Mag. 21, 609 (1936).

[17] H. J. Hoge, Phys. Rev. **48**, 615 (1935).

[18] A. van Itterbeek and W. Duchateau, Physica 23, 169 (1957).

[19] E. C. Stoner, Proc. Roy. Soc. **A152**, 672 (1935).

[20] G. E. Zil'berman and F. I. Itskovich, JETP 32, 158 (1957), Soviet Phys. JETP **5**, 119 (1957).

[21] R. Lingelbach and E. Vogt, Acta Met. **7**, 441 (1959).

[22] N. E. Alekseevskiĭ and Yu. P. Gaĭdukov, JETP 37, 672 (1959), Soviet Phys. JETP **10**, 481 (1960).

[23] G. B. Bokiĭ, Введение в кристаллохимию (Introduction to Crystal Chemistry) p. 243, 1954.

Translated by Z. Barnea
7

SOVIET PHYSICS JETP VOLUME 12, NUMBER 1 JANUARY, 1961

A POSSIBLE NEUTRAL CASCADE MESON DECAY

I. A. IVANOVSKAYA, E. V. KUZNETSOV, É. I. MAL'TSEV, A. PROKESH, G. M. STASHKOV, and I. V. CHUVILO

Joint Institute of Nuclear Studies

Submitted to JETP editor February 15, 1960

J. Exptl. Theoret. Phys. (U.S.S.R.) **39**, 44-46 (July, 1960)

An examination of 20000 photographs obtained by irradiating a xenon bubble chamber by a beam of 3-Bev/c negative π mesons revealed an event which can be interpreted as a decay of a heavy neutral meson according to the scheme

$$D^0 \to K^+ + \pi^- + Q.$$

The mass of this particle computed on the basis of the K^+ and π^- meson momenta was found to be $m_{D^0} = (660 \pm 50)$ Mev.

WANG Kang-chang and co-workers[1] and Sinha and Sengupta[2] observed during an investigation of cosmic radiation several events which were interpreted by the authors as the decay of a neutral particle according to the scheme

$$D^0 \to K^+ + \pi^- + Q, \tag{1}$$

where Q = 10 — 50 Mev. In this connection, an experiment involving high-energy accelerators to search for particles with analogous decay schemes would be of interest.

An examination of 20000 photographs obtained by irradiating the two-liter xenon bubble chamber of the Institute of Theoretical and Experimental Physics of the U.S.S.R. Academy of Sciences[3] in a beam of 3 Bev/c negative π mesons disclosed the

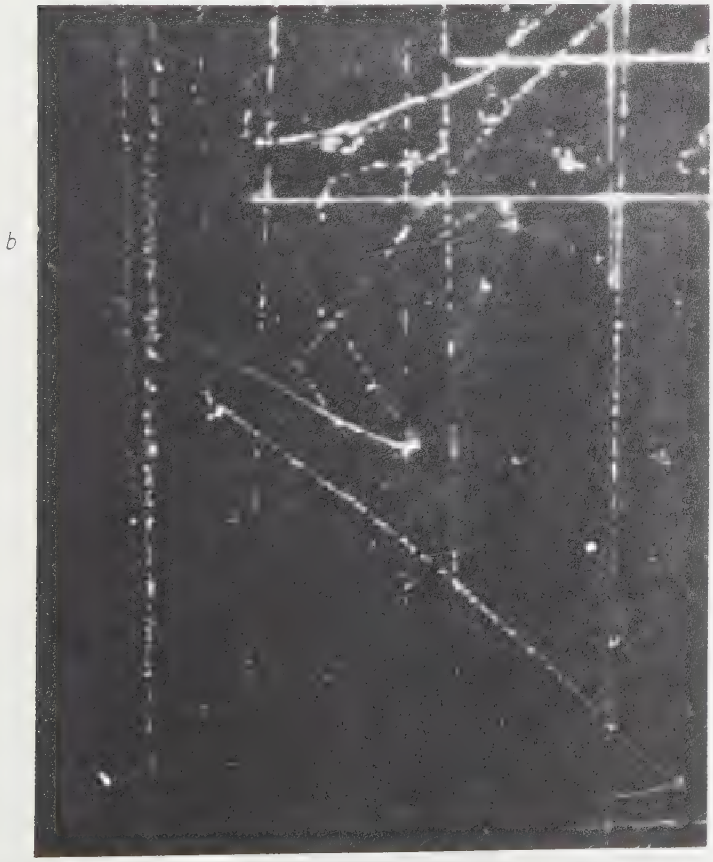

FIG. 1. Suggested decay of a heavy meson by the scheme $D^0 \to K^+ + \pi^-$. The point of decay is denoted by the letter b.

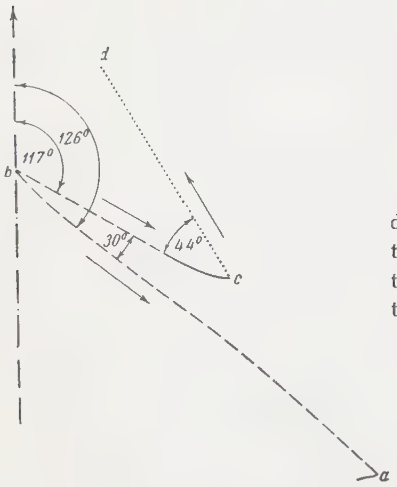

FIG. 2. Diagram of decay: bc – K⁺-meson track; cd – $\pi^+(\mu^+)$-meson track; ba – π^--meson track.

event shown in Fig. 1. The geometrical diagram is shown in Fig. 2. The direction of the primary beam is shown by the dash-dot arrow. Points a, b, c lie in the working volume. Track cd escapes into the glass.

The chamber was operated without a magnetic field. The identification of the particles was made by means of ionization and multiple scattering. The data of the measurements are given in the table. The errors shown in the table are statistical.

The mean values of $p\beta$ along the track were measured by the multiple-scattering method. The momentum p of the particle with track bc (henceforth referred to as particle "bc" etc.) was determined from its range, the remaining momenta were calculated from the $p\beta$ values.

The mass of particle "bc" was determined from the multiple scattering — residual range relation, the mass of particle "ba" was determined from the ionization — multiple scattering relation. The values of the ionization shown in the table were measured by the "porosity" method (by the ratio of the total gap length to the total track length).[4] Track cd was used for calibration (the value of the ionization along track cd was taken as equal to 1.46, i.e. equal to the ionization of a π^+ meson from a K_{π_2} decay). The calculated values of the ionization were computed from the momentum values p.

The ionization and multiple scattering measurements indicate that the particles move in the directions shown by the arrows in Fig. 2. The mass of particle "bc", which stops in the chamber, turned out to be (490 ± 190) Mev, i.e., coinciding, within the limits of statistical error, with the mass of a K meson. Measurement of the quantity $p\beta$ for particle "cd" by the multiple scattering method gave the value (180 ± 54) Mev/c, in good agreement with the values for K_{π_2} or K_{μ_2} decays. We note that for a μ^+ meson from a K_{μ_2} decay $p\beta = 216$ Mev/c, for a π^+ meson from a K_{π_2} decay $p\beta = 170$ mev/c, while the maximum value of $p\beta$ for an electron from a $\mu - e$ decay is 53 Mev/c (the mean value of $p\beta$ for a $\mu - e$ decay[5] is $p\beta = 38$ Mev/c). Thus both the measurement of the mass along track bc and the measurement of $p\beta$ for track cd is evidence of the fact that the sequence "bc" — "cd" is the decay of a K⁺ meson, and not a $\pi - \mu - e$ decay. The ionization of tracks bc and cd does not contradict this conclusion.

Particle "ba" experiences in the chamber a nuclear interaction, giving at point a a small star of the evaporation type. The value of $p\beta$ for this particle, measured by the multiple scattering method, is equal to (113 ± 22) Mev/c. The mass of particle "ba" determined from the ionization — multiple scattering relation proved to be (195 ± 55) Mev, i.e. close to the mass of a π or μ meson. Since particle "ba" gives a nuclear interaction at the end of its range, it may be assumed that it is a π meson.

The measurements and the results of the calculations show that the given case cannot be interpreted as the production of a π^+ meson in a star caused by a neutron at point a with a subsequent scattering at point b and a $\pi - \mu - e$ decay at point c, nor the production of a K⁺ meson in the same star with scattering at point b and a K_{μ_2} decay at point c.

The event described can likewise not be interpreted as a star produced by a neutron at point b, in which two strange particles and a π meson are produced (the reaction $n + n \rightarrow \Lambda^0 + K^+ + \pi^- + n$), since the calculations indicate that the threshold for such a reaction is approximately 0.9 Bev above the maximum energy of neutrons which can be produced in the chamber under the given conditions of irradiation. The high threshold is associated

Track	Particle	Range, (g/cm²)	$p\beta$,(Mev/c)	Momentum, (Mev/c)	Mass, (Mev)	Ionization	
						exp	calc
bc	K^+	6.4	—	225±20	490±190	5.0±1.4	5.7
cd	$\pi^+(\mu^+)$	>11.06	180±54	214±65	—	(1,46)	1.44
ba	π^-	14.5	113±22	172±35	19±555	2.4±0.4	1.8

with the fact that K^+ and π^- mesons in the laboratory system travel backwards with respect to the direction of the primary beam, while in the center-of-mass system of the colliding particles they should have a very high kinetic energy.

The event may be interpreted as the result of the reaction $K^0 + n \rightarrow n + K^+ + \pi^-$. However, interactions of K mesons with Xe nuclei in which π mesons are produced usually lead to multi-pronged stars. Therefore it seems to us more probable to interpret the given case as the decay of a neutral particle according to the scheme (1). The mass of this particle calculated from the momenta of the $K^\pm$ and π^- mesons and from their angle of divergence proves to be equal to

$$m_{D^0} = (660 \pm 50)\ \text{Mev}.$$

An attempt was also made to compute the mass of the D^0-meson from the kinematics of its production under the assumption that it is produced in the reaction

$$\pi^- + p \rightarrow n + D^0. \qquad (2)$$

If the calculation is made under the assumption that the D^0-meson is produced in a collision of a π^- meson with a proton at rest, then the value of the mass of the D^0 meson is found to be equal to 440 Mev. If one also takes into account the Fermi motion of the nucleons in the nucleus and assumes, for example, that the π meson collides with a proton moving towards it with a kinetic energy of 10 Mev (momentum 170 Mev/c), then the mass of the D^0 is found to equal 660 Mev. We see that the determination of the mass from the kinematics of reaction (2) has a very large error owing to the motion of the nucleons in the nucleus, but, nevertheless, this does not conflict with the possibility of the reaction taking place. The same is true for the reaction

$$\pi^- + p \rightarrow \Xi^0 + D^0. \qquad (3)$$

Bearing in mind the above possibility, and also the communication about the D^+ meson[6] of mass $m_{D^+} = (742 \pm 25)$ Mev, one may apparently speak about the existence of three particles: the D^+, D^0, and D^- mesons with close values of mass and the same decay schemes of the type

$$D \rightarrow K + \pi.$$

The question of the place of the D^0-meson in the system of elementary particles and the consequences that result from its existence are discussed in reference 7.

---

[1] Wang Kang-Chang, Hsiao Cheng, Cheng Yen-Ch'ih, and Liu Ming, Physics J. (in Chinese) 11, 493 (1955).

[2] M. S. Sinha and S. N. Sengupta, Nuovo cimento **5**, 1153 (1957).

[3] E. V. Kuznetsov and I. Ya. Timoshin, Приборы и техника эксперимента (Instrum. and Meas. Techniques) No. **4**, 40 (1959).

[4] M. F. Lomanov and B. V. Chirikov, ibid. No. **5**, 22 (1957).

[5] H. Bethe and F. de Hoffmann, Mesons and Fields, Part 2, Row, Peterson and Company, 1955, Russ Trans. IIL, M., 1957, p. 441.

[6] Wang Kang-Chang, Communication at the International Conference on High Energy Physics, Kiev, 1959.

[7] I. V. Chuvilo, Preprint, Joint Institute for Nuclear Research, 1959.

Translated by E. Marquit
8

SOVIET PHYSICS JETP VOLUME 12, NUMBER 1 JANUARY, 1961

POLARIZATION OF Sc^{46} *NUCLEI IN IRON*

A. V. KOGAN, V. D. KUL'KOV, L. P. NIKITIN, N. M. REINOV, I. A. SOKOLOV, and M. F. STEL'MAKH

Leningrad Physico-Technical Institute, Academy of Sciences, U.S.S.R.

Submitted to JETP editor February 20, 1960

J. Exptl. Theoret. Phys. (U.S.S.R.) 39, 47-52 (July, 1960)

The asymmetry of the γ radiation from polarized Sc^{46} nuclei in an alloy with pure iron was measured for temperatures of $(1.5 - 3) \times 10^{-2}$ °K. The effect observed shows that the introduction of scandium into the ferromagnet results in the appearance of an effective magnetic field H_{eff} of the order of 10^5 oe acting on the nucleus. In the case of Co^{60} introduced into iron the effective field is $(3 \text{ to } 4) \times 10^5$ oe.

THE theoretical treatment[1-3] of the correlations between β particles and γ quanta, following an allowed β transition, shows that for the case of oriented nuclei, the correlation function should be asymmetric with respect to the direction of the momentum of the β particle if combined parity is not conserved and symmetric if it is.

It has by now been established in various experiments that parity is conserved within the limits of error ~10%. In order for experiments on β-γ correlation from oriented nuclei to give a result with a greater or comparable accuracy, it is necessary to choose a nucleus in which the term in the β decay corresponding to interference between the Fermi and Gamow-Teller interactions is large. Of the known nuclei, this condition is best satisfied by Sc^{46}, Mn^{52} (which has already been investigated by Ambler and co-workers[4]) and, to a lesser degree, by V^{48}. The β decays of Co^{56} and Co^{58}, which are allowed β transitions, cannot be used for experiments concerning time parity because the interference term is equal to zero.[5,6] For this same reason, one cannot use allowed β transitions which occur with a change of spin of $1(Co^{60})$, in which there is a pure Gamow-Teller interaction.

Experiments with Sc^{46}, which are the most promising in this respect, could not be done, since the scandium ions are not paramagnetic, and one therefore could not use the method of Bleaney and Gorter-Rose for orienting the nuclei. The use of the method of a strong field (Simon) requires practically unattainable steady magnetic field intensities of $10^5 - 10^6$ oe for obtaining a noticeable degree of polarization.*

The work of Samoĭlov, Sklyarevskiĭ, and Stepanov,[8-10], who polarized the nuclei of weakly magnetic elements in alloys of these elements with ferromagnets, opened the possibility for the orientation of nuclei of various new elements including scandium.

In the present paper we present the first results obtained by us on orientation of Sc^{46}, introduced into iron.

The apparatus used by us for orientation of nuclei introduced into ferromagnets is shown in Fig. 1.

The sample 1 in the form of a thin disk was cooled by adiabatic demagnetization of a mixture of chromium potassium alum and propyl alcohol 2, in a container of organic glass 3; heat was transferred from the sample to the cooling mixture by means of a "cold pipe" 4. To improve the thermal contact between the paramagnetic salt and the cold pipe a "whisk broom" 5 of small copper wires 0.5 mm in diameter was soldered to its end. The separation between the wires did not exceed 1.5 mm. The sample was soldered to the cold pipe with tin (as in the experiments of references 8 — 10) and covered electrolytically with a layer of copper. To reduce the heat flow to the working cooling mixture it was attached by means of three small quartz tubes 6 to an upper "ballast" salt pressed in the shape of a hollow cylinder 7, which was fixed into the glass collar of the envelope by two sliders 8 made of stainless steel. The container 3 was centered with respect to the surrounding removable cover of the glass envelope by stainless steel springs 9 bonded to the cylinder of the lower "ballast" salt 10. The "ballast" salt was joined to the container by a quartz tube 11.

The magnetic field H_0 needed for magnetization of the iron was produced by means of a superconducting cylinder[11] 12 in the helium dewar. The niobium cylinder, which during the adiabatic demag-

---

*A description of the various methods for orienting atomic nuclei can be found in the survey paper of G. R. Khutsishvili.[7]

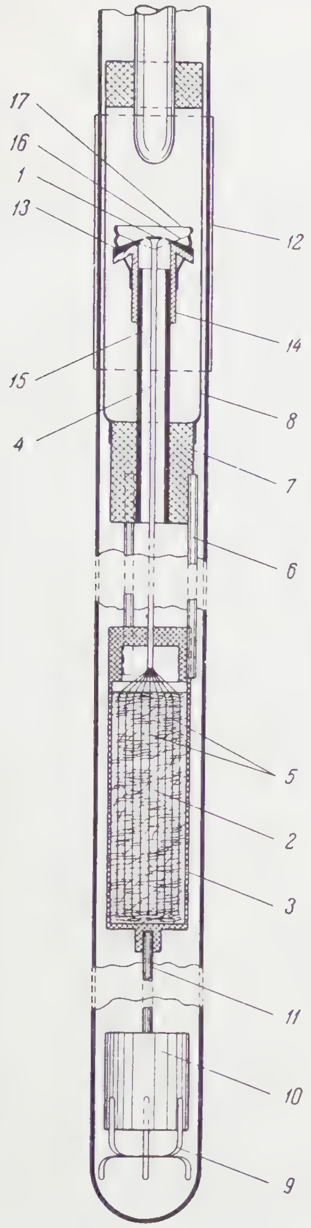

FIG. 1. Schematic drawing of the equipment.

netization is in a quite high field, preserves within its volume, after demagnetization to zero field, a field which is close to the critical value. For the niobium which we had at our disposal this residual field was ~ 900 oe. To increase the magnetic field in the neighborhood of the sample up to ~ 1600 to 1800 oe, we used wedge-shaped ''concentrators'' 13 of Armco iron. The ''concentrators'' were fixed to bracket supports 14 attached with BF-4 adhesive to a silvered glass tube 15, pressed into the upper ''ballast'' salt 7. The upper end of the cold pipe was centered with respect to the ''concentrators'' by means of caprone tension members 16 bonded to the housing 17 of stainless steel; the housing had a temperature close to the temperature of the ''ballast'' salt.

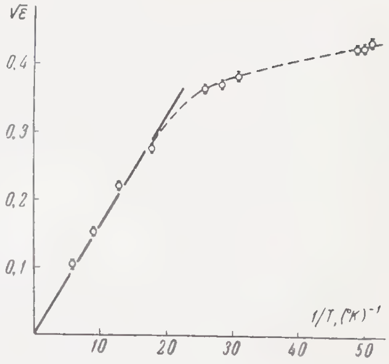

FIG. 2. Dependence of the asymmetry ε of γ radiation of Co^{60} on thermodynamic temperature T. The points shown on the graph are the average values of $\sqrt{\varepsilon}$ in a certain temperature interval.

The use of ''ballast'' salts enabled us to mount the apparatus in an envelope with small clearances (internal diameter 20 mm) and to reduce the heat leak to a value < 10 erg/min at temperatures $\sim 0.01°$K.

EXPERIMENTS WITH Co^{60}

To check the operation of the equipment, we carried out experiments on orientation of Co^{60} nuclei dissolved in pure iron obtained by heating in vacuum. The cobalt content of the iron did not exceed 0.02%. In Fig. 2 we show the dependence of the square root of the asymmetry of the γ-radiation

$$\varepsilon = [I(\pi/2) - I(0)]/I(\pi/2)$$

on the thermodynamic temperature T of the cooling mixture. For low values of the nuclear polarization, when the condition $\mu H_{eff}/kTI \ll 1$ is satisfied, where μ is the magnetic moment of the nucleus, H_{eff} is the effective magnetic field acting on the nucleus and I is the nuclear spin, we have $\sqrt{\epsilon} \sim H_{eff}/T$. Then the relation between $\sqrt{\epsilon}$ and T^{-1} should be represented by a straight line if the thermodynamic temperature T of the cooling mixture is correctly determined and the temperatures of sample and salt coincide. The magnetic temperature was determined from the susceptibility of the cooling mixture by using a mutual inductance bridge. As in the papers of Samoĭlov and coworkers, to change from magnetic to thermodynamic temperature we used the old scale for a single crystal of chromium potassium alum.[12-13] Later it was shown that this scale is not exact for low temperatures $(1/T > 20)$.

As we see from Fig. 2, when $1/T \approx 25 - 30$ one already observes a significant deviation of the experimental points from a straight line. This effect is mainly caused by a temperature drop between the sample and salt. If we use the results of references 14 and 15 for the change to the thermodynamic temperature scale, the curve $\sqrt{\epsilon} = f(T)$

deviates from the straight line at the smallest values of 1/T. However, for the determination of the effective internal field one can use the straight line for values $1/T < 20$, and the difference between the temperature scales has practically no effect on the value of H_{eff} obtained in the experiment.

From Fig. 2 it follows that the effective magnetic field acting on a Co^{60} nucleus in an alloy with iron is equal to 3.5×10^5 oe, for cobalt content < 1%. This value is in good agreement with results for H_{eff} for the case of an alloy of iron with 5% cobalt, obtained both from the asymmetry of the γ radiation of Co^{60} and from the nuclear specific heat of Co^{59} (reference 16) ($H_{eff} = (3.1 - 3.2) \times 10^5$ oe). The values for alloys with low cobalt content are somewhat higher than for permendur[17] ($H_{eff} = 2.4 \times 10^5$ oe) and for a cobalt single crystal[18,19] ($H_{eff} = (1.8 - 2.0) \times 10^5$ oe).

These data were interpreted by Kurti[16] as a confirmation of the theoretical estimate made by Marshall of the effect of the main component of the cobalt-iron alloy on the internal field produced by the d-shell electrons of the cobalt ion. However, recently Daniels and Le Blanc[20] found that the internal field in a hexagonal single crystal of cobalt is $H_{eff} = 2.7 \times 10^5$ oe; this value practically coincides with the data for alloys with low cobalt content. It was shown that the values $H_{eff} \approx 2 \times 10^5$ oe found in earlier work are explained by the presence in the cobalt crystals of the high-temperature cubic crystalline phase.

It is obvious that for a satisfactory comparison of experimental data with theory it is necessary to increase significantly the accuracy of the experiment. We note that the quite sizeable differences between data obtained in various laboratories may arise simply because of errors in the determination of the absolute temperature of the sample in the range $\sim 10^{-2}$ °K.

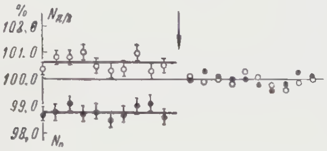

FIG. 3. Asymmetry of γ radiation of Sc^{46} nuclei polarized in an alloy with iron. On the graph we indicate (in percent) the ratios of the number of pulses recorded by scintillation counters over a time interval of 64 sec, in the direction of the axis of orientation, N_0, (solid dots), and at an angle of 90°$-N_{\pi/2}$, (open circles), to the average number of pulses recorded in the corresponding counters after heating of the sample. The arrow shows the time when the sample was heated from 0.03°K to 1.2°K. The mean square statistical errors of the measurements are indicated.

EXPERIMENTS WITH Sc^{46}

Scandium irradiated with neutrons was introduced into pure iron in the form of a metal. The scandium content in the iron did not exceed 0.5%, the activity of the sample was equivalent to ~ 1 μC of Sc^{46}.

The solubility of scandium in iron has not yet been investigated and it was not known whether a solid solution of scandium in iron occurs*.

We carried out a long series of measurements of the asymmetry of the γ radiation of Sc^{46} for a temperature of the cooling mixture down to 0.015°K. The asymmetry obtained at these temperatures was $\epsilon = 2.5\%$. Its sign is in agreement with the known dipole character of the cascade γ transitions in Ti^{46}. As was already stated above, the thermal contact used by us did not achieve equality of temperatures of sample and cooling mixture for $1/T > 25$.

In Fig. 3 we give the data on the asymmetry of the γ radiation of polarized Sc^{46} nuclei for temperatures of the cooling mixture of 0.025 — 0.03°K. The counting of the γ quanta lasted ten minutes on the cold sample, during which time the temperature of the sample hardly changed. After forced heating, measurements for this same length of time were made at a temperature ~ 1.2°K. The asymmetry value $\epsilon = 1.8\%$ obtained here was somewhat lower than the maximum value given above which was obtained for a temperature of the cooling salt T ~ 0.015°K. For a temperature ~ 0.04 — 0.05°K, the value of ϵ for Sc^{46} is only 1%, so that the temperature dependence of the asymmetry of the γ radiation cannot be investigated for low values of 1/T with sufficient accuracy. The magnetic moment of Sc^{46} has not been determined experimentally, but its value can be estimated sufficiently well on the basis of the shell model. The values of μ obtained from the formulas for a spherical and an elongated nucleus are close to one another, and their average is 3.5 nuclear magnetons, with an error not exceeding 0.5 magnetons. The comparison of the theoretical formula for the asymmetry of the γ radiation of Sc^{46} with the experimental value for $1/T = 25$ enables us to determine the effective magnetic field acting on the scandium nucleus in the alloy of scandium and iron: $H_{eff} \approx 10^5$ oe.

---

*L. M. Shestopalov of the Physico-Technical Institute, Academy of Sciences, U.S.S.R., made a study of microslices of two samples of iron-scandium alloy with contents ~ 1% and ~ 8% Sc, obtained by melting without crucible in vacuum. The results obtained show that formation of a solid solution occurs at normal temperature for a scandium content somewhat less than 1%. For large scandium content the more clearly observed phase inhomogeneities indicate a limited solubility.

EXPERIMENTAL ERRORS

Errors in the determination of H_{eff} are caused by: a) error in the determination of the magnetic moment of the nucleus, b) error in the measurement of ϵ (the asymmetry of the γ radiation), c) error in the determination of the absolute temperature, and d) possible error because of incomplete orientation of domains.

For Co^{60} the first and second sources of error are unimportant since its magnetic moment is known to high accuracy and the precision of the measurement of the asymmetry of the γ radiation is sufficiently high.

The error in determining the absolute temperature results from: 1) errors in going from magnetic temperature to thermodynamic temperature (according to the estimate of the authors it amounts to ~ 10%) and 2) errors in converting from magnetic temperatures measured for the cylindrical sample to magnetic temperatures for spherical samples for which all the computations were made. The overall error is around 15%.

The error mentioned in point d) is related to the fact that the external magnetic field used by us may not have completely oriented the domains of the ferromagnetic sample.

One might assume that iron with a small impurity of cobalt will be practically saturated for a field of 1500 oe; for the alloy of iron with scandium the situation may be somewhat worse since the magnetic properties of the iron-scandium alloy are not known. The inclusion of the corresponding correction would require additional investigations.

Taking account of all this we may state that the values of effective magnetic field measured by us lie within the following limits:

1) for Co^{60}: $3.0 \cdot 10^5 \leqslant H_{\text{eff}} \leqslant 4.0 \cdot 10^5$ oe,

2) for Sc^{46}: $0.70 \cdot 10^5 \leqslant H_{\text{eff}} \leqslant 1.30 \cdot 10^5$ oe.

POSSIBILITY OF INVESTIGATION OF β-γ CORRELATION FOR ORIENTED Sc^{46} NUCLEI

According to computation, the limiting anisotropy of γ radiation for completely oriented Sc^{46} nuclei is 80%. It is obvious that, for the insignificant degree of orientation achieved by us, experiments on β-γ correlation can give no information concerning the conservation of combined parity. However, if one achieves temperatures of the sample of 0.01° K or lower, one can obtain up to 25% polarization of the nuclei and then the precision of the experiment will increase significantly. There is information in the literature concerning indirect cooling which reached a temperature of 0.015° K.[21] If one succeeds in obtaining still lower temperatures and maintaining them sufficiently long, one may count on successful correlation measurements with Sc^{46}.

The authors express their profound gratitude to Prof. N. P. Sazhin for providing the metallic scandium and to Prof. A. Z. Dolginov for computing the formula for the asymmetry of the γ radiation of Sc^{46}.

---

[1] A. Z. Dolginov, JETP **33**, 1363 (1957), Soviet Phys. JETP **6**, 1047 (1958). Nucl. Phys. **5**, 512 (1958).

[2] M. Morita and R. S. Morita, Phys. Rev. **107**, 1381 (1957).

[3] R. B. Curtis and R. R. Lewis, Phys. Rev. **107**, 1381 (1957).

[4] Ambler, Hayward, Hoppes, and Hudson, Phys. Rev. **110**, 787 (1958).

[5] Ambler, Hayward, Hoppes, and Hudson, Phys. Rev. **108**, 503 (1957).

[6] F. Boehm and A. H. Wapstra, Phys. Rev. **107**, 1462 (1957).

[7] G. R. Khutsishvili, Usp. Fiz. Nauk **53**, 381 (1954).

[8] Samoĭlov, Sklyarevskiĭ, and Stepanov, JETP **36**, 644 (1959), Soviet Phys. JETP **9**, 448 (1959).

[9] Samoĭlov, Sklyarevskiĭ, and Stepanov, JETP **36**, 1944 (1959), Soviet Phys. JETP **9**, 1383 (1959).

[10] Samoĭlov, Sklyarevskiĭ, and Stepanov, Поляризация ядер диамагнитных элементов, растворенных в железе (Polarization of Nuclei of Diamagnetic Elements Dissolved in Iron), Moscow, 1959.

[11] Kogan, Kul'kov, Nikitin, and Reinov, J. Tech. Phys. (U.S.S.R.) **29**, 1419 (1959), Soviet Phys.-Tech. Phys. **4**, 1308 (1960).

[12] DeKlerk, Steenland, and Gorter, Physica **15**, 649 (1949).

[13] A. H. Cooke, Proc. Phys. Soc. **A62**, 269 (1949).

[14] J. M. Daniels and N. Kurti, Proc. Roy. Soc. **A221**, 243 (1954).

[15] Beun, Miedema, and Steenland, Physica **23**, 1 (1957).

[16] N. Kurti, J. Appl. Phys. Suppl. **30**, 215S (1959).

[17] Samoĭlov, Sklyarevskiĭ, and Stepanov, JETP **36**, 1366 (1959), Soviet Phys. JETP **9**, 972 (1959).

[18] C. V. Heer and R. A. Erickson, Phys. Rev. **108**, 896 (1957).

[19] Arp, Kurti, and Peterson, Bull. Am. Phys. Soc. Ser. II, **2**, 388 (1957).

[20] J. M. Daniels and M. A. R. LeBlanc, Can. J. Phys. **37**, 1321 (1959).

[21] Miedema, Postma, Van der Vlugt, and Steenland, Physica **25**, 509 (1959).

Translated by M. Hamermesh

SOVIET PHYSICS JETP VOLUME 12, NUMBER 1 JANUARY, 1961

QUADRUPOLE EFFECTS IN NUCLEAR MAGNETIC RESONANCE IN $NaNO_3-AgNO_3$ MIXED CRYSTALS

M. I. KORNFEL'D and V. V. LEMANOV

Semiconductor Institute, Academy of Sciences U.S.S.R.

Submitted to JETP editor February 19, 1960

J. Exptl. Theoret. Phys. (U.S.S.R.) 39, 53-56 (July, 1960)

A study has been made of the intensity of satellites in $NaNO_3-AgNO_3$ mixed crystals as a function of the $AgNO_3$ content. The critical sphere model has been shown to be applicable, and the sphere radius has been determined and found equal to 13 A.

At present there exist several publications[1,2] dealing with quadrupole effects in nuclear magnetic resonance (NMR) in crystals containing impurities. All this work deals with cubic crystals.

In a perfect cubic crystal the energy of the quadrupole interaction of the nucleus with the electric field of the crystalline lattice is equal to zero, since in virtue of the high symmetry of the crystal the gradient of the electric field at the nucleus is equal to zero. This leads to the result that in a cubic crystal the system of the energy levels of the nucleus in a magnetic field remains equidistant, i.e., the frequencies of all the possible N.M.R. transitions coincide. As a result of this coincidence only one "total" absorption line is observed in a cubic crystal. In the presence of an impurity the cubic symmetry of the lattice near the impurity atom or ion is destroyed and this leads to gradients different from zero. The interaction of nuclei with such gradients leads to a displacement of the nuclear energy levels and, correspondingly, to a displacement in the transition frequency. Since the magnitude of the gradient is different for nuclei situated at different distances from the impurity the frequency shift will also be different, and this in turn leads to a broadening of the absorption line. According to Pound's theory,[3] in the first approximation a broadening of the satellites occurs (the $m \rightarrow m-1$ transitions for $m \neq \frac{1}{2}$, where m is the magnetic quantum number), and in the second approximation a broadening of the central line $m = \frac{1}{2} \rightarrow m = -\frac{1}{2}$) takes place.

Experiments with cubic crystals have shown that at low impurity concentrations the intensity of the absorption line diminishes with increasing concentration of the impurity, attaining a value corresponding to the intensity of the central line. This effect is explained in the cited publications with the aid of the so-called critical-sphere model. According to this model the frequency shift is so great for nuclei situated at a distance from the impurity which is smaller than the radius of the critical sphere that these nuclei cease making a contribution to the absorption line, whereas nuclei situated at greater distances contribute only to the initial line. It might appear natural to suppose that the nuclei can have intermediate positions which must lead to a broadening of the line. But such broadening is not observed in cubic crystals. However, experiments with cubic crystals do not yield complete certainty that the satellites are not broadened, since in such crystals we cannot observe the satellites independently of the central line. More definite information on the behavior of the satellites can be obtained from a study of crystals of symmetry lower than cubic. In such crystals the gradient of the electric field in the lattice is different from zero, and the absorption line is split into components, i.e., into a central line and satellites. The amount of splitting is given for the case when the gradient is sufficiently small and has cylindrical symmetry by the following formula:[3]

$$\Delta\nu = \frac{3e^2 qQ\,(2m-1)}{8I\,(2I-1)\,h}\,(3\cos^2\varphi - 1), \qquad (1)$$

where I is the nuclear spin, eq is the component of the gradient along the symmetry axis, φ is the angle between the axis of symmetry and the magnetic field, and Q is the nuclear quadrupole moment.

Thus, by carrying out investigations on a noncubic crystal, we are able to make separate observations of the behavior of the satellites. We have utilized $NaNO_3$ for such a crystal. These crystals belong to the rhombohedral system, and the Na^{23} NMR spectrum in them consists of three lines: a central line and two symmetrically situated satellites. In accordance with (1), the magnitude of the splitting depends on the orientation of the crystal in the magnetic field. The experimental curves fall smoothly on the curve:[3]

$$\Delta\nu = 83.5\,(3\cos^2\varphi - 1)\ \text{kc/sec} \qquad (2)$$

where φ is the angle between the third order axis and the magnetic field.

In order to study the effect of impurities on the Na^{23} spectrum in $NaNO_3$, we have studied $NaNO_3$—$AgNO_3$ mixed crystals in which an Ag^+ ion replaces a Na^+ ion.

$NaNO_3$ crystals and mixed crystals, weighing from 100 to 250 g, were grown in a crucible furnace by Steber's method[4] from chemically pure substances. Cylindrical samples of 1.2 cm diameter and from 1.42 to 2.7 cm high were cut from these crystals by means of a wet thread and were then polished on damp cloth.

The absorption spectra were studied (with apparatus described elsewhere[5]) under the following conditions: intensity of the magnetic field 4400 oe, modulation amplitude 0.7 oe, and synchronous-detector time constant 10 sec. The voltage in the oscillator circuit was set at 0.15 v in order to obtain the best signal-noise ratio. Such a voltage leads to some saturation of the central line,[3] but experiment has shown that a decrease in the voltage does not alter the results obtained, and leads only to a slight increase in the intensity of the central line.

The single crystals of $NaNO_3$ and $NaNO_3$—$AgNO_3$ grown by us had a sufficiently pronounced mosaic structure. In the investigation of the absorption spectra in these crystals it was found that the widths of the satellites depended on the orientation. For $\varphi = 0$ and 90° the satellites and the central line have a width of the order of 2 or 2.5 kc/sec, which approximately corresponds to the dipole-dipole width;[3] at intermediate angles the satellites become broader, but their intensity remains constant independently of the orientation. This effect can be explained by the mosaic structure referred to previously. Indeed, as can be seen from (2), the "disorientation" of individual regions of the sample even within 5° can lead to considerable broadening for $\varphi = 45°$ without producing any noticeable broadening of the satellites for $\varphi = 0$ and 90°.

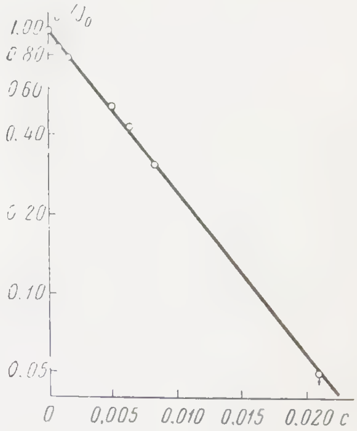

FIG. 2. Dependence of the relative intensity of the satellites on the concentration of $AgNO_3$.

Figure 1 gives as an example some NMR spectra in $NaNO_3$ and $NaNO_3$—$AgNO_3$ for $\varphi = 90°$, which are derivatives of absorption lines. (For $\varphi = 0°$, completely analogous spectra are obtained.) Figure 2 shows the dependence of the intensities of the satellites on the concentration of Ag^+ on a semi-logarithmic scale. It is seen that a decrease in the intensity of the satellites becomes noticeable even at a concentration of 0.001, which corresponds to 1 Ag^+ ion for each 1000 Na^+ ions. At a concentration of 0.021 the satellites disappear completely while the central line still remains practically undistorted. The decrease in the intensity of the satellites is not accompanied by broadening. The width of the satellites measured between points of the maximum and minimum of the derivative of the absorption line remains the same in mixed crystals as in pure $NaNO_3$, and only a slight broadening of the wings of the line is observed.

Since the width and the shape of the satellites remain approximately the same, their intensity is

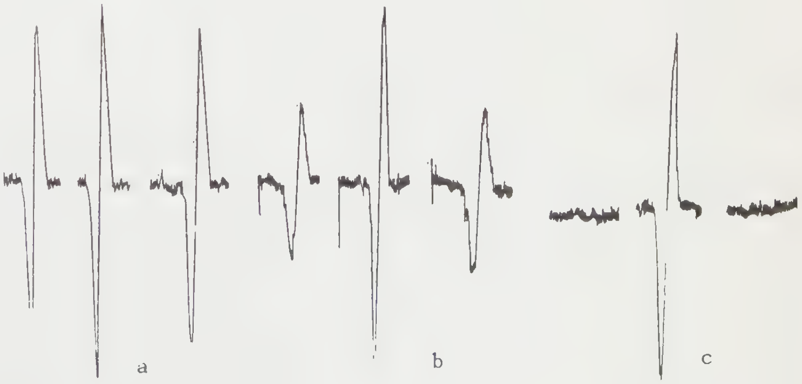

FIG. 1. NMR spectra in various crystals: a) $NaNO_3$, b) $NaNO_3$ + 0.5% $AgNO_3$, c) $NaNO_3$ + 2.1% $AgNO_3$.

proportional to the maximum value of the derivative. Therefore in Fig. 2 the maximum values of the derivative have been adopted as a measure of the intensity of the satellites.

The lack of broadening of the satellites allows us in our case also to utilize the critical sphere model for the analysis of the results, i.e., to consider only two cases: either the Ag^+ ion lies inside the critical sphere, so that for a Na^+ nucleus lying at the center of this sphere the frequency shift is so great that the given nucleus ceases to make a contribution to the observed absorption line, or the Ag^+ ion lies outside the critical sphere and then the Na^+ nucleus at the center of the sphere makes a contribution to the initial unbroadened line. For a random distribution of the Ag^+ ions, the intensity of the satellites must consequently be proportional to the probability that the impurity ion does not lie inside the critical sphere, i.e.,

$$J/J_0 = (1-c)^n, \qquad (3)$$

where J_0 and J are the intensities of the satellites in a pure and a mixed crystal, c is the molar concentration, n is the number of lattice points containing Na^+ ions inside the critical sphere. Since c is small, we can rewrite (3) in the following form

$$\ln(J/J_0) = n \ln(1-c) \approx -nc.$$

As may be seen from Fig. 2 the dependence of J/J_0 on c does indeed have the shape of a straight line on a semilogarithmic scale. From the slope of this straight line we obtain n = 138, i.e., the critical sphere contains 138 Na^+ ions. This number of ions corresponds to a critical sphere radius approximately equal to 13 A. (In the case of a noncubic crystal we should really introduce a critical ellipsoid, but the absence of any angular dependence in the observed spectra gives some justification for using a spherical model.)

The results presented above show that in noncubic crystals, too, an impurity leads only to a decrease in the intensity of the satellites without broadening. This fact, together with the fact that the experimental dependence of the intensity of the satellites on the concentration of the impurity has the form (3), supports the view that the critical sphere model is applicable. Nevertheless, the reasons for the absence of satellite broadening are not sufficiently clear, as has been noted previously, and this question requires further investigation.

---

[1] T. J. Rowland, Acta Met. 3, 74 (1955).

[2] Kawamura, Otsuka, and Ishiwatari, J. Phys. Soc. Japan 11, 1064 (1956).

[3] R. V. Pound, Phys. Rev. 79, 685 (1950).

[4] V. D. Kuznetsov, Кристаллы и кристаллизация (Crystals and Crystallization), Gostekhizdat, 1953.

[5] V. V. Lemanov, Приборы и техника эксперимента (Instrum. and Meas. Techniques), in press.

Translated by G. Volkoff
10

SOVIET PHYSICS JETP VOLUME 12, NUMBER 1 JANUARY, 1961

ELECTRON PARAMAGNETIC RESONANCE AND SPIN-LATTICE RELAXATION OF Co^{2+} *IN CORUNDUM*

G. M. ZVEREV and A. M. PROKHOROV

Institute of Nuclear Physics, Moscow State University

Submitted to JETP editor February 25, 1960

J. Exptl. Theoret. Phys. (U.S.S.R.) **39**, 57-63 (July, 1960)

The electron paramagnetic resonance of Co^{2+} in corundum has been observed and the spin-Hamiltonian constants for the two nonequivalent ion systems have been measured. The temperature dependence of the spin-lattice relaxation time has been studied. It was found that at liquid helium temperatures Co^{2+} has an anomalously large relaxation time. Effects were observed which are associated with spin-spin cross relaxation between hyperfine structure components.

IT is important to investigate the electron paramagnetic resonance (EPR) of iron-group ions in corundum for both theoretical and practical reasons. For example, the working material in most paramagnetic amplifiers is corundum containing an admixture of chromium or iron ions.[1-3] An important part in the future development of paramagnetic amplifiers may be played by corundum containing two paramagnetic ions, one of which serves as the working material for the amplifier while the other shortens the spin-lattice relaxation time of the first ion. In one investigation[4] cerium ions were used to modify the relaxation time of gadolinium ions in lanthanum ethyl sulfate.

In the present work the EPR spectrum of Co^{2+} in corundum was studied, the spectrum was interpreted theoretically and the spin-lattice relaxation time was investigated.

1. The ground state of the free Co^{2+} ion is ^4F of the $3d^7$ configuration. The other term of the same symmetry, ^4P, is located 14 000 cm^{-1} above the ground level. In the corundum single crystal the Co^{2+} ion levels undergo Stark splitting induced by the electric field of neighboring ions. The crystalline electric field is generated by an octahedron of O^{2-} ions and is of cubic symmetry with a small admixture of trigonal symmetry.

The behavior of Co^{2+} energy levels in crystalline fields of different symmetries has been investigated in references 5 and 6. In a cubic field the lowest level, which possesses sevenfold orbital degeneracy, is split into a singlet and two triplets, with the triplets lying below the singlet. The trigonal field further splits a triplet into a singlet and a doublet (neglecting the spin-orbit interaction). The singlet can lie either above or below the doublet, depending on the specific form of the crystalline field. Each orbital level possesses fourfold spin degeneracy. When spin-orbit coupling is taken into account the trigonal field splits the lower triplet into six Kramers doublets. Abragam and Pryce[7] have shown that the orbital moment $l' = 1$ can be assigned to the lower orbital triplet and that the behavior of the energy levels in the trigonal field with spin-orbit coupling can be described by the fine-structure Hamiltonian

$$W = \Delta (1 - \hat{l}_z'^2) - \alpha\lambda \hat{l}_z' \hat{S}_z - \alpha'\lambda (\hat{l}_x' \hat{S}_x + \hat{l}_y' \hat{S}_y), \qquad (1)$$

where Δ is the splitting of the lower triplet by the trigonal field, λ is the spin-orbit coupling constant ($\lambda = -180\ cm^{-1}$), α and α' are factors depending on the admixture of higher states belonging to the ^4F and ^4P terms in the wave functions of the lower triplet. When these admixtures are omitted we have $\alpha = \alpha' = 3/2$.[6] The z axis of the rectangular system is a trigonal crystal axis. α and α' can be calculated only if the complete scheme of level splitting by the crystalline field is known.

The fine-structure levels can be classified by means of the quantum number $m = l'_z + S_z$. In the representation where $\hat{l}'_z$ and $\hat{S}_z$ are diagonal it is easy to write the secular determinant of the Hamiltonian (1), which undergoes triple splitting corresponding to $m = \pm 1/2, \pm 3/2, \pm 5/2$. The solution of the secular equation gives three Kramers doublets belonging to $m = \pm 1/2$, two doublets for $m = \pm 3/2$, and one doublet for $m = \pm 5/2$; The lowest energy level is a doublet with $m = \pm 1/2$; its wave functions are superpositions of the wave functions for the states with $m = \pm 1/2$:

$$|{}^1\!/_2\rangle = a|-1;\ {}^3\!/_2\rangle + b|\ 0;\ {}^1\!/_2\rangle + c|\ 1;\ -{}^1\!/_2\rangle,$$

$$|-{}^1\!/_2\rangle = a|\ 1;\ -{}^3\!/_2\rangle + b|\ 0;\ -{}^1\!/_2\rangle + c|-1;\ {}^1\!/_2\rangle \qquad (2)$$

with the coefficients a, b, c depending on α, α', Δ. When the wave functions of the lowest doublet are known we can calculate the spectroscopic splitting factors $g_{\parallel}$ and $g_{\perp}$ of the level.[6] Vice versa, when the g factors are known, Δ, α, α', can be calculated.

The hyperfine splitting constants can be represented as the sums of three terms:[6]

$$A = A_L + A_{Ss} + A_{Sd}; \qquad B = B_L + B_{Ss} + B_{Sd}. \qquad (3)$$

Here A_L and B_L depend on electron orbital motion, A_{sd} and B_{sd} result from the d-electron spin, and A_{Ss} and B_{Ss} are associated with the admixture of configurations containing unpaired s electrons. The first and second terms in (3) can be represented as follows:

$$A_L = Pg_{L\parallel},\ B_L = Pg_{L\perp},\ A_{Ss} = -(k/2)\,Pg_{S\parallel},$$

$$B_{Ss} = -(k/2)\,Pg_{S\perp}. \qquad (4)$$

Here g_L and g_S are the orbital and spin parts of the g factors; $P = 2\gamma\beta\beta_n\overline{r^{-3}}$, where γ is the nuclear gyromagnetic ratio, β is the Bohr magneton, β_n is the nuclear magneton and k characterizes the admixture of s electrons.

The terms A_{Sd} and B_{Sd} make only a small contribution and may be neglected in approximate calculations.

2. We have reported our observation of the EPR of Co^{2+} in corundum at 4.2°K in an earlier paper.[8] The spectrum consists of two strong lines, each having eight hyperfine components (corresponding to the nuclear spin $I = {}^7\!/_2$ of Co^{59}), and a few weak lines which also exhibit the characteristic hyperfine structure of cobalt.

All lines become stronger with decreasing temperature. They therefore belong to transitions between levels of the lowest Kramers doublet and are not associated with excited states.

The strong lines can be interpreted by means of the spin Hamiltonian with effective spin $S' = {}^1\!/_2$:

$$\hat{\mathcal{H}} = g_{\parallel}\beta H_z\hat{S}'_z + g_{\perp}\beta(H_x\hat{S}'_x + H_y\hat{S}'_y)$$
$$+ A\hat{I}_z\hat{S}'_z + B\,(\hat{I}_x\hat{S}'_x + \hat{I}_y\hat{S}'_y), \qquad (5)$$

where $\hat{S}'_x$, $\hat{S}'_y$, $\hat{S}'_z$, are projections of the spin, $\hat{I}_x$, $\hat{I}_y$, $\hat{I}_z$ are projections of the nuclear spin, and H_x, H_y, H_z are the external magnetic field components. Measurements of the EPR spectrum at 9000 and 38 000 Mcs yielded the following values of the constants in the Hamiltonian:

line I: $g_{\parallel} = 2.292 \pm 0.001$, $g_{\perp} = 4.947 \pm 0.003$,
$A = 3.24 \pm 0.01$, $B = 9,72 \pm 0.05$;

line II: $g_{\parallel} = 2.808 \pm 0.003$, $g_{\perp} = 4.855 \pm 0,005$,
$A = 2,08 \pm 0.09$, $B = 15.10 \pm 0.11$.

A and B are given in units of 10^{-3} cm^{-1}.

Line I of Co^{2+} in corundum was also measured at 9100 Mcs and T = 1.6°K by Geusic,[9] whose hyperfine constants are in good agreement with our values, although there is a small but appreciable difference of the g factor.

The hyperfine splitting of both cobalt lines is greater for perpendicular than for parallel orientation. Therefore the parallel orientation is accompanied by strong second-order effects which destroy the equal separation of hyperfine components for line I and even cause partial overlapping of the components at one end of the spectrum of line II (Fig. 1).

As the crystal departs from parallel orientation a slight splitting of each hyperfine component appears, which disappears for both $\theta = 0°$ and $\theta > 30°$.

Lines I and II evidently belong to different nonequivalent ion systems. The existence of two Co^{2+} ion systems in corundum may be accounted for as follows. The lattice contains two kinds of octahedral cavities in which the cobalt ion may be located. One system of cavities in the normal lattice is occupied by aluminum ions, while the second system is not entirely occupied and there is one unoccupied site for every two occupied cavities.[10] Aluminum is included in the corundum lattice as the trivalent ion Al^{3+} while the cobalt ion is divalent. Charge neutralization therefore requires the replacement of two Al^{3+} ions by three Co^{2+} ions, two of which occupy the Al^{3+} ion sites while one fills an unoccupied octahedral cavity. The separation of cobalt ion centers from the centers of the nearest oxygen ions is identical for both ion systems, so that the cubically symmetric field should be approximately the same for both systems. However, the trigonal field may differ considerably, since in the trigonal axis direction a Co^{2+} ion has one Al^{3+} ion as its nearest neighbor, while in the second case there are two Al^{3+} ions (Fig. 2). The measured ratio of integrated intensities for lines I and II in the case of parallel orientation was 2.3:1, in good agreement with the expected value of 2:1. The weaker cobalt lines in corundum probably result from ions having anomalous crystalline environments resulting from other cobalt ions, dislocations, etc.

Using the values obtained for $g_{\parallel}$ and $g_{\perp}$, we calculated α, α', Δ, the constants of the Hamil-

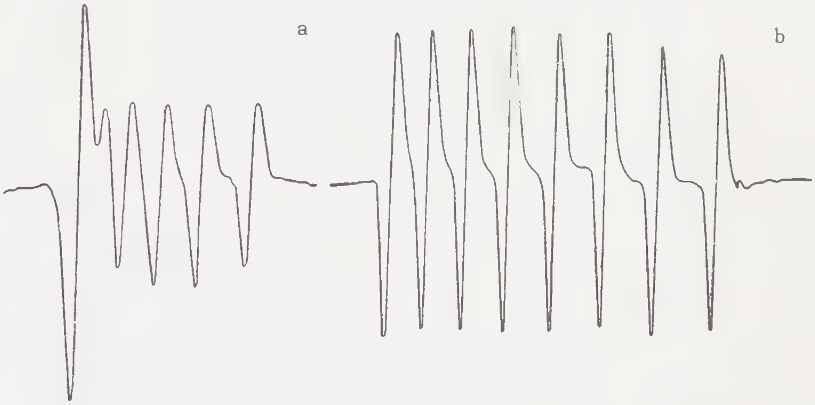

FIG. 1. Traces of the derivative of the EPR lines of Co^{2+} in corundum for parallel orientation at 4.2°K. a – line II, b – line I. The magnetic field increases from left to right.

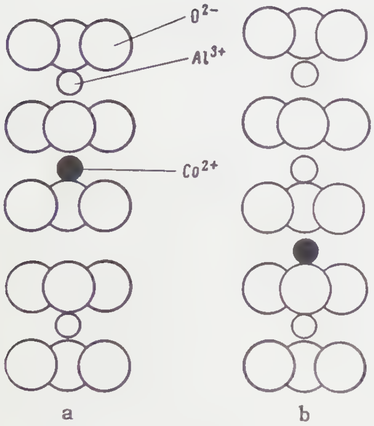

FIG. 2. Positions of two nonequivalent Co^{2+} ions in the corundum lattice.

tonian (1), in first approximation. When only one ion system is considered, two equations for the g factors cannot determine all three unknown constants. We therefore imposed the additional condition that α and α' should approximately agree for both ion systems. The calculations gave $\alpha = 1.32$, $\alpha' = 1.38$, $\Delta = -760\ cm^{-1}$ for line I, and $\Delta = -400\ cm^{-1}$ for line II. It is difficult to obtain the complete level scheme of Co^{2+} from an investigation of EPR alone. It is desirable to use optical data in addition, as was done by Low for Co^{2+} in the MgO lattice.[11]

It is interesting that the parameter Δ for Co^{2+} in corundum does not have the same sign as in zinc fluosilicate, which also possesses a crystalline field of trigonal symmetry.[6]

An attempt to calculate the hyperfine interaction constants A and B by using the values $P = 0.0225\ cm^{-1}$ and $k = 0.325$, which were selected by Abragam and Pryce, did not yield satisfactory agreement with experiment. For line I we must have $P = 0.017\ cm^{-1}$ and $k = 0.27$; for line II we must have $P = 0.027\ cm^{-1}$ and $k = 0.30$. These values are fairly rough estimates, but we note that even for reasonable changes of α, α', Δ the values of P and k that are calculated from experimental hyperfine data do not change much.

3. At room temperature Co^{2+} has a very short spin-lattice relaxation time τ_1, which hinders the observation of EPR lines. This difficulty is associated with the closeness of the lower orbital levels, which have separations of a few hundred cm^{-1}. The short relaxation time τ_1 hinders detection of EPR even at the temperature of liquid nitrogen.

τ_1 was measured at liquid helium temperatures for the saturated 9500 Mcs resonance line, using corundum single crystals containing $10^{-2}\%$ cobalt. The absolute accuracy of τ_1 in the saturation technique was ±50%, although the relative error was considerably smaller. For line I in parallel orientation at 4.2°K we obtained $\tau_1 = 1$ sec and the temperature law $\tau_1 \sim T^{-1}$ in the range 1.8–4.2°K. Relaxation above 4.2°K was investigated during the heating of the cavity resonator from liquid helium temperature to liquid nitrogen temperature. In the range 4.2–22°K the relaxation time drops off sharply from 1 sec at 4.2°K to 3×10^{-8} sec at 22°K.

In the range 22–50°K we were able to calculate τ_1 from the broadening of the EPR line as a result of spin-lattice relaxation. Below 22°K the magnetic field width of a single hyperfine component of line I at half maximum is 7.5 oe. The line begins to broaden with heating up to 22°. At 31° the width is 15 oe; with further heating the hyperfine components begin to overlap. At 50°K the line is ~200 oe wide with no trace of hyperfine structure. The temperature dependence of τ_1 in the interval 22–50° fits the formula $\tau_1 \sim T^{-n}$ with $n = 5 \pm 0.5$. Figure 3 shows the overall temperature dependence of τ_1.

A few additional remarks are needed regarding the use of the saturation technique for measuring τ_1. This procedure does not determine τ_1 but rather the product $\tau_1\tau_2$, where τ_2 is the spin-spin relaxation time. τ_2 can be calculated from the line width $\Delta\nu$ when the latter is associated with homogeneous broadening, i.e., when it is induced,

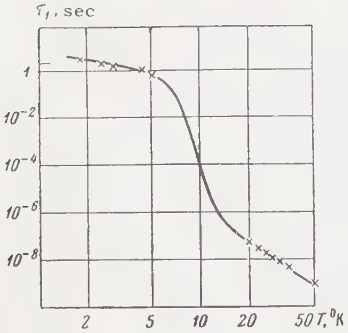

FIG. 3. Temperature dependence of the relaxation time τ_1 of Co^{2+} line I.

for example, by dipole-dipole interaction or spin-lattice relaxation.[12] We employed very dilute samples with $\sim 10^{-2}\%$ concentration. Consideration of the hyperfine structure reduces the concentration of ions with identical nuclear spin projections by an additional factor of 8. At such a low concentration the dipole-dipole interaction makes an extremely small contribution to the total line width, which in this case is determined mainly by spin interaction with the nuclear magnetic moments of the diamagnetic environment and by crystal imperfections. An analysis showed that at liquid helium temperatures the line shape is Gaussian with somewhat broadened wings and that it is not affected by saturation. The hypothesis that homogeneous broadening determines the line widths is thus confirmed. For small concentrations of paramagnetic ions the interactions that cause homogeneous broadening result in a Lorentz line shape.[13] The concept of cross relaxation[14] enables us to conclude that even in the case of inhomogeneous broadening the line is saturated identically over its entire contour and that the saturation factor in $(1 + \gamma^2 H_1^2 \tau_1 \tau_2)^{-1}$ requires replacement of τ_2 by τ_2^*, which is determined from the observed line width. We performed this substitution.

We also note that cobalt exhibits a spin-spin cross interaction between different hyperfine components. This was first noted by Townes et al.[15] for copper ions, and when one component is saturated leads to partial saturation of the other components. This effect distorts the measurements obtained by the saturation technique and results in lowered values of τ_1.

The results presented here for the spin-lattice relaxation time of Co^{2+} exhibit an anomalously long relaxation time of this ion at liquid helium temperatures compared with Cr^{3+} and Fe^{3+}. These ions are weakly coupled to the lattice and spin-lattice relaxation does not impede the observation of EPR lines even at room temperature, while at liquid helium temperatures τ_1 is of the order $10^{-1} - 10^{-2}$ sec. We might attempt to attribute the anomalous relaxation time of cobalt to low thermal conductivity of the corundum lattice containing cobalt, i.e., we may assume that the true spin-lattice relaxation time is short but that the rate of energy removal from the spin system is limited by the process of energy transfer from lattice phonons to the helium bath. This hypothesis is refuted as follows. When one hyperfine component of line I was saturated at frequency ν_1 we were able to observe the behavior of another hyperfine component at frequency ν_2, both components being observed in the same external magnetic field. In this case an emission line was obtained at ν_2 instead of an absorption line, i.e., a negative spin temperature was attained. In the presence of strong ion-lattice coupling a negative temperature cannot exist between levels, since the lattice temperature is always positive because of the absence of an upper limit to the phonon energy spectrum. The cause of the anomalous relaxation of Co^{2+} in corundum must therefore be sought in the nature of the ion itself. We note that in experiments using parallel fields Van den Broek et al[16] also observed anomalously large values of τ_1 in certain cobalt salts at liquid helium temperatures.

The relationship $\tau_1 \sim T^{-1}$ at liquid helium temperatures may be associated with the relaxation mechanism resulting from direct emission and absorption of single phonons. The steep drop of the relaxation time in the range 4.2—22° is still unexplained. The relationship between τ_1 and T at higher temperatures may be represented as the superposition of direct processes and combination scattering of phonons, resulting in a strong temperature dependence $(\tau_1 \sim T^{-7})$. We note that the temperature dependence of line II relaxation in parallel orientation practically coincides with that for line I (Fig. 3). Since lines I and II originate in ions having different schemes of the lowest orbital levels, the relaxation anomalies cannot be accounted for by specific features of a level scheme (for example, the existence of an excited level ~ 10 cm^{-1} directly above the lowest level). The observed angular dependence of the relaxation time for line I at 4.2° and 2° showed that, within experimental error, τ_1 is independent of crystal orientation in an external magnetic field.

4. EPR of Co^{2+} results in several properties associated with spin-spin cross interactions between different components. As already mentioned, when a component at frequency ν_1 is saturated an emission line can be obtained for a neighboring component at frequency ν_2. When $\nu_1 > \nu_2$ this effect is observed for components lying on the stronger magnetic-field edge of the line. When $\nu_2 > \nu_1$ the effect is observed for components on the other edge of the line. This effect can be utilized in a paramagnetic amplifier with working frequency above that of the auxiliary radiation.

The cross relaxation processes of cobalt in corundum are now being investigated in greater detail.

The authors wish to thank R. P. Bashuk and A. S. Bebchuk for preparing the samples of corundum containing cobalt, and L. S. Kornienko for valuable discussions.

---

[1] Zverev, Kornienko, Manenkov, and Prokhorov, JETP **34**, 1660 (1958), Soviet Phys. JETP **7**, 1141 (1958).

[2] Makhov, Kikuchi, Lambe, and Terhune, Phys. Rev. **109**, 1399 (1958).

[3] L. S. Kornienko and A. M. Prokhorov, JETP **36**, 919 (1959), Soviet Phys. JETP **9**, 649 (1959).

[4] Scovil, Feher, and Seidel, Phys. Rev. **105**, 762 (1957).

[5] R. Schlapp and W. G. Penney, Phys. Rev. **42**, 666 (1932).

[6] A. Abragam and M. H. L. Pryce, Proc. Roy. Soc. (London) **A206**, 173 (1951).

[7] A. Abragam and M. H. L. Pryce, Proc. Roy. Soc. (London) **A205**, 135 (1951).

[8] G. M. Zverev and A. M. Prokhorov, JETP **36**, 647 (1959), Soviet Phys. JETP **9**, 451 (1959).

[9] J. E. Geusic, Bull. Am. Phys. Soc. II, **4**, 261 (1959).

[10] E. S. Rudnitskaya, Тр. Ин-та кристаллографии (Trans. Crystallographic Inst.) **8**, 13 (1953).

[11] W. Low, Phys. Rev. **109**, 256 (1958).

[12] A. M. Portis, Phys. Rev. **91**, 1071 (1953).

[13] C. Kittel and E. Abrahams, Phys. Rev. **90**, 238 (1953).

[14] Bloembergen, Shapiro, Pershan, and Artman, Phys. Rev. **114**, 445 (1959).

[15] Giordmaine, Alsop, Nash, and Townes, Phys. Rev. **109**, 302 (1958).

[16] Van den Broek, Van der Marel, and Gorter, Physica **25**, 371 (1959).

Translated by I. Emin
11

SOVIET PHYSICS JETP VOLUME 12, NUMBER 1 JANUARY, 1961

OBSERVATION OF CHARGED RELATIVISTIC PARTICLES IN A LUMINESCENT CHAMBER

B. A. DEMIDOV and S. D. FANCHENKO

Submitted to JETP editor March 17, 1960

J. Exptl. Theoret. Phys. (U.S.S.R.) **39**, 64-66 (July, 1960)

Luminescent chamber photographs of cosmic ray μ meson tracks have been obtained with ionization close to minimum. The density of the tracks of these μ mesons was measured.

E. K. ZAVOĬSKIĬ and his co-workers[1-3] recorded in a luminescent chamber the tracks of relatively slow protons, mesons and α particles. Recently, Jones, Perl, Reynolds, et al.[4] obtained tracks in luminescent chambers of fast cosmic ray particles, but they did not show quantitatively that the tracks recorded were those of particles with minimum ionization density. The clarity of the tracks in these experiments far exceeded those achieved in Zavoĭskiĭ's luminescent chamber.

The present work was undertaken for the purpose of observing singly-charged minimum ionization particles in a luminescent chamber, with high sharpness of imaging, and for a quantitative determination of the density of such tracks. A knowledge of the minimum value of the density of tracks in the chamber enables one to establish an absolute calibration of ionization density for all tracks observed in it.

A schematic diagram of the equipment is shown in Fig. 1. The working volume of the chamber is the crystal K_1 [NaI(Tl) crystal 7 cm in diameter, with a thickness actually used ~1 cm]. The objective 0 of the "Yupiter" type projects an image of the luminous track of a particle on to the input photocathode Φ of the multi-stage electron optical converter EOC, which has the maximum coefficient of amplification of brightness of imaging.[2,3,5,6] The long magnet winding K produces the longitudinal magnetic field which is needed for focusing the electron image in the EOC. The EOC is operated in a "slaved" pulse mode on the first, second and last electron optical stages. The image of each track in the crystal is "held" on the luminescent screen S_1 of the first stage for ~100 μsec.[7] If during this time a gating pulse arrives at the input of the control circuit (CC), the image is "accepted" from the screen S_1, passes to the output luminescent screen S_{out} and is photographed by the automatic photographic apparatus PA. In Fig. 1 we also show the shape of the control pulses which go from the circuit CC to the EOC and to the relay for moving the plates of the photographic apparatus.

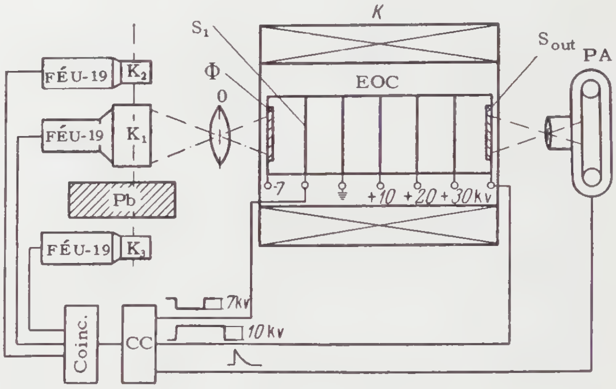

FIG. 1

Most of the photographs were obtained in this synchronized type of operation of the EOC, in which the gating pulse to the input of CC came directly from the FÉU-19 photomultiplier "looking at" the working volume of the luminescent chamber. About 1,000 track photographs were obtained in this way. In 125 of these, there are visible well-focused single tracks most of which passed through the whole working volume of the chamber in directions close to the vertical. Five such tracks were recorded per minute on the average, apparently belonging to relativistic cosmic-ray mesons (Fig. 2a). In addition, there were recorded several stars and showers (Fig. 2b).

To measure the track density for minimum ionizing particles, a special experiment was done in which relativistic particles were selected by a telescope system of three counters (K_1, K_2, K_3) connected in coincidence (Fig. 1). A 115 g/cm^2 lead absorber was placed between K_1 and K_3. The gating pulse to the CC came from the coincidence circuit (Coinc). The coincidence circuit (Coinc) operated once every 2 – 2.5 hours. With the absorber thickness used in this experiment we could record only particles with an ionization differing by no more than a factor of $1\frac{1}{2}$ from minimum. If we consider that the cosmic radiation at sea level consists predominantly of μ mesons, it is

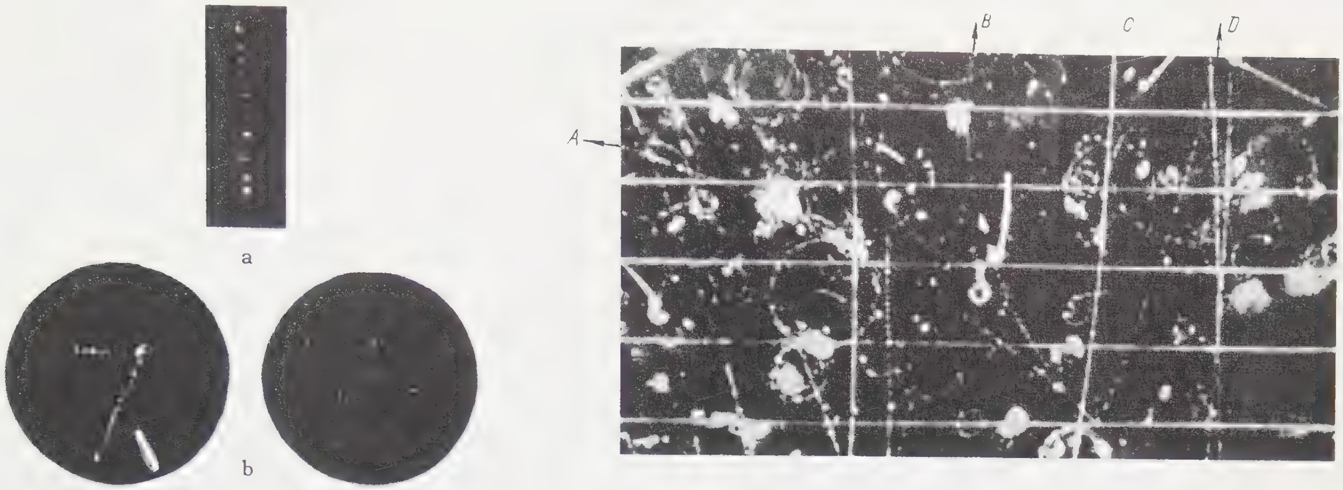

FIG. 2

easy to show that the difference in density of the tracks recorded from minimum did not exceed 10 — 20%. Under these conditions we photographed and measured on the negative a total track length of 10.4 cm (this corresponds to 41.6 cm in the crystal). In the photographs a track consists of individual points, each of which is formed by a single photoelectron emerging from the input photocathode.*

The number of "points" m appearing on the image of 1 cm of track in the crystal, is given by the formula:[2]

$$m = [\gamma k^2 B^2 / 1600(1+k)^2 n^2 \varepsilon] \, (dE/dx),$$

$$\gamma = 100\, C_{IP} \eta \, (1 - f) \qquad (1)$$

In this expression dE/dx is the energy loss of the particle per cm path in the luminescent crystal; n, C_{IP} and ϵ are, respectively, the index of refraction, the efficiency and the mean energy of photons of the luminescence in the crystal; η is the quantum yield of the photo cathode of the EOC; f is the coefficient for absorption and scattering of light along the path from the track in the crystal to the photocathode of the EOC; B and k are the aperture and magnification of the objective O. The experiment gave for the density of tracks of minimum ionizing particles a value $m_{exp} = 5\ \mathrm{cm}^{-1}$, from which it follows that the coefficient in formula (1) is $\gamma_{exp} = 0.4$ for our chamber. This is half the computed value γ_{comp}, obtained on the assumption that $f = 0$, $C_{IP} = 0.08$ and $\eta = 0.1$. Thus, because of light losses in the objective and crystal and possibly also because of a somewhat reduced quantum yield of the photocathode used in the particular EOC employed in this experiment, or because of a reduced quantum yield of the luminescence of the NaI(Tl) crystal which we used, the density of tracks in our apparatus was half as great as the maximum possible.

In conclusion the authors express their gratitude to E. K. Zavoĭskiĭ for valuable advice and discussion, and to L. S. Danelyan and V. V. Sklyarevskiĭ for providing the crystals.

---

*Neighboring points sometimes may fuse together, forming a "conglomerate."

[1] Zavoĭskiĭ, Smolkin, Plakhov, and But-slov, Dokl. Akad. Nauk SSSR, 100, 241 (1955).

[2] Zavoĭskiĭ, But-slov, Plakhov, and Smolkin, Атомная энергия (Atomic Energy), 1, 34 (1956).

[3] Zavoĭskiĭ, But-slov, and Smolkin, Dokl. Akad. Nauk SSSR, 111, 956 (1956), Soviet Phys.-Doklady, 1, 743 (1956).

[4] L. W. Jones and M. L. Perl, International Conference on High-Energy Accelerators and Instrumentation, CERN, Geneva (1959).

[5] But-slov, Zavoĭskiĭ, Plakhov, Smolkin, and Fanchenko, Успехи научной фотографии (Advances in Scientific Photography), 6, 84 (1959).

[6] But-slov, Zavoĭskiĭ, Plakhov, Smolkin, and Fanchenko, Report to the Fourth International Congress on High-speed Photography, Cologne, (1958).

[7] G. H. Smolkin, Приборы и техника эксперимента (Instrum. and Meas. Techniques), 4, 60 (1957).

Translated by M. Hamermesh
12

SOVIET PHYSICS JETP VOLUME 12, NUMBER 1 JANUARY, 1961

FOUR-PRONGED DECAY OF THE LONG LIVED K^0 MESON

É. O. OKONOV, N. I. PETROV, A. M. ROZANOVA, and V. A. RUSAKOV

Joint Institute for Nuclear Research

Submitted to JETP editor March 18, 1960

J. Exptl. Theoret. Phys. (U.S.S.R.) **39**, 67-69 (July, 1960)

Among 140 decays of long-lived K_2^0 mesons observed in a cloud chamber, one case of a four-pronged star was observed, which most probably can be interpreted as a $K_2^0 \rightarrow \pi^+ + \pi^- + \pi^0$ decay with a subsequent $\pi^0 \rightarrow \gamma + e^+ + e^-$ decay.

In an exposure of a cloud chamber (see reference 1) to a beam of neutral particles from the proton synchrotron of the Joint Institute for Nuclear Research, at a distance of 8 m from the internal target, there were registered 140 K_2^0 decays* and among them one four-prong event, a photograph of which is shown in the figure. Tracks A, B, and D are directed upward relative to the plane of the photograph and track C downward. For tracks A, B, and D the radii of magnetic curvature were measured; for the short track C it was possible to determine only the angle and sign of the magnetic curvature. The results of the measurements are shown in the table. All tracks, including the positive particle tracks A and D, have an ionization close to minimum.

From the data of the measurements, it follows that the positive particles cannot be protons, and tracks A and B are probably an electron — positron pair. Therefore it is quite natural to consider the observed star to be the result of the decay of a neutral particle.

In fact, of the possible reactions of the interaction of neutrons (in the beam) with the gas of the chamber, the only events of this kind which may occur are those involving the production, in the same act, of two neutral π mesons or two charged π mesons and a neutral one in the absence of protons associated with the disintegration of a nucleus. In both cases we can observe a four-pronged star if each π^0 meson decays into γ quanta and an e^+, e^- pair (Dalitz pair). Under our conditions, however, such an event is extremely improbable, since the neutrons have a low energy. As a matter of fact, the mean energy of protons knocked out from the walls of the chamber by neutrons is 75 Mev, while among 10,000 recoil protons none were found to have an energy greater than 400 Mev. Moreover, among 15,000 stars recorded in the chamber gas, only 15 were observed to involve the production of one π^- meson; no reliable cases of pair production of π mesons (not to mention acts of triple production) were found. An estimate of the probability of observing one four-pronged star with the production, in one act, of two or three π mesons can be made on the basis of the experimental facts and investigations[2-4] of the meson production process in the interaction of nucleons. This estimate, in both cases, gives the value $\approx 10^{-7}$. The probability of a chance observation of two V^0 decays which might resemble a four-pronged star is also very small.

At the present time there is known only one type of decay which gives rise to four charged particles: This is the decay of a neutral π meson into two electron — positron pairs. In our case this extremely rare decay is practically excluded both from the magnitude of the probability of its observation, and from the kinematic relations. In particular, the divergence angle of the electrons in one of the pairs (tracks C and D) is very large (66°); moreover, the divergence angle is not in agreement with the energy of the γ quanta. It would be most natural to ascribe the event to a decay, not observed thus far, of a long-lived K^0 meson. There are two possible decays of this type allowed from the viewpoint of CP invariance:

$$K_2^0 \rightarrow \pi^+ + \pi^- + \gamma \rightarrow e^+ + e \ , \qquad (1)$$

$$K_2^0 \rightarrow \pi^+ + \pi^- + \pi^0 \begin{array}{l} \nearrow e^+ + e^- \\ \\ \searrow \gamma \end{array} \qquad (2)$$

According to the theoretical estimate of Dalitz,[5] the probability of a decay of the first type is only 4% of the probability of the decay of the second type; therefore it is more probable to interpret the

---

*The direction of the beam of neutral particles was at an angle of 97° to the direction of the protons incident on the target.

Track	Momentum (Mev/c)	Sign of charge	Angle of flight (deg)	Dip angle (deg)	Divergence angle (deg)
A	89±5	+	43.5±1.5	13.5±0.5	3
B	31,5±2	—	43.0±1.5	11.0±0.5	
C	?	—	33±5	33±5	66
D	160±16	+	32.0±1.5	16.5±0.5	

four-pronged event observed by us as the decay of a K_2^0 meson into three π mesons with a subsequent decay of the π^0 meson through a Dalitz pair.

For the decay in accordance with scheme (1), we can determine the mass of the decaying particle; it proved to be equal to (400 ± 40) Mev. In the case of the more probable scheme (2), we found the kinetic energy of the K_2^0 particle to be 80 Mev, where it was assumed that the K^0 mass was 496 Mev.

It should be noted that among the previously reported[6-8] decays of long-lived K^0 mesons there are three V^0 events in agreement with the assumption that the unobserved neutral decaying particle is a π^0 meson. The discovery of a four-pronged decay of the K_2^0 meson is direct evidence of the correctness of this assumption, and consequently is evidence of the existence of the decay of the long-lived K^0 meson in accordance with scheme (2). A few years ago a four-pronged decay[7] was observed in cosmic radiation* similar to that observed by us. The authors interpreted it as the decay of a τ^0 meson with a lifetime of 3×10^{-10} sec. Along with this, they recorded 43 decays of short-lived K^0 mesons. It is difficult, however, to bring these facts into agreement with the subsequent theoretical and experimental data, which indicate that the decay of the short-lived K^0 meson into three π mesons is strongly forbidden. At the same time, the probability of observing a similar decay of a long-lived K^0 meson under the conditions of their experiment, was small ($\approx 10^{-3}$). In our case, we were definitely dealing with the decay of a long-lived K^0 meson, since the internal target, which was the source of the neutral particles, was at a distance of 8 m from the point of observation. Even if we make the improbable assumption that the production of the decaying particle took place in the chamber wall, then its lifetime would exceed the value of the mean lifetime of the K_1^0 meson by one order of magnitude. As regards the expected probability of observation of a decay of a K_2^0 meson in accordance with scheme (2), it is 0.1 — 0.2, in agreement with the available experimental data.

We also observed two electron — positron pairs whose direction of flight was at a large angle ($\approx 90°$) with the collimator axis, so that it could not be caused by γ quanta present in the incident beam. There are grounds for considering these electron — positron pairs as Dalitz pairs arising from the decay $K_2^0 \rightarrow 3\pi^0$, the probability of which, apparently is not too different from the probability of the decay $K_2^0 \rightarrow \pi^+ + \pi^- + \pi^0$.*

To arrive at a final conclusion, however, it is necessary to accumulate further data and study the background conditions more carefully.

In conclusion, the authors express their gratitude to the members of the proton synchrotron crew for providing the experimental arrangement for this work; to B. Pontecorvo for his constant interest in, and attention to, this work; to M. A. Markov and M. I. Podgoretskiĭ for discussion and critical comments. The authors also thank D. Nyag for help in the calculations, and M. Kh. Anikina and P. I. Zhabin for taking part in the measurements.

[1] Dzhelepov, Kozodaev, Osipenkov, Petrov, and Rusakov, Приборы и техника эксперимента (Instrum. and Meas. Techniques) No 3, 3 (1956).

[2] E. L. Grigor'ev and L. P. Solov'eva, J. Exptl. Theoret. Phys. (U.S.S.R.) **31**, 932 (1956), Soviet Phys. JETP **4**, 801 (1957).

[3] Fowler, Shutt, Thorndike, and Whittemore, Phys. Rev. **95**, 1026 (1954).

[4] W. A. Wallenmeyer, Phys. Rev. **105**, 1058 (1957).

[5] R. H. Dalitz, Phys. Rev. **99**, 915 (1958).

[6] Bardon, Lande, Lederman, and Chinowsky, Ann. Phys. **5**, 156 (1958).

[7] Cooper, Filthuth, Newth, Petrucci, Salmeron, and Zichichi, Nuovo cimento **4**, 1433 (1956); Cooper, Filthuth, Montanet, Newth, Petrucci, Salmeron, Zichichi, Nuovo cimento **8**, 471, (1958).

[8] Crawford, Cresti, Douglass, Good, Kalbfleisch, Stevenson, and Ticho, Phys. Rev. Letters **2**, 266 (1959).

Translated by E. Marquit
13

---

*For this case the signs of the charges of two decay products were not determined.

*If it is assumed that the $K_{3\pi}^0$ decay results in a "symmetrical" state with an isospin I = 1 (as is the case for $K_{3\pi}^+$ decay), then, in good agreement with experiment, the selection rule $|\Delta I| = \frac{1}{2}$ leads in this case to the relation $w(K_2^0 \rightarrow 3\pi^0)/w(K_2^0 \rightarrow \pi^+ + \pi^- + \pi^0) = 3/2$.

SOVIET PHYSICS JETP VOLUME 12, NUMBER 1 JANUARY, 1961

MEASUREMENT OF THE ENERGY OF ALPHA PARTICLES FROM SOME EMITTERS

A. A. VOROB'EV, A. P. KOMAR, and V. A. KOROLEV

Leningrad Physico-Technical Institute, Academy of Sciences, U.S.S.R.

Submitted to JETP editor March 22, 1960

J. Exptl. Theoret. Phys. (U.S.S.R.) **39**, 70-72 (July, 1960)

Precise measurements of the energies of α particles from At^{217}, Fr^{221}, Po^{213}, U^{235}, and U^{238} have been performed with an ionization α spectrometer.

By means of an ionization α spectrometer we measured the energy of the α particles from some emitters. The measurement of the value of the ionization was carried out by the method of comparison of the pulse amplitudes from the α particles with generator pulses, whose amplitude was measured with great precision (~ 0.01%). In order to completely exclude the effect of positive ions, we used two screening grids. The chamber was filled with a mixture of argon and methane (97% Ar, 3% CH_4). Here, the correction for the pulse rise time was negligibly small. The half-width of the α lines was 35 kev. The required stability of the gain of the amplifier channel was provided by a forced-stabilization circuit. In determining the energy of the α particles it is necessary to know the relation between the ionization and energy. The calibration measurements shown in Table I indicated that the relation between the ionization and energy can be represented by a straight line intersecting the energy axis at $E_\alpha = 84$ kev, which coincides with the results of reference 1. Therefore the energy of the α particles was calculated from the formula

$$(E_e - 84)/(E_\alpha - 84) = I_e/I_\alpha, \qquad (1)$$

where E_e and E_α are the energies (in kev) of the α particles from the standard and the investigated emitters; I_e and I_α are the values of the produced ionization.

In Table I are shown the results of the measurement of the energies of some emitters used for calibration. We took the Th^{228} line as a standard.

TABLE I

Element	E_{mag} (Mev)	I	E_{ioniz} (Mev)
Th^{228}	5.421	1.0000	5.421
Ra^{224}	5,681	1.0485	5.680
Rn^{220}	6.278	1,1602	6.276
Po^{216}	6.775	1.2533	6.773
Po^{212}	8,780	1.6306	8.786

In the first column are shown the results of the energy measurements known from magnetic analysis,[2] in the second column is shown the value of ionization in relative units, and in the third column is shown the α-particle energy determined from (1). The measured values of the energies are in good agreement with the known values, which indicates the reliability of the α-particle energy measurements by means of the ionization α spectrometer.

Table II lists the results of the measurements of the α-particle energy of some emitters.

The measurement of the At^{217}, Fr^{221}, and Po^{213} spectra were made simultaneously with the measurement of the energy-ionization relation. Therefore the check points shown in Table I serve as standards in the given case.

$\underline{At^{217}}$. The measured energy values sharply differ from the results of references 3 and 5, and exceed by 14 kev the energy values obtained by Stephens.[4] In the first two experiments an ionization chamber was used. The results of the energy measurement in reference 3 should be considered only as an estimate. As regards Cranshaw and Harvey,[5] their method of energy measurement is highly inaccurate. Moreover, errors due to the poor screening of the grid and the low resolving power of the spectrometer are possible. It is characteristic that the energy values of other α emitters (U^{233}, Pu^{239}) obtained in this work differ from subsequent measurements by 10 — 15 kev, although the error of measurement indicated by the authors is 3 and 5 kev. Thus, there are grounds for considering the results of the energy measurements in reference 5 to be in error. The difference between the energy value measured by us and that measured on the magnetic spectrometer[4] lies within the limits of experimental error.

$\underline{Fr^{221}}$. The measured energy value is in good agreement with the results of Stephens,[4] but, as in the case of At^{217}, it sharply differs from the energy

TABLE II

Element	E_α, (Mev)	
	our data	data of other authors
At^{217}	7,064±0.005	7.00±0,05 [3]; 7.05 ±0.01 [4]; 7,023±0.01 [5]
Fr^{221}	6,336±0.005	6.30±0.05 [3]; 6.332±0.01 [4]; 6,298±0.01 [5]
Po^{213}	8,368±0.010	8.34±0.01 [3]; 8.35 ±0.01 [4]; 8.336±0.005 [5]
U_I^{235}	4,396±0,003	4.354 [6]; 4.40 [7]
U_{II}^{235}	4.211±0.003	4.117 [6]; 4.20 [7]
U^{238}	4,190±0.005	4.195 [1]; 4.18 [9]

values obtained in references 3 and 5.

Po^{213}. In this case the basic line broadens out towards the higher energies, owing to the ionization produced by the β particles preceding α decay, which decreases the accuracy of the energy measurement. The value obtained is 18 kev greater than the result of the energy measurement by the magnetic spectrometer. The results differ from those of references 3 and 5 by approximately 30 kev.

U^{235}. For the energy measurement the basic line from U^{234} present in the same source (E_α = 4.768 Mev) was used as a standard. In Table II are shown the energy values for the two largest intensities of the lines of U_I^{235} and U_{II}^{235}. These values are in sharp disagreement with the results of the energy measurements of Pilger et al. on the magnetic spectrometer.[6] Better agreement was observed with the results of Ghiorso,[7] although these measurements bore only a qualitative character. Recently, an investigation of the α spectra of U^{235} was made on a new magnetic spectrometer of greater luminosity (Baranov, Zelenkov, et al.[8]); the following energy values of the line spectra we are considering were obtained:

$$E_I = 4.394 \pm 0.002, \qquad E_{II} = (4.213 \pm 0.002)\ \text{Mev}.$$

These values are in excellent agreement with our results. The obtained agreement is also evidence of the fact that the ionization — energy relation remains linear, at least up to the energies of E_α = 4 Mev.

U^{238}. The measurement of the energy of the ground line of U^{238} was carried out with a source containing a natural mixture of uranium isotopes. The U^{238} ground line served as the standard. The obtained energy value coincides with the results of reference 1.

---

[1] Harvey, Jackson, Eastwood, and Hanna, Can. J. Phys. **35**, 258 (1957).

[2] Strominger, Hollander, and Seaborg, Revs. Modern Phys. **30**, 585 (1958).

[3] Hagemann, Katzin, Studier, Seaborg, and Ghiorso, Phys. Rev. **79**, 435 (1950).

[4] F. S. Stephens, Thesis, University of California 1955.

[5] T. E. Cranshaw and J. A. Harvey, Can. J. Research **26**, 243 (1948).

[6] Pilger, Stephens, Asaro, and Perlman, Bull. Am. Phys. Soc., Ser. II, **2**, 394 (1957).

[7] A. Ghiorso, Phys. Rev. **82**, 979 (1951).

[8] S. A. Baranov and A. G. Zelenkov, Report at the 10th Annual Conference on Nuclear Spectroscopy, M., 1960.

[9] Clark, Spencer-Palmer, and Woodward, J. South African Chem. Inst. **10**, 2, 74 (1957).

Translated by E. Marquit
14

SOVIET PHYSICS JETP VOLUME 12, NUMBER 1 JANUARY, 1961

FINITE-AMPLITUDE WAVES IN A MULTI-COMPONENT CONDUCTING MEDIUM

V. S. TKALICH

Submitted to JETP editor October 22, 1959

J. Exptl. Theoret. Phys. (U.S.S.R.) 39, 73-77 (July, 1960)

The set of equations for a non-ideal plasma in the hydrodynamic approximation is reduced to a linear one without assuming that the signal is small. Propagation of finite amplitude waves in the presence of a magnetic field is investigated; a comparison is made with well known results obtained on the basis of other assumptions.

1. The set of equations of the hydrodynamic approximation for a plasma consisting of N kinds of ions (each of which is treated as an incompressible fluid) has the following form[1-7]

$$\operatorname{curl}\mathbf{e} = -\frac{\mu}{c}\frac{\partial\mathbf{h}}{\partial t}, \qquad \operatorname{curl}\mathbf{h} = \frac{\varepsilon}{c}\frac{\partial\mathbf{e}}{\partial t} + \frac{4\pi}{c}\sum_{l=1}^{N} e_l n_l \mathbf{v}_l,$$

$$\operatorname{div}\mathbf{h} = 0, \qquad \operatorname{div}\varepsilon\mathbf{e} = 4\pi\sum_{l=1}^{N} e_l n_l, \qquad \operatorname{div}\mathbf{v}_k = 0,$$

$$\partial\mathbf{v}_k/\partial t + \nabla w_k = [\mathbf{v}_k\times[\operatorname{curl}\mathbf{v}_k + (\mu e_k/cm_k)\,\mathbf{h}]] + (e_k/m_k)\,\mathbf{e}$$
$$+\sum_{l=1}^{N}\nu_{kl}(\mathbf{v}_l-\mathbf{v}_k) - \nu_k\operatorname{curl}\operatorname{curl}\mathbf{v}_k$$
$$(k,\ l = 1,\ 2,\ \ldots,\ N), \tag{1}$$

where $w_k \equiv v_k^2/2 + p_k/m_k n_k + F_k$ is the sum of the kinetic, thermal and potential energy per unit mass of ions of the k-th kind; ν_k is the kinematic coefficient of viscosity; ν_{kl} is the effective frequency of collisions of an ion of type k with ions of type l.

We resolve the field π consisting of the set of quantities ($\mathbf{h}$, $\mathbf{e}$, $\mathbf{v}_k$, w_k) into a field Π_0 ($\mathbf{H}_0$, $\mathbf{E}_0$, $\mathbf{V}_{k0}$, W_{k0}) which represents some known solution of the system (1), and an auxiliary field to be determined Π ($\mathbf{H}$, $\mathbf{E}$, $\mathbf{V}_k$, W_k)

$$\mathbf{h} = \mathbf{H}_0 + \mathbf{H}, \qquad \mathbf{e} = \mathbf{E}_0 + \mathbf{E},$$
$$\mathbf{v}_k = \mathbf{V}_{k0} + \mathbf{V}_k, \qquad w_k = W_{k0} + W_k. \tag{2}$$

On introducing the vector potential $\mathbf{A}$ for the auxiliary field Π

$$\mathbf{H} = \operatorname{curl}\mathbf{A}, \qquad \mathbf{E} = -c^{-1}\,\partial\mathbf{A}/\partial t, \tag{3}$$

the system of equations for the field Π($\mathbf{A}$, $\mathbf{V}_k$, W_k) may be re-written in the form

$$\operatorname{div}\mathbf{A} = 0, \qquad \operatorname{div}\mathbf{V}_k = 0,$$

$$\left(\operatorname{curl}\operatorname{curl} + \frac{\varepsilon\mu}{c^2}\frac{\partial^2}{\partial t^2}\right)\mathbf{A} = \frac{4\pi}{c}\sum_{l=1}^{N} e_l n_l \mathbf{V}_l, \tag{4}$$

$$\frac{\partial}{\partial t}\left(\mathbf{V}_k + \frac{\mu e_k}{cm_k}\mathbf{A}\right) + \nabla W_k = \left[\mathbf{V}_k\times\operatorname{curl}\left(\mathbf{V}_k + \frac{\mu e_k}{cm_k}\mathbf{A}\right)\right]$$
$$+\sum_{l=1}^{N}\nu_{kl}(\mathbf{V}_l-\mathbf{V}_k) - \nu_k\operatorname{curl}\operatorname{curl}\mathbf{V}_k + \left[\mathbf{V}_k\times\left(\operatorname{curl}\mathbf{V}_{k0}\right.\right.$$
$$\left.\left.+\frac{\mu e_k}{cm_k}\mathbf{H}_0\right)\right] + \left[\mathbf{V}_{k0}\times\operatorname{curl}\left(\mathbf{V}_k + \frac{\mu e_k}{cm_k}\mathbf{A}\right)\right]. \tag{5}$$

Equation (5) can be made linear if we restrict ourselves to the consideration of "helical" motions

$$\operatorname{curl}[\mathbf{V}_k + (\mu e_k/cm_k)\mathbf{A}] = a_k\mathbf{V}_k, \tag{6}$$

where $a_k = a_k(\mathbf{r},\ t)$ satisfies the condition $(\mathbf{V}_k\nabla)\,a_k = 0$. The method of linearizing helical fields in ordinary hydrodynamics,[8,9] applied[10] to stationary helical motions of the form (6) is generalized in this paper to non-stationary fields. On setting $a_k = a_k(t)$ ("homogeneous" helical motion) and on substituting (6) into the equation of motion (5), we obtain

$$\frac{\partial}{\partial t}\left(\mathbf{V}_k + \frac{\mu e_k}{cm_k}\mathbf{A}\right) + \nabla W_k = \sum_{l=1}^{N}\nu_{kl}(\mathbf{V}_l-\mathbf{V}_k)$$
$$-\nu_k\operatorname{curl}\operatorname{curl}\mathbf{V}_k + \left[\mathbf{V}_k\times\left((\operatorname{curl}-a_k)\,\mathbf{V}_{k0} + \frac{\mu e_k}{cm_k}\mathbf{H}_0\right)\right]. \tag{7}$$

On replacing (7) by the condition that the equations are soluble (by taking the curl) and on taking (6) into account we obtain

$$\frac{\partial}{\partial t}(a_k\mathbf{V}_k) = \sum_{l=1}^{N}\nu_{kl}\operatorname{curl}(\mathbf{V}_l-\mathbf{V}_k) - \nu_k(\operatorname{curl})^3\,\mathbf{V}_k$$
$$+\left\{\left[(\operatorname{curl}-a_k)\,\mathbf{V}_{k0} + \frac{\mu e_k}{cm_k}\mathbf{H}_0\right]\nabla\right\}\mathbf{V}_k$$
$$-(\mathbf{V}_k\nabla)\left[(\operatorname{curl}-a_k)\,\mathbf{V}_{k0} + \frac{\mu e_k}{cm_k}\mathbf{H}_0\right]. \tag{8}$$

In the simplest case when the quantity in the square brackets does not depend on the coordinates, i.e., when

$$(\operatorname{curl}-a_k)\,\mathbf{V}_{k0} + (\mu e_k/cm_k)\,\mathbf{H}_0 = \mathbf{f}_k(t),$$

equation (8) assumes a particularly simple form

$$\frac{\partial}{\partial t}(a_k\mathbf{V}_k) = \sum_{l=1}^{N} \nu_{kl}\,\mathrm{curl}\,(\mathbf{V}_l - \mathbf{V}_k) - \nu_k\,(\mathrm{curl}\,)^3\mathbf{V}_k + \{[(\mathrm{curl} - a_k)\,\mathbf{V}_{k0} + (\mu e_k/cm_k)\,\mathbf{H}_0]\,\nabla\}\,\mathbf{V}_k. \tag{9}$$

Thus, when the set Π_0 — a certain solution of the system (1) — is known, then (4), (6), and (8) represent a system of linear partial differential equations. Since this system is linear, the vector fields $\Pi\,(\mathbf{A}, \mathbf{V}_k)$ satisfy the superposition principle. We note that the problem of the validity of the superposition principle for finite amplitude fields has been previously studied in a number of papers.[6–12]

2. By utilizing the method developed for stationary helical motion[10] we obtain an equation for the vector potential $\mathbf{A}$, and also expressions for the partial currents. On introducing the notation

$$\Omega_k^2 \equiv 4\pi e_k^2 n_k/m_k, \qquad \Omega^2 \equiv \sum_{l=1}^{N} \Omega_l^2, \quad \mathbf{U}_k \equiv 4\pi e_k n_k c^{-1}\mathbf{V}_k,$$
$$\hat{\alpha}_k \equiv a_k - \mathrm{curl},\ \hat{\alpha}_0 \equiv -\mathrm{curl},\ \hat{\beta} \equiv \mathrm{curl\ curl} + \varepsilon\mu c^{-2}\partial^2/\partial t^2, \tag{10}$$

where all the operators $\hat{\alpha}_k$ and $\hat{\alpha}_0$ commute[13,14] with each other (and also with $\hat{\beta}$, if a_k = const), we rewrite the system (4) and (6) in the following form

$$\sum_{l=1}^{N} \mathbf{U}_l = \hat{\beta}\mathbf{A}, \qquad \hat{\alpha}_k\mathbf{U}_k + (\Omega_k/c)^2\hat{\alpha}_0\mathbf{A} = 0,$$
$$\mathrm{div}\,\mathbf{A} = 0, \quad \mathrm{div}\,\mathbf{U}_k = 0. \tag{11}$$

On multiplying the first equation of (11) by the operator $\hat{L}$

$$\hat{L} \equiv \prod_l \hat{\alpha}_l \equiv \hat{L}_k\hat{\alpha}_k, \tag{12}$$

where the product is taken over all the different $\hat{\alpha}_k$, and on utilizing the second equation of (11), we obtain the equation for the vector potential $\mathbf{A}$

$$\left[\hat{L}\hat{\beta} + \hat{\alpha}_0 \sum_{l=1}^{N} (\Omega_l/c)^2\hat{L}_l\right]\mathbf{A} = 0. \tag{13}$$

On multiplying the second equation of (11) by a_k^{n-1} and on summing over all k we obtain the recurrence relation[10]

$$\sum_{l=1}^{N} a_l^n\mathbf{U}_l = \mathrm{curl}\left[\sum_{l=1}^{N} a_l^{n-1}\mathbf{U}_l + \mathbf{A}\sum_{l=1}^{N} a_l^{n-1}(\Omega_l/c)^2\right],$$

from which with the aid of the first of relations (11) we obtain

$$\sum_{l=1}^{N} a_l^n\mathbf{U}_l = \left[(\mathrm{curl})^n\hat{\beta} + \sum_{l=1}^{N}(\Omega_l/c)^2 \sum_{m=1}^{n} a_l^{n-m}(\mathrm{curl})^m\right]\mathbf{A}. \tag{14}$$

On setting in (14) n = 1, 2, , . . . , N − 1 we obtain together with the first equation of (11) a system of algebraic equations linear in $\mathbf{U}_k$. It is soluble if among the a_k there are no equal ones ($a_k \neq a_l$, $k \neq l$), since its determinant is a Vandermonde determinant.[14] On solving it we obtain a linear differential operator $\hat{\gamma}_k$ which on being applied to the vector potential $\mathbf{A}$ yields

$$\mathbf{U}_k = \hat{\gamma}_k\mathbf{A}. \tag{15}$$

3. We consider fields in a neutral plasma in the presence of a constant homogeneous magnetic field $\mathbf{H}_0$ = const. On setting

$$\mathbf{E}_0 = \mathbf{V}_{k0} = \nu_{kl} = \nu_k = 0, \qquad a_k = \mathrm{const},$$
$$W_{k0} = \mathrm{const}, \qquad \varepsilon = \mu = 1,$$

we obtain from (9) with the aid of (15) the following equation

$$\hat{\gamma}_k\,[a_k\partial/\partial t - (e_k/cm_k)\,(\mathbf{H}_0\nabla)]\,\mathbf{A} = 0, \tag{16}$$

which must be solved simultaneously with (13).

For a progressive wave of the simple harmonic form

$$\mathbf{A} = \mathbf{A}_0\exp\{i(\omega t - \varkappa\mathbf{nr})\}, \qquad \mathbf{V}_k = \mathbf{V}_{0k}\exp\,\{i(\omega t - \varkappa\mathbf{nr})\} \tag{17}$$

(ω is the frequency, κ is the wave number, $\mathbf{n}$ is a unit vector in the direction of motion of the wave, $\mathbf{A}_0$ and $\mathbf{V}_{0k}$ are complex amplitudes) on substituting (17) into (16) we obtain

$$a_k = -\varkappa\mathbf{n}\boldsymbol{\omega}_k/\omega, \qquad \boldsymbol{\omega}_k \equiv e_k\mathbf{H}_0/cm_k. \tag{18}$$

On substituting (17) into (6) we obtain the amplitudes

$$\mathbf{V}_{0k} = (e_k/cm_k)\,(s\mathbf{n}\boldsymbol{\omega}_k/\omega - 1)^{-1}\mathbf{A}_0,\ \mathbf{A}_0 = [\mathbf{n}\times\mathbf{b}] + is\,[\mathbf{n}\times[\mathbf{n}\times\mathbf{b}]], \tag{19}$$

where $\mathbf{b}$ is an arbitrary constant vector, the quantity s characterizes the polarization of the wave $s = \pm 1$. The vectors $\mathbf{A}$ and $\mathbf{V}_k$ whose amplitudes satisfy a relation of the form $\mathbf{A}_0\mathbf{A}_0 = 0$ are circularly polarized.

On utilizing (4), (17), and (19) we obtain in the usual manner[1,2] the dielectric constant of the plasma ϵ_0

$$\varepsilon_0 = 1 - \sum_{l=1}^{N} (\Omega_l/\omega)^2 \,/\, [1 - (s\mathbf{n}\boldsymbol{\omega}_l/\omega)], \tag{20}$$

and from the condition that the equations are soluble we obtain the phase velocity $V_{ph} \equiv \omega/\kappa$

$$V_{\mathrm{ph}} = \pm c/\sqrt{\varepsilon_0}. \tag{21}$$

It follows from (20) and (21) that there exist two waves (corresponding to $s = \pm 1$) of different polarization (leading to different ϵ_0) which are propagated with different phase velocities.

If $\omega \to s\mathbf{n}\boldsymbol{\omega}_k$, then for a fixed $\mathbf{A}_0$ the velocity $\mathbf{V}_{0k}$ should in accordance with (19) increase without limit. However, the relation (19) and the approximation itself cease to hold when V_{0k} becomes comparable to the corresponding thermal velocity V_{kT}.

4. We now give the principal conditions under which the hydrodynamic approximation is applic-

able to plasma. Let L and T be the characteristic length and time for the process; let λ_k and τ_k be the mean free path and the corresponding time, and let V_{kT} be the thermal velocity for the k-th type of ions. We can consider the medium to be continuous if the process is sufficiently slow $(T \gg \tau_k)$ and the gas is sufficiently dense $(L \gg \lambda_k)$. The pressure p_k is scalar if the magnetic fields are sufficiently weak $(2\pi c m_k/He_k \gg \tau_k, \lambda_k/V_{kT})$.

The plasma may be regarded as incompressible if its temperature is sufficiently great, i.e., if the velocity of thermal motion V_{kT} is considerably greater than both the velocity of ordered motion v_k $(V_{kT} \gg |v_k|)$, and also the velocity of propagation of the disturbance being considered in the given approximation $(V_{kT} \gg V_{ph})$.

If for a certain type of motion one of the kinds of ions (there may be several such kinds) plays no essential role (for example, the partial currents due to it are small), then the above conditions need not necessarily be satisfied for it. The latter conditions are similar to the conditions for the applicability of ordinary magnetohydrodynamics,[4,12,15] but are not so restrictive.

We assume that the plasma has two components. Then with the aid of (20) and (21) we obtain the expression for the phase velocity

$$V_{\mathrm{ph}}^2 = (c\omega / \Omega)^2 (1 - s\mathbf{n}\boldsymbol{\omega}_l/\omega)(s\mathbf{n}\boldsymbol{\omega}_i/\omega - 1), \qquad (22)$$

which coincides with the expression obtained from formula (13) of Braginskiĭ's paper[3] if the plasma is regarded as incompressible, and if the transition is made to the limit $c_l, c_i \to \infty$.

On assuming that the frequencies in formula (22) are small $(\mathbf{n}\boldsymbol{\omega}_i \gg \omega)$ we obtain an expression for the phase velocity

$$V_{\mathrm{ph}} \approx (H_0/\sqrt{4\pi M n}) \cos(\widehat{\mathbf{n}\mathbf{H}_0}),$$

which coincides respectively with expressions (2.23) and (2.18) of Syrovat-skiĭ's paper[15] for the Alfven and for the slow magnetoacoustic waves (in the limiting case of high temperature $V_T \to \infty$).

We note that the well known expressions[1,2] for the dielectric permittivity tensor were obtained for the case of zero temperature $(V_{kT} \to 0)$ and for infrequent collisions $(T \ll \tau_k)$, i.e., in a limiting case which is the opposite to the one considered here.

5. The boundary conditions which have to be adopted in solving the system (1) assume different forms depending on the properties of the plasma boundary and on the nature of the process. If an ideal $(\nu_{kl} = \nu_k = 0)$ plasma is bounded by a dielectric, then on integrating (1) in the simplest case when there are no surface charges or currents we obtain the following boundary conditions:[5]

$$[\mathbf{h}_t] = [\mathbf{e}_t] = [\mu \mathbf{h}_n] = [\varepsilon \mathbf{e}_n] = \mathbf{v}_{kn} = 0. \qquad (23)$$

The square brackets denote the difference between the values of the quantity contained within the brackets taken on the two sides of the boundary; the index t denotes the tangential (to the plasma boundary) components of the vectors, while the index n denotes the normal components. On utilizing (2) we bring the conditions (23) into the form

$$[(\mathbf{H}_0 + \mathbf{H})_t] = [(\mathbf{E}_0 + \mathbf{E})_t] = [\mu(\mathbf{H}_0 + \mathbf{H})_n]$$

$$= [\varepsilon(\mathbf{E}_0 + \mathbf{E})_n] = (\mathbf{V}_{k0} + \mathbf{V}_k)_n = 0,$$

which is the most convenient one for the solution of problems by means of the present method.

In conclusion the author expresses his deep gratitude to N. V. Saltanov and E. F. Tkalich for discussions.

---

[1] E. Aström, Ark. f. Fys. 2, 443 (1951).

[2] Al'pert, Ginzburg, and Feĭnberg, Распространение радиоволн (Propagation of Radio Waves), Gostekhizdat, (1953).

[3] S. I. Braginskiĭ, Dokl. Akad. Nauk SSSR, 115, 473 (1957).

[4] S. I. Braginskiĭ, Collection Вопросы магнитной гидродинамики и динамики плазмы (Problems of Magnetohydrodynamics and Plasma Dynamics), Riga, 1959, p. 67.

[5] Chandrasekhar, Kaufman, and Watson, Ann. Phys. 5, 1 (1958).

[6] V. S. Tkalich, loc. cit. ref. 4, p. 191.

[7] V. S. Tkalich, Izv. Akad. Nauk SSSR Ser. Fiz., OTN, MM, No 5, (1959).

[8] I. S. Gromeka, Collected Works, USSR Acad. Sci., 1952, p. 76.

[9] O. F. Vasil'ev, Основы механики винтовых и циркуляционных потоков (Fundamentals of the Mechanics of Helical and Circulating Flows), Gosenergoizdat, (1958).

[10] E. F. Tkalich and V. S. Tkalich, Izv. Akad. Nauk SSSR Ser. Fiz., OTN, MM, in press.

[11] J. N. Kapur, Appl. Sci. Research 8A, 2-3, 198 (1959).

[12] H. Alfen, Cosmical Electrodynamics, Oxford, (1950).

[13] N. E. Kochin, Векторное исчисление и начала тензорного исчисления (Vector Calculus and Intro-

duction to Tensor Calculus), USSR Acad. Sci., (1951).

[14] V. I. Smirnov, Курс высшей математики (Course of Higher Mathematics), Vol. 3, part 1, Gostekhizdat, (1953).

[15] S. I. Syrovat-skiĭ, Usp. Fiz. Nauk, 62, 247 (1957).

Translated by G. Volkoff
15

SOVIET PHYSICS JETP VOLUME 12, NUMBER 1 JANUARY, 1961

π^--MESIC DECAY OF THE $_\Lambda H^3$ HYPERNUCLEUS

V. A. LYUL'KA

Submitted to JETP editor February 4, 1960

J. Exptl. Theoret. Phys. (U.S.S.R.) **39**, 78-79 (July, 1960)

The ratio of the lifetimes of the decays $_\Lambda H^3 \rightarrow He^3 + \pi^-$ and $_\Lambda H^3 \rightarrow d + p + \pi^-$ is considered in the impulse approximation, with the interaction in the proton — deuteron system taken into account. It is shown that for a spin j = ½ of the $_\Lambda H^3$ hypernucleus the value of this ratio is in good agreement with the experimental value.

As is known, the study of the different channels of decay of hypernuclei can supply information on the character of the Λ-nucleon forces and the spin of hypernuclei.[1-3] Picasso and Rosati[1] showed that the ratio of the half-lives for

$$H^3_\Lambda \rightarrow He^3 + \pi^-, \tag{1}$$

$$H^3_\Lambda \rightarrow d + p + \pi^- \tag{2}$$

indicates that for the spin of the $_\Lambda H^3$ hypernucleus the value ½ is a preferable one; however, full agreement on the values of this ratio obtained from experiment is still lacking.

In the present article we shall show that, by taking into account the effect of the interaction in the final state, which has not been done in references 1 and 2, one may obtain better agreement between theory and the experimental data. The interaction of π mesons with other decay products at the energies considered is small, since the basic effect is associated with the interaction in the proton — deuteron system.

The amplitude of the Λ-particle decay in a hypernucleus has the form

$$M = g_s + g_p (\sigma \mathbf{k}) / k_0,$$

where k_0 is the π-meson momentum in the decay of a free Λ particle (~101 Mev/c).

The square of the matrix element of the decay (2) as a function of the spin j of the $_\Lambda H^3$ hypernucleus, after averaging over the spin states (our choice of the wave function for the p — d system was analogous to that of Buckingham and Massey[4]), takes the form

$$|M_{if}|^2 = \left(g_s^2 + \frac{1}{9} g_p^2 \frac{k^2}{k_0^2}\right) |I^d|^2 + \frac{8}{9} g_p^2 \frac{k^2}{k_0^2} |I^q|^2 \text{ for } j = 1/2,$$

$$|M_{if}|^2 = \frac{4}{9} g_p^2 \frac{k^2}{k_0^2} |I^d|^2 + \left(g_s^2 + \frac{5}{9} g_p^2 \frac{k^2}{k_0^2}\right) |I^q|^2 \text{ for } j = 3/2. \tag{3}$$

Here

$$I^{q,d} = \int \Psi^{q,d+}_{\mathbf{k}_f} (\mathbf{r}_\Lambda, \mathbf{r}_p, \mathbf{r}_n) \Psi_d (r_n r_p) e^{-2i\mathbf{k}\rho/3} \Psi_{H^3_\Lambda}$$
$$\times (\mathbf{r}_\Lambda, \mathbf{r}_p, \mathbf{r}_n)\, d\mathbf{r}_\Lambda d\mathbf{r}_p d\mathbf{r}_n,$$

$$\Psi^{q,d}_{\mathbf{k}_f} = e^{i\mathbf{k}_f \rho} + (k_f \rho)^{-1} e^{-i\mathbf{k}_f \rho}$$
$$\times \sum_l (-1)^l (2l + 1) \exp\{-i\delta_l^{q,d}\} \sin \delta_l^{q,d} P_l (\cos\theta),$$

$\delta l^{q,d}$ are the phase shifts in the states with spins 3/2 and ½ (reference 5), **k** is the π-meson momentum, $\mathbf{k}_f$ is the relative momentum of the p — d system, $\boldsymbol{\rho} = \mathbf{r}_\Lambda - \frac{1}{2}(\mathbf{r}_p + \mathbf{r}_n)$.

We took into account for the p — d system only states with $l = 0$ and $l = 1$, since at the energies under consideration the phase shifts for $l \geq 2$ are small. Thus, inclusion of the interaction in the final state leads to the probability of decay (2) being dependent on the spin of the $_\Lambda H^3$ hypernucleus (cf. reference 1). In the absence of such an interaction $I^q = I$, and from (3) we find that the probability of this decay does not depend on j (conclusion from reference 1).

For a decay of the type (1) the square of the matrix elements was calculated by Picasso and Rosati:[1]

$$|M_{if}|^2 = \tfrac{1}{12} (9g_s^2 + g_p^2 k^2/k_0^2) |I|^2 \text{ for } j = 1/2,$$

$$|M_{if}|^2 = \tfrac{1}{3} g_p^2 (k^2/k_0^2) |I|^2 \qquad \text{for } j = 3/2. \tag{4}$$

Here

$$I = \int \Psi^+_{He_3} (\mathbf{r}_\Lambda, \mathbf{r}_p, \mathbf{r}_n)\, e^{-i\mathbf{k}\mathbf{r}_\Lambda} \Psi_{H^3_\Lambda} (\mathbf{r}_\Lambda, \mathbf{r}_p, \mathbf{r}_n)\, d\mathbf{r}_\Lambda d\mathbf{r}_p d\mathbf{r}_n.$$

Using (2) and (3), one may calculate, as in reference 1, the ratio of the lifetimes w^j of decays (1) and (2) for the two spin values of j of the $_\Lambda H^3$ hypernucleus. The wave functions $\Psi_{_\Lambda H^3}$ and Ψ_{He^3} were taken the same as in reference 1. The account of the Coulomb interaction was similar to that used by Tang.[6] In accordance with recent data, the ratio $x = g_s^2/g_p^2$

was limited to the values $1 \leq x \leq 5$. With a change of x in the given limits, the ratio of the lifetimes of decays (1) and (2) changes within the following limits:

$$0.67 \geqslant w^{1/2} \geqslant 0.53; \qquad 1.42 \leqslant w^{3/2} \leqslant 5.31.$$

Thus the spin value $j = 1/2$ for the $_\Lambda H^3$ hyperfragment is in satisfactory agreement with experiment, which gives $w_{exp} \lesssim 1$. Here, the agreement is better than in the case of Picasso and Rosati, who obtained for the same x values of $w^{1/2}$ greater than unity.

In conclusion, I thank Professor D. D. Ivanenko for his interest in this work, and also N. S. Il'ina for performing the numerical calculations.

[1] L. E. Picasso and S. Rosati, Nuovo cimento **11**, 711 (1959).

[2] M. Leon, Phys. Rev. **113**, 1604 (1959).

[3] R. H. Dalitz, Phys. Rev. **112**, 605 (1958).

[4] R. A. Buckingham and H. S. W. Massey, Proc. Roy. Soc. (London) **A179**, 123 (1942).

[5] H. S. W. Massey, Progr. in Nuclear Phys. **3**, 249 (1953).

[6] Y. C. Tang, Nuovo cimento **10**, 780 (1958).

Translated by E. Marquit
16

SOVIET PHYSICS JETP VOLUME 12, NUMBER 1 JANUARY, 1961

EXPERIMENTAL INVESTIGATION OF CYCLOTRON RESONANCE IN METALS

M. Ya. AZBEL' and É. A. KANER

Physico-Technical Institute, Academy of Sciences, Ukr. S.S.R.

Submitted to JETP editor December 16, 1959

J. Exptl. Theoret. Phys. (U.S.S.R.) 39, 80-87 (July, 1960)

The results of some recent studies of cyclotron resonance in metals are discussed. Some additional opportunities for an experimental investigation of this phenomenon are indicated.

1. Many recent papers have been devoted both to experimental[1-13] and to the theoretical[14-26] investigations of cyclotron resonance in metals. Fawcett,[1] Bezuglyĭ and Galkin,[2] Kip et al.[3] and Khaĭkin[4] observed resonance in tin, while Bezuglyĭ and Galkin carried out additional investigations on lead[5] and indium.[6] Bismuth and its alloys with tin and thallium were studied by Aubrey and Chambers[7] and Galt et al.,[8] copper by Fawcett[1] and Langenberg et al.,[9,10] zinc by Galt et al.[11] and aluminum by Langenberg and Moore[12] and also by Fawcett.[13] Thus, cyclotron resonance has been observed by now in seven metals. It is consequently of interest to evaluate the experimental results, to ascertain the degree of their agreement with theoretical predictions, and to indicate certain supplementary possibilities of experimental investigation of cyclotron resonance in metals. This is the purpose of the present article.

The authors have shown earlier[22-26] that in metals at low temperatures in a constant magnetic field **H** parallel to the surface of the metal there is resonant absorption of energy from the high frequency field. The absorption has a minimum at resonance. The resonance takes place in magnetic fields corresponding to the values of the cyclotron frequency* $\Omega_q \approx \omega/q$, where ω is the frequency of the alternating magnetic field and $q = 1, 2, 3\ldots$. Variation of only the resonant frequencies $\Omega = eH/mc$ or the distances between them (e is the absolute value of the electron charge and c the velocity of light) permits a direct determination of the effective mass m of the electrons ("holes") in the metal and its anisotropy.†

The effective mass will be determined the more accurately, the greater, on the one hand, the average mean free time of the electrons τ_0 (that is, $\omega\tau_0$) and the more accurately, on the other hand, are satisfied in the experiment the theoretical requirements that the magnetic field be parallel to the surface of the metal and that this surface be of highest quality. As $\omega\tau_0$ tends to infinity, the equation $\Omega = \omega/q$, which determines the position of the resonance, becomes exact and not approximate, as in the case of finite value $\omega\tau_0$. If $\omega\tau_0$ does not have the finite value called for by the theory, the absorption minimum shifts towards the smaller magnetic fields. However, independently of the satisfaction of these requirements, the value obtained for the effective mass will be approximately correct.

In contradistinction, the shape of the resonance curve and the sharpness of the resonance are quite sensitive to the parallelness of the magnetic field and to the surface finish; furthermore, the stronger the magnetic field, the more stringent these requirements. Failure to satisfy these requirements may lead to a change in the order of magnitude of the depth and width of the resonance. A quantitative comparison of these characteristics of the resonant curves with theory is possible only when the theoretically predicted law of decrease of surface impedance of the metal, $Z \sim H^{-1/3}$, is satisfied in strong magnetic fields, where $Z = R + iX$ (see references 20, 24, and 25). If the theoretical requirements are satisfied and the dependence $R \sim H^{-1/3}$ is experimentally satisfied in a strong field, a more detailed quantitative comparison of the experimental data with theory is possible. Since the law of dispersion of current carriers in the metals is not known beforehand, and the dependence of Z on H is essentially connected with the form of the dispersion law, comparison with theory must be carried out either near resonance, or in strong fields where all the dependences can be determined in explicit form.

---

*We emphasize that the multiplicity of the resonant frequencies is connected with the anomalous character of the skin effect, and not with the deviation of the dispersion from quadratic, and takes place even with a square-law dispersion.

†In the case of a non-quadratic dispersion, when the effective mass depends on the projection p_z of the electron momentum p in the direction of the magnetic field $\mathbf{H} \parallel z$, we have in mind here the extremal value of $m(p_z)$ with respect to p_z. In this case the sharpness and width of each resonant line differs for the minimum and maximum (with respect to p_z) values of the effective mass.[22-26]

The use of a simple formula for the quadratic dispersion law in the reduction of the experimental data, as was done in many papers (see, for example, reference 11), is naturally not permissible in the general case.

2. All the experiments[1-13] have confirmed the theoretically predicted high "sensitivity" of the effect to the parallelness of the constant magnetic field to the specimen surface finish. A large number of harmonics are observed in tin, copper, zinc, and aluminum (up to 15 or 17 in tin,[3,4] up to 12 in copper[10] and up to 8 in zinc[11]), thus splendidly confirming the multiplicity of the resonant frequencies.[10,4]

The anisotropy of the effective mass in one of the crystallographic planes was fully investigated for single crystals of tin,[3,4] bismuth,[7] and copper.[10] In particular, the data of Aubrey and Chambers[7] and of Galt et al.[8] have confirmed the three-ellipsoid Fermi-surface model proposed by Shoenberg[27] for electrons in bismuth, and made possible the calculation of some of their parameters.

The results of the investigation of cyclotron resonance in copper[10] agree with the shape obtained by Pippard[28] for the Fermi surface. The shape of the surface is thus confirmed for copper by four independent methods: the anomalous skin effect (Pippard[28]), the de Haas—van Alphen effect (Shoenberg[29]), galvanomagnetic phenomena (Alekseevskiĭ and Gaĭdukov[30]) and cyclotron resonance (Langenberg and Moore[10]).

The low effective-mass values, $m \sim 0.2m_0$, obtained by Langenberg and Moore[12] and by Fawcett[13] with cyclotron resonance in aluminum, agree with the "cushion-like" Fermi surface for "holes" in aluminum, constructed by Gunnersen[31] from data on the de Haas—van Alphen effect. This Fermi surface, according to Heine,[32] is located in the corners of the first Brillouin zone and corresponds to a "hole" concentration on the order of 4×10^{-3} per atom. The "heavy" carriers with mass on the order of $1.5m_0$, not observed in the de Haas—van Alphen effect and observed by Langenberg and Moore[12] with cyclotron resonance, are connected with the main group of carriers in aluminum, the Fermi surface of which is located in the second Brillouin zone. The smallest electron group ($\sim 10^{-5}$ per atom), responsible for the long-wave oscillations in the de Haas-van Alphen effect and located at the corners of the third Brillouin zone, was naturally not observed in cyclotron-resonance experiments.

3. Many experimenters[3,9,10,12] measured directly not the surface resistance R(H), but its derivative dR/dH with respect to the magnetic field. Plots of dR/dH vs. H have a clearly pronounced resonant character. The resonant cyclotron frequencies and the effective masses are determined from the position of maximum of the derivative dR/dH. At first glance this may appear to be incorrect, since R(H) has a minimum at resonance,[22-25] and it is natural to expect dR/dH to vanish at the resonance point. It must be borne in mind, however, that the function R(H) has a cusp at the resonance points when $\omega\tau_0 = \infty$, and the derivative dR/dH goes to infinity when $H = H_{res} + 0$.

By way of illustration, let us consider a quadratic dispersion law, when

$$Z(H) = 2R(0)\,[1 - \exp(-2\pi i\omega/\Omega)]^{1/3}\exp(i\pi/3),$$

$$\frac{dZ}{dH} = -\frac{2\pi}{3}\,Z(0)\,\frac{1 + i\omega\tau_0}{H\Omega\tau_0}\left[1 - \exp\left\{-\frac{2\pi(1 + i\omega\tau_0)}{\Omega\tau_0}\right\}\right]^{-2/3}$$
$$\times \exp\{-2\pi i(1 + i\omega\tau_0)/\Omega\tau_0\}. \tag{1}$$

The phase $1 - \exp(-2\pi i\omega/\Omega)$ is chosen in the interval $(-\pi/2, \pi/2)$ to make R(H) positive. Near resonance, when $|\kappa_1| \ll 1$ ($\kappa_1 = 1 - q\Omega_{res}/\omega$, and q is an integer),

$$R(H) = 2(2\pi q)^{1/3}R(0)\,|\varkappa_1|^{1/3}\cos(\pi/3 + \tfrac{1}{3}\tan^{-1}(\pi q\varkappa_1)^{-1}). \tag{2}$$

To the right of resonance ($H > H_{res}$, $\kappa_1 < 0$)

$$R(H) = \sqrt{3}\,(2\pi q)^{1/3}R(0)\,|\varkappa_1|^{1/3}, \tag{3}$$

$$dR/dH = 3^{-1/2}R(0)H^{-1}(2\pi q)^{1/3}|\varkappa_1|^{-2/3}, \tag{4}$$

To the left of resonance ($H < H_{res}$, $\kappa_1 > 0$)

$$R(H) = R(0)\,(2\pi q\varkappa_1)^{4/3}, \tag{5}$$

$$dR/dH = -\tfrac{4}{3}R(0)H^{-1}(2\pi q)^{4/3}\,\varkappa_1^{1/3}. \tag{6}$$

Thus, dR/dH tends to zero to the left of resonance and to infinity on the right. Consequently, the position of resonance is best determined from the maximum of dR/dH. The position of the minimum of dR/dH does not coincide with $H = H_{res}$. Figure 1 shows schematically the variation of R(H) and of dR/dH as a function of the magnetic field near one of the resonance points.

Similar curves are obtained in the case of a non-quadratic dispersion, when the resonant frequency corresponds to the minimum effective mass. In the case when the resonance corresponds to the largest value of effective mass with respect to p_z, $dR/dH = -\infty$ when $H = H_{res} - 0$ and $dR/dH = +\infty$ when $H = H_{res} + 0$ (see Fig. 2). In the latter case the resonant magnetic field can be determined both from the maximum and from the minimum of the derivative dR/dH. The fact that the minimum and the maximum of dR/dH are close together (even for a finite value of $\omega\tau_0$), makes it possible to distinguish between the maximum and minimum effective masses.

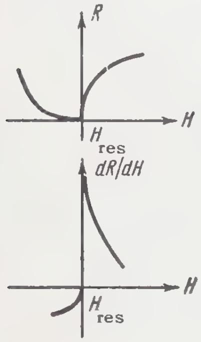

FIG. 1

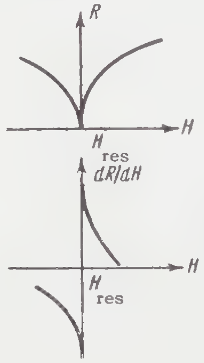

FIG. 2

4. The resonant frequencies can be determined and were determined experimentally both by the minimum of absorption, and by the maximum of its derivative with respect to the magnetic field. Many experimental curves show clearly (see, for example, reference 10) that the resonance is much more clearly pronounced in the dR/dH curves than in the R(H) curves. To understand the reason for this, it is necessary to consider the dependence of R and dR/dH on the magnetic field at large but finite value of $\omega\tau_0 = \xi^{-1}$, $\xi \ll 1$.

Differentiating the expressions for the surface resistance given in Eqs. (3.18), (4.6), (6.3), and (6.8) of reference 24, we readily obtain equations for both the height of the resonance maximum dR/dH and for the shift in the resonant cyclotron frequency relative to ω/q. The results of these calculations and of their comparison with the calculated values of R(H) (see reference 24) are listed in the table, where H_1 is the magnetic field at which $\Omega = \omega$ and τ_0 is the mean free time.*

Thus, only when the dispersion is quadratic does the relative depth of the resonance minimum of R(H) have the order of magnitude of the resonance height of the maximum of dR/dH. For any essentially non-quadratic dispersion law, the relative height of the maximum of dR/dH is greater than the relative depth of the minimum of R(H), by $(\omega\tau_0)^{2/3}$ and $(\omega\tau_0)^{7/18}$ for the maximum and minimum effective masses, respectively. This agrees well with experiment. The comparison of the R(H) and dR/dH curves affords an additional deduction of the dispersion law (naturally, if the theoretical requirements are satisfied).

The relative shift of the resonant cyclotron frequency (magnetic field) for dR/dH, for any dispersion law, is positive and on the order of $\xi = (\omega\tau_0)^{-1} \ll 1$, i.e., it is of opposite sign and substantially smaller than the corresponding shift for R(H) when the dispersion is quadratic ($\kappa \sim \xi^{1/2}$), or non-quadratic with $m = m_{min}$ ($\kappa_1 \sim \xi^{2/3}$).[24] This conclusion can be used for an experimental determination of the effective mass.

The minimum of dR/dH does not have a resonant character when the dispersion is quadratic and the mass is a minimum (with respect to p_z), since it is far removed from $H = H_{res}$. For the maximum mass (with respect to p_z)

$$(dR/dH)_{min} \sim -(R(0)/H_1)q^{4/3}(\omega\tau_0)^{5/6}, \tag{7}$$

$$\frac{\Omega_{res} - \omega/q}{\omega/q} = -\left(\omega\tau_0 \tan\frac{\pi}{11}\right)^{-1}; \tag{8}$$

the minimum of dR/dH is a resonant one, and $(dR/dH)_{min}$ tends to $-\infty$ as $\tau_0 \rightarrow \infty$, as already mentioned (see Fig. 2).

5. A characteristic feature of the experimental curves is their considerable asymmetry in the vicinity of resonance: the derivative of dR/dH to the left of the maximum (like the value of R(H) to the right of the minimum) changes much more rapidly than on the right (see, for example, references 3 and 10). This feature is manifest also in the theoretical curves — see Figs. 1 and 2. A similar variation of dR/dH and R(H) with the magnetic field can be seen also in Fig. 5 of reference 24; it must be borne in mind, however, that R is plotted in this figure as a function of 1/H and not of H.

6. Certain experimental curves exhibit an increase in the height of the maximum with increasing magnetic field (this is seen particularly clearly on the figure of reference 10), beginning with harmonics of a definite order. This can be attributed to the fact that when $2\pi/\Omega\tau_0 > 1$, the derivative dR/dH diminishes exponentially [$\sim \exp(-2\pi/\Omega\tau_0)$] with diminishing magnetic field and the resonance maxima disappear. This affords a convenient method for estimating the value of τ_0 from the number q_0 of the distinctly noticed resonant harmonics $\tau_0 \sim 2\pi q_0/\omega$. Thus, for example, $q_0 \sim 10$ in the experiments of Kip, Langenberg, et al.[3] on tin and $q_0 = 9$ in the experiments of Langenberg and Moore[10] on copper. When $\omega = 2\pi \cdot 24 \times 10^9$ cps this yields

---

*The mean free time τ_0 for the anomalous skin effect was cogently introduced in reference 26.

Resonant values of the surface resistance R_{res}, the derivative $(dR/dH)_{res}$, and the relative shift of the minimum of R and of the maximum of dR/dH; $-\kappa_1 = q\Omega_{res}/\omega - 1$

	$R_{res}/R(0)$	$(dR/dH)_{res}/R(0)H_1$	$-\varkappa_1$ for $R(H)$	$-\varkappa_1$ for dR/dH
Quadratic dispersion law, $m(p_z) = \text{const}$	$(2\pi q/\omega\tau_0)^{2/3}$	$\sim (q^2\omega\tau_0)^{2/3}$	$-(2\pi q\,\omega\tau_0),^{-1/2}$	$\left(\omega\tau_0 \cot\frac{\pi}{10}\right)^{-1}$
Non-quadratic dispersion law, $m(p_z) = m_{min}$	$\sim(q^2/\omega\tau_0)^{4/9}$	$\sim q^{4/3}(\omega\tau_0)^{5/6}$	$\sim -(q\,\omega\tau_0)^{-2/3}$	$\left(\omega\tau_0 \cot\frac{\pi}{22}\right)^{-1}$
Non-quadratic dispersion law, $(p_z) = m_{max}$	$\sim(q^2/\omega\tau_0)^{1/6}$	$\sim q^{4/3}(\omega\tau_0)^{5/6}$	$-\left(\omega\tau_0 \tan\frac{\pi}{5}\right)^{-1}$	$\left(\omega\tau_0 \cot\frac{3\pi}{22}\right)^{-1}$

$\tau_0 \sim 3 \times 10^{-10}$ sec, in good agreement with the values $\tau_0 \sim 3 \times 10^{-10}$ sec given in these papers.

There is, however, a circumstance that casts doubts on this conclusion. The point is that, according to theory, the instant that a clearly pronounced resonance appears, the height of the resonance maxima should decrease with increasing magnetic field (i.e., with decreasing number of the harmonic q):

$$(dR/dH)_{max} \sim q^{4/3} \sim H_q^{-4/3}.$$

The opposite takes place in the experiments of Langenberg and Moore: the resonant maxima increase with increasing H. This can be explained only by assuming that even in relatively strong magnetic fields on the order of 2000 oe, we get $\Omega\tau_0 \gtrsim 2\pi$, owing to failure to maintain the magnetic field strictly parallel to the surface of the metal and to the insufficiently smooth surface; an alternative is to consider the presence of anomalous zones. Such factors can cause the value of τ_0, which determines the surface impedance, to be itself dependent on the magnetic field and to be considerably less than in the bulk metal.[24] In this case, when the effective magnetic field is weak, the formulas of references 22 – 25 are naturally inapplicable.

When $\Omega\tau/2\pi \ll 1$, strictly speaking, there is no resonance, but the impedance Z has a small periodic increment ΔZ:

a) in the case of quadratic dispersion

$$\Delta Z/Z \approx \frac{1}{3} \exp\left\{-\frac{2\pi}{\Omega\tau} - 2\pi i\,\frac{\omega}{\Omega}\right\},$$

b) in the general case

$$\Delta Z/Z = \frac{1}{6p_0}\left\{\frac{1}{2}\left[\frac{d^2}{dp_z^2}(\Omega\tau)\right]_{p_z = p_0}\right\}^{1/2}$$

$$\times \quad \exp\left\{-\frac{2\pi}{(\Omega\tau)_{max}} - 2\pi i \frac{\omega}{\Omega(p_0)}\right\}$$

[p_0 is the point of maximum of $\Omega(p_z)\tau(p_z)$]. There exists, naturally, in addition to this increment, the increment obtained in reference 24, which is monotonic in H and of order $(l^2/\delta_{eff})^2$ (l is the mean free path, r the radius of the orbit, and ω_0 the plasma frequency). Obviously

$$d \ln X/dH \sim q^n \exp(-2\pi q/\omega\tau)$$

(n = 2 for quadratic dispersion and n = 3/2 for a nonquadratic law).

Unfortunately, the knowledge of $\Omega(p_0)$ determines the effective mass at an unknown point and thus affords merely an estimate of the order of magnitude of m*. The substantial temperature dependence of d ln X/dH in the experiments of Khaĭkin[4] shows that the measurements have been performed, possibly for the most part, in the region where $\Omega\tau/2\pi \gtrsim 1$. Nevertheless, the effect is quite noticeable because of the high accuracy of the experiment.

When $\Omega\tau \gg 1$, the derivative d ln X/dH depends little on the temperature and $(d \ln X/dH)_{res} \approx \pm\omega\tau_0/24H\pi q$ when $(\Omega_{res} - \omega/q)/(\omega/q) = \pm 2\pi q/\omega\tau_0$. The high-frequency oscillations (relative to the magnetic field) observed in Khaĭkin's experiments may be due to the quantum oscillations predicted in reference 33 for the high-frequency region, oscillations which are quite useful for the construction of the Fermi surface.

For a detailed comparison of the theory with experiment, an experimental verification of the theoretical requirements becomes particularly important. It is convenient to study for this purpose the measurements of dR/dH and d ln X/dH in a strong magnetic field. In a strong field we have, independently of the dispersion law

$$dR/dH \sim H^{-7/3} \quad \text{for} \quad 2\pi\omega \ll \Omega \ll \pi\omega^2\tau_0,$$

$$dR/dH \sim H^{-4/3},\ d\ln X/dH \approx -\tfrac{1}{3} \quad \text{for} \quad \Omega \gg \pi\omega^2\tau_0.$$

We emphasize that the law of decrease of dR/dH in a strong magnetic field strictly parallel to the surface of the metal should be independent of the rotation of the vector **H** in the plane of the sample. Another criterion for the satisfaction of the theoretical requirements is the "regular" dependence of the height of the maximum $(dR/dH)_{max}$ or $(d\ln X/dH)_{res}$ on the number of the harmonic q $(dR/dH \sim q^{4/3}$, $d\ln X/dH \sim q^{-1})$.

7. In spite of the large number of experiments on cyclotron resonance in metals, the dependence of the absorption on the direction of polarization of the alternating electric field (direction of the high-frequency current) was not investigated for a fixed direction of **H**. Therefore, naturally, the previously predicted "resonance at a selected polarization" was not observed[24,25] at effective masses corresponding to a central section and elliptical reference points (at which the electron velocity **v** is parallel to **H**) of the Fermi surface. The result is modified for dR/dH in the following manner: resonance will be observed for any direction of polarization of the electric field **E** relative to **H**, with the exception of those directions, at which **E** is perpendicular to the direction of the electron velocity at the reference point $(\mathbf{E} \perp \mathbf{H})$ and at the point of the central section of the Fermi surface $p_z = 0$ for $v_n = 0$ (v_n is the projection of **v** on the normal to the surface of the metal).

8. Let us emphasize again that, generally speaking, only the ratio $\Omega \approx \omega/q$ is "stable," at sufficiently large $\omega\tau_0$ and in the absence of a noticeable superposition of the resonant frequencies, with respect to experimental errors and with respect to different assumptions of the theory. Thus, for example, the discrepancy between the experimental and theoretical values of the phase shift of the oscillation, pointed out by many authors,[7,10,11] can be caused by many factors: insufficiently large $\omega\tau_0$, the approximate character of Eq. (3.16) of reference 24 [used to determine the impedance and in which the complex terms of order $(\delta/r)^{1/2}$ have been discarded], the rotation of the principal axes of the surface-impedance tensor $R_{\mu\nu}$ with variation of the magnetic field (even near resonance — in the next higher approximations), **H** not parallel to the surface of the metal, etc.

9. To establish the form of the Fermi surface in metals and the electron velocities on it, it would be quite desirable to investigate further the anisotropy of the resonance, both in different crystallographic directions and in an inclined magnetic field, where the resonance may be due to diamagnetic quantum oscillations.[33-34] In particular, it is interesting to measure simultaneously the classical and the quantum parts of dR/dH. We note that cyclotron resonance is particularly useful in explaining the features of closed plane sections of the Fermi surface. Open surfaces affect little the form of the resonance curves, since for a given direction of **H**, they are encountered as a rule together with closed ones. It is possible to determine the direction of the open trajectories only from the reduction and vanishing (for a certain direction of **H**) of a given resonant frequency in an investigation of the anisotropy of the resonance. Data on galvanomagnetic phenomena can be used to obtain open trajectories.[30,35]

In conclusion, we take this opportunity to note that the solutions obtained by Mattis and Dresselhaus[17] and Rodriguez[18] for the kinetic equation of electrons in a magnetic field parallel to the surface of a metal do not satisfy the boundary conditions. Actually, owing to violation of the symmetry of the problem by the magnetic field, the continuation of the distribution function (even or zero) to the surface outside the metal does not correspond to the boundary conditions for any orientation of **H** (see references 20, 23, 26, 34, and 37), unlike the case $\mathbf{H} = 0$. The only exception is a perpendicular magnetic field with isotropic dispersion. In a parallel magnetic field, the problem becomes more complicated by the discontinuity of the distribution function.[36,37]

The situation is still more complicated in the quantum case, where the character of the reflection of the electrons from the surface of the metal changes the electron energy levels (see reference 33 for more details). The particular error made by these authors is that in solving the kinetic equation by Laplace transforms they did not account for the jump in the distribution function on the boundary between the metal and the vacuum. It was precisely an incorrect allowance for the boundary condition that has led to differences between the formulas of references 17 and 18 and those of references 22 — 24 and 33. Incidentally, in the case of a quadratic dispersion law, the reflection of the electrons from the surface of the metal does not influence greatly the results in either the classical or quantum case (with exception of the case of pure specular reflection, which is only of academic interest[26]), so that the results of Mattis and Dresselhaus and of Rodriguez are qualitatively correct.

The authors are grateful to A. F. Kip, D. N. Langenberg, E. Fawcett, and I. Phillips for graciously supplying preprints of their papers.

---

[1] E. Fawcett, Bull. Amer. Phys. Soc. **1**, 217 (1956); Phys. Rev. **103**, 1582 (1956).

[2] P. A. Bezuglyĭ and A. A. Galkin, JETP **33**,

1076 (1957) and **34**, 237 (1958), Soviet Phys. JETP **6**, 831 (1958) and **7**, 164 (1958).

[3] Kip, Langenberg, Rosenblum, and Wagoner, Phys. Rev. **108**, 494 (1958).

[4] M. S. Khaĭkin, JETP **37**, 1473 (1959), Soviet Phys. JETP **10**, 1044 (1960).

[5] P. A. Bezuglyĭ and A. A. Galkin, JETP **34**, 236 (1958), Soviet Phys. JETP **7**, 163 (1958).

[6] P. A. Bezuglyĭ and A. A. Galkin, JETP **37**, 1480 (1959), Soviet Phys. JETP **10**, 1049 (1960).

[7] J. E. Aubrey and R. G. Chambers, J. Phys. Chem. Solids **3**, 128 (1957).

[8] Galt, Yager, Merrit, Cetlin, and Brailsford, Phys. Rev. **114**, 1396 (1959).

[9] Langenberg, Kip, and Rosenblum, Bull. Amer. Phys. Soc. **3**, 416 (1958).

[10] D. N. Langenberg and T. W. Moore, Phys. Rev. Lett. **3**, 328 (1959).

[11] Galt, Merritt, Yager, and Dail, Phys. Rev. Lett. **2**, 292 (1959).

[12] D. N. Langenberg and T. W. Moore, Phys. Rev. Lett. **3**, 137 (1959).

[13] E. Fawcett, Phys. Rev. Lett. **3**, 139 (1959).

[14] R. G. Chambers, Canad. J. Phys. **34**, 1395 (1956).

[15] B. Lax, Revs. Modern Phys. **30**, 122 (1958).

[16] V. Heine, Phys. Rev. **107**, 431 (1957).

[17] D. C. Mattis and G. Dresselhaus, Phys. Rev. **111**, 403 (1958).

[18] S. Rodriguez, Phys. Rev. **112**, 1616 (1958).

[19] I. C. Phillips, Phys. Rev. Lett. **3**, 327 (1959).

[20] M. Ya. Azbel', Dokl. Akad. Nauk SSSR **100**, 437 (1955).

[21] M. Ya. Azbel' and M. I. Kaganov, Dokl. Akad. Nauk SSSR **95**, 41 (1954).

[22] M. Ya. Azbel' and É. A. Kaner, JETP **30**, 411 (1956), Soviet Phys. JETP **3**, 450 (1956).

[23] M. Ya. Azbel' and É. A. Kaner, JETP **32**, 896 (1957), Soviet Phys. JETP **5**, 730 (1957).

[24] M. Ya. Azbel' and É. A. Kaner, J. Phys. Chem. Solids **6**, 113 (1958).

[25] É. A. Kaner and M. Ya. Azbel', JETP **33**, 1461 (1957), Soviet Phys. JETP **6**, 1126 (1958).

[26] É. A. Kaner, JETP **33**, 1472 (1957), Soviet Phys. JETP **6**, 1135 (1958).

[27] D. Shoenberg, JETP **8**, 1271 (1938). Phil. Trans. **A245**, 1 (1952).

[28] A. B. Pippard, Phil. Trans. **A250**, 325 (1957).

[29] D. Shoenberg, Nature **183**, 171 (1959).

[30] N. E. Alekseevskiĭ and Yu. P. Gaĭdukov, JETP **37**, 672 (1959), Soviet Phys. JETP **10**, 481 (1960).

[31] E. M. Gunnersen, Phil. Trans. **A249**, 299 (1957).

[32] V. Heine, Proc. Roy. Soc. **A240**, 341 (1957).

[33] M. Ya. Azbel', JETP **34**, 969, 1158 (1958), Soviet Phys. JETP **7**, 669, 801 (1958). J. Phys. Chem. Solids **7**, 105 (1958).

[34] M. Ya. Azbel', Doctoral dissertation, Moscow, 1958.

[35] I. M. Lifshitz and V. G. Peschanskiĭ, JETP **35**, 1251 (1958), Soviet Phys. JETP **8**, 875 (1959).

[36] M. Ya. Azbel', Dokl. Akad. Nauk SSSR **99**, 519 (1954).

[37] É. A. Kaner, JETP **34**, 658 (1958), Soviet Phys. JETP **7**, 454 (1958).

Translated by J. G. Adashko
17

SOVIET PHYSICS JETP VOLUME 12, NUMBER 1 JANUARY, 1961

GENERALIZED RECIPROCITY PRINCIPLE

L. M. BIBERMAN and B. A. VEKLENKO

Moscow Power Institute

Submitted to JETP editor December 24, 1959

J. Exptl. Theoret. Phys. (U.S.S.R.) **39**, 88-93 (July, 1960)

Relations are derived for the generalized reciprocity principle (GRP) in the case when the radiation frequency changes during the transfer process. The limits of validity of the GRP are determined. The connection between the GRP and the concept of thermodynamic equilibrium is established.

THE reciprocity principle was quite useful in the development of the theory of radiation transfer and in the solution of many of its specific problems. In this connection, considerable attention has been paid recently to this question and to its mathematical formulation.[1-6] Nevertheless, the presently used treatment of the reciprocity principle appears to us to be far from complete, since it is usually assumed that the frequency of radiation does not change during the transfer process.

The authors have indicated earlier[7] that the application of the theory of random processes to radiation-transfer phenomena lead to two systems of equations, which correspond to the Kolmogorov-Feller equations. It was noted there that a simultaneous analysis of both systems leads to a formulation of the generalized reciprocity principle (GRP) and to an establishment of its limits of applicability. This approach is similar to an analysis of the reciprocity of Brownian motion, used in the theory of random processes.[8-10]

1. DERIVATION OF FUNDAMENTAL RELATIONS

The transfer of radiation in a scattering, absorbing, and reradiating medium filling a certain volume V is best described by introducing the four functions f_c^c, f_0^c, f_c^0, and f_0^0. The quantity

$$f_c^c(\mathbf{r}_1,\boldsymbol{\eta}_1,\nu_1,t_1;\mathbf{r}_2,\boldsymbol{\eta}_2,\nu_2,t_2)\,dV_2d\boldsymbol{\eta}_2d\nu_2 = f_c^c(1;\ 2)\,dV_2d\boldsymbol{\eta}_2d\nu_2$$

is the probability that a photon of frequency ν_1, moving at the instant of time t_1 at the point $\mathbf{r}_1$ in the direction of the unit vector η_1, will be located at the instant t_2 in the vicinity of the point $\mathbf{r}_2$, will have a frequency $(\nu_2,\ \nu_2 + d\nu_2)$, and will move in a direction specified in the interval $(\eta_2,\ \eta_2 + d\eta_2)$. The quantity

$$f_c^0(1;\ 2)\,dV_2d\boldsymbol{\eta}_2d\nu_2$$

is the probability that the excited atom will be at the instant t_2 in a state $(\mathbf{r}_2,\ \eta_2,\ \nu_2)$ if it was excited by a photon whose parameters were $(\mathbf{r}_1;\ \eta_2,\ \nu_1)$ at the instant t_1. By η_2 and ν_2 are meant here the parameters of the photon at the instant of time preceding the absorption.

The functions $f_0^c(1;\ 2)$ and $f_0^0(1;\ 2)$ need no explanation.

In reference 7 we gave two systems of equations defining the functions f(1; 2). We present these systems here in expanded form, under the assumption that the characteristics of the medium are independent of the time. The latter is a necessary condition for the GRP to be valid.

$$\begin{aligned}\partial f_c^c(1;\ 2)/\partial t_2 = &\int f_c^0(1;\ \mathbf{r}_2,\ \boldsymbol{\eta}_3,\ \nu_3,\ t_2)\\ &\times A_{21}p_k(\mathbf{r}_2;\ \boldsymbol{\eta}_3,\ \nu_3;\ \boldsymbol{\eta}_2,\ \nu_2)\,d\boldsymbol{\eta}_3d\nu_3\\ &+\int f_c^c(1;\ \mathbf{r}_2,\ \boldsymbol{\eta}_3,\ \nu_3,\ t_2)\,\varkappa(\mathbf{r}_2;\ \nu_3)\,cp_\varkappa(\mathbf{r}_2;\ \boldsymbol{\eta}_3,\ \nu_3;\ \boldsymbol{\eta}_2,\ \nu_2)\,d\boldsymbol{\eta}_3\,d\nu_3\\ &- f_c^c(1;\ 2)\,[k(\mathbf{r}_2;\ \nu_2)\,c+\varkappa(\mathbf{r}_2;\ \nu_2)\,c+\sigma_c(\mathbf{r}_2;\ \nu_2)\,c]\\ &- c\boldsymbol{\eta}_2\,\mathrm{grad}_{\mathbf{r}_2}f_c^c(1;\ 2),\end{aligned} \tag{1}$$

$$\begin{aligned}\partial f_c^0(1;\ 2)/\partial t_2 = &\ f_c^c(1;\ 2)\,ck(\mathbf{r}_2;\ \nu_2)\\ &- [A_{21}+\sigma_0(\mathbf{r}_2)]\,f_c^0(1;\ 2),\end{aligned} \tag{2}$$

$$\begin{aligned}&\partial f_0^c(1;\ 2)/\partial t_2\\ &=\int f_0^0(1;\ \mathbf{r}_2,\ \boldsymbol{\eta}_3,\ \nu_3,\ t_2)\,A_{21}p_k(\mathbf{r}_2;\ \boldsymbol{\eta}_3,\ \nu_3;\ \boldsymbol{\eta}_2,\ \nu_2)\,d\boldsymbol{\eta}_3d\nu_3\\ &+\int f_0^c(1;\ \mathbf{r}_2,\ \eta_3,\ \nu_3,\ t_2)\,c\varkappa(\mathbf{r}_2;\ \nu_2)\,p_\varkappa(\mathbf{r}_2;\ \boldsymbol{\eta}_3,\ \nu_3;\ \boldsymbol{\eta}_2,\ \nu_2)\,d\boldsymbol{\eta}_3d\nu_3\\ &- f_0^c(1;\ 2)\,[k(\mathbf{r}_2;\ \nu_2)\,c+\varkappa(\mathbf{r}_2;\ \nu_2)\,c+\sigma_c(\mathbf{r}_2;\ \nu_2)\,c]\\ &- c\boldsymbol{\eta}_2\,\mathrm{grad}_{\mathbf{r}_2}f_0^c(1;\ 2),\end{aligned} \tag{3}$$

$$\begin{aligned}\partial f_0^0(1;\ 2)/\partial t_2 = &\ f_0^c(1;\ 2)\,k(\mathbf{r}_2;\ \nu_2)\\ &- [A_{21}+\sigma_0(\mathbf{r}_2)]\,f_0^0(1;\ 2),\end{aligned} \tag{4}$$

$$\begin{aligned}-\partial f_c^c(1;2)/\partial t_1 &= k(\mathbf{r}_1;\nu_1)\,cf_0^c(1;2)\\ &+\varkappa(\mathbf{r}_1;\nu_1)\,c\int p_\varkappa(\mathbf{r}_1;\boldsymbol{\eta}_1,\nu_1;\boldsymbol{\eta}_3,\nu_3)\\ &\times f_c^c(\mathbf{r}_1,\boldsymbol{\eta}_3,\nu_3,t_1;2)\,d\boldsymbol{\eta}_3\,d\nu_3 - f_c^c(1;2)\,[k(\mathbf{r}_1;\nu_1)\,c\\ &+\varkappa(\mathbf{r}_1;\nu_1)\,c+\sigma_c(\mathbf{r}_1;\nu_1)\,c]+c\boldsymbol{\eta}_1\operatorname{grad}_{\mathbf{r}_1} f_c^c(1;2), \end{aligned} \qquad (1')$$

$$\begin{aligned}-\partial f_0^c(1;2)/\partial t_1 &\\ &=\int A_{21}p_k(\mathbf{r}_1;\boldsymbol{\eta}_1,\nu_1;\boldsymbol{\eta}_3,\nu_3)\,f_c^c(\mathbf{r}_1,\boldsymbol{\eta}_3,\nu_3,t_1;2)\,\mathrm{d}\boldsymbol{\eta}_3 d\nu_3\\ &-f_0^c(1;2)\,[A_{21}+\sigma_0(\mathbf{r}_1)]; \end{aligned} \qquad (2')$$

$$\begin{aligned}-\partial f_c^o(1;2)/\partial t_1 &= k(\mathbf{r}_1;\nu_1)\,cf_0^0(1;2)\\ &+\varkappa(\mathbf{r}_1,\nu_1)\,c\int p_\varkappa(\mathbf{r}_1;\boldsymbol{\eta}_1,\nu_1;\boldsymbol{\eta}_3,\nu_3)\,f_c^0(\mathbf{r}_1,\boldsymbol{\eta}_3,\nu_3,t_1;2)\,d\boldsymbol{\eta}_3 d\nu_3\\ &-f_c^0(1;2)\,[k(\mathbf{r}_1;\nu_1)\,c+\varkappa(\mathbf{r}_1;\nu_1)\,c+\sigma_c(\mathbf{r}_1,\nu_1)\,c]\\ &+c\boldsymbol{\eta}_1\operatorname{grad}_{\mathbf{r}_1} f_c^0(1;2); \end{aligned} \qquad (3')$$

$$\begin{aligned}-\partial f_0^0(1;2)/\partial t_1 &\\ &=\int A_{21}p_k(\mathbf{r}_1;\boldsymbol{\eta}_1,\nu_1;\boldsymbol{\eta}_3,\nu_3)\,f_c^0(\mathbf{r}_1,\boldsymbol{\eta}_3,\nu_3,t_2;2)\,d\boldsymbol{\eta}_3 d\nu_3\\ &-f_0^0(1;2)\,[A_{21}+\sigma_0(\mathbf{r}_1)]. \end{aligned} \qquad (4')$$

The following notation is used here: $k(\mathbf{r};\nu)$ is the coefficient of absorption of a photon by the atoms, A_{21} is the probability of photon emission, $p_k(\mathbf{r};\boldsymbol{\eta}_1;\nu_1;\boldsymbol{\eta}_2,\nu_2)$ is the radiation indicatrix, $\kappa(\mathbf{r};\nu)$ is the scattering coefficient, $p_\kappa(\mathbf{r};\boldsymbol{\eta}_1;\nu_1;\boldsymbol{\eta}_2,\nu_2)$ is the scattering indicatrix, $\sigma_0(\mathbf{r})$ is the probability of collisions of second kind per excited atom, $\sigma_c(\mathbf{r};\nu)$ is the coefficient of true absorbtion, and c is the velocity of light.

We introduce the function $g_c^c(\mathbf{r}_1,\boldsymbol{\eta}_1,\nu_1,t_1;\mathbf{r}_2,\boldsymbol{\eta}_2,\nu_2,t_2,)$, which represents the probability density of the photon being at the instant t_1 in a state $(\mathbf{r}_1,\boldsymbol{\eta}_1,\nu_1)$ if its state corresponds in a subsequent instant of time t_2 to the parameters $(\mathbf{r}_2,\boldsymbol{\eta}_2,\nu_2)$.

Let us define the generalized reciprocity principle for the function $f_c^c(1;2)$ in the following manner:*

$$\begin{aligned}f_c^c(\mathbf{r}_1,\boldsymbol{\eta}_1,\nu_1,t_1;\mathbf{r}_2,\boldsymbol{\eta}_2,\nu_2,t_2)&\\ &=g_c^c(\mathbf{r}_2,-\boldsymbol{\eta}_2,\nu_2,t_1;\mathbf{r}_1,-\boldsymbol{\eta}_1,\nu_1,t_2). \end{aligned} \qquad (5)$$

On the other hand, another connection can be established between the functions f_c^c and g_c^c.

According to the Bayes theorem (see, for example, reference 11), we have

$$g_c^c(1;2)=f_c^c(1;2)\,\varphi(\mathbf{r}_1,\boldsymbol{\eta}_1,\nu_1)/\varphi(\mathbf{r}_2,\boldsymbol{\eta}_2,\nu_2), \qquad (6)$$

where the function φ characterizes a certain stationary distribution of the photons.

From (5) and (6) we obtain

$$\varphi(\nu_1)\,f_c^c(1;2)=\varphi(\nu_2)\,f_c^c(\mathbf{r}_2,-\boldsymbol{\eta}_2,\nu_2,t_1;\mathbf{r}_1,-\boldsymbol{\eta}_1,\nu_1,t_2). \quad (7)$$

We have left out the arguments $\boldsymbol{\eta}$ and $\mathbf{r}$ of the function $\varphi(\nu)$, since the necessary condition for (7) to be valid is that $\varphi(\nu)$ be independent of these parameters. The latter can be readily established by taking the limit as $\Delta t = t_2 - t_1 \rightarrow 0$.

Expressing $f_c^c(1;2)$ in explicit form in this limiting transition

$$f_c^c(1;2)=c\,\Delta t\varkappa(\mathbf{r};\nu)p_\varkappa(\mathbf{r};\boldsymbol{\eta}_1,\nu_1;\boldsymbol{\eta}_2,\nu_2),$$

we obtain the necessary condition imposed on the characteristics of a medium for which the GRP is valid

$$\begin{aligned}\varphi(\nu_1)\,\varkappa(\mathbf{r};\nu_1)\,p_\varkappa(\mathbf{r};\boldsymbol{\eta}_1,\nu_1;\boldsymbol{\eta}_2,\nu_2)&\\ &=\varphi(\nu_2)\,\varkappa(\mathbf{r};\nu_2)\,p_\varkappa(\mathbf{r};-\boldsymbol{\eta}_2,\nu_2;-\boldsymbol{\eta}_1,\nu_1). \end{aligned} \qquad (8)$$

Let us proceed now to examine the functions f_c^0, f_0^c, and f_0^0.

We substitute in (1) the function $f_c^c(1;2)$ as given by (7), and multiply the result by $\varphi(\nu_1)$. Then

$$\begin{aligned}\partial\varphi(\nu_2),\,f_c^c(\mathbf{r}_2,-\boldsymbol{\eta}_2,\nu_2,t_1;\mathbf{r}_1,-\boldsymbol{\eta}_1,\nu_1,t_2)/\partial t_2&\\ &=\varphi(\nu_1)\int f_c^0(1;\mathbf{r}_2,\boldsymbol{\eta}_3,\nu_3,t_2)\,A_{21}p_k(\mathbf{r}_2;\boldsymbol{\eta}_3,\nu_3;\boldsymbol{\eta}_2,\nu_2)\,d\boldsymbol{\eta}_3 d\nu_3\\ &+\int\varphi(\nu_3)\,f_c^c(\mathbf{r}_2,-\boldsymbol{\eta}_3,\nu_3,t_2;\mathbf{r}_1,-\boldsymbol{\eta}_1,\nu_1,t_2)\\ &\times\varkappa(\mathbf{r}_2;\nu_3)\,cp_\varkappa(\mathbf{r}_2;\boldsymbol{\eta}_3,\nu_3;\boldsymbol{\eta}_2,\nu_2)\,d\boldsymbol{\eta}_3 d\nu_3\\ &-\varphi(\nu_2)\,f_c^c(\mathbf{r}_2,-\boldsymbol{\eta}_2,\nu_2,t_1;\mathbf{r}_1,-\boldsymbol{\eta}_1,\nu_1,t_2)\,[k(\mathbf{r}_2;\nu_2)\\ &\times\ c+\varkappa(\mathbf{r}_2;\nu_2)\,c+\sigma_c(\mathbf{r}_2;\nu_2)\,c]\\ &-c\boldsymbol{\eta}_2\operatorname{grad}_{\mathbf{r}_2}\varphi(\nu_2)\,f_c^c(\mathbf{r}_2,-\boldsymbol{\eta}_2,\nu_2,t_1;\mathbf{r}_1,-\boldsymbol{\eta}_1,\nu_1,t_2). \end{aligned}$$

Let us interchange the indices in this equation, remembering that this interchange implies replacement of $\mathbf{r}_1$ by $\mathbf{r}_2$, of ν_1 by ν_2, of $\boldsymbol{\eta}_1$ by $-\boldsymbol{\eta}_2$, and of $\boldsymbol{\eta}_2$ by $-\boldsymbol{\eta}_1$. We subtract from the resultant equation the equation (1′) multiplied by $\varphi(\nu_1)$. Taking (8) into account,we get

$$\begin{aligned}\varphi(\nu_1)\,k(\mathbf{r}_1;\nu_1)\,cf_0^c(1;2)&\\ &=A_{21}\varphi(\nu_2)\int f_c^0(\mathbf{r}_2,-\boldsymbol{\eta}_2,\nu_2,t_1;\mathbf{r}_1,\boldsymbol{\eta}_3,\nu_3,t_2)\\ &\times\ p_k(\mathbf{r}_1;\boldsymbol{\eta}_3,\nu_3;-\boldsymbol{\eta}_1,\nu_1)\,d\boldsymbol{\eta}_3 d\nu_3. \end{aligned} \qquad (9)$$

As $t_2 - t_1 \rightarrow 0$, this equation becomes

$$\begin{aligned}\varphi(\nu_1)\,k(\mathbf{r};\nu_1)\,p_k(\mathbf{r};\boldsymbol{\eta}_1,\nu_1;\boldsymbol{\eta}_2,\nu_2)&\\ &=\varphi(\nu_2)\,k(\mathbf{r};\nu_2)p_k(\mathbf{r};-\boldsymbol{\eta}_2,\nu_2;-\boldsymbol{\eta}_1,\nu_1). \end{aligned} \qquad (10)$$

---

*This definition of the GRP coincides with the definition of the reciprocity of a random process, used in probability theory.[8-10]

This is the second necessary condition that must be satisfied by a medium for which the GRP is valid.

Analogously, we obtain from (3) and (3′), with account of (7), (8), and (9),

$$\varphi(\nu_1)\, k(\mathbf{r}_1; \nu_1) \int f_0^0(1; \mathbf{r}_2, \boldsymbol{\eta}_3, \nu_3, t_2)\, p_k(\mathbf{r}_2; \boldsymbol{\eta}_3, \nu_3; \boldsymbol{\eta}_2, \nu_2)\, d\boldsymbol{\eta}_3 d\nu_3$$

$$= \varphi(\nu_2)\, k(\mathbf{r}_2; \nu_2) \int f_0^0(\mathbf{r}_2, -\boldsymbol{\eta}_2, \nu_2, t_1; \mathbf{r}_1, \boldsymbol{\eta}_3, \nu_3, t_2)$$

$$\times\; p_k(\mathbf{r}_1, \boldsymbol{\eta}_3, \nu_3; -\boldsymbol{\eta}_1, \nu_1)\, d\boldsymbol{\eta}_3, d\nu_3. \qquad (11)$$

The remaining equations do not yield any new relations for the GRP.

2. RANGE OF VALIDITY OF THE RESULTANT RELATIONS

Relations (8) and (10) express the conditions that must be met by a medium in which the GRP holds. Let the medium be in the state of thermodynamic equilibrium. Then (8) and (10) express the principle of detailed balancing. The function $\varphi(\nu)$ now acquires a clearer physical meaning: it is proportional to the energy distribution of the photons in the spectrum of equilibrium radiation. From this point of view, relations (7), (9), and (11) can be treated as a generalization of the principle of detailed balancing to include the case of coupling between different elements of space.

The function $\varphi(\nu)$ is determined by the temperature; it was shown above that it should be independent of the coordinates. It follows therefore that the GPR can hold only in isothermal media.

The requirement of thermodynamic equilibrium is not mandatory for the GRP. Thus, for example, relations (8) and (10) are satisfied if the distribution of the neutral and the charged particles over the energy states is in equilibrium while the radiation field is not. A similar situation takes place, for example, in the case of a gas occupying a finite volume, in which kinetic processes cause an outflow of radiation and an intense exchange of energy between different states.

The existence of an equilibrium distribution over all the energy states insures satisfaction of the GRP for any mechanism by which the radiation frequency is changed, including transitions between different energy levels.

It is obvious that in each specific case it is enough to stipulate equilibrium distribution only over the states that influence the transfer of the given type of radiation. In no case are we interested in the state of the radiation field. This is connected with the fact that the transfer of photons is determined by their interaction with matter and is not directly dependent on the radiation field.

The role of induced emission must be considered separately. The radiation-transfer equations that include induced emission are nonlinear, since they take into account the interaction between the photons and the excited atoms. Naturally, the linear equations which we derived in reference 7 and which we cite here cannot account for induced emission. This does not impose, however, any additional limitation on the validity of (7), (9), and (10). We have already noted that the GRP holds in the presence of an equilibrium energy distribution. Under these conditions the induced emission, as is well known, is accounted for by multiplying the absorbtion coefficient by $(1 - e^{-h\nu/kT})$.

3. SOME PARTICULAR CASES

a) Let the radiation indicatrix $p_k(\mathbf{r}; \boldsymbol{\eta}_1, \nu_1; \boldsymbol{\eta}_2, \nu_2)$ be independent of the first indices $\boldsymbol{\eta}_1$ and ν_1, i.e., let it be spherical, and let a complete redistribution of photon frequencies take place. It follows from (1)–(4) that the functions f_0^c and f_0^0 will also be independent of the initial parameters $\boldsymbol{\eta}_1$ and ν_1, and consequently the mathematical expressions for the GRP will be noticeably simplified.

Such is the situation with Eq. (9) which, after integrating with respect to $\boldsymbol{\eta}_1$ and ν_1, can be written in the form

$$n^0(\mathbf{r}_1)\, f_0^c(\mathbf{r}_1, t_1; \mathbf{r}_2, \boldsymbol{\eta}_2, \nu_2, t_2)$$

$$= \varphi(\nu_2) \int f_c^0(\mathbf{r}_2, -\boldsymbol{\eta}_2, \nu_2, t_1;\ \mathbf{r}_1, \boldsymbol{\eta}_3, \nu_3, t_3)\, d\boldsymbol{\eta}_3\, d\nu_3. \qquad (12)$$

We use here the relation

$$n^0(\mathbf{r})\, A_{21} = c \int \varphi(\nu)\, k(\mathbf{r}; \nu)\, d\nu,$$

where $n^0(\mathbf{r})$ is the concentration of the excited atoms in thermodynamic equilibrium.

We introduce the notation

$$f_c^0(\mathbf{r}_2, -\boldsymbol{\eta}_2, \nu_2, t_1; \mathbf{r}_1, t_2)$$

$$= \int f_c^0(\mathbf{r}_2, -\boldsymbol{\eta}_2, \nu_2, t_1; \mathbf{r}_1, \boldsymbol{\eta}_3, \nu_3, t_2)\, d\boldsymbol{\eta}_3\, d\nu_3.$$

Then

$$n^0(\mathbf{r}_1)\, f_0^c(\mathbf{r}_1, t_1; \mathbf{r}_2, \boldsymbol{\eta}_2, \nu_2, t_2)$$

$$= \varphi(\nu_2)\, f_c^0(\mathbf{r}_2, -\boldsymbol{\eta}_2, \nu_2, t_1; \mathbf{r}_1, t_2). \qquad (13)$$

Similarly, integrating (11) with respect to $\boldsymbol{\eta}_1$, ν_1, $\boldsymbol{\eta}_2$, and ν_2 and introducing the analogous notation

$$f_0^0(\mathbf{r}_1, t_1; \mathbf{r}_2, t_2) = \int f_0^0(\mathbf{r}_1, t_1; \mathbf{r}_2, \boldsymbol{\eta}_2, \nu_2, t_2)\, d\boldsymbol{\eta}_2\, d\nu_2,$$

we obtain

$$n^0(\mathbf{r}_1) f_0^0(\mathbf{r}_1, t_1; \mathbf{r}_2, t_2) = n^0(\mathbf{r}_2) f_0^0(\mathbf{r}_2, t_1; \mathbf{r}_1, t_2).$$

Relation (7) remains unchanged in appearance.

b) Let $\nu_1 - \nu_2 = \Delta\nu$ be small. Then $\varphi(\nu_1) \approx \varphi(\nu_2)$, as a result of which the range of validity of relations (7), (9), and (11) is increased, since the function $\varphi(\nu)$ vanishes in conditions (8) and (10), thus lifting the requirement that the medium be isothermal. In this case the GRP will be satisfield, in particular, in a medium with a coordinate-dependent temperature, provided local thermodynamic equilibrium obtains.

c) Let us now make simultaneously both foregoing assumptions, which are usually made in studies of the diffusion of resonant absorbtion with complete redistribution of photon frequency. We are interested only in the form of Eq. (13), which becomes, using the Wien distribution and interchanging the the indices

$$8\pi g f_c^0(1;\ 2) = \lambda_0^2 c n(\mathbf{r}_2)\, g_a f_0^c(\mathbf{r}_2, t_1; \mathbf{r}_1, -\boldsymbol{\eta}_1, \nu_1, t_2). \quad (14)$$

Here λ_0 is the wavelength corresponding to the center of the spectral line, $n(\mathbf{r})$ is the concentration of the atoms in the normal state, and g and g_a are the statistical weights of the normal and excited levels. It is curious that the connection between f_0^c and f_c^0, expressed by (14), is independent of the specific processes that cause the broadening of the spectral lines.

4. CONCLUSION

The results of the present paper contain, as particular cases, the mathematical expressions obtained earlier by other authors for the GRP.

Thus, considering the case of pure scattering and putting $\nu_1 = \nu_2$, we obtain instead of (7)

$$f_c^c(\mathbf{r}_1, \boldsymbol{\eta}_1, t_1; \mathbf{r}_2, \boldsymbol{\eta}_2, t_2) = f_c^c(\mathbf{r}_2, -\boldsymbol{\eta}_2, t_1; \mathbf{r}_1, -\boldsymbol{\eta}_1, t_2). \quad (15)$$

Here the condition (8) degenerates into the trivial requirement that the scattering indicatrix be dependent only on the angle between the vectors η_1 and η_2.

Relation (15) coincides with the formulation of the reciprocity principle as given by Minnaert,[1] Chandrasekhar,[4] and others. Case[6] obtained several specific mathematical expressions for the reciprocity principle as applied to neutron diffusion, in which the parameter corresponding to the frequency was the neutron velocity. He assumed that the neutron velocity did not change during the diffusion process, and obtained relations similar to (15). Actually it is necessary to start out with relation (7), with $\varphi(\nu)$ taken here as the Maxwellian distribution of the neutron velocities.

Kadomtsev[12] considered radiation transfer in scattering and absorbing media, allowing for changes in frequency and disregarding re-radiation processes. Putting

$$p_\times(\mathbf{r}; \boldsymbol{\eta}_1, \nu_1; \boldsymbol{\eta}_2, \nu_2) = p_\times(\mathbf{r}; -\boldsymbol{\eta}_2, \nu_2; -\boldsymbol{\eta}_1, \nu_1), \quad (16)$$

which contradicts the principle of detailed balancing when $\nu_1 \neq \nu_2$, he arrived at the particular relation (15), which holds only when $\nu_1 \approx \nu_2$. Furthermore, he required that the absorption coefficient be independent of the frequency. This requirement is superfluous.

Sobolev,[13] considering radiation transfer in the spectral line for a plane-parallel scattering atmosphere, also arrived at relation (15).

It must be noted that radiation transfer is far from always produced in a narrow spectral interval. Thus, for example, the role of $\varphi(\nu)$ becomes quite important if the foregoing results are applied to the investigation of luminescence. In this case a relation similar to (7) connects the absorption and luminescence spectra in the Stokes and anti-Stokes regions.

It is appropriate to note, in conclusion, that all the previously published papers give only particular relations between the function $f_c^c(1;\ 2)$. There are no relations in the literature for f_c^0, f_0^c, or f_0^0.

---

[1] M. Minnaert, Astrophys. J. **93**, 403 (1941).

[2] V. A. Ambartsumyan, Астрономический журнал (Astronom. J.) **19**, No. 5, 30 (1942).

[3] V. V. Sobolev, ibid. **28**, 355 (1951).

[4] S. Chandrasekhar, Transfer of Radiant Energy, (Russ. Transl.) IIL, 1953.

[5] V. V. Sobolev, Перенос лучистой энергии в атмосфере звезд и планет (Transfer of Radiant Energy in the Atmospheres of Stars and Planets), Gostekhizdat, 1956.

[6] K. M. Case, Revs. Modern Phys. **24**, 651 (1957).

[7] L. M. Biberman and B. A. Veklenko, JETP **31**, 341 (1956), Soviet Phys. JETP **4**, 440 (1957).

[8] E. Schrödinger, Sitzungsber. der Preuss. Akad. der Wiss. Math. Klasse, 144, 1931.

[9] A. N. Kolmogoroff, Math. Ann. **113**, 766 (1937).

[10] A. M. Yaglom Математический сборник (Math. Collection) **24**, 455 (1949).

[11] B. V. Gnedenko, Курс теории вероятностей (Course of Probability Theory), Gostekhizdat, 1954.

[12] B. B. Kadomtsev, Dokl. Akad. Nauk SSSR **113**, 541 (1957), Soviet Phys.-Doklady 2, 139 (1958).

[13] V. V. Sobolev, Вестник. ЛГУ, серия мат. (Bulletin, Leningrad State Univ. Math. Series), No. 11, 99 (1955).

Translated by J. G. Adashko
18

SOVIET PHYSICS JETP VOLUME 12, NUMBER 1 JANUARY, 1961

INTERFERENCE BETWEEN COULOMB AND NUCLEAR SCATTERING AT HIGH ENERGIES

B. P. BANNIK and V. G. GRISHIN

Joint Institute for Nuclear Research

Submitted to JETP editor December 28, 1959; resubmitted April 7, 1960

J. Exptl. Theoret. Phys. 39, 94-96 (July, 1960)

Interference between Coulomb and nuclear scattering is considered in the quasi-classical approximation. Results of calculations are presented for scattering of 8.7-Bev protons on light and heavy emulsion nuclei. The magnitude and sign of the real part of the amplitude for scattering of protons on protons are discussed.

THE amplitude of elastic scattering of nucleons on nucleons and nuclei has, in the general case, the form

$$f(\vartheta) = A(\vartheta) + (B\sigma_i, \vartheta), \tag{1}$$

where $A(\vartheta)$ is some complex function, and $B(\sigma_i, \vartheta)$ is the part of the amplitude dependent on the spins of the interacting particles. At high energies it is usually assumed that the real part of $A(\vartheta)$ and the term $B(\sigma_i, \vartheta)$ in expression (1) are equal to zero. Experiments on elastic scattering of 8.7-Bev protons on hydrogen[1] and on emulsion nuclei[2] apparently indicate that this assumption is incorrect. However, the results of these experiments, in essence, only raise the question of taking into account the real part of $A(\vartheta)$ and the spin dependence of the nuclear forces, but do not give any clue as to their role in the interaction. In the present article we consider the interference between nuclear and Coulomb scattering, the study of which can give the magnitude and sign of Re A.

In the quasi-classical approximation for spin-zero particles the scattering amplitude has the form

$$A(\vartheta) = ik\int_0^\infty [1 - e^{2i\beta(\rho)}]\, J_0(k\vartheta\rho)\, \rho\, d\rho, \tag{2}$$

where $\beta(\rho)$ is the sum of the Coulomb and nuclear scattering phase shifts. Thus the Coulomb interference is determined by the value and sign of the nuclear phase shifts. In the optical approximation, the latter depends in turn on the magnitude and sign of the real part of the nucleon—nucleon forward scattering amplitude, Re $f_{NN}(0)$.

Formula (2) is approximately valid also for the case of the scattering of particles with spin on spin-zero nuclei, for example, for the scattering of protons on light emulsion nuclei (C^{12}, N^{14}, O^{16}). Strictly speaking, the spin-orbit interaction should be taken into account in this case, but it does not play an important role in the small-angle region.

We used expression (2) to calculate the interference between Coulomb and nuclear scattering of 8.7-Bev protons on light and heavy (Ag, Br) emulsion nuclei.* The phase shifts of the nuclear scattering were calculated by the usual method (see, for example, reference 2). The Coulomb scattering phase shifts were obtained from the formula of Bethe.[3] The magnitude of Re $f_{NN}(0)$, according to the data of Markov, Tsyganov, Shafranova, and Shakhbazyan (see reference 4), was set equal to 14.4×10^{-13} cm. The results of the calculations are shown in Fig. 1. In order to obtain the differential cross section for the mixture of emulsion nuclei, it is necessary to combine the cross sections for the light and heavy nuclei with respective weights of 0.58 and 0.42.

The differential cross section was also calculated from the approximate formula of Bethe:[3]

$$d\sigma/d\Omega = |g_n(0) - (2n/k\vartheta^2)e^{2i\eta}|^2 F^2(k\vartheta a),$$
$$n = Ze^2/\hbar v, \qquad \eta = n(0.058 - \ln ka - \ln\vartheta), \tag{3}$$

where $g_n(0)$ is the forward nuclear scattering amplitude, a is the mean square radius multiplied by $\sqrt{2/3}$. The form factor was taken in the form $F = \exp\{-(k\vartheta a)^2/4\}$. Here we wished to consider the degree of applicability of this approximate formula in connection with the critical remarks of Batty.[5] As a result of the calculations, it turned

---

*We neglect the spin of the heavy nuclei as it does not play an important role in the scattering process. This is connected with the fact that the ratio of the spin of heavy nuclei to their mass number is small.

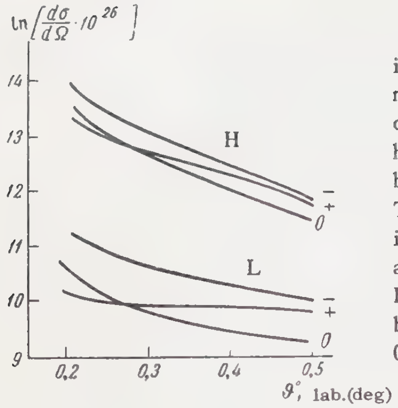

FIG. 1. Interference in the case of emulsion nuclei. The curves calculated for light and heavy nuclei are denoted by the letters L and H. The curves corresponding to positive, negative, and zero values of Re $f_{NN}(0)$ are denoted by the symbols +, –, and 0. ($d\sigma/d\Omega$ in cm^2)

out that the difference between the cross sections obtained from the approximate formula and the quasi-classical approach is no greater than a few percent for light nuclei.

In the case of scattering of 8.7-Bev protons on protons, it was assumed that the effect of their spins can be neglected.* The differential cross section was calculated from formula (3). The form factor in the same form as for the nuclei was calculated for $a = 0.86 \times 10^{-13}$ cm — the value taken from the data of Preston.[4] The results of the calculations (in the c. m. s.) are shown in Fig. 2. It is seen that the choice of the value Re $f_{NN}(0) = 13.5 \times 10^{-13}$ cm does not contradict the experimental results if its sign is positive. This statement, however, should not be considered conclusive, since the errors on the histogram are large, and the assumptions made above are based on insufficiently accurate experimental data.

The authors thank I. I. Levintov, M. I. Podgoretskiĭ, and Y. A. Smorodinskiĭ for their helpful discussions.

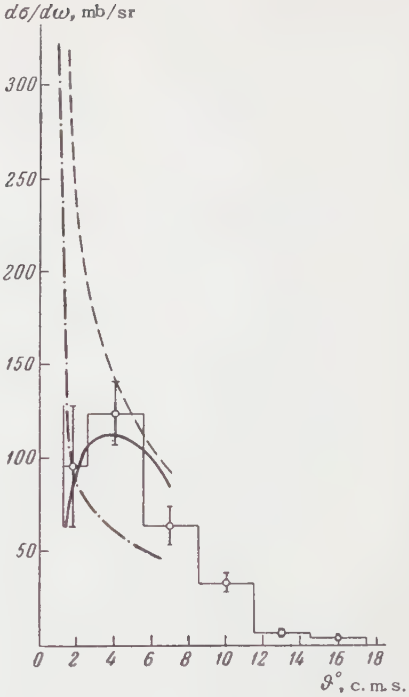

FIG. 2. Interference in the case of hydrogen. The solid, dashed and dot-dash lines refer to the positive, negative, and zero values of Re $f_{NN}(0)$. The histogram represents the experimental results of Markov et al.

---

[1] Lyubimov, Markov, Tsyganov, Cheng Pu-Ying, and Shafranova, JETP **37**, 910 (1959); Soviet Phys. JETP **10**, 651 (1960).

[2] Bannik, Grishin, Danysz, Lyubimov, and Podgoretskiĭ, JETP **37**, 1575 (1959); Soviet Phys. JETP **10**, 1118 (1960).

[3] H. Bethe, Ann. Phys. **3**, 190 (1958).

[4] V. I. Veksler, Report at the 9th International Conference on High Energy Physics, Kiev, 1959.

[5] C. J. Batty, Proc. Phys. Soc. (London) A **73**, 185 (1959).

Translated by E. Marquit
19

---

*Some basis for this assumption may be found in the fact that comparison of the scattering of 8.7-Bev protons on hydrogen[1,4] and on emulsion[2] indicates that the effect of the spin-dependent interaction is small.

SOVIET PHYSICS JETP VOLUME 12, NUMBER 1 JANUARY, 1961

A RESONANCE MODEL FOR THE $\pi + N \rightarrow \pi + \pi + N$ REACTION AT MESON ENERGIES OF 300 — 450 Mev

V. V. ANISOVICH

Leningrad Physico-Technical Institute, Academy of Sciences, U.S.S.R.

Submitted to JETP editor January 8, 1960

J. Exptl. Theoret. Phys. U.S.S.R) **39**, 97-104 (July, 1960)

It is assumed that the energy dependence of the matrix element is only due to a resonance interaction between the nucleon and one of the mesons in the final state $(^3/_2, {}^3/_2)$, and that these particles carry away most of the energy of the system. Under these assumptions, expressions containing six parameters are given for the reaction cross sections. It is shown that the results based upon such a model are in agreement with the available experimental data.

IT is not possible at present to calculate the cross sections for the $\pi + N \rightarrow \pi + \pi + N$ reaction using the field theory. It is therefore very desirable to describe the process using some general properties of strong interactions or, at least, by means of phenomenological models. At not too high energies of the incident meson (up to 250 Mev) the reaction was studied by Ansel'm and Gribov,[1] who succeeded in showing that the zero-energy amplitudes of the meson-meson scattering can be found from the study of the behavior of the reaction cross section near the threshold. At energies in the 1 — 1.5 Bev range, single π-meson production in meson-nucleon collisions was investigated quite successfully using the isobar model.[2] In the 300 — 600 Mev range, Peierls[3] and Barshay[4] studied the possibility of obtaining information on the meson-meson interaction from the angular correlation of the particles produced in the reaction.

1. BASIC ASSUMPTIONS. RELATIONS BETWEEN THE TOTAL CROSS SECTIONS FOR DIFFERENT REACTIONS.

In the present article we consider the case where the kinetic energy of the particles produced lies within the 100 — 200 Mev range in the c.m.s. We assume that the meson-meson interaction in the energy range under consideration is much smaller than the resonance meson-nucleon interaction. It is further assumed that, in the final state, one of the mesons and the nucleon are produced in the $(^3/_2, {}^3/_2)$ state with an energy which is, in the majority of events, close to resonance energy. The kinetic energy of the second meson will, in general, be not higher than 50 Mev. The last assumption can be submitted to an experimental test. The matter will be discussed in detail below.

In addition, it is assumed that the energy dependence of the matrix element is determined by the interaction of the particles in the final state only. In the majority of cases one of the mesons and the nucleon are in the resonant state with high energy, while the second meson has an energy not higher than 50 Mev. The interaction of a 50-Mev meson with a nucleon is considerably weaker than at 100 — 200 Mev. We neglect therefore the interaction between the second meson and the nucleon in the final state. Since it is assumed that the meson-meson interaction at energies below 200 Mev is also weak compared with the resonance interaction, it can be neglected as well.

Thus, only the interaction between one of the mesons and the nucleon in the $(^3/_2, {}^3/_2)$ state is considered in the final state. A diagram of the process is shown in Fig. 1a; it is assumed that the shaded circle is constant in the energy range under consideration. The upper part of the diagram represents the scattering of the meson on the nucleon, in which one meson vertex is missing (Fig. 1b). If the product $r_0 q$ of the meson-nucleon interaction radius by the meson momentum is small, then the matrix element corresponding to Fig. 1b is given, disregarding angle-dependent factors, by the following expression (neglecting the nucleon recoil):

$$q^{-2} e^{i\delta(q)} \sin \delta (q). \quad (1)$$

where $\delta(q)$ is the phase of meson-nucleon scattering in the $(^3/_2, {}^3/_2)$ state for meson momentum q. Since the second meson possesses an energy of the order of 50 Mev, we shall assume that it is in a state with orbital angular momentum L equal to 0

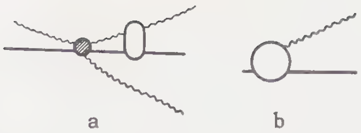

FIG. 1

or 1 with respect to the center of mass of the two remaining particles.

It is necessary to note that when the energy of the incident meson is higher than 450 Mev the kinetic energy of the particles produced will be higher than 200 Mev. The energies of both mesons can then be close to the resonance energy, and it becomes necessary to consider the interaction of both mesons with the nucleon in the final state. The results obtained in the present article are, therefore, not applicable to higher energies.

Similar assumptions were made by Mandelstam[5] in a study of the $N + N \rightarrow \pi + N + N$ reaction. His results are in good agreement with experiment, and one can hope, therefore, that a similar approach may be useful in the treatment of the present problem.

Let us now consider the consequences resulting only from the assumption that, in the final state, one of the mesons and the nucleon are produced in the $(\frac{3}{2}, \frac{3}{2})$ resonance state and carry away most of the energy of the system.

If the meson and the nucleon are characterized by the isotopic spin projections ζ and ν in the initial state, and if in the final state the first and second meson and the nucleon have the isotopic spin projections ξ, η, and μ respectively, then, according to the requirement of isotopic invariance, the transition matrix element is

$$\sum_T (\alpha_T F^T(1,2) + \beta_T F^T(2,1)),$$

$$\alpha_T = C^{T\tau}_{1\zeta^1/_2\nu} C^{T\tau}_{1\eta^3/_2\mu+\xi} C^{^3/_2\mu+\xi}_{1\xi^1/_2\mu}, \quad \beta_T = C^{T\tau}_{1\zeta^1/_2\nu} C^{T\tau}_{1\xi^3/_2\mu+\eta} C^{^3/_2\mu+\eta}_{1\eta^1/_2\mu}, \quad (2)$$

where T and τ are the total isotopic spin of the system and its projection on the z axis (T can have the values $\frac{1}{2}$ and $\frac{3}{2}$), 1 and 2 are the energy and momentum of the first and second meson, respectively, and $F^T(1, 2)$ is the transition amplitude, which is dependent on the total isotopic spin and on the energies and momenta of the particles produced. The term containing $F^T(1, 2)$ corresponds to the production of the first π meson in resonance with the nucleon, while the term with $F^T(2, 1)$ corresponds to the production of the second meson in the resonance state. The actual values of α_T and β_T for different processes are given in the Appendix.

The square of the matrix element contains terms with $F^{T'}(1, 2) F^{T*}(1, 2)$ and $F^{T'}(1, 2) F^{T*}(2, 1)$. Moreover, $F^T(1, 2)$ and $F^T(2, 1)$ cannot be simultaneously large: if one meson is produced in resonance with the nucleon, little energy is available for the second meson and the amplitude $F^T(2, 1)$ is small, and vice versa. We can therefore neglect the terms containing $F^{T'}(1, 2) F^{T*}(2, 1)$. The square of the matrix element can then be written in the following form:

$$\sum_{TT'} \{\alpha_T \alpha_{T'} \operatorname{Re}(F^{T^*}(1,2) F^{T'}(1,2)) + \beta_T \beta_{T'} \operatorname{Re}(F^{T^*}(2,1) F^{T'}(2,1))\}. \quad (3)$$

The contributions of the real parts of Eq. (3) to the total cross section are equal. Using Eq. (3) and Eq. (A1) of the Appendix we thus obtain the following expressions for the total cross sections for the processes under consideration:

$$\sigma(\pi^+ + p \rightarrow n + \pi^+ + \pi^+) = {}^4/_{15} A_3, \quad \sigma(\pi^+ + p \rightarrow p + \pi^0 + \pi^+) = {}^{13}/_{15} A_3,$$

$$\sigma(\pi^- + p \rightarrow n + \pi^- + \pi^+) = {}^{10}/_{27} A_1 + {}^{26}/_{135} A_3 - {}^{14}/_{27} \sqrt{{}^2/_5} A_{13},$$

$$\sigma(\pi^- + p \rightarrow n + \pi^0 + \pi^0) = {}^8/_{27} A_1 + {}^4/_{135} A_3 + {}^8/_{27} \sqrt{{}^2/_5} A_{13},$$

$$\sigma(\pi^- + p \rightarrow p + \pi^- + \pi^0) = {}^4/_{27} A_1 + {}^{17}/_{135} A_3 + {}^{10}/_{27} \sqrt{{}^2/_5} A_{13}. \quad (4a)$$

A_2, A_3, and A_{13} are functions of the total energy only. A_1 and A_3 are obtained by integrating the squares of the absolute values of the amplitudes, with total isotopic spins equal to $\frac{1}{2}$ and $\frac{3}{2}$ respectively, over the phase volume, and A_{13} is the result of integrating the interference term. A_1 and A_3 are therefore positive, and A_{13} satisfies the inequality $|A_{13}| \leq \sqrt{A_1 A_3}$.

The following two relations between the total cross sections are a consequence of Eq. (4a):

$$\sigma(\pi^+ + p \rightarrow n + \pi^+ + \pi^+) = 0.3\,\sigma(\pi^+ + p \rightarrow p + \pi^0 + \pi^+),$$

$$1.4\sigma(\pi^+ + p \rightarrow n + \pi^+ + \pi^+) + 2\sigma(\pi^- + p \rightarrow n + \pi^0 + \pi^0) = 0.6\sigma(\pi^- + p \rightarrow n + \pi^- + \pi^+) + 2.5\,\sigma(\pi^- + p \rightarrow p + \pi^0 + \pi^-). \quad (4b)$$

Thus, using only the assumption that one of the mesons is produced in the resonance state $(\frac{3}{2}, \frac{3}{2})$, two relations between the cross sections in the energy range under consideration have been obtained. A comparison of Eqs. (4b) with experimental data will constitute a test of the assumption made above that one of the mesons and the nucleon are produced in the $(\frac{3}{2}, \frac{3}{2})$ state with an energy which, in general, is close to the resonance energy.

2. TRANSITION-MATRIX ELEMENT

Let us now consider the problem in greater detail. The following transitions are possible under the assumptions made above:

$$D^{-}_{3/2} \to P_{3/2}s_{3/2}, \quad P^{+}_{3/2} \to P_{3/2}\, p_{3/2},$$
$$P^{+}_{1/2} \to P_{3/2}p_{1/2}, \quad F^{+}_{3/2} \to P_{3/2}p_{5/2}. \tag{5}$$

In (5), the expression $P^{+}_{1/2} \to P_{3/2}p_{1/2}$ denotes, e.g., that in the initial state the meson and the nucleon had orbital angular momentum 1, total angular momentum $1/2$, and positive parity, while in the final state on the mesons and the nucleon are in the $P_{3/2}$ resonance state and the second meson is in a p state with respect to the center of mass of the first two particles. We shall neglect the transitions from an initial F state since, at energies on the order of 400 Mev, the contribution of the F state to meson-nucleon scattering is considerably smaller than the contribution of other states.

As will be shown in the following, the assumption that one of the mesons and the nucleon are in the $(3/2, 3/2)$ state with an energy close to the resonance energy in the majority of cases is, for the given model, equivalent to the assumption that the principal transition is

$$D^{-}_{3/2} \to P_{3/2}s_{3/2}.$$

It is possible to write down the matrix element $F^T(1, 2)$ in an approximation in which the nucleon mass is assumed to be infinite. For the case when the total angular momentum of the system and its projection on the z axis are equal to j and M, respectively, $F^T(1, 2)$ is given by

$$a^T_{jL} q_1^{-2}\, e^{i\delta(q_1)} \sin\delta(q_1)\, q_2^L \sum_{ms} C^{jM}_{LM-m\,3/2\,m} C^{3/2\,m}_{1\,m-s\,1/2\,s}$$
$$\times Y_{1\,m-s}(\mathbf{q}_1)\, Y_{LM-m}(\mathbf{q}_2), \tag{6}$$

where $\mathbf{q}_1$ is the momentum of the meson which is in the $(3/2, 3/2)$ state, $\delta(\mathbf{q}_1)$ is the phase shift for the given momentum in the resonance state, $\mathbf{q}_2$ and L are the momentum and angular momentum of the second meson with respect to the center of mass of the first two particles, and a^T_{jL} are certain constants varying with T, j, and L. It follows from Eq. (5) and the assumption about the small contribution of the F state that there are three such constants for a given T.

The matrix element, as given by Eq. (6), is correct to a term of the order of the ratio of the kinetic energy of the particles in the final state to the nucleon mass.

The constants a^T_{jL} should still satisfy certain relations that follow from the fact that the S matrix is a unitary one. As in reference 6, it can be found that

$$a^T_{jL} = b^T_{jL} \exp(i\eta^T_{jL}), \tag{7}$$

where η^T_{jL} is the phase of the meson-nucleon scattering with given T, j, and L corresponding to the incident meson energy, and b^T_{jL} are real (though not necessarily positive) quantities which should be determined by comparing the expressions for the cross sections with experimental data.

3. EXPRESSIONS FOR THE CROSS SECTIONS

In calculating the cross sections for the investigated process we assume the nucleon to be at rest in the final state. The cross sections can be then easily calculated in the usual way. It is only necessary to multiply the amplitudes F^T given in Eq. (6) by a factor $k^{-1/2}C^{jM}_{\lambda 0 \frac{1}{2} M}$, which is due to the expansion of the plane wave in terms of the total angular momentum eigenfunctions of the system (k is the meson momentum in the initial state, and λ is the angular momentum of the meson-nucleon system in the initial state).

The energy distribution of mesons moving within a solid angle element with a given θ (angle between the z axis and the direction of meson emission in the c.m.s.) is given by the expression

$$d\sigma = [a_0 + a_1\cos\theta + \tfrac{1}{2}a_2(3\cos^2\theta - 1)]\, d\omega\, d\Omega/4\pi,$$
$$a_0 = S(\omega)[A_1 + ((\varepsilon-\omega)^2 - 1)B_1] + S(\varepsilon-\omega)[A_2 + (\omega^2 - 1)B_2],$$
$$a_1 = S(\varepsilon - \omega)\ \sqrt{\omega^2 - 1}\ C,$$
$$a_2 = S(\omega)[D_1 + ((\varepsilon-\omega)^2 - 1)E_1] + S(\varepsilon-\omega)(\omega^2 - 1)E_2,$$
$$S(\omega) = \frac{\sqrt{1+k^2}\sqrt{M^2+k^2}}{k^2(\sqrt{1+k^2} + \sqrt{M^2+k^2})}$$
$$\times (\varepsilon - \omega)\sqrt{(\varepsilon-\omega)^2 - 1}\ \omega \frac{\sin^2\delta(\omega)}{(\omega^2-1)^{3/2}}. \tag{8}$$

where M is the nucleon mass, $\omega = \sqrt{1+q^2}$ is the energy of the meson under consideration (meson mass equal zero), ϵ is the energy of both mesons in the final state (including rest energy) in the c.m.s. (it should be remembered that we neglect the kinetic energy of the nucleon in the final state), $d\Omega = 2\pi \sin\theta\, d\theta$ is the solid-angle element, and $\delta(\omega)$ is the phase shift in the $(3/2, 3/2)$ resonance state. A_1, A_2, ... E_1, E_2 are constants varying with a^T_{jL}, α_T, and β_T (i.e., they are different for different processes). In addition, these constants vary depending on which one of the mesons produced is considered. Explicit expressions for the constants are given in the Appendix.

The total cross section is obtained from Eq. (8) by integrating over all possible values of ω and the angle θ. Using the data of reference 7 to determine $\sin^2\delta(\omega)$, we can calculate the total cross section for the investigated process

$$\sigma = (A_1 + A_2)I_1 + (B_1 + B_2)I_2, \tag{9}$$

where I_1 and I_2 are functions of the total energy only. Numerical values of these functions are given in the table.

Energy of the incident meson in the laboratory system, Mev.	$I_1 \cdot 10^2$	$I_2 \cdot 10^2$	$I_3 \cdot 10^2$
290	0.83	0.42	0.60
320	1.5	1.0	1.2
370	3.2	2.9	3.0
430	6.3	6.6	6.4

The following expression gives the meson angular distribution:

$$4\pi d\sigma/d\Omega = b_0 + b_1 \cos\theta + {}^1/_2 b_2 (3\cos^2\theta - 1),$$

$$b_0 = (A_1 + A_2) I_1 + (B_1 + B_2) I_2,$$

$$b_1 = C I_3, \quad b_2 = D I_1 + (E_1 + E_2) I_2. \tag{10}$$

The values of I_3 are given in the table.

According to the assumptions made, the course of the process is such that one of the mesons is produced in a $(^3/_2, {}^3/_2)$ resonance state and, in general, the energy of this meson lies in the resonance range, i.e., is relatively high.

It is essential to check whether the formulas obtained fulfill the requirement that the number of cases in which the meson produced in the $(^3/_2, {}^3/_2)$ state has an energy substantially different from the resonance energy be really small. Integrating Eq. (8) over the angle θ, we obtain the energy distribution for the meson which, to be specific, we shall denote as the "first" meson:

$$d\sigma/d\omega = S(\omega)[A_1 + ((\varepsilon - \omega)^2 - 1) B_1]$$

$$+ S(\varepsilon - \omega)[A_2 + (\omega^2 - 1) B_2].$$

The first term is responsible for the production of the "first" meson in the $(^3/_2, {}^3/_2)$ state. It is necessary to check if this term really decreases sufficiently fast with decreasing energy of the "first" meson. The energy dependence of the first term is determined by the quantities $A_1 S(\omega)$ and $B_1(\epsilon - \omega^2 - 1) S(\omega)$, of which the first has, in fact, a maximum for $\omega \sim \omega_{res}$ $(\omega_{res} \sim \epsilon - 1)$, while the second attains a maximum for smaller ω. This is a result of the additional factor $(\epsilon - \omega)^2 - 1 = q_2^2$, which appears in the matrix element (6) because of the production of the "second" meson with $L = 1$.

If the process goes in such a way that the "second" meson is, in general, produced in a state with $L = 0$, i.e., if $A_1 \gg B_1$ (the quantities $S(\omega)$ and $S(\omega)[(\epsilon - \omega)^2 - 1]$ are of the same order of magnitude), then the basic assumptions are satisfied. The same can be said about the second term, responsible for the production of the "second" meson in the $(^3/_2, {}^3/_2)$ state. This term should decrease sufficiently fast with increasing ω if $\epsilon - \omega$ becomes smaller than ω_{res}.

It is thus necessary that $A_1 + A_2 \gg B_1 + B_2$ (for the results it is sufficient that $A_1 + A_2$ be greater than $B_1 + B_2$ by a factor of two or three at least). As will be seen in the following from the analysis of experimental data, the condition $A_1 + A_2 \gg B_1 + B_2$ can, in fact, be satisfied, although B_1 and B_2 cannot be assumed to vanish, for if all mesons produced are in resonance interaction with the nucleon the term $a_1 \cos\theta$, which is essential for the agreement with experiment, disappears from the cross section (8) in the P state.

4. COMPARISON WITH EXPERIMENTAL DATA

The results given above for the cross sections have been compared with the experimental data of Perkins et al.,[8] who measured the cross sections for the $\pi^- + p \rightarrow \pi^+ + \pi^- + n$ reaction at 260, 320, 370, and 430 Mev (Fig. 2). The expression for the total cross section (9) is in good agreement with the experimental results. Attention should be drawn to the fast increase of the cross section between 300 and 450 Mev, which cannot be explained by the increase of the phase volume only. The curve showing the increase of the phase volume with energy is given for comparison in Fig. 2 by the dashed line. It should also be noted that, essentially, the total cross sections (9) depend only on one parameter $A_1 + A_2$, since $B_1 + B_2$ is small under the assumptions made above.

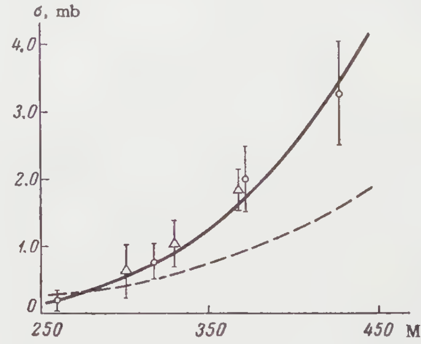

FIG. 2. Total cross section for the $\pi^- + p \rightarrow n + \pi^+ + \pi^-$ reaction, calculated according to Eq. (9) for $A_1 + A_2 = 53$ mb, $B_1 + B_2 = 3$ mb (solid line). Dashed line represents the increase in the phase volume. o – values of the total cross section $\sigma(\pi^- + p \rightarrow n + \pi^+ + \pi^-)$,[8] Δ – values of $\sigma(\pi^- + p \rightarrow n + \pi^+ + \pi^-) + 0.35\sigma(\pi^- + p \rightarrow \pi^- + \pi^0 + p)$.[9] The x axis represents the incident meson energy in the laboratory system.

It can be seen from Figs. 3 and 4 that the data on the angular distribution of positively charged mesons at 320 and 430 Mev also are in agreement with the theoretical curves.

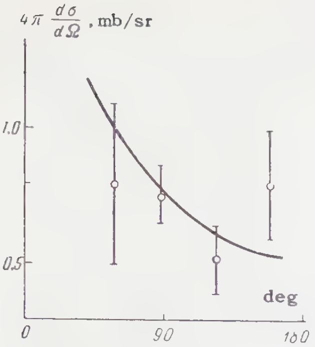

FIG. 3. Angular distribution in the c.m.s. of the mesons produced in the $\pi^- + p \rightarrow n + \pi^+ + \pi^-$ reaction at 320 Mev incident meson energy.[8] Solid curve represents the angular distribution calculated according to Eq. (10) for C = 30 mb, D_1 = 2.5 mb, and $E_1 + E_2$ = 2.5 mb.

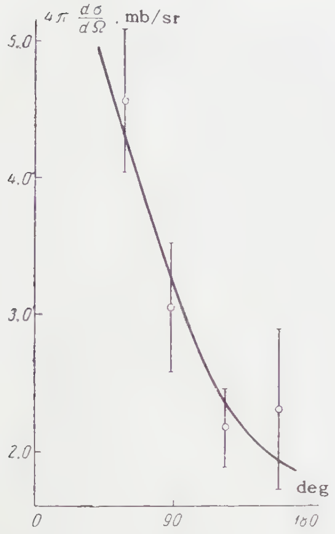

FIG. 4. Angular distribution in c.m.s. of π^+ mesons produced in the $\pi^- + p \rightarrow n + \pi^+ + \pi^-$ reaction at 430 Mev incident meson energy.[8]

The mean value of $\sigma(\pi^+ + p \rightarrow \pi^+ + \pi^+ + n) + \sigma(\pi^+ + p \rightarrow \pi^+ + \pi^0 + p)$ was estimated[9] for the energy range 300 — 575 Mev. It was found to be equal to (1.8 ± 0.6) mb. It follows then from Eq. (4a) that $A_3 = (1.6 \pm 0.5)$ mb and that the contribution of the term containing A_3 to the total cross sections $\sigma(\pi^- + p \rightarrow n + \pi^+ + \pi^-)$, $\sigma(\pi^- + p \rightarrow n + \pi^0 + \pi^0)$, and $\sigma(\pi^- + p \rightarrow p + \pi^0 + \pi^-)$ is of the order of 0.3, 0.05, and 0.2 mb respectively, i.e., is small. Neglecting it, we obtain an additional relation between the total cross sections

$$\sigma(\pi^- + p \rightarrow n + \pi^+ + \pi^-) + 4\sigma(\pi^- + p \rightarrow p + \pi^0 + \pi^-) = 3\sigma(\pi^- + p \rightarrow n + \pi^0 + \pi^0). \qquad (11)$$

It follows from reference 8 that the mean value of $\sigma(\pi^- + p \rightarrow p + \pi^+ + \pi^-)$ in the energy range under consideration is of the order of 2 — 2.5 mb. Since $A_3 \sim 1.6$ mb and $A_{13} \leq \sqrt{A_1 A_3}$, one finds easily from Eq. (4a) that the mean value of $\sigma(\pi^- + p \rightarrow p + \pi^0 + \pi^-) \leq 2$ mb in the investigated energy range.

This fact is confirmed by the results of Zinov and Korenchenko[10] who measured the quantity $2\sigma(\pi^- + p \rightarrow n + \pi^+ + \pi^-) + 0.7\,\sigma(\pi^- + p \rightarrow p + \pi^0 + \pi^-)$ (see Fig. 2). From their data, as well as those of reference 8, it follows that the cross section $\sigma(\pi^- + p \rightarrow p + \pi^0 + \pi^-)$ cannot be large.

The available experimental data are not sufficient to establish how well the proposed model describes the two-meson production process in meson-nucleon collisions in the energy range under consideration. The agreement between the experimental and the theoretical angular distributions of π^+ mesons and the total cross sections does not provide a decisive proof for the validity of the model because of the large number of unknown parameters a^T_{jL} (six constants). It should be mentioned, however, that the model yields a correct increase of the cross sections with the energy, which depends only on the variation of I_1 with the energy but is independent of the constants a^T_{jL}. The model also predicts an increase of the coefficients b_1 and b_2 with the energy in the expressions (10) for the angular meson distribution, which is in agreement with experiment.

The author is greatly indebted to V. N. Gribov for indicating the subject of the investigation and for advice, and to A. A. Ansel'm for helpful discussion.

APPENDIX

We give here the values of α_T and β_T for the various processes:

I. $\pi^+ + p \rightarrow n + \pi^+ + \pi^+$

$$\alpha_{1/2} = \beta_{1/2} = 0, \quad \alpha_{3/2} = \beta_{3/2} = \sqrt{2/15}.$$

II. $\pi^+ + p \rightarrow p + \pi^0(1) + \pi^+(2)$

$$\alpha_{1/2} = \beta_{1/2} = 0, \quad \alpha_{3/2} = -2/\sqrt{15}, \quad \beta_{3/2} = \sqrt{3/5}.$$

III. $\pi^- + p \rightarrow n + \pi^-(1) + \pi^+(2)$

$$\alpha_{1/2} = 1/\sqrt{3}, \quad \beta_{1/2} = 1/3\sqrt{3},$$

$$\alpha_{3/2} = -\sqrt{2/15}, \quad \beta_{3/2} = \frac{2}{3}\sqrt{2/15}.$$

IV. $\pi^- + p \rightarrow n + \pi^0 + \pi^0$

$$\alpha_{1/2} = \beta_{1/2} = -2/3\sqrt{3}, \quad \alpha_{3/2} = \beta_{3/2} = -\frac{1}{3}\sqrt{2/15}.$$

V. $\pi^- + p \rightarrow p + \pi^-(1) + \pi^0(2)$

$$\alpha_{1/2} = -\frac{1}{3}\sqrt{2/3}, \quad \beta_{1/2} = \frac{1}{3}\sqrt{2/3},$$

$$\alpha_{3/2} = -1/3\sqrt{15}, \quad \beta_{3/2} = 4/3\sqrt{15}. \qquad \text{(A1)}$$

The expressions for the cross sections (8) — (10) contain the constants $A_1, A_2, \ldots E_1, E_2$. If we are interested in the cross section for the meson denoted in (A1) by π (1), the constants are

$$A_1 = D = \frac{2}{5}\sum_{TT'} \alpha_T \alpha_{T'} \operatorname{Re}(a^{T*}_{3/2\,0} a^{T'}_{3/2\,0}),$$

$$B_1 = \sum_{TT'} \alpha_T \alpha_{T'} \left\{\frac{1}{3}\operatorname{Re}(a^{T*}_{1/2\,1} a^{T'}_{1/2\,1}) + \frac{2}{3}\operatorname{Re}(a^{T*}_{3/2\,1} a^{T'}_{3/2\,1})\right\},$$

$$C = \sum_{TT'} \beta_T \beta_{T'} \left\{-2\sqrt{\frac{2}{15}}\operatorname{Re}(a^{T*}_{1/2\,1} a^{T'}_{3/2\,0}) + \frac{4}{5\sqrt{3}}\operatorname{Re}(a^{T*}_{3/2\,1} a^{T'}_{3/2\,0})\right\},$$

$$E_1 = \sum_{TT'} \alpha_T \alpha_{T'} \left\{ -\frac{4}{3} \sqrt{\frac{2}{5}} \operatorname{Re}\left(a^{T*}_{1/2\,1} a^{T'}_{3/2\,1}\right) - \frac{2}{15} \operatorname{Re}\left(a^{T*}_{3/2\,1} a^{T'}_{3/2\,1}\right) \right\},$$

$$E_2 = \sum_{TT'} \beta_T \beta_{T'} \left\{ -\frac{2}{3} \sqrt{\frac{2}{5}} \operatorname{Re}\left(a^{T*}_{1/2\,1} a^{T'}_{3/2\,1}\right) - \frac{8}{15} \operatorname{Re}\left(a^{T*}_{3/2\,1} a^{T'}_{3/2\,1}\right) \right\}. \tag{A2}$$

A_2 and B_2 can be obtained from the expressions for A_1 and A_2 by substituting β_T for α_T.

For the meson denoted in (A1) by π (2), the constants $A_1, \ldots, E_2$ are obtained from the corresponding constants in Eq. (A2) by substituting β_T for α_T. Thus, e.g., the cross section for the π^- meson in the $\pi^- + p \rightarrow n + \pi^+ + \pi^-$ reaction is obtained by substituting into Eq. (A2) the values $\alpha_{1/2} = 1/\sqrt{3}$, $\beta_{1/2} = 1/3\sqrt{3}$, $\alpha_{3/2} = -\sqrt{2/15}$, $\beta_{3/2} = \frac{2}{3}\sqrt{2/15}$, and the cross section for the π^+ meson is obtained by substituting into Eq. (A2) the values $\alpha_{1/2} = 1/3\sqrt{3}$, $\beta_{1/2} = 1/\sqrt{3}$, $\alpha_{3/2} = \frac{2}{3}\sqrt{2/15}$, $\beta_{3/2} = -\sqrt{2/15}$.

---

[1] A. A. Ansel'm and V. N. Gribov, JETP **36**, 1890 (1959) and **37**, 501 (1959), Soviet Phys. JETP **9**, 1345 (1959) and **10**, 354 (1960).

[2] S. I. Lindenbaum and R. M. Sternheimer, Phys. Rev. **106**, 1107 (1957).

[3] R. F. Peierls, Phys. Rev. **111**, 1373 (1958).

[4] S. Barshay, Phys. Rev. **111**, 1651 (1958).

[5] S. Mandelstam, Proc. Roy. Soc. **A244**, 491 (1958).

[6] E. Fermi, Nuovo cimento Suppl. **2**, 1 (1955), V. N. Gribov, JETP **33**, 1431 (1957), Soviet Phys. JETP **6**, 1102 (1958).

[7] H. Bethe and F. Hoffmann, Mesons and Fields, Vol. II, (Russ. Transl.) I I L, 1957, p. 34, B. Pontecorvo, Материалы Киевской конференции 1959 Materials of the Kiev Conference, 1959, p. 30.

[8] Perkins, Caris, Kenny, Knopp, and Perez-Mendes (Berkeley). Cited by B. Pontecorvo, ibid. pp. 86-89.

[9] Blevins, Block, and Leitner (Durham). Cited by B. Pontecorvo, ibid. 1959, p. 76.

[10] V. G. Zinov and S. M. Korenchenko, JETP **34**, 301 (1958), Soviet Phys. JETP **7**, 210 (1958).

Translated by H. Kasha
20

SOVIET PHYSICS JETP VOLUME 12, NUMBER 1 JANUARY, 1960

ENERGY SPECTRUM OF CASCADE ALPHA PARTICLES IN PHOTOGRAPHIC EMULSION STARS PRODUCED BY HIGH-ENERGY PROTONS

V. I. OSTROUMOV, N. A. PERFILOV, and R. A. FILOV

Radium Institute, Academy of Sciences, U.S.S.R.

Submitted to JETP editor January 15, 1960

J. Exptl. Theoret. Phys. (U.S.S.R.) 39, 105-107 (July, 1960)

The energy spectrum of α particles with energies above 30 Mev and emitted in the disintegration of heavy photographic emulsion nuclei induced by 140, 200, 360 and 660 Mev protons has been computed. The calculations are based on the assumption of a single elastic collision between cascade nucleons and particles inside the nucleus. The calculated and experimental distributions are compared and found to be in good agreement if the kinetic energy of the α particle in the nucleus is assumed to equal 5-10 Mev.

IN our previous work[1] we presented the results of calculations of the effective cross sections for the emission of α particles of energy greater than 30 Mev in the disintegration of emulsion nuclei induced by high energy protons. The calculations were based on the assumption of single elastic collisions between the secondary fast nucleons produced in the cascade stage of the disintegration process and clusters of nucleons of the α-particle type, which may exist in the nucleus as a temporary formation. Comparison with the corresponding experimental data allowed the determination of the relative time during which the nucleons remain in the group of α clusters for light emulsion nuclei (C, O, N) and in the peripheral region of heavy nuclei (Ag and Br). The probability for the production of α particles in the nucleus calculated in this way proved to be a decreasing function of the value assumed for the momentum of the α particles inside the nucleus.

In the present article we present a calculation of the energy spectrum of fast cascade α particles in order to obtain definite information on the value of the velocity of the α particles in the nucleus, since it is natural to expect that the shape of the energy distribution curve of the recoil particles will depend on their initial momentum.

The computational and experimental methods are quite analogous to those described earlier.[1,2] In order to obtain the energy spectrum of the emitted α particles, formulas[1] with the corresponding values of T (the lower limit of the kinetic energy of the recorded α particles) were used.

Shown in the figure is the experimental α-particle spectrum (with a lower limit of 30 Mev) obtained from the observation of stars produced in Ag and Br nuclei by protons of energy E_0 = 660 Mev. The α-particle spectra obtained in the experiments for proton energies of 140, 200, and 360 Mev have the same shape and therefore are not shown. The statistics of the observations are given in reference 2. The calculated results are shown in the same figure. The calculated and experimental distributions are reduced to the same total number of particles. In view of the fact that the energy spectra of the emitted α particles, calculated for α-particle kinetic energies in the nucleus of W = 5, 10, and 20 Mev, lie very close to one another, only the curves for W = 0 and W = 5 Mev are given in the figure. It is seen from the figure that the experimental data corresponds to the calculations based on elastic collisions of nucleons with moving α particles; the same good agreement is also obtained at E_0 = 140, 200, and 360 Mev.

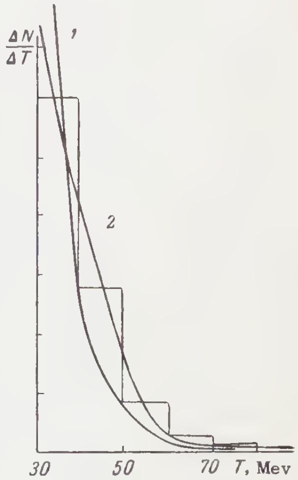

Energy spectrum of α particles knocked out of Ag and Br nuclei by 660-Mev protons. The histogram represents the experimental data; curve 1 was calculated for W = 0 Mev; curve 2 was calculated for W = 5 Mev.

The choice of the particular value of the α-

particle momentum is not critical for the shape of the observed energy spectrum (at least if W remains between 5 and 20 Mev). Therefore attempts to choose some function for the momentum distribution of the α particles inside the nucleus in order to obtain good agreement between the calculated and experimental spectra serve no purpose. Thus, for example, a uniform momentum distribution within W = 0 to 20 Mev or a Gaussian distribution with the value e^{-1} corresponding to an energy of 5 or 10 Mev give practically the same good agreement with experiment.

A certain excess of high energy α particles above the calculated value can be attributed, at least in part, to an admixture of He^3 nuclei, which have a smaller energy for the same range. If we take the amount of He^3 nuclei as equal to 20%[3] and assume that the spectra for He^4 and He^3 are identical, then the correction to the experimental spectrum brings it closer to the calculated one. Moreover, a certain effect in this direction can result from the dependence of the α-particle mean free path in the nucleus on its kinetic energy.

Detailed calculations of the energy spectra of cascade α particles emitted from light emulsion nuclei lead approximately to the same results, since the distribution function of the emitted α particles is related to the concrete type of nucleus only by the shape of the energy spectrum of the cascade nucleons, which spectrum changes little from nucleus to nucleus. Comparison with experiment, however, is difficult, owing to the low accuracy of observation of stars from light nuclei. This was done for the disintegration of light nuclei induced by 360-Mev protons. In this case, too, the values W = 5 or 10 Mev proved to be most suitable. This result does not contradict the data of Cüer and Samman[4], who found that α particles in the C^{12} nucleus have a broad energy distribution with a mean value W = 6 Mev.

Comparing the data on the value of W obtained in the present work with that calculated from the expression for w (W) (see reference 1), where w is the probability for the production of an α particle, we can conclude that there is a strong tendency for the nucleons at the periphery of the heavy nuclei to produce α clusters which behave as a single entity in the cascade process of nuclear disintegration. Of course, the agreement between the calculated results and the experimental data is not yet sufficient to establish the absoluteness and uniqueness of the chosen model. The possibility of some other mechanism, for example, of the complex "pick-up" type (p, α) cannot be completely excluded.

For further verification of the correctness of the ideas we have developed to account for the occurrence of high energy α particles in nuclear disintegration, it is necessary to have additional criteria. Such a criterion can be the agreement between the calculated angular distribution of the cascade α particles and the expermental distribution, since it is difficult to expect that any two different mechanisms lead to the same angular and energy distributions over a wide energy range of incident nucleons. Extrapolation of the calculated curves to lower α-particle energies will probably not be successful, since the application of the model based on collisions between a single nucleon and an α particle is not suitable for low energies.

---

[1] V. I. Ostroumov and R. A. Filov, JETP **37**, 643 (1959), Soviet Phys. JETP **10**, 459 (1960).

[2] Ostroumov, Perfilov, and Filov, JETP **36**, 367 (1959), Soviet Phys. JETP **9**, 254 (1959).

[3] A. A. Rimskiĭ-Korsakov, Thesis, Leningrad Polytechnical Institute, 1959.

[4] A. Samman and P. Cüer, J. phys. radium **19**, 13 (1958).

Translated by E. Marquit
21

SOVIET PHYSICS JETP VOLUME 12, NUMBER 1 JANUARY, 1961

THE POSITION OF THE GIANT RESONANCE IN THE DIPOLE ABSORPTION OF GAMMA QUANTA BY ATOMIC NUCLEI

V. G. NEUDACHIN, V. G. SHEVCHENKO, and N. P. YUDIN

Nuclear Physics Institute, Moscow State University

Submitted to JETP editor January 28, 1960; resubmitted March 11, 1960

J. Exptl. Theoret. Phys. (U.S.S.R.) **39**, 108-111 (July, 1960)

The giant-resonance curves for a number of intermediate nuclei (Ca^{40}, V^{51}, Ni^{58}, and $Cu^{63,65}$) are calculated on the basis of the shell model. It is shown that if spectroscopic data on the lower nuclear levels are employed the shell theory calculations yield in a natural manner the correct position of the giant resonance.

WILKINSON'S[1] application of the shell theory to calculate the dipole absorption of gamma quanta has permitted a qualitative explanation of the width and area of the giant resonance. However, the energy of the giant resonance turned out to be approximately half as large as the experimental value. To obtain agreement with the experimental value, Wilkinson made use of the concept of "effective mass"; the correct position of the giant resonance is obtained for an effective mass equal to half the true mass of the nucleon. For such a value of the effective mass the distance between single-particle levels belonging to neighboring shells is increased by a factor of two and amounts to ~ 14 Mev for the usually accepted dimensions of the nucleus. However, the latest experimental data[2] show that the spacing between the above levels is, just as in the usual shell model, 6 — 7 Mev.

We wish to show that for nuclei with $A < 70$ account of the residual pair interactions in the calculations of the giant resonance according to the shell model, and a more accurate estimate of the nucleon binding energy in closed shells yield an energy value in agreement with experiment, so that the giant-resonance phenomenon can be understood within the framework of the usual shell theory without the introduction of an "effective mass." The effect of the residual interactions is apparent from empirical data on the lower states of nuclei without the introduction of any kind of explicit pair potential.

The method of taking account of these effects will be presented below by the example of a calculation of the dipole absorption curve for the Ca^{40} and V^{51} nuclei for which sufficient spectroscopic material is available.

For instance, in the E1 absorption of a gamma quantum by the V^{51} nucleus the following transition is possible:

$$(\nu f_{7/2})^8 (\pi f_{7/2})^3 \rightarrow (\nu f_{7/2})^8 (\nu d_{3/2}^{-1}) (\nu f_{5/2}) (\pi f_{7/2})^3. \qquad (1)$$

We have no direct information on the energy of the final state, but we can calculate this energy by analyzing the data on the lower states of neighboring nuclei. The literature contains information on the position of the single-particle levels $1f_{7/2}$, $2p_{3/2}$, $2p_{1/2}$, $1f_{5/2}$, $1g_{9/2}$, and $2d_{5/2}$, in the Ca^{41} and Sc^{41} nuclei.[2] For the calculation we must, in addition, know the following:

a) the change in the binding energy of the $1f_{5/2}$, $2p_{3/2}$, $2p_{1/2}$, $1g_{9/2}$, and $2d_{5/2}$ nucleons in the transition from Ca^{41} and Sc^{41} to a heavier nucleus with a configuration of $(\pi\nu f_{7/2})^n f_{5/2}$, or $(\pi\nu f_{7/2})^n g_{9/2}$, etc;

b) the change in the binding energy of the whole nucleus in the transition from $(\pi\nu f_{7/2})^n$, for instance, to $(\nu d_{3/2}^{-1})(\pi\nu f_{7/2})^n$;

c) the value of the spin-orbit splitting constant of $d_{3/2}^{-1} - d_{5/2}^{-1}$ in Ca^{39}.

To obtain this information we make use of the following experimental data:

a) the energy $E(f_{5/2})$ of the single-particle level $f_{5/2}$ is equal to 2.0 Mev in Ca^{41} (reference 2), 7.8 Mev in Ni^{61} (references 3 and 4), 7.0 Mev in Cr^{53} (references 3, 5 and 6), and 4.1 Mev in Sc^{49} (reference 6), and must on the average depend linearly on the number of $f_{7/2}$ nucleons above Ca^{40} (cf., for example, reference 7), which is in approximate agreement with the values cited above. As a result $\Delta E(f_{5/2}) \approx (0.3 \text{ to } 0.4) n$ Mev (where n is the number of $f_{7/2}$ nucleons), i.e., there occurs, by comparison with Ca^{41}, a shift to lower energies. Analogously, we conclude from data on the Ca^{41} (reference 2), $Ca^{45,49}$ (reference 9), Ni^{57}, Cr^{53} (reference 3), and Fe^{55} (reference 8) nuclei that $\Delta E(2p_{3/2}) \approx (0.3 \text{ to } 0.4) n$ Mev. From the more scanty data on the Ca^{41}, Zn^{71}, and Ge^{73} (reference 3) nuclei we obtain $\Delta E(g_{9/2}) \sim 0.1\, n$ Mev.

b) In the K^{40} nucleus the neutron is bound more weakly than in Ca^{41}, on the average by 0.95 Mev [the $d^{-1}_{3/2}f_{7/2}$ states form a system consisting of four levels in an interval of 0.9 Mev (reference 9)]; in the K^{41} nucleus the two $f_{7/2}$ nucleons are bound more weakly than in the Ca^{42} nucleus by 1.95 Mev (reference 9), and in the K^{43} nucleus[4] the $f^4_{7/2}$ nucleons are bound more weakly than in Ca^{44} by 3.90 Mev, i.e., the energy change is, as was expected, approximately linear with the number of $f_{7/2}$ nucleons, and can be described by the formula $\Delta E\,(d^{-1}_{3/2}) \approx (0.9 \text{ to } 1.0)\,n$ Mev. When we deal with a "hole," the energy of the system no longer increases, but decreases instead. This last effect is thus the most important manifestation of residual interactions.

c) We take the spin-orbit splitting constant for $d^{-1}_{3/2} - d^{-1}_{5/2}$ in Ca^{39} to be the same as for $p^{-1}_{1/2} - p^{-1}_{3/2}$ in N^{15} (reference 10), so that $\Delta E\,(d^{-1}_{3/2} - d^{-1}_{5/2}) \sim 8$ to 10 Mev. In the following we will take the excitation energy of the $2s^{-1}_{1/2}$ state to be 3 — 4 Mev, corresponding to the position of the unsplit d level.

Now it is possible to estimate the energy of transition (1). We have ΔE = 15.8 — 6 + (9 to 10) = 19 to 20 Mev; this is one of the most intense transitions.

The calculation of the absorption cross sections is carried out according to the shell-theory formulas for mixed configurations with a summation over all the spins of the final states for a given final configuration, so that very simple expressions for the cross section are obtained:

a) in transitions from an unfilled shell

$$\int_\Delta \sigma(E)\,dE = \tfrac{4}{3}\,(\pi^2 e'^2/\hbar c)\,E_\gamma n_1 (2l_1+1)(2l_2+1)(2j_2+1) \times \begin{pmatrix} l_1 & 1 & l_2 \\ 0 & 0 & 0 \end{pmatrix}^2 \begin{Bmatrix} l_2 & j_2 & 1/2 \\ j_1 & l_1 & 1 \end{Bmatrix}^2 \langle l_2 | r | l_1 \rangle^2; \qquad \text{(a)}$$

b) for transitions from a filled shell

$$\int_\Delta \sigma(E)\,dE = \tfrac{4}{3}\,(\pi^2 e'^2/\hbar c)\,E_\gamma (2j_2+1-n_2)(2l_1+1)(2j_1+1) \times (2l_2+1) \begin{pmatrix} l_2 & 1 & l_1 \\ 0 & 0 & 0 \end{pmatrix}^2 \begin{Bmatrix} l_2 & j_2 & 1/2 \\ j_1 & l_1 & 1 \end{Bmatrix} \langle l_2 | r | l_1 \rangle^2. \qquad \text{(b)}$$

Here e′ is the effective nucleon charge equal to Ne/A for a proton and — Ze/A for a neutron, n_1 is the number of nucleons in the unfilled shell, n_2 is the number of nucleons in the shell into which the transition takes place (n_1 and n_2 refer to the initial state), l_1, j_1, l_2, j_2 are the orbital and total momenta of the nucleon in the initial and final state, respectively. The integration is over the region Δ in which the levels of the given configuration are located.

The results for V^{51} and Ca^{40} are presented in the figure. Without account of residual interactions the curve for V^{51} would have been shifted to the left by ~ 6 Mev. For Ca^{40}, for which additional account of residual interactions is naturally unnecessary, the maximum of the curve is in the region of 17 — 18 Mev, and not 14 Mev, owing to the fact that in Ca^{40} a decisive role is played by the high-energy $1d_{5/2} \rightarrow 1f_{7/2}$ transitions, while in V^{51}, in which the neutron $1f_{7/2}$ shell is filled, these transitions are less important than the sum of the $\pi\nu 1d_{3/2} \rightarrow 1f_{5/2}$ and $\pi\nu 2s_{1/2} \rightarrow 2p_{3/2}$ transitions which makes the main contribution to the giant-resonance maximum.

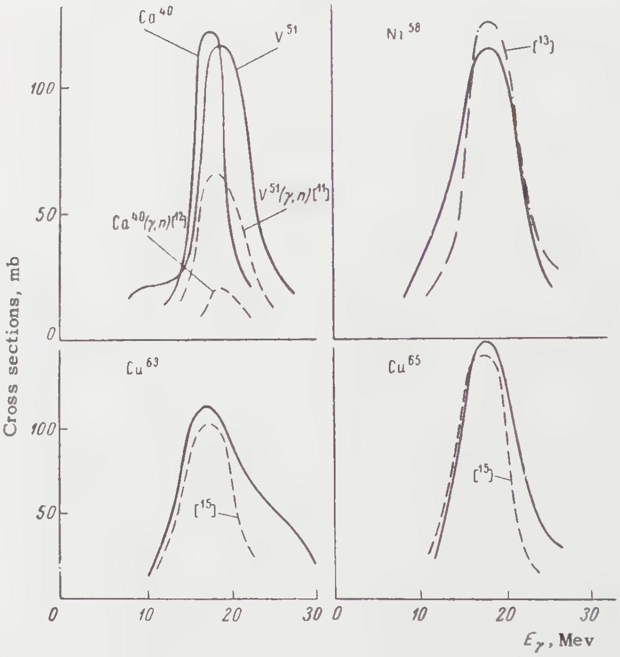

E1 absorption curves for various elements. The solid curves are calculated; the dot-dash curve is the experimental curve of the total absorption cross section for Ni^{58}; the dashed curves are the experimental curves for (γ, n) reactions.

For V^{51} and Ca^{40} only the excitation curves for the (γ, n) reactions have been measured.[11,12] A comparison of the integral cross sections of these reactions with the theoretical curves for the total absorption cross section shows that $\int \sigma(\gamma, p)\,dE$ should be somewhat larger than, $\int \sigma(\gamma, n)\,dE$ for V^{51}, and considerably larger for Ca^{40}. Experiments to measure the total absorption cross section of gamma quanta by nuclei close to those considered [Ni^{58} and Ar^{40} (references 13 and 14)] confirm this conclusion.

In all substantial transitions with neutron excitation in nuclei in which N is close to Z the excited neutron is bound with respect to the framework in spite of the fact that the excitation energy is larger than the energy of the neutron threshold. Such excited states can emit nucleons but only on account of the mixing of configurations, i.e., the nucleon disintegration will, apparently, obey the laws of the statistical model of the nucleus. However, proton excitation, due to the fact that the Coulomb energy raises the proton levels, will, in the majority of cases, lead to the emission of ''direct'' protons with energies larger than those predicted by the statistical model. For instance, in the $\nu 1d_{3/2} \rightarrow \nu 1f_{5/2}$ transition the excited V^{51} nucleus cannot emit a $1f_{5/2}$ neutron (the direct photoeffect is forbidden), and in the $\pi 1d_{3/2} \rightarrow \pi 1f_{5/2}$ a $1f_{5/2}$ proton with an energy of ~ 3 Mev can be emitted. We note that although such terms as ''neutron excitation'' are not fully correct if the isotopic spin is considered a good quantum number, their use nevertheless has a certain intuitive advantage for the description of the disintegration of a state.

We have also calculated the dipole-absorption curves for Ni^{58}, Cu^{63}, and Cu^{65}. The figure shows a comparison of these curves with experimental data.[13,15] The agreement of the experimental data with the calculations is entirely satisfactory. It must be noted that for the calculations of Ni^{58}, Cu^{63}, and Cu^{65} the spectroscopic material is considerably scantier and the results are, therefore, of a more approximate nature.

In conclusion, we again emphasize that our analysis indicates good correspondence of the calculated giant-resonance position and the spectroscopic data on the lower states of nuclei in the investigated region. It seems important to us that extensive spectroscopic investigations be conducted in the same order in which they are needed for the analysis of photonuclear reactions. Until now such investigations have been carried out only for a small number of nuclei, and their absence hampers the analysis of photonuclear reactions in many portions of the periodic table.

The authors express their gratitude to V. V. Balashov and Yu. F. Smirnov for useful advice and help in the work, and also to Yu. M. Shirokov for a discussion of the obtained results.

---

[1] D. H. Wilkinson, Physica **22**, 1039 (1956).

[2] Class, Davis, and Johnson, Phys. Rev. Lett. **3**, 41 (1959).

[3] B. S. Dzhelepov and L. K. Peker Схемы распада радиоактивных ядер (Decay Schemes of Radioactive Nuclei), Acad. of Sci. Press, 1958.

[4] V. A. Kravtsov, Usp. Fiz. Nauk **65**, 451 (1958).

[5] A. J. Elwyn and F. B. Shull, Phys. Rev. **111**, 925 (1958).

[6] R. H. Nussbaum, Phys. Rev. **28**, 423 (1956).

[7] C. Schwarz, Phys. Rev. **94**, 95 (1954).

[8] R. D. Lawson and J. L. Uretsky, Phys. Rev. **108**, 1300 (1957).

[9] P. M. Endt and C. M. Braams, Revs. Modern Phys. **29**, 683 (1957).

[10] J. P. Elliot and A. M. Lane, Phys. Rev. **96**, 1160 (1954).

L. Katz and J. Chidli, Trans. of the All-Union Conference on Nuclear Reactions at Small and Medium Energies, Moscow 1957, Acad. of Sci. Press 1958, pp. 371-385.

[12] J. Goldemberg and L. Katz, Can. J. Phys. **32**, 49 (1954); Summers-Gill, Haslam, and Katz, Can. J. Phys. **31**, 70 (1953).

[13] J. H. Carver and W. Turchinetz, Proc. Phys. Soc. **73**, 585 (1959).

[14] A. S. Penfold and E. L. Garwin, Phys. Rev. **114**, 1139 (1959).

[15] L. Katz and A. G. W. Cameron, Can. J. Phys. **29**, 518 (1951).

Translated by Z. Barnea
22

SOVIET PHYSICS JETP VOLUME 12, NUMBER 1 JANUARY, 1961

DISPERSION RELATIONS AND ANALYSIS OF THE ENERGY DEPENDENCE OF CROSS SECTIONS NEAR THRESHOLDS OF NEW REACTIONS

L. I. LAPIDUS and CHOU KUANG-CHAO

Joint Institute for Nuclear Research

Submitted to JETP editor February 5, 1960

J. Exptl Theoret. Phys. (U.S.S.R.) 39, 112-119 (July, 1960)

The application of dispersion relations to the analysis of the energy dependence of scattering (and reaction) amplitudes near thresholds of new reactions is discussed. General expressions are obtained which characterize the nonmonotonic behavior of forward-scattering amplitudes as functions of the energy. The energy dependence of one of the amplitudes for elastic scattering of γ-ray quanta by deuterons is examined near the threshold for photodisintegration of the deuteron.

1. An examination of the scattering of γ-ray quanta by nucleons near the threshold for pion production[1] has shown that the dispersion relations automatically lead to the appearance of discontinuities of the derivative of the real part of the amplitude, if one takes account of the energy dependence of the reaction cross section near threshold.* Within the framework of the dispersion relations the problem of the appearance of discontinuities of the derivative of the forward scattering amplitude involves the analysis of integrals of the form

$$\frac{k_0^2}{4\pi^2} \mathrm{P} \int \frac{d\omega}{k} \frac{\sigma(\omega)}{\omega \mp \omega_0},$$

where the usual notation is used, and the total cross section $\sigma(\omega)$ includes both the elastic scattering cross section $\sigma_s(\omega)$ and the inelastic interaction cross section $\sigma_c(\omega)$.

The behavior of $\sigma_c(\omega)$ near the threshold of the binary reaction

$$a + b \to c + d \qquad (2)$$

involving particles with masses μ (incident), M (target), m and $\mathfrak{M}$ is given by the expression

$$\sigma_c(\omega) = Bq_c/k_c, \qquad (3)$$

where q_c and k_c are the momenta before and after the collision (in the c.m.s.) and B is a constant. It is not hard to see that

$$(q_c/k_c)^2 = (\omega - \omega_t)(\omega + \omega_t - \delta)/(\omega^2 - \mu^2), \qquad (4)$$

where $\omega = (k^2 + \mu^2)^{1/2}$ is the total energy of the incident particle in the laboratory system (l.s.),

$$\omega_t - \mu = [(\mathfrak{M} + m)^2 - (M + \mu)^2]/2M \qquad (5)$$

is the threshold energy of the reaction (2), and

$$\delta = \{\mathfrak{M}^2 + m^2 - \mu^2 - M^2\}/M. \qquad (6)$$

The application of dispersion relations makes it possible to examine both "local effects" near the very threshold, which in some cases lead to sharp "peaks," "dips," and "steps," and also the general influence of inelastic processes occurring in some energy range on the processes at a given energy. We recall that the unitarity relations for the S matrix make it possible to take into account the influence on a given process of other processes occurring at the same energy.

2. The study of γ-N scattering has shown that there are "local effects" in only two of the six scalar amplitudes needed to describe the transition matrix in this case. The presence of other strongly energy-dependent amplitudes hinders the analysis. For a detailed analysis of the inelastic processes it is necessary to examine the dispersion relations for nonvanishing momentum transfers Q^2, and possibly also double dispersion relations.

In the present paper we confine ourselves to the examination of dispersion relations in the total energy for $Q^2 = 0$ for a scalar function $A(\omega)$, which is the trace of the scattering matrix,

$$A(\omega) = \mathrm{Sp}\, M(\omega, Q^2 = 0), \qquad (7)$$

and whose imaginary part is related to the total cross section. The contribution of inelastic processes to $D = \mathrm{Re}\, A(\omega)$ is characterized by the two integrals

---

*The nonmonotonic behavior of the cross section near the threshold has been treated phenomenologically in a diploma research by G. Ustinova, and also by Capps and Holladay.[2]

$$\frac{k_0^2}{4\pi^2}\,\mathrm{P}\int\frac{d\omega}{k}\,\frac{\sigma_c^-(\omega)}{\omega-\omega_0}, \tag{8}$$

$$\frac{k_0^2}{4\pi^2}\,\mathrm{P}\int\frac{d\omega}{k}\,\frac{\sigma_c^+(\omega)}{\omega+\omega_0}, \tag{9}$$

where $\sigma_c^-(\omega)$ is the total cross section of reaction (2) and $\sigma_c^+(\omega)$ is the cross section of the reaction cross-symmetrical to (2).

Being interested in the energy dependence of the real part of the quantity $A(\omega)$ in Eq. (7), let us calculate the integrals

$$\frac{k_0^2}{4\pi^2}\,\mathrm{P}\int_{\omega_t}^{\omega_1}\frac{d\omega}{k}\,\frac{\sigma_c^-}{\omega-\omega_0}=\frac{k_0^2B^-}{4\pi^2}\,\mathrm{P}\int_{\omega_t}^{\omega_1}\frac{d\omega}{k^2}\,\frac{[(\omega-\omega_t)(\omega+\omega_t-\delta)]^{1/2}}{\omega-\omega_0}$$

$$=\frac{B^-k_0^2}{4\pi^2}\,\Pi(\omega_0), \tag{10}$$

$$\frac{k_0^2}{4\pi^2}\,\mathrm{P}\int_{\omega_t}^{\omega_1}\frac{d\omega}{k}\,\frac{\sigma_c^+}{\omega+\omega_0}=\frac{k_0^2B^+}{4\pi^2}\,\Pi(-\omega_0); \tag{11}$$

in these integrals the range of integration is from the threshold ω_t to ω_1, the limit of the region of the s state in σ_c in which Eq. (3) is still valid. If we introduce the notations

$$a(\omega_0)=(\omega_0-\omega_t)(\omega_0+\omega_t-\delta),$$

$$a(-\omega_0)=(\omega_0+\omega_t)(\omega_0-\omega_t+\delta),$$

$$R=(\omega_1-\omega_t)(\omega_1+\omega_t-\delta), \tag{12}$$

it is not hard to show that

$$k_0^2\Pi(\omega_0)=-\{\psi(\omega_0)-\tfrac{1}{2}(1+\omega_0/\mu)\psi(\mu)$$

$$-\tfrac{1}{2}(1-\omega_0/\mu)\psi(-\mu)\}, \tag{13}$$

where

$$\psi(\mu)=\sqrt{-a(\mu)}\left[\frac{\pi}{2}+\tan^{-1}\frac{(2\mu-\delta)(\omega_1-\mu)+2a(\mu)}{2\sqrt{-a(\mu)R}}\right],$$

$$\psi(-\mu)=\sqrt{-a(-\mu)}\left[\frac{\pi}{2}\right.$$

$$\left.-\tan^{-1}\frac{(2\mu+\delta)(\omega_1+\mu)-2a(-\mu)}{2\sqrt{-a(-\mu)R}}\right]. \tag{13'}$$

For the function $\psi(\omega)$ at the point ω_0 we get the expressions

$$\psi(\omega_0)=\sqrt{-a(\omega_0)}\left[\frac{\pi}{2}+\tan^{-1}\frac{(2\omega_0-\delta)(\omega_1-\omega_0)+2a(\omega_0)}{2\sqrt{-a(\omega_0)R}}\right],$$

$$\omega_0\leqslant\omega_t; \tag{14}$$

$$\psi(\omega_0)=\sqrt{a(\omega_0)}\ln\left|\frac{2a(\omega_0)+(2\omega_0-\delta)(\omega_1-\omega_0)+2\sqrt{a(\omega_0)R}}{(\omega_1-\omega_0)(2\omega_t-\delta)}\right|,$$

$$\omega_0\geqslant\omega_t. \tag{14'}$$

The expression for $k_0^2\Pi(-\omega_0)$ is obtained from (13) and (14) by the replacement $\omega_0\to-\omega_0$.

It follows from (14) and (14′) that the first derivative has a discontinuity at the point ω_0. The resulting energy dependence has the characteristic feature that the derivative is infinite on the side $\omega_0<\omega_t$ and has a finite value when we approach the point $\omega_0=\omega_t$ from the region $\omega_0<\omega_t$.

It might seem that the quantity $k_0^2\Pi(-\omega_0)$ obtained as the result of substituting (3) and (4) in (9) would also have a discontinuity of the derivative at $\omega_0=\omega_t-\delta$. On changing the sign of ω_0 in (14), however, we easily verify that this is not so. The values of the derivative of $k_0^2\Pi(-\omega_0)$ calculated with approach to $\omega_0=\omega_t$ from the two sides are identical. Thus although in a relativistic treatment cross-symmetrical inelastic processes indeed contribute to the real part of the scattering amplitude, they do not lead to nonmonotonic energy dependence of the amplitude.

The application of dispersion relations enables us to get detailed information about the magnitude and half-width of the anomaly near the threshold. The half-width ϵ of the drop in the region $\omega_0<\omega_t$ can be estimated roughly in the following way. Near $\omega_0=\omega_t\,(\omega_0<\omega_t)$ the argument of the arc tangent is large; using this fact, we find

$$\psi(\omega_0)=\sqrt{-a}\;\pi. \tag{15}$$

Defining the half-width ϵ by the condition

$$D(\omega_t-\varepsilon)=\tfrac{1}{2}D(\omega_t) \tag{16}$$

and using Eq. (15), we then get

$$D(\omega_t)-(B/4\pi)\sqrt{(\omega_t-\omega_0)(\omega_0+\omega_t-\delta)}=\tfrac{1}{2}D(\omega_t), \tag{17}$$

from which we have

$$\varepsilon\approx\tfrac{1}{8}(\omega_t-\delta/2)^{-1}\,[4\pi D(\omega_t)/B]^2. \tag{18}$$

In the limiting case in which the contribution to $D(\omega_t)$ not associated with the expressions (10) and (11) can be neglected,

$$D(\omega_t)=BJ(\omega_t)/4\pi^2, \tag{19}$$

and from Eq. (13) we have the result that

$$J(\omega_t)=\tfrac{1}{2}\,[(1+\omega_t/\mu)\psi(\mu)+(1-\omega_t/\mu)\psi(-\mu)]. \tag{20}$$

3. Let us consider the photoproduction of neutral pions

$$\gamma+p\to p+\pi^0 \tag{21}$$

near the threshold of the reaction

$$\gamma+p\to n+\pi^+. \tag{22}$$

In this energy range it suffices to consider the electric-dipole transition. We denote by E^0 and E^+ the transition elements for neutral and charged mesons, respectively. From the condition of unitarity and the experimental fact that $\mathrm{Re}\,E^0 \approx 0$, we get the result

$$\mathrm{Im}\,E^0 = \sqrt{2/3}\,(\alpha_3 - \alpha_1)\,\mathrm{Re}\,E^+, \tag{23}$$

where α_3 and α_1 are the phase shifts for π-N scattering. Substituting the experimental data for α_3, α_1, and E^+, we get

$$\mathrm{Im}\,E^0 = \sqrt{2/3}\,(a_3 - a_1)\,q_0^{1/2} q_+^{1/2} \sqrt{q_+/\nu}\cdot 3{,}3\cdot 10^{-15}\ \mathrm{cm}, \tag{24}$$

where

$$q_0^{1/2} \approx (\nu^2 - \nu_{0t}^2)^{1/4}, \quad q_+ \approx (\nu^2 - \nu_{+t}^2)^{1/2}$$

(ν is the energy of the photon, and a_3, a_1 are the scattering lengths). The anomalies at the threshold are determined by an integral of the form

$$P\int_{\nu_{+t}}^{\nu_1} d\nu\,(\nu^2 - \nu_{0t}^2)^{1/4}(\nu^2 - \nu_{+t}^2)^{1/2}/\nu^{1/2}(\nu - \nu_0), \tag{25}$$

which undoubtedly gives "peak" singularities.

In analogy with this, in the general case we can consider the cross section of the reaction

$$a + b \rightarrow c + d \tag{26}$$

near the threshold of the reaction

$$a + b \rightarrow e + f. \tag{27}$$

If the threshold of reaction (27) is far from that of reaction (26), we can always find an energy range where

$$\mathrm{Im}\,M\,(ab \rightarrow cd) = M\,(ab \rightarrow ef)\,M^+(ef \rightarrow cd) + \ldots = Aq + \ldots; \tag{28}$$

here A is a weakly varying function of the energy and q is the relative momentum of the system ef. The other terms in the sum (28) are also slowly varying functions of the energy if there are no thresholds of other reactions in the neighborhood. In this case the dispersion integral has the usual form, and we can determine the magnitude and half-width of the "peak" or "dip" in the same way as for the case of scattering.

In the case of such a process as the photoproduction of pions

$$\mathrm{Im}\,M\,(ab \rightarrow cd) = Aqq_0^{1/2} + \ldots, \tag{29}$$

since the threshold of the reaction ab → ef is close to that of the reaction ab → cd. In these cases the dispersion integrals are rather complicated and we have not been able to carry out the integration.

4. It thus follows from the conditions of causality and unitarity, together with Eqs. (3) and (4), that the first derivative of the real part of the scattering amplitude has a discontinuity, and that the derivative from the side $\omega_0 < \omega_t$ is infinite. That it is precisely the first derivative that is infinite is due to the form of the relations (3) and (4). The behavior of the cross section for the reaction (2), when its products are in states with nonvanishing angular momentum l, is given by the expression

$$\sigma_c^{(l)} = B^{(l)}\,[(\omega - \omega_t)(\omega + \omega_t - \delta)/(\omega^2 - \mu^2)]^{l+1/2}. \tag{30}$$

Substitution of (3) in (8) makes the lth derivative infinite.

It is perhaps interesting to note that, unlike the nonrelativistic treatment, this use of the dispersion relations has not required the assumption that the partial amplitudes are analytic. It has turned out that it is enough to use only the analytic character of the scattering amplitude with respect to the total energy, with a bounded value of the momentum transfer, $Q^2 < Q^2_{\mathrm{max}}$.

As Baz' has pointed out, the unitarity of the S matrix has the consequence that as the number of channels increases the effect in each channel decreases. An analysis of γ-N scattering near the threshold for photoproduction of pions, for which there are "peak" effects in only two out of six scalar functions, has shown that there is also a smearing of the effect with increase of the spin of the particles.

An important feature of the theory of dispersion relations is the discussion of the convergence of the dispersion integrals at high energies or, what is the same thing, of the number of subtractions. The main calculations in the present paper are made for dispersion relations with one subtraction. In the case of dispersion relations without subtraction one must make the replacement

$$k_0^2\int\frac{d\omega}{k}\,\frac{\sigma}{\omega - \omega_0} \rightarrow \int\frac{d\omega\,k\sigma}{\omega - \omega_0}. \tag{31}$$

With sufficiently high experimental accuracy the difference between Eq. (8) and Eq. (31) can give information about the number of subtractions.

Let us note briefly what sort of singularities can appear near the threshold of the reaction

$$a + b \rightarrow c + d + f. \tag{32}$$

By substituting in Eq. (8) the cross section of the reaction (32) in the form

$$\sigma_c = B' k_c^{-1} P_{c\,max}^4 \approx \Gamma\,(\omega - \omega_t)^2$$

(reaction products in the s state), we get

$$\int_{\omega_t}^{\omega_1}\frac{\sigma d\omega}{\omega - \omega_0} \approx \Gamma\int_{\omega_t}^{\omega_1}\frac{d\omega\,(\omega - \omega_t)^2}{\omega - \omega_0} = \Gamma\Big\{\frac{1}{2}[(\omega_1 - \omega_0)^2 - (\omega_t - \omega_0)^2] + 2(\omega_0 - \omega_t)(\omega_1 - \omega_t) + (\omega_0 - \omega_t)^2\ln|(\omega_1 - \omega_0)/(\omega_t - \omega_0)|\Big\}, \tag{33}$$

which leads to a logarithmic infinity in the second derivative of $D(\omega)$ with respect to ω.

For a reaction with four particles in a final s state the quantity $(\omega_0 - \omega_t)^2 \ln|\omega_t - \omega_0|$ is replaced by $(\omega_0 - \omega_t)^5 \ln|\omega_0 - \omega_t|$. Similar behavior of the real part of the scattering amplitude appears at the thresholds of all reactions.

An example of the application of dispersion relations that is well known in the literature is the analysis of the coherent scattering of photons in the Coulomb field of a nucleus[3] (cf. also reference 4). It is not hard to convince oneself that near $\omega = 2m$ ($\gamma \equiv \omega/2m = 1$) — the threshold for production of an electron-positron pair — the real part of the scattering amplitude has an energy dependence of the type $x^k \ln x$ ($x = \gamma - 1$). To see this we have only to examine the expression for the real part of the amplitude:

$$D(\omega) = \frac{Z^2}{m}\left(\frac{e^2}{4\pi}\right)^3 \left\{\frac{1}{\gamma\pi}\,[2C_1(\gamma) - D_1(\gamma)] + \frac{\gamma}{27\pi}\left[\left(109 + \frac{64}{\gamma^2}\right)E_1(\gamma) - \left(67 - \frac{6}{\gamma^2}\right)\left(1 - \frac{1}{\gamma^2}\right)F_1(\gamma)\right] - \frac{1}{9\gamma^2} - \frac{9}{4}\right\}, \tag{34}$$

where

$$C_1(\gamma) = \mathrm{Re}\int_0^\gamma \frac{\arcsin x}{x}\cosh^{-1}\left(\frac{\gamma}{x}\right)dx, \quad C_1(1) = 1.62876;$$

$$D_1(\gamma) = \mathrm{Re}\int_0^\gamma \frac{\cosh^{-1}(\gamma/x)}{(1 - x^2)^{1/2}}\,dx, \qquad D_1(1) = 1{,}83193;$$

$$E_1(\gamma) = \begin{cases} E(\gamma^{-1}), & \gamma \geqslant 1 \\ \gamma^{-1}E(\gamma) + (\gamma - \gamma^{-1})K(\gamma), & \gamma \leqslant 1 \end{cases};$$

$$F_1(\gamma) = \begin{cases} K(\gamma^{-1}), & \gamma \geqslant 1 \\ \gamma K(\gamma), & \gamma \leqslant 1 \end{cases},$$

and $K(\gamma)$ and $E(\gamma)$ are the complete elliptic integrals of the first and second kinds. As is well known, for $1 - \gamma^2 \ll 1\,[\Lambda = \ln(4(1 - \gamma^2)^{-1/2}]$,

$$K(\gamma) = \Lambda + \tfrac{1}{4}(\Lambda - 1)(1 - \gamma^2) + \tfrac{9}{64}\left(\Lambda - \tfrac{7}{6}\right)(1 - \gamma^2)^2 + \tfrac{25}{256}\left(\Lambda - \tfrac{37}{30}\right)(1 - \gamma^2)^3 + \ldots,$$

$$E(\gamma) = 1 + \tfrac{1}{2}\left(\Lambda - \tfrac{1}{2}\right)(1 - \gamma^2) + \tfrac{3}{64}\left(\Lambda - \tfrac{13}{12}\right)(1 - \gamma^2)^2 + \ldots, \tag{35}$$

which indeed shows that the dependence is of the form $x^k \ln x$. It is not hard to check that the scattering of light by light near the threshold of the reaction $\gamma + \gamma \rightarrow e^+ + e^-$ is a process, well known in quantum electrodynamics, for which the amplitude is characterized by a "local" anomaly (cf. Figs. 2–4 in the paper by Karplus and Neuman[5])*. The amplitude for the Compton effect near the threshold of the reaction $\gamma + e \rightarrow 2e + e^+$ has the characteristic dependence $x^2 \ln x$.

5. The elastic scattering of γ rays by deuterons near the threshold for photodisintegration of the deuteron is an example of a process for which use of dispersion relations is necessary for the analysis of the anomaly near the threshold. The nonmonotonic behavior near the threshold in this case comes from the magnetic-dipole disintegration. The electric-dipole disintegration leads to appreciable changes in the energy dependence of the amplitude for elastic γ-d scattering in a certain relatively wide range of energies.

The amplitude for forward elastic γ-d scattering can be represented in the form

$$e_i' T_{ik} e_k = A\mathbf{e}'\mathbf{e} + iB\mathbf{S}\,[\mathbf{e}'\mathbf{e}] + \tfrac{1}{2}C\,[(\mathbf{S}\mathbf{e})(\mathbf{S}\mathbf{e}') + (\mathbf{S}\mathbf{e}')(\mathbf{S}\mathbf{e})] + \tfrac{1}{2}D\,[(\mathbf{S}\,[\mathbf{k}\times\mathbf{e}])(\mathbf{S}\,[\mathbf{k}\times\mathbf{e}']) + (\mathbf{S}\,[\mathbf{k}\times\mathbf{e}'])(\mathbf{S}\,[\mathbf{k}\times\mathbf{e}])]. \tag{36}$$

The cross section for scattering of unpolarized γ rays by unpolarized deuterons then takes the form

$$\sigma_s(0^\circ) = |A + \tfrac{2}{3}(C + D)|^2 + \tfrac{1}{18}|C + D|^2 + \tfrac{2}{3}|B|^2 + \tfrac{1}{3}|D - C|^2, \tag{37}$$

and we have

$$k\sigma_t = 4\pi\,\mathrm{Im}\,(A + \tfrac{2}{3}C + \tfrac{2}{3}D).$$

By means of the dispersion relation for the quantity $L = A + {}^2\!/_3 C + {}^2\!/_3 D$,

$$\mathrm{Re}\,L(\omega) = -\frac{e^2}{M_d} + \frac{2\omega^2}{\pi}\,\mathrm{P}\int_{\omega_d}^{\infty} \frac{\mathrm{Im}\,L(\omega')}{\omega'(\omega'^2 - \omega^2)}\,d\omega', \tag{38}$$

where ω_d is the threshold for photodisintegration of the deuteron, let us examine the effect of inelastic processes on the energy dependence of the real part of the amplitude L. In the calculation of the dispersion integral it is convenient to use the theoretical expressions for the cross sections for photodisintegration of the deuteron (cf., e.g., reference 8).

Let us begin with the examination of the "local effects." The expression for the cross section for magnetic-dipole disintegration is

$$\sigma_c^{(m)} = \frac{2\pi}{3}\frac{e^2}{\hbar c}\left(\frac{\hbar}{Mc}\right)^2(\mu_p - \mu_n)^2\,\frac{(\gamma - 1)^{1/2}\left(1 + \sqrt{\varepsilon'/|\varepsilon|}\right)^2}{\gamma\,[\gamma - 1 + \varepsilon'/|\varepsilon|]}, \tag{39}$$

where $\gamma = \omega/|\epsilon|$, ω being the energy of the photon; $|\epsilon| = 2.22$ Mev and $\epsilon' \sim 70$ kev are the binding energies of the np system in the ${}^3S_1$ and ${}^1S_0$ states; and the rest of the notation is as usual. Because of the factor $[\gamma - 1 + \epsilon'/|\epsilon|]^{-1}$ the expression (39) does not admit of the simple analytic continuation

---

*Regarding effects of the Coulomb interaction see papers by Baz'[6] and by Fonda and Newton.[7]

$$\varkappa = \sqrt{\gamma - 1} \rightarrow i\,|\varkappa|,$$

since in this case $\gamma\sigma_c^{(m)}$ goes to infinity below the threshold at $|\kappa|^2 = \epsilon'/|\epsilon|$. Substitution of Eq. (39) in the dispersion integral

$$Z_L(\gamma_0) = \varepsilon \frac{\gamma_0^2}{2\pi^2} \mathrm{P} \int_1^\infty \frac{d\gamma\sigma_c^{(m)}(\gamma)}{\gamma^2 - \gamma_0^2}$$

for $\gamma_0 \neq \delta$ gives

$$Z_L(\gamma_0) = \frac{2}{3}\frac{e^2}{2Mc^2}\frac{\varepsilon}{Mc^2}(\mu_p - \mu_n)^2 \left(1 + \sqrt{\varepsilon'/|\varepsilon|}\right)^2 \times \left\{\frac{\sqrt{1-\gamma_0}}{\delta - \gamma_0}\theta(1-\gamma_0) + \frac{\sqrt{1+\gamma_0}}{\delta+\gamma_0} - \frac{2}{\delta} - \frac{2\gamma_0^2\sqrt{\varepsilon'/|\varepsilon|}}{\delta(\delta^2-\gamma_0^2)}\right\}, \tag{40}$$

where $\delta = 1 - \epsilon'/|\epsilon|$, $\theta(x) = 1$ for $x \geq 1$, and $\theta(x) = 0$ for $x < 1$; for $\gamma_0 = \delta$

$$Z_L(\delta) = \frac{2}{3}\frac{e^2}{2Mc^2}\frac{\varepsilon}{Mc^2}(\mu_p - \mu_n)^2\left(1 + \sqrt{\varepsilon'/|\varepsilon|}\right)^2 \times\left\{\sqrt{1+\delta}/2\delta - 2/\delta + 2\sqrt{\varepsilon'/|\varepsilon|}/3\delta + \sqrt{|\varepsilon|/\varepsilon'}/2\right\}. \tag{41}$$

The dependence of the quantity $\Delta_L(\gamma_0) = Z_L(\gamma_0)/(e^2/2Mc^2)$ on the γ-ray energy is shown in the diagram (curve 1)

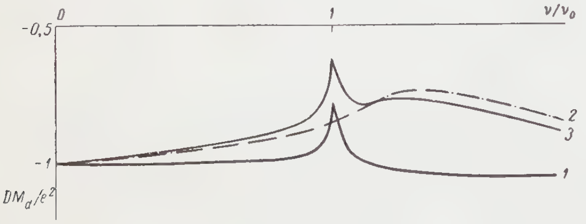

For extreme values of γ_0 we get from Eq. (40)

$$\Delta_L(\gamma_0) = \frac{2}{3}\frac{\varepsilon}{Mc^2}(\mu_p - \mu_n)^2\left(1 + \sqrt{\frac{\varepsilon'}{|\varepsilon|}}\right)^2 \times\left\{\frac{3}{8} + 2\frac{\varepsilon'}{|\varepsilon|} - \sqrt{\frac{\varepsilon'}{|\varepsilon|}}\left(1 + 2\frac{\varepsilon'}{|\varepsilon|}\right)\right\}\gamma_0^2 \approx \frac{2}{3}\frac{\varepsilon}{Mc^2}(\mu_p - \mu_n)^2\left(1 + \sqrt{\frac{\varepsilon'}{|\varepsilon|}}\right)^2\frac{1}{4}\gamma_0^2, \quad \gamma_0 \ll 1; \tag{42}$$

$$\Delta_L(\gamma_0) = -\frac{4}{3}\frac{\varepsilon}{Mc^2}(\mu_p - \mu_n)^2\left(1 + \sqrt{\frac{\varepsilon'}{|\varepsilon|}}\right)^2, \quad \gamma_0 \gg 1. \tag{43}$$

At the photodisintegration threshold with $1 - \delta = 1/30$.

$$Z_L(1) = 0.24\,e^2/2Mc^2.$$

On the side of energies smaller than the threshold energy the half-width of the peak is somewhat smaller than ϵ', i.e., about 50 or 60 kev.

The contribution of the cross section for dipole absorption

$$\sigma_c^{(d)} = 4\pi\frac{e^2}{Mc^2}\frac{\hbar c}{\varepsilon}\frac{(\gamma-1)^{3/2}}{\gamma^3} \tag{44}$$

at $D = \mathrm{Re}\,L$ is of the form

$$\Delta_p(\gamma_0) = 2Mc^2 Z_p(\gamma_0)/e^2 = 2\left\{\gamma_0^{-2}\left[(1-\gamma_0)^{3/2}\theta(1-\gamma_0) + (1+\gamma_0)^{3/2} - 2\right] - {}^3/_4\right\}. \tag{45}$$

The quantity $\Delta_p = \Delta_p(\gamma_0)$ is shown in the diagram by curve 2. In the limiting cases

$$\Delta_p(\gamma_0) = \tfrac{3}{32}\gamma_0^2, \quad \gamma_0 \ll 1; \tag{46}$$

$$\Delta_p(\gamma_p) = -\tfrac{3}{2}, \quad \gamma_0 \gg 1. \tag{47}$$

At the threshold for photodisintegration

$$\Delta_p(1) = 0{,}156.$$

The total effect of the dipole and magnetic-dipole disintegrations on the real part of the amplitude L is shown in the diagram by curve 3. Right at the threshold the effect of photodisintegration leads to a change of the amplitude by about 40 percent.

The contribution of photodisintegration of the deuteron to the polarizability of the deuteron can be seen from Eqs. (42) and (46). Since the value of the cross section for photodisintegration of the deuteron at high energies is larger than the sum of the expressions (39) and (44), the estimates obtained here can be regarded as lower limits on the quantities, although the contribution of high energies is small.

The treatment carried through here for one amplitude of the γ-d scattering can serve as an indication that inclusion of the effects of inelastic processes, and primarily those of the photodisintegration of the deuteron, in the analysis of elastic γ-d scattering can be important over a wide range of energies.

Similar effects must naturally occur also in the scattering of γ rays by heavier nuclei. A study of the elastic scattering of γ rays by nuclei shows[9] that for quite a number of elements the cross section for nuclear scattering of γ rays near the threshold of the reaction (γ, n) is characterized by a peak of considerable height with an energy width of about ±2 Mev, which is evidently due to nonmonotonic effects near the threshold. Further improvement of the accuracy of the experimental data on elastic scattering of γ rays and on the energy dependence of the cross sections of (γ, n) reactions near threshold is necessary for a more reliable analysis of this effect.

---

[1] L. I. Lapidus and Chou Kuang-Chao, JETP **37**, 1714 (1959), Soviet Phys. JETP **10**, 1213 (1960); JETP **38**, 201 (1960), Soviet Phys. JETP **11**, 147 (1960).

[2] R. H. Capps and W. G. Holladay, Phys. Rev. **99**, 931 (1955), Appendix B.

[3] F. Rohrlich and R. L. Gluckstern, Phys. Rev. **86**, 1 (1952).

[4] A. I. Akhiezer and V. B. Berestetskiĭ, Квантовая электродинамика (Quantum Electrodynamics), Fizmatgiz, 1959, Sec. 55.

[5] R. Karplus and M. Neuman, Phys. Rev. **83**, 776 (1951).

[6] A. I. Baz', JETP **36**, 1762 (1959), Soviet Phys. JETP **9**, 1256 (1959).

[7] L. Fonda and R. G. Newton, Ann. Phys. **7**, 133 (1959).

[8] A. I. Akhiezer and I. Ya. Pomeranchuk, Некоторые вопросы теории ядра (Some Problems of Nuclear Theory), Gostekhizdat 1958, Secs. 11 and 12.

[9] E. G. Fuller and E. Hayward, Phys. Rev. **101**, 692 (1956).

Translated by W. H. Furry
23

SOVIET PHYSICS JETP VOLUME 12, NUMBER 1 JANUARY, 1961

AN ASYMPTOTICALLY EXACT SOLUTION FOR THE MODEL HAMILTONIAN OF THE THEORY OF SUPERCONDUCTIVITY

N. N. BOGOLYUBOV, D. N. ZUBAREV, and Yu. A. TSERKOVNIKOV

Mathematics Institute, Academy of Sciences, U.S.S.R.

Submitted to JETP editor February 13, 1960

J. Exptl. Theoret. Phys. (U.S.S.R.) 39, 120-129 (July, 1960)

It is shown that it is possible to satisfy with asymptotic exactness the entire chain of equations for Green's functions constructed on the basis of the model Hamiltonian of Bardeen, Cooper, and Schrieffer. Thus the asymptotic exactness of the known solution for the superconducting state is proved without the use of perturbation theory. It is shown that the trivial solution that corresponds to the normal state must be rejected at temperatures below the critical temperature.

INTRODUCTION

In a previous paper[1] it has been shown on the basis of the model Hamiltonian of Bardeen, Cooper, and Schrieffer (BCS)[2] that the thermodynamic functions of a superconducting system, which were obtained by a variation method in BCS, are asymptotically exact for $V \to \infty$, $N/V = \text{const}$ (V is the volume of the system, and N the number of particles). This conclusion was based on the fact that each term of the perturbation-theory series, by means of which the correction to that solution is calculated, is asymptotically small for $V \to \infty$. Certain objections can, however, be raised against such a proof. In fact, if in the model Hamiltonian of BCS one takes as the zeroth approximation the Hamiltonian of noninteracting particles, then each term of the thermodynamic perturbation theory will also be asymptotically small, whereas it is well known that the existing theory of superconductivity is based on the inclusion of precisely these terms. On the basis of a partial summation of the diagrams (ladder approximation), Prange[3] has even expressed a doubt that a solution of the superconducting type with a gap in the spectrum of elementary excitations exists at all for the model Hamiltonian of BCS.

In the present paper we show how to obtain the same asymptotically exact solution as in references 2 and 1 without resorting to perturbation theory. Besides this it will be shown that for temperatures Θ below the phase-transition temperature Θ_0 the solution that appears for $V \to \infty$ and corresponds to the nonsuperconducting state (the trivial solution) must be rejected as failing to satisfy the necessary conditions for the exact Green's functions. Arguments about the absence of the trivial solution for $\Theta < \Theta_0$ have already been put forward by Wentzel[4] and by Thouless.[5] Thouless based his argument on an examination of a special model that admits of exact solution.

2. THE MODEL AND APPROXIMATING HAMILTONIANS IN THE THEORY OF SUPERCONDUCTIVITY

The model Hamiltonian of BCS is of the form

$$H = \sum_f T_f a_f^+ a_f - \frac{1}{2V} \sum_{ff'} J(f, f') a_f^+ a_{-f}^+ a_{-f'} a_{f'} + \nu\mathfrak{A},$$

$$\mathfrak{A} = \tfrac{1}{2} \sum_f w_f (a_{-f} a_f + a_f^+ a_{-f}^+), \quad \nu \geqslant 0, \tag{2.1}$$

where $f = (\mathbf{k}, \sigma)$, $-f = (-\mathbf{k}, -\sigma)$; σ is the spin index, which takes the values $+\frac{1}{2}$ and $-\frac{1}{2}$, and $\mathbf{k}$ is the momentum; $T_f = k^2/2m - \mu$, and μ is the chemical potential; and a_f and a_f^+ are operators that satisfy the commutation relations of Fermi statistics. $J(f, f')$ and w_f are real functions which have the properties

$$J(f, f') = J(f', f) = -J(-f, f'), \quad w_{-f} = -w_f. \tag{2.2}$$

For example,

$$J(f, f') = \tfrac{1}{2} J(\mathrm{k}, \mathrm{k}') [\delta(\sigma - \sigma') - \delta(\sigma + \sigma')], \quad J(\mathrm{k}, \mathrm{k}')$$

$$= J(\mathrm{k}', \mathrm{k}) = J(-\mathrm{k}, \mathrm{k}') \tag{2.3}$$

[$\delta(\sigma - \sigma')$ is the Kronecker symbol].

In the Hamiltonian (2.1) we have introduced a supplementary operator $\nu\mathfrak{A}$, which will play an auxiliary part in the selection of the required solutions (see later argument, Sec. 4). In the final results we shall set $\nu = 0$.

Following reference 1, we introduce certain real functions A_f and write the Hamiltonian (1) in the form

$$H = H_0 + H_1, \tag{2.4}$$

$$H_0 = \sum_f H_f = \sum_f \{\tfrac{1}{2} A_f(\nu w_f - C_f) + T_f a_f^+ a_f$$

$$+ \tfrac{1}{2} C_f (a_f^+ a_{-f}^+ + a_{-f} a_f)\}, \tag{2.5}$$

$$H_1 = -\frac{1}{2V} \sum_{ff'} J(f, f') B_f^+ B_{f'}, \tag{2.6}$$

$$B_f = a_{-f} a_f - A_f, \tag{2.7}$$

$$C_f = \nu w_f - \frac{1}{V} \sum_f J(f, f') A_{f'}. \tag{2.8}$$

We now set

$$A_f = \langle a_{-f} a_f \rangle_0 = \langle a_f^+ a_{-f}^+ \rangle_0, \tag{2.9}$$

where the symbol $<\ldots>_0$ means that the averaging is taken over a grand ensemble with the Hamiltonian H_0. (We note that the operator H_0 does not satisfy the condition that the total number of particles $N = \Sigma_f a_f^+ a_f$ is conserved, and therefore in general $A_f \neq 0$). Then

$$\langle B_f \rangle_0 = 0 \tag{2.10}$$

and it can be shown (cf. reference 1) that the operator H_1, treated as a perturbation, gives an asymptotically small contribution for $V \to \infty$ ($N/V = \text{const}$) in each term of the thermodynamic perturbation theory. Neglecting the term H_1 in Eq. (2.4) for this reason, we get the following expression for the thermodynamic potential:

$$\Omega = -\Theta \ln \mathrm{Sp}\, \{e^{-H_0/\Theta}\}. \tag{2.11}$$

The Hamiltonian H_0, which we shall hereafter call the approximating Hamiltonian, is a quadratic form in the operators a_f, a_f^+, and can be diagonalized by means of a linear transformation (cf. reference 6):

$$a_f = u_f \alpha_f + v_f \alpha_{-f}^+, \quad u_f^2 + v_f^2 = 1,$$

$$u_f = u_{-f}, \quad v_f = -v_{-f}. \tag{2.12}$$

We get as the result

$$H_0 = U + \sum_f E_f \alpha_f^+ \alpha_f, \tag{2.13}$$

$$\Omega = U - \Theta \sum_f \ln (1 + e^{-E_f/\Theta}), \tag{2.14}$$

$$U = \tfrac{1}{2} \sum_f \{A_f(\nu w_f - C_f) + T_f - E_f\}. \tag{2.15}$$

The energy of an elementary excitation is given by

$$E_f = \sqrt{T_f^2 + C_f^2}. \tag{2.16}$$

The parameters of the canonical transformation (2.12) are connected with C_f and E_f by the relations

$$u_f^2 - v_f^2 = T_f / E_f, \qquad u_f v_f = -C_f / 2E_f. \tag{2.17}$$

Carrying out the averaging over the grand ensemble with the Hamiltonian (2.13) explicitly, we get the following expressions for the quantities A_f and the mean occupation numbers $\bar{n}_f$:

$$A_f = \langle a_{-f} a_f \rangle_0 = -(C_f / 2E_f) \tanh (E_f / 2\Theta), \tag{2.18}$$

$$\bar{n}_f = \langle a_f^+ a_f \rangle_0 = \tfrac{1}{2} \{1 - (T_f / E_f) \tanh (E_f / 2\Theta)\}. \tag{2.19}$$

Substituting Eq. (2.18) in Eq. (2.8), we get the equation for C_f:

$$C_f = \nu w_f + \frac{1}{2V} \sum_{f'} J(f, f') \tanh (E_{f'} / 2\Theta) C_{f'} / E_{f'}. \tag{2.20}$$

These same results can be obtained starting from the equations for the two-time (retarded or advanced) Green's functions constructed for the approximating Hamiltonian H_0:

$$i dG_f(t - t') / dt = \delta(t - t') + T_f G_f(t - t') + C_f \Gamma_f(t - t'),$$

$$-i d\Gamma_f(t - t') / dt = T_f \Gamma_f(t - t') - C_f G_f(t - t'), \tag{2.21}$$

where, for example, the retarded functions are given by (cf. references 7, 8)

$$G_f(t - t') = \langle\langle a_f(t);\ a_f^+(t') \rangle\rangle_0^{adv}$$

$$= -i\theta(t - t') \langle [a_f(t);\ a_f^+(t')]_+ \rangle_0,$$

$$\Gamma_f(t - t') = \langle\langle a_{-f}^+(t);\ a_f^+(t') \rangle\rangle_0^{adv}$$

$$= -i\theta(t - t') \langle [a_{-f}^+(t);\ a_f^+(t')]_+ \rangle_0 \tag{2.22}$$

and $[\ldots]_+$ is the anticommutator. The system of equations (2.21) can be solved by means of spectral representations, which supplement it with the necessary boundary conditions. (Analogous equations for the causal Green's functions have been considered by Gor'kov.[9]) The system (2.21) is closed and reduces to (2.20). For $\Theta < \Theta_0$, where Θ_0 is the temperature of the transition from the superconducting to the normal state, this equation has two solutions, one of which, $C_f = 0$, is trivial. The nontrivial solution goes to zero for $\Theta = \Theta_0$. If we adopt for $\Theta < \Theta_0$ the nontrivial solution, which corresponds to the lowest value of the thermodynamic potential (2.14), the thermodynamic functions will give a good description of the properties of superconducting systems.

3. THE ASYMPTOTICALLY EXACT SOLUTION OF THE CHAIN OF EQUATIONS FOR THE GREEN'S FUNCTIONS

We shall now prove, without resorting to perturbation theory, that Eq. (2.14) is indeed asymptotically exact for $V \to \infty$ $(N/V = \text{const})$ as the expression for the thermodynamic potential Ω of the system with the model Hamiltonian (2.1), and (in Sec. 4) that for $\Theta < \Theta_0$ and $\nu = 0$ the trivial solution $C_f = 0$ of Eq. (2.20) must be rejected.

Starting from the Hamiltonian (2.1), we get for the operator $a_f(t)$ in the Heisenberg representation the equation

$$i\frac{da_f}{dt} = T_f a_f - \frac{1}{V}\sum_{f'} J(f, f')\, a_{-f}^{+} a_{-f'}\; a_{f'} + \nu w_f a_{-f}^{+}. \tag{3.1}$$

Let us consider Green's functions of the form

$$G_{f,\mathfrak{M}}(t-t') = \langle\langle a_f(t)\,\mathfrak{M}(t);\; a_f^{+}(t')\rangle\rangle, \tag{3.2}$$

$$\Gamma_{f,\mathfrak{N}}(t-t') = \langle\langle a_{-f}^{+}(t)\,\mathfrak{N}(t);\; a_f^{+}(t')\rangle\rangle, \tag{3.3}$$

where the operators $\mathfrak{M}$ and $\mathfrak{N}$ are products of pairs of operators $a_q^{+}a_q$, $a_g^{+}a_{-g}^{+}$, and $a_{-h}a_h$, for example,

$$\mathfrak{M} = a_{q_1}^{+} a_{q_1} \ldots a_{q_k}^{+} a_{q_k} \ldots a_{g_i}^{+} a_{-g_i}^{+} \ldots a_{-h_j} a_{h_j} \ldots, \tag{3.4}$$

and where all the indices $f, q_1, \ldots, q_k, \ldots, g_i, \ldots, h_j, \ldots$ are different. We note that for the Hamiltonian (3.1) the operator for the total number of particles, $N = \Sigma a_f^{+} a_f$, is not an integral of the motion, and therefore the Green's functions (3.3) are different from zero.

Using Eq. (3.1), we get for the functions $G_{f,\mathfrak{M}}$ and $\Gamma_{f,\mathfrak{N}}$ the equations

$$\begin{aligned} i\,dG_{f,\mathfrak{M}}/dt &= \delta(t-t')\langle [a_f\mathfrak{M},\, a_f^{+}]_{+}\rangle + T_f G_{f,\mathfrak{M}} \\ &- \frac{1}{V}\sum_{f'} J(f,f')\,\langle\langle a_{-f}^{+} a_{-f'}\, a_{f'}\mathfrak{M}; a_f^{+}(t')\rangle\rangle \\ &+ \nu w_f \Gamma_{f,\mathfrak{M}} + \langle\langle a_f\, i\frac{d\mathfrak{M}}{dt};\; a_f^{+}(t')\rangle\rangle, \end{aligned} \tag{3.5}$$

$$\begin{aligned} i\,d\Gamma_{f,\mathfrak{N}}/dt &= \delta(t-t')\langle [a_{-f}^{+}\mathfrak{N},\, a_f^{+}]_{+}\rangle - T_f \Gamma_{f\mathfrak{N}} \\ &- \frac{1}{V}\sum_{f'} J(f,f')\,\langle\langle a_{f'}^{+} a_{-f'}^{+}\, a_f\mathfrak{N};\; a_f^{+}(t')\rangle\rangle \\ &+ \nu w_f G_{f\mathfrak{N}} + \langle\langle a_{-f}^{+}\, i\frac{d\mathfrak{N}}{dt};\; a_f^{+}(t')\rangle\rangle \end{aligned} \tag{3.6}$$

(for brevity we omit the argument t in the operators).

These equations are an infinite system of coupled equations. We shall assume that the summation in (3.5) and (3.6) is taken over those values of f' that are equal neither to $\pm f$ nor to any of the indices of the operators involved in $\mathfrak{M}$ and $\mathfrak{N}$. We are then making in each equation an error of the order $1/V$, which is admissible. But then the Green's functions under the summation signs in (3.5) and (3.6) will belong to the same class as the functions $G_{f,\mathfrak{M}}$ and $\Gamma_{f,\mathfrak{N}}$, and consequently the chain of equations for these functions will be a closed one.

We shall now show that we can satisfy the entire chain (3.5) and (3.6) to within terms of order $1/V$ if we carry out the averaging in (3.2) and (3.3) not with the model Hamiltonian (2.1), but with the approximating Hamiltonian (2.5), i.e., if we set

$$G_{f,\mathfrak{M}} = \langle\mathfrak{M}\rangle_0 G_f, \qquad G_f = \langle\langle a_f(t)\, a_f^{+}(t')\rangle\rangle_0; \tag{3.7}$$

$$\Gamma_{f,\mathfrak{N}} = \langle\mathfrak{N}\rangle_0 \Gamma_f, \qquad \Gamma_f = \langle\langle a_{-f}^{+}(t)\, a_f^{+}(t')\rangle\rangle_0, \tag{3.8}$$

where, for example,

$$\langle\mathfrak{M}\rangle_0 = \bar{n}_{q_1} \ldots \bar{n}_{q_k} \ldots A_{g_i}^{*} \ldots A_{h_j} \ldots \tag{3.9}$$

and $\bar{n}_q$ and A_g are defined by the relations (2.18) and (2.19). Then the entire chain of equations reduces to the pair of equations (2.21) for G_f and Γ_f.

In fact, substituting (3.7) and (3.8) in (3.5) and (3.6), we get

$$\begin{aligned} \langle\mathfrak{M}\rangle_0\, i\,dG_f/dt &= \langle\mathfrak{M}\rangle_0 \delta(t-t') + T_f \langle\mathfrak{M}\rangle_0 G_f \\ &- \frac{1}{V}\sum_{f'} J(f, f')\,\langle a_{-f'}\, a_{f'}\mathfrak{M}\rangle_0 \Gamma_f \\ &+ \nu w_f \langle\mathfrak{M}\rangle_0 \Gamma_f + i\langle d\mathfrak{M}/dt\rangle_0 G_f, \end{aligned} \tag{3.10}$$

$$\begin{aligned} \langle\mathfrak{N}\rangle_0\, i\,d\Gamma_f/dt &= -T_f\langle\mathfrak{N}\rangle_0\Gamma_f - \frac{1}{V}\sum_{f'} J(f, f')\,\langle a_{f'}^{+} a_{-f'}^{+}\mathfrak{N}\rangle_0 G_f \\ &+ \nu w_f \langle\mathfrak{N}\rangle_0 G_f + \langle i\,d\mathfrak{N}/dt\rangle_0 \Gamma_f. \end{aligned} \tag{3.11}$$

We now use the fact that

$$\langle a_{-f'}\, a_{f'}\mathfrak{M}\rangle_0 = A_{f'}\langle\mathfrak{M}\rangle_0, \qquad \langle a_{f'}^{+} a_{-f'}^{+}\mathfrak{N}\rangle_0 = A_{f'}\langle\mathfrak{N}\rangle_0.$$

Then, according to (3.1) and (2.18)–(2.20), we have apart from terms of order $1/V$

$$\begin{aligned} \langle i\,da_q^{+}a_q/dt\rangle_0 &= \frac{1}{V}\sum_{q'} J(q, q')\,\langle a_q^{+}a_{-q}^{+}a_{-q'}\, a_{q'} - a_{q'}^{+}a_{-q'}^{+}a_{-q}\, a_q\rangle \\ &+ \nu w_f\langle a_q^{+}\, a_{-q}^{+} - a_{-q}\, a_q\rangle_0 = 0, \end{aligned}$$

$$\begin{aligned} -\langle i\,da_g^{+}a_{-g}^{+}/dt\rangle_0 &= 2T_g A_g - \frac{1}{V}\sum_{g'} J(g, g')(1-2\bar{n}_g) A_{g'} \\ &+ \nu w_g(1-2\bar{n}_g) = 0 \end{aligned}$$

and consequently

$$\langle i\,d\mathfrak{M}/dt\rangle_0 = 0, \qquad \langle i\,d\mathfrak{N}/dt\rangle_0 = 0. \tag{3.12}$$

Thereupon (3.10) and (3.11) reduce to the system (2.21).

Thus we see that (3.7) and (3.8) are an asymptotically exact solution (for $V \to \infty$, $N/V = \text{const}$) of the entire chain of equations for the Green's functions. We have convinced ourselves [see Eqs. (3.7)–(3.9)] that all the Green's functions for the model Hamiltonian (2.1) and the approximating Hamiltonian (2.5) coincide, and consequently these Hamiltonians are equivalent in an asymptotic sense.

We have here considered Green's functions (3.2) and (3.3) which, in general, do not satisfy the condition of conservation of the number of particles (the number of creation operators is not equal to the number of annihilation operators), and for $\nu = 0$ [cf. Eq. 2.1)] averages of the type $\langle a_{-f}a_f \rangle$, where the averaging is over a grand ensemble with the Hamiltonian H, are equal to zero. We can, however, obtain all of the results of the theory of superconductivity by starting with a chain of equations for Green's functions in which the numbers of creation and annihilation operators are equal to each other.

Let us consider Green's functions of the forms

$$G_{f,\mathfrak{M}}(t-t') = \langle\langle a_f(t)\,\mathfrak{M}(t);\; a_f^+(t')\rangle\rangle, \tag{3.13}$$

$$\Gamma_{f,f',\mathfrak{N}}(t-t') = \langle\langle a_{-f}^+(t)\,a_{-f'}(t)\,a_{f'}(t)\,\mathfrak{N}(t);\; a_f^+(t')\rangle\rangle, \tag{3.14}$$

where the operators $\mathfrak{M}$ and $\mathfrak{N}$ are made up of products of operators of the form $a_q^+a_qa_g^+a_{-g}^+a_{-h}a_h$:

$$\mathfrak{M} = \ldots a_q^+\,a_q \ldots a_g^+\,a_{-g}^+\,a_{-h}\,a_h \ldots \tag{3.15}$$

Assuming that all the indices of the operators occurring in the Green's functions (3.13) and (3.14) are different, we have the following closed chain of equations:

$$\begin{aligned} i\,dG_{f,\mathfrak{M}}/dt &= \delta(t-t')\langle\mathfrak{M}\rangle + T_f G_{f,\mathfrak{M}} \\ &\quad - \frac{1}{V}\sum_{f''} J(f,\,f'')\langle\langle a_{-f}^+ a_{-f''}\,a_{f''}\,\mathfrak{M};\; a_f^+(t')\rangle\rangle \\ &\quad + \langle\langle a_f\, i\,\frac{d\mathfrak{M}}{dt};\; a_f^+(t')\rangle\rangle, \\ i\,d\Gamma_{f,f',\mathfrak{N}}/dt &= -T_f\Gamma_{f,f',\mathfrak{N}} \\ &\quad - \frac{1}{V}\sum_{f''} J(f,\,f'')\langle\langle a_f a_{f''}^+ a_{-f''}^+\,a_{-f'}\,a_{f'}\,\mathfrak{N};\; a_f^+(t')\rangle\rangle \\ &\quad + \langle\langle a_{-f}^+\, i\,\frac{da_{-f'}\,a_{f'}}{dt}\,\mathfrak{N};\; a_f^+(t')\rangle\rangle \\ &\quad + \langle\langle a_{-f}^+a_{-f'}\,a_{f'}\, i\,\frac{d\mathfrak{N}}{dt};\; a_f^+(t')\rangle\rangle \end{aligned} \tag{3.16}$$

(the summation index f′ is not equal to any of the other indices).

It is easy to verify that the system (3.16) can be satisfied, apart from terms of order 1/V, if we perform the averaging in (3.13) and (3.14) with respect to the approximating Hamiltonian, i.e., if we set

$$G_{f,\mathfrak{M}} = \langle\mathfrak{M}\rangle_0 G_f, \quad \Gamma_{f,f',\mathfrak{N}} = \langle\mathfrak{N}\rangle_0 A_{f'}\Gamma_f. \tag{3.17}$$

The system (3.16) then again reduces to the system of equations (2.21).

By repeating these same arguments one can show that the chain for the many-time causal Green's functions of the form

$$\begin{aligned} &G(t_1, \ldots, t_n) \\ &\quad = \langle T a_{f'_1}(t_1) \ldots a_{f_l}(t_l)\,a_{f_{l+1}}^+(t_{l+1}) \ldots a_{f_n}^+(t_n)\rangle, \end{aligned} \tag{3.18}$$

where T is the chronological-ordering operator and the averaging is taken with respect to the model Hamiltonian (2.1) ($\nu \neq 0$ or $\nu = 0$), can also be solved with asymptotic exactness.

Let us now examine the solutions of (2.20). We set

$$\begin{aligned} C_f = C\varphi_f = (-1)^{\sigma+1/2}\,C\,\varphi_k, &\qquad \varphi_{k_0} = 1, \\ \omega_f \cdot J_f = \tfrac{1}{2}(-1)^{\sigma+1/2}J_k, & \end{aligned} \tag{3.19}$$

where k_0 is the magnitude of the momentum at the Fermi surface, C is the size of the gap at the Fermi surface, $J_k = J_{k,k_0}$, and $J_{k,k'}$ is the kernel $J(\mathbf{k},\mathbf{k}')$ averaged over the angular variables. Setting $k = k_0$ in (2.20) and using (3.19), we have

$$C = \nu J + \frac{C}{2V}\sum_f J_f \tanh\frac{E_f}{2\Theta}\,\frac{\varphi_f}{E_f}, \tag{3.20}$$

where $J = \tfrac{1}{2}J_{k_0}$. Multiplying (3.20) by J_f/J and subtracting the result from (2.20), we get an equation for φ_f:

$$\varphi_f = \frac{J_f}{J} + \frac{1}{2V}\sum_{f'}\left\{J(f,f') - \frac{J_fJ_{f'}}{J}\right\}\tanh\frac{E_{f'}}{2\Theta}\,\frac{\varphi_{f'}}{E_{f'}}. \tag{3.21}$$

Unlike the corresponding expression in (2.20) the integrand in (3.21) already has no singularities as $C \to 0$ and $\Theta \to 0$.

For sufficiently small interaction parameter (cf. references 1 and 6), $C \sim \Theta \sim e^{-1/\rho}$ are small quantities ($\rho \ll 1$), and we can set $C = 0$ and $\Theta = 0$ in (3.21). As the result we then get a linear inhomogeneous equation for φ_f:[10]

$$\varphi_f = \frac{J_f}{J} + \frac{1}{2V}\sum_{f'}\left\{J(f,f') - \frac{J_fJ_{f'}}{J}\right\}\frac{\varphi_{f'}}{|T_{f'}|}, \tag{3.22}$$

from which, confining ourselves to the first step of iteration, we have

$$\varphi_f \approx J_f/J. \tag{3.23}$$

Substituting (3.23) in (3.20), we bring the equation for the gap C into the following form:

$$C = \nu J + \frac{CJ}{2V}\sum_f \frac{J_f^2}{J^2}\,\frac{\tanh(E_f/2\Theta)}{E_f}. \tag{3.24}$$

We note that in the case of a factorizable kernel

$$J(f,f') = J_fJ_{f'}/J, \qquad J_{-f} = -J_f, \tag{3.25}$$

the function (3.23) is an exact solution of (3.21) as well as (3.22). Consequently (3.24) will in this case be valid also for strong interaction. For definiteness we shall hereafter assume that the interaction is factorizable.

Equation (3.24) has two solutions. One of them goes over for $\nu \to 0$ into the well known solution of (2.20) (cf. references 1 and 2), which gives a gap in the spectrum of the elementary excitations (for small interaction ρ we have $C \sim e^{-1/\rho}$), and the other goes to zero for $\nu \to 0$ [the "trivial" solution of Eq. (2.20)].

Let us find the solution that goes to zero as $\nu \to 0$. In doing so we confine ourselves to the case of zero temperature, $\Theta = 0$. The extension to the case of nonzero temperature presents no difficulties (cf. reference 10), and does not change the character of the solution.

Let us set $\Theta = 0$ in (3.24) and go over from the summation over $f = (\mathbf{k}, \sigma)$ to integration over the variable $\xi = k^2/2m - \mu$ ($\xi \equiv T_f$), assuming that the Fermi energy is much larger than the mean Debye frequency ω ($\omega/\mu \ll 1$) at which the kernel in (3.20) changes rapidly. We get

$$C = \nu J + \rho C \int_0^\infty d\xi \varphi^2(\xi) / \sqrt{\xi^2 + C^2\varphi^2(\xi)}, \qquad (3.26)$$

where [cf. Eq. (2.3)].

$$\rho = mk_0 J/\pi^2, \qquad \varphi^2(\xi) = (J_f/J)^2.$$

For small C (we are looking for the solution $C \to 0$ as $\nu \to 0$) we can set $\varphi(\xi) \approx \varphi(0) = 1$ in the radicand in (3.26). Integrating by parts and neglecting the small quantity C/ω where possible, we get

$$C = \nu J - C\rho \ln (C/\tilde{\omega}), \qquad (3.27)$$

$$\tilde{\omega} = \omega \exp\left\{-\int_0^\infty \ln \frac{2\xi}{\omega} \frac{d\varphi^2(\xi)}{d\xi} d\xi\right\}. \qquad (3.28)$$

Solving the equation (3.27), we find

$$C \approx \nu J / \rho \ln \frac{\nu J}{\rho\tilde{\omega}} \to 0 \text{ for } \nu \to 0 \ (\nu > 0). \qquad (3.29)$$

For weak interaction ($\rho \ll 1$), C/ω is small, and on setting $\nu \to 0$ in the same equation (3.27), we get the well known expression for the gap in the spectrum of elementary excitations of superconductors:

$$C = \tilde{\omega} e^{-1/\rho}. \qquad (3.30)$$

4. THE UNACCEPTABILITY OF THE TRIVIAL SOLUTION AT TEMPERATURES BELOW THE CRITICAL TEMPERATURE

We shall now show that the "trivial" solution (3.29) must be rejected. For this purpose we use the following exact property of the average of the operator $\mathfrak{A}$ that appears in the Hamiltonian (2.1):

$$\frac{d}{d\nu}\langle\mathfrak{A}\rangle \leqslant 0. \qquad (4.1)$$

This property can be established in the following way. Regarding the operator $\Delta\nu\mathfrak{A}$ as a small perturbation, we have for the increment of the average value (cf. reference 8)

$$\Delta\langle\mathfrak{A}\rangle = (\Delta\nu/2\pi)\langle\langle\mathfrak{A}|\mathfrak{A}\rangle\rangle_{E=0}, \qquad (4.2)$$

where $\langle\langle\mathfrak{A}|\mathfrak{A}\rangle\rangle_E$ is the Fourier component of the corresponding retarded Green's function $\langle\langle\mathfrak{A}(t); \mathfrak{A}(t')\rangle\rangle$. For $\Delta\nu \to 0$ we get from (4.2)

$$\frac{d}{d\nu}\left\langle\frac{\mathfrak{A}}{V}\right\rangle = \frac{1}{2\pi}\left\langle\left\langle\frac{\mathfrak{A}}{V}\middle|\mathfrak{A}\right\rangle\right\rangle_{E=0}. \qquad (4.3)$$

On the other hand,

$$\langle\langle\mathfrak{A}|\mathfrak{A}\rangle\rangle_{E=0} = -\frac{1}{2\pi}\int_{-\infty}^{\infty} J(\omega)(e^{\omega/\Theta} - 1)\omega^{-1} d\omega, \qquad (4.4)$$

where $J(\omega)$ is the spectral intensity of the two-time correlation function $\langle\mathfrak{A}(t)\mathfrak{A}(t')\rangle$.[7] Since $\mathfrak{A}^+ = \mathfrak{A}$, we have $J(\omega) > 0$. The second factor in the integrand in (4.4) is also always positive, and from this there follows the property (4.1).

One comment must be made about the formula (4.3), namely that the averaging in its right member must be done not with the approximating Hamiltonian H_0, but with the complete Hamiltonian H. In fact, the quantity whose derivative is taken in the left member of (4.3) is given by

$$\langle V^{-1}\mathfrak{A}\rangle = \frac{1}{V}\sum_f J_f\langle a_{-f}a_f\rangle \qquad (w_f = J_f), \qquad (4.5)$$

which remains finite as $V \to \infty$. In the right member of (4.3), on the other hand, we have

$$\langle\langle V^{-1}\mathfrak{A}|\mathfrak{A}\rangle\rangle = \frac{1}{4V}\sum_{f, f'} J_f J_{f'}\langle\langle a_f^+a_{-f}^+ + a_{-f}a_f \,|\, a_{f'}^+a_{-f'}^+ + a_{-f'}a_{f'}\rangle\rangle. \qquad (4.6)$$

The summation in (4.6) is taken over two indices. Therefore in Eq. (4.6) the terms of order 1/V that are dropped in averaging over the ensemble with the Hamiltonian H_0 give a finite contribution and must be taken into account. If we were to do the averaging in the right member of (4.3) with the Hamiltonian H_0, we would get zero, whereas the left member, as we shall see, is different from zero. In the left member of (4.3) we obviously can do the averaging with the approximating Hamiltonian H_0.

Using the formula (2.18) (averaging with the Hamiltonian H_0) and the solution (3.23), we rewrite the expression (4.5) in the form

$$\langle V^{-1}\mathfrak{A}\rangle = -\gamma J = -\frac{CJ}{2V}\sum_f \varphi_f^2 \frac{\tanh(E_f/2\Theta)}{E_f}. \qquad (4.7)$$

According to Eq. (3.24),

$$C = (\nu + \gamma) J, \qquad (4.8)$$

and for the quantity γ we get the transcendental equation

$$\gamma = \frac{(\gamma + \nu) J}{2V}\sum_f \varphi_f^2 \frac{\tanh(E_f/2\Theta)}{E_f},$$

$$E_f = \sqrt{T_f^2 + (\nu + \gamma)^2 J_f^2}. \qquad (4.9)$$

The condition (4.1) can written in the form

$$d\gamma / d\nu \geqslant 0. \tag{4.10}$$

Calculating this derivative by using (4.9), we have

$$\frac{d\gamma}{d\nu} = \Big[\frac{J}{2V}\sum_f \varphi_f^2 \frac{T_f^2}{E_f^3} \tanh\frac{E_f}{2\Theta} + \frac{(\nu+\gamma)^2 J^3}{4\Theta V}\sum_f \varphi_f^4 E_f^{-2} \cosh^{-1}\frac{E_f}{2\Theta}\Big] \times \Big[1 - \frac{J}{2V}\sum_f \varphi_f^2 \frac{T_f^2}{E_f^3}\tanh\frac{E_f}{2\Theta} - \frac{(\nu+\gamma)^2 J^3}{4\Theta V}\sum_f \varphi_f^4 E_f^{-2}\cosh^{-1}\frac{E_f}{2\Theta}\Big]^{-1} \geqslant 0. \tag{4.11}$$

Let us now set $\nu \rightarrow 0$. The first factor in the expression (4.11) is always positive. For $\gamma \neq 0$ ($C \neq 0$, $\Theta < \Theta_0$) the second factor is also positive, since by using (4.9) we can put it in the form

$$\frac{JC^2}{2V}\sum_f \varphi_f^4 E_f^{-3}\ \frac{\sinh(E_f/\Theta) - E_f/\Theta}{2\cosh^2(E_f/2\Theta)} > 0.$$

For the trivial solution $\gamma = 0$ ($C = 0$) the second factor in the expression (4.11) is given by

$$1 - \frac{J}{2V}\sum_f \varphi_f^2 \frac{\tanh(|T_f|/2\Theta)}{|T_f|} = \frac{J}{2V}\sum_f \varphi_f^2 \frac{\tanh(|T_f|/2\Theta) - \tanh(|T_f|/2\Theta_0)}{|T_f|},$$

where the phase-transition temperature Θ_0 is determined from Eq. (4.9) under the condition $\gamma = 0$ or $C = 0$ (the condition that the gap in the spectrum (2.16) of the elementary excitations vanishes):

$$1 = \frac{J}{2V}\sum_f \varphi_f^2 \frac{\tanh(|T_f|/2\Theta_0)}{|T_f|}. \tag{4.12}$$

Consequently, in this case the second factor is positive for $\Theta > \Theta_0$ and negative for $\Theta < \Theta_0$; that is, for $\Theta = \Theta_0$ the trivial solution $C = 0$ ($\gamma = 0$) does not satisfy the relation (4.1), which is a direct consequence of the spectral representation, and therefore this solution must be rejected at temperatures below the critical temperature.

Thus the exact criterion (4.1), which is obtained without neglect of terms of order 1/V, enables us to reject the superfluous solution $C = 0$ that was obtained as a result of the passage to the limit $V \rightarrow \infty$ ($N/V = \text{const}$).

In conclusion we formulate briefly the results we have obtained.

1) It has been shown that with asymptotic accuracy, dropping terms of order 1/V from the equations, one can satisfy the entire chain of equations for the Green's functions constructed on the basis of the BCS model Hamiltonian. In this connection we verify that one can use instead of the model Hamiltonian a simpler approximating Hamiltonian, which is a quadratic form in the operators.

2) It has been shown that at temperatures below the critical temperature the "trivial solution" does not satisfy the necessary conditions for the exact Green's functions and must be rejected.

3) Thus without resorting to perturbation theory we again confirm the asymptotic accuracy of the results obtained in references 1 and 2.

From a rigorous mathematical point of view, however, certain objections can be raised against the proofs presented here. It still has to be shown that when terms of order 1/V are dropped from the equations the solution also changes by an infinitesimal amount. One of the writers[11] has carried out all the necessary estimations by an entirely different method and has shown that the fractional discrepancies between the eigenvalues of the model Hamiltonian and the approximating Hamiltonian, and also between the corresponding Green's functions, will vanish in the limit $V \rightarrow \infty$ ($N/V = \text{const}$).

---

[1] Bogolyubov, Zubarev, and Tserkovnikov, Dokl. Akad. Nauk SSSR **117**, 788 (1957), Soviet Phys.-Doklady **2**, 535 (1958).

[2] Bardeen, Cooper, and Schrieffer, Phys. Rev. **108**, 1175 (1957).

[3] R. E. Prange, Bull. Am. Phys. Soc. **4**, 225 (1959).

[4] G. Wentzel, Preprint.

[5] D. J. Thouless, Preprint (UCRL-8758, 1959).

[6] N. N. Bogolyubov, JETP **34**, 58 (1958), Soviet Phys. JETP **7**, 40 (1958).

[7] N. N. Bogolyubov and S. V. Tyablikov, Dokl. Akad. Nauk SSSR **126**, 53 (1959), Soviet Phys.-Doklady **4**, 589 (1959).

[8] D. N. Zubarev, Usp. Fiz. Nauk **71**, 1 (1960), Soviet Phys. Uspekhi **3**, (1960).

[9] L. P. Gor'kov, JETP **34**, 735 (1958), Soviet Phys. **7**, 505 (1958).

[10] D. N. Zubarev and Yu. A. Tserkovnikov, Науч. докл. Высш. школы., физ.-мат. науки (Scient. Report of the Colleges, Phys. Math. Sci.) No. 2, 133 (1959).

[11] N. N. Bogolyubov, On the Problem of the Model Hamiltonian in the Theory of Superconductivity, Preprint P-511, Joint Inst. Nuc. Res., Dubna, 1960.

Translated by W. H. Furry
24

SOVIET PHYSICS JETP VOLUME 12, NUMBER 1 JANUARY, 1961

PERIPHERAL INTERACTIONS BETWEEN π MESONS AND NUCLEONS AT HIGH ENERGIES

I. M. DREMIN

P. N. Lebedev Physics Institute, Academy of Sciences, U.S.S.R.

Submitted to JETP editor February, 1960

J. Exptl. Theoret. Phys. (U.S.S.R.) **39**, 130-133 (July, 1960)

The inelastic interaction between a π meson and a nucleon is considered, taking into account the exchange of one virtual π meson. The cross section of a process in which two mesons are produced is computed. Relations between the cross sections for various channels of the process $\pi^- + p \rightarrow N + 3\pi$ are given.

In the present paper we consider the peripheral interaction between a π meson and a nucleon (πN) using the method proposed earlier in reference 1. In this method the cross section for the peripheral interaction is expressed approximately in terms of the cross sections of two real processes which are either known experimentally or about which reasonable assumptions can be made on the basis of known experiments. We compute the cross section for an inelastic πN interaction which leads to three π mesons in the final state. It is assumed in the calculation that the interaction is effected through the exchange of a single virtual π meson while the nucleon and the meson go into excited states with the masses $\mathfrak{M}_1 \geq m + \mu$ and $\mathfrak{M}_2 \geq 2\mu$, respectively, i.e., we consider the Feynman graph shown in the figure (m is the mass of the nucleon and μ the mass of the meson). This method is of interest in view of the fact that there is experimental information on the important role of such processes at high energies.[2,3]

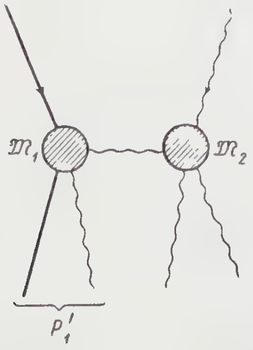

In analogy with Eq. (3) of reference 1, we can write the cross section for the process under consideration in the form*

$$E_1E_2J\sigma_{\pi N} = \frac{1}{\pi^4}\int d^4P_1'(k^2+\mu^2)^{-2}\,\omega E_1J_1\sigma_{\pi\pi}\omega E_2J_2\sigma_2(\omega), \quad (1)$$

where E_1 and E_2 are the energies of the colliding particles, P_1' is the momentum of the isobar, k is the four-momentum of the virtual meson, $k^2 = \mathbf{k}^2 - \omega^2$, J is the current density of the particles, and $\sigma_{\pi\pi}$ is the cross section for the interaction of a π meson with another π meson. Here (as in reference 1) we neglect the difference between the Lorentz-invariant expressions $\omega EJ\sigma$ and the corresponding expressions for the real π meson. To obtain from this information about the cross section for the πN interaction, we must make some definite assumptions concerning the cross section $\sigma_{\pi\pi}$.

We assume that the cross section for the ππ interaction is constant, i.e., independent of the energy of the π meson. We note, however, that if there really is a resonance in the ππ cross section for $p^2 \sim 3.5\mu^2$ (reference 4), where p^2 is the square of the momentum in the center-of-mass system of the two π mesons, this implies that the cross section for the πN interaction will have a maximum at $\epsilon \sim 5$ Bev (ε is the energy of the π meson in the laboratory system), since the function under the integral sign also has a maximum at $p^2 \sim 3.5\mu^2$ for such energies (see below).

With these assumptions we have, in the center-of-mass system of the π meson and the nucleon [writing $k^2 = \kappa_1^2 + 2p_0P_1'(1-\cos\vartheta)$],

$$\frac{\sigma_{\pi N}}{\sigma_{\pi\pi}} = \frac{2p_0}{\pi^3m^2\varepsilon^2}\int\limits_{m\mu}^{z_{max}} dz \int\limits_{\mu^2}^{y_{max}} dy \int\limits_{\beta}^{1} d(\cos\vartheta)$$

$$\times\,\frac{P_1'\sqrt{z^2-m^2\mu^2}\sqrt{y^2-\mu^4}\,\sigma(z/m)}{[\mu^2+\varkappa_1^2+2p_0P'_1(1-\cos\vartheta)]^2},$$

$$z = (\mathfrak{M}_1^2 - m^2 - \mu^2)/2, \qquad y = (\mathfrak{M}_2^2 - 2\mu^2)/2.$$

Expanding the quantity κ_1^2 in terms of the ratios $z/E^2 \ll 1$, and $y/E^2 \ll 1$, we find

$$\varkappa_1^2 = 4zy/E^2 + 4y(z+y)(2z+m^2)/E^4 \equiv ay^2 + by,$$

---

*Unless noted otherwise, we use the notation of reference 1.

where E is the total energy of the system in the center-of-mass system. The limits of integration z_{max}, y_{max}, and β are determined from the requirement that the degree of "virtualness" of the π meson be smaller than a certain given value: $k^2 \leq \delta^2$. It is clear that this method is valid for $\delta \sim \mu$ and invalid for $\delta \gg \mu$. However, at the present moment it is impossible to give the exact theoretical value of δ corresponding to the upper limit up to which our method is applicable. A separate paper will be devoted to the discussion of this question. We propose here a method of obtaining δ from the experimental data on peripheral πN and NN collisions. After integrating, we rewrite (2) in the form

$$\frac{\sigma_{\pi N}}{\sigma_{\pi\pi}} \approx \frac{1}{2\pi^3 p_0^2 E^2} \int\limits_{m\mu}^{z_{max}} dz \sqrt{z^2 - m^2\mu^2}$$

$$\times \left[\frac{1}{a} \ln \frac{\delta^2 (\delta^2 + \mu^2)}{by_{max}(by_{max} + \mu^2)} - \frac{y_{max}^2 - \mu^4}{\delta^2 + \mu^2}\right] [2\sigma_{3/2}(z) + \sigma_{1/2}(z)],$$

$$ay_{max}^2 + by_{max} - \delta^2 = 0. \tag{3}$$

We have made four different assumptions with respect to the interaction amplitudes in the different isotopic states of the two π mesons. According to the experimental data, probably the most correct assumption is that the amplitudes are equal in magnitude and mutually orthogonal (see the Appendix). We note that in this case the cross section for the inelastic peripheral interaction with nucleons is the same for π^- and π^+ mesons. Expression (3) was integrated numerically* for the π meson energy $\epsilon = 5$ Bev and the cut-off parameter $\delta^2 = 4\mu^2$. This yields $\sigma_{\pi N}/\sigma_{\pi\pi} \approx 0.13$. If we assume that the cross section for the $\pi\pi$ interaction is equal to the geometrical value, i.e., $\sigma_{\pi\pi} \approx 65$ mb, we obtain $\sigma_{\pi N} \approx 8.5$ mb. This value is in satisfactory agreement with the data of references 2 and 3.

It must be noted, however, that we can speak only of a good qualitative, but not of a strict quantitative, agreement, because there is some arbitrariness in the choice of the value of the $\pi\pi$ interaction cross section, and moreover, expression (3) depends strongly on δ (approximately like δ^3).

An analogous integration for the case of the NN interaction was performed in reference 1, but these authors did not take for the cut-off parameter the degree of "virtualness" of the π meson, but the average value of the perpendicular component of the momentum transfer, which was taken from experiment; this is, of course, less rigorous on account of the large experimental errors. If in this case the cut-off is also determined by the degree of "virtualness", one easily obtains the formula

$$\sigma_{NN} = \frac{1}{(2\pi)^3 p_0^2 E_0^2} \int\limits_{m\mu}^{z_{max}} dz$$

$$\times \int\limits_{m\mu}^{y_{max}} dy \sqrt{z^2 - m^2\mu^2} \sqrt{y^2 - m^2\mu^2} \left[\frac{1}{\varkappa^2 + \mu^2} - \frac{1}{\delta^2 + \mu^2}\right]$$

$$\times \left\{\begin{matrix} {}^{10}/_9\sigma_{3/2}\sigma_{3/2} + {}^{16}/_9\sigma_{3/2}\sigma_{1/2} + {}^{1}/_9\sigma_{1/2}\sigma_{1/2} \\ {}^{14}/_9\sigma_{3/2}\sigma_{3/2} + {}^{8}/_9\sigma_{3/2}\sigma_{1/2} + {}^{5}/_9\sigma_{1/2}\sigma_{1/2} \end{matrix}\right\}. \tag{4}$$

The top row in the curly brackets corresponds to processes of the type p + p → N + N + 2π, the lower row corresponds to processes of the type n + p → N + N + 2π, and $\sigma_i = \sigma_{i\,el}$. The values of z_{max} and y_{max} are determined from the requirement $\kappa^2 = \delta^2$.

We note the following relation

$$\sigma_{\pi N}/\sigma_{NN} = \sigma_{\pi\pi}/\sigma_{geom},$$

where α is a function only of the energy of the incident particles in the πN and NN interactions and is independent of δ^2, as was shown by the numerical computation. Indeed, $\sigma_{\pi N}$ is given by a formula analogous to formula (4), the only difference being that one of the σ_i in the curly brackets is replaced by $\sigma_{\pi\pi}$. The difference in the energy dependence of σ_i and $\sigma_{\pi\pi}$ has practically no effect on the value of this integral if $\delta \geq 2\mu$. It would therefore be desirable to determine the ratio of the cross section for the peripheral πN interaction with formation of two π mesons over the cross section for the peripheral NN interaction also with formation of two mesons by an evaluation of the corresponding experimental data. This will enable one to determine the $\pi\pi$ interaction uniquely. The value of $\sigma_{\pi\pi}$ obtained in this way will, of course, indeed agree with the cross section for the $\pi\pi$ interaction, if the latter does not depend on the energy of the colliding π mesons or does so only very weakly.

The constancy of the value of $\sigma_{\pi\pi}$, as obtained from the above-quoted ratio of the πN and NN interactions for various energies, will serve as a criterion of the correctness of our assumptions.

Furthermore, the parameter δ is directly determined by formula (4) if the exact value of σ_{NN} is known for some fixed energy of the colliding particles. The experimental data quoted in the re-

---

*In this case the integration goes over the region where $\sigma_{1/2} \ll \sigma_{3/2}$. The numerical values of $\sigma_{3/2}$ and $\sigma_{1/2}$ were taken from the report of Piccioni.[5] The integration over y is equivalent to the integration over the energies of the π meson in the $\pi\pi$ loop up to $\varepsilon' \approx 3.5$ Bev; the function in the integrand has a maximum at the kinetic energy of the π meson $\varepsilon'_{kin} \approx 0.8$ Bev in the rest system of the other π meson.

Ratio of cross sections*	Theoretical values				Experimental data	
	a	b	c	d	[2]	[3]
p^{-00}/p^{+--}	0.5	4	0.23	0.43	$\leqslant 2$	$\leqslant 1.2$
n^{+-0}/p^{+--}	2	4	0.12	0.36	$\leqslant 2.5$	$\leqslant 1.1$
n^{000}/p^{+--}	1	0	0.02	0.05	0	$\leqslant 0.4$

*p^{-00} denotes the cross section for the process $\pi^- + p \rightarrow p + \pi^- + \pi^0 + \pi^0$, etc.

port of Veksler[6] indicate that $\delta \sim 3\mu$. For a unique choice of δ it is desirable to find its value from formula (3) with $\sigma_{\pi\pi}$ obtained by the above-mentioned method. The presently available experimental data are not sufficiently accurate to use this procedure.

The author thanks D. S. Chernavskiĭ for valuable advice and discussion of the results obtained.

APPENDIX

The isotopic spin relations for the process under consideration were determined in a way similar to that proposed in the report of Tamm.[7] The calculations were carried out for four different assumptions with respect to the matrix elements of the $\pi\pi$ interaction. If we denote the matrix element of the interaction of two π mesons in a state with the total isotopic spin I by (I), these assumptions can be written in the following fashion:

a) $(0)\neq 0, \quad (1) = (2) = 0$[8];

b) $(1)\neq 0, \quad (0) = (2) = 0$[9];

c) $(2)\neq 0, \quad (0) = (1) = 0$;

d) states of the $\pi\pi$ system with different total isotopic spin are mutually orthogonal and $|(0)| = |(1)| = |(2)|$.

We note that the contribution of the excited state of the nucleon with isospin ½ to processes of the type considered will be negligibly small for π meson energies of $\epsilon \sim 5$ Bev. With the above-mentioned assumptions we can therefore obtain exact relations between the cross sections for various processes. These relations and their comparison with experiment are given in the table. The data in this table definitely point to the important role played by the interaction of the two mesons in the state with total isotopic spin 2. However, it has not yet been possible to discriminate in a unique way between, for example, the assumptions c) and d).

---

[1] I. M. Dremin and D. S. Chernavskiĭ, JETP **38**, 229 (1960), Soviet Phys. JETP **11**, 167 (1960).

[2] Maenchen, Fowler, Powell, and Wright, Phys. Rev. **108**, 850 (1957).

[3] W. D. Walker, Phys. Rev. **108**, 872 (1957).

[4] T. Frazer and J. Fulco, Phys. Rev. Lett. **2**, 365 (1959).

[5] O. Piccioni, Proc. of the Annual Intern. Conf. on High Energy Physics at CERN, 1958, p. 65.

[6] V. I. Veksler, Report at the International Conference on the Physics of High Energy Particles, Kiev, 1959.

[7] I. E. Tamm, Report at the International Conference on the Physics of High Energy Particles, Kiev, 1959.

[8] F. J. Dyson, Phys. Rev. **99**, 1037 (1955).

[9] G. Takeda, Phys. Rev. **100**, 440 (1955).

Translated by R. Lipperheide
25

SOVIET PHYSICS JETP VOLUME 12, NUMBER 1 JANUARY, 1961

RADIATION EMITTED BY A CHARGED PARTICLE PASSING THROUGH A PLATE

V. E. PAFOMOV

P. N. Lebedev Physics Institute, Academy of Sciences, U.S.S.R.

Submitted to JETP editor February 15, 1960

J. Exptl. Theoret. Phys. (U.S.S.R.) **39**, 134-137 (July, 1960)

Results of calculation of the angular distribution of the radiation emitted by a charged particle passing through an isotropic ferrodielectric plate and through a crystalline plate are presented. In the case of thick plates the main contribution is due to the Cerenkov radiation. An investigation of the solution shows that in the frequency range in which the projections of the wave vector and the Poynting vector on the particle velocity have opposite signs, the Cerenkov radiation is emitted through the back wall of the plate.

The radiation emitted by a charged particle moving through thin dielectric plates is also considered.

1. The problem of energy transfer through boundaries is of a considerable importance in the theory of the Vavilov-Cerenkov effect. In particular, it is interesting to study the angular distribution of the radiation emitted by a charged particle penetrating through a plate. Omitting the calculations, which are analogous to those carried out in reference 1, we give here the final results. The angular distribution of the radiation energy behind the plate is:

a) for the case of a ferrodielectric plate

$$\frac{dW_\omega}{d\Omega} = \frac{e^2v^2}{\pi^2c^3}\frac{\sin^2\vartheta\cos^2\vartheta}{(1-\beta^2\cos^2\vartheta)^2}\,|f(\omega,\vartheta)|^2,$$

$$\begin{aligned}f(\omega,\vartheta) = \{&[(\varepsilon-1)(1-\beta x)-\beta^2(\varepsilon\mu-1)](1+\beta x)\\ &\times(x+y)e^{i\omega xd/c}+[(\varepsilon-1)(1+\beta x)-\beta^2(\varepsilon\mu-1)](1-\beta x)\\ &\times(x-y)e^{-i\omega xd/c}-2x[(\varepsilon-1)(1-\beta^2x^2)\\ &-\beta^2(\varepsilon\mu-1)(1+\beta y)]e^{i\omega d/v}\}\times[(x+y)^2e^{i\omega xd/c}\\ &-(x-y)^2e^{-i\omega xd/c}]^{-1}(1-\beta^2x^2)^{-1},\end{aligned}$$

$$x=\sqrt{\varepsilon\mu-\sin^2\vartheta}\quad(\operatorname{Im}x<0),$$

$$y=\varepsilon\cos\vartheta,\quad d\Omega=\sin\vartheta\,d\vartheta\,d\varphi; \tag{1}$$

b) for the case of a plate cut from a uniaxial crystal perpendicular to its optical axis*

$$\frac{dW_\omega}{d\Omega} = \frac{e^2v^2}{\pi^2c^3}\frac{\sin^2\vartheta\cos^2\vartheta}{(1-\beta^2\cos^2\vartheta)^2}\left|\frac{\varepsilon_0}{\varepsilon_e}F(\omega,\vartheta)\right|^2,$$

$$\begin{aligned}F(\omega,\vartheta) = [&(\gamma_1+\chi\gamma_2)(\chi+\eta)e^{i\omega\chi d/c}+(\gamma_1-\chi\gamma_2)(\chi-\eta)e^{-i\omega\chi d/c}\\ &-2\chi(\gamma_1+\eta\gamma_2)e^{i\omega d/v}][(\chi+\eta)^2e^{i\omega\chi d/c}\\ &-(\chi-\eta)^2e^{-i\omega\chi d/c}]^{-1}(1-\beta^2\chi^2)^{-1},\end{aligned}$$

$$\gamma_1=\beta^2\sin^2\vartheta+1-\beta^2-\varepsilon_0\beta^2\sin^2\vartheta-\varepsilon_e+\varepsilon_0\varepsilon_e\beta^2,$$

$$\gamma_2=\beta(1-\beta^2-\varepsilon_e/\varepsilon_0+\varepsilon_e\beta^2),\qquad\chi=[\varepsilon_0-(\varepsilon_0/\varepsilon_e)\sin^2\vartheta]^{1/2}$$

$$(\operatorname{Im}\chi<0),\quad\eta=\varepsilon_0\cos\vartheta. \tag{2}$$

In deriving the formulas it was assumed that the particle moves perpendicularly to the plate with constant velocity. The following notation has been used in Eqs. (1) and (2): e and v are the charge and velocity of the particle, respectively, β is the ratio of the particle velocity to the velocity of light in vacuum, d is the plate thickness, ϑ is the angle between the normal to the plate and the direction of observation, φ is the azimuth angle, and ϵ_0 and ϵ_e are the transverse and longitudinal components (with respect to the crystal axis) of the dielectric permittivity tensor. In the derivation, all the quantities were expanded in Fourier integrals and, therefore, in the presence of damping it was assumed that the imaginary parts of ϵ, μ, ϵ_0, and ϵ_e are negative.

The formulas for the angular distribution of the radiation energy in front of the plate can be obtained from Eqs. (1) and (2) by replacing β by $-\beta$.* It should be noted that (1) and (2) are valid at sufficiently large distances, where the total field forms a spherical wave.

It is of interest to consider the results obtained from the point of view of the Vavilov-Cerenkov effect. For simplicity, let us assume in the following that the plates are ideally transparent. For the direction of the refracted Cerenkov angles, satisfying the equations

$$\text{a) } \beta^2(\varepsilon\mu-\sin^2\vartheta)=1,\quad\text{b) } \beta^2(\varepsilon_0-\varepsilon_0\varepsilon_e^{-1}\sin^2\vartheta)=1. \tag{4}$$

an infinity of the type $\lim_{\alpha\to0}\sin^2(\alpha d)/\alpha^2$, where d is the plate thickness, occurs in (1) and (2). In the case of thick plates (compared with the wavelength), (1) and (2) exhibit sharp intensity maxima, proportional to the square of the plate thickness. The width of these maxima is inversely proportional to d. As the result of reflection of the Cerenkov radiation from the front surface, similar maxima appear in front of the plate also. A study of the formulas reveals that the ratio of the Cerenkov radiation energy emitted backward (W_b) to the energy emitted forward (W_f) is, in the two cases considered, given by the expressions*

---

*Formula (2) has been derived earlier.[4] The results given in the present article, in the part concerning the crystal plate, were obtained in that investigation.

*For $\mu = 1$ and $\varepsilon_0 = \varepsilon_e = \varepsilon$, Eqs. (1) and (2) coincide with the results of the author given in references 1 and 2. [In reference 2, typographical errors occurred in the signs of the second and third exponents in the numerator of Eq. (2)].

$$\text{a)}\ \frac{W_b}{W_f} = \frac{(1-\varepsilon\beta\cos\vartheta_r)^2}{(1+\varepsilon\beta\cos\vartheta_r)^2}, \qquad \text{b)}\ \frac{W_b}{W_f} = \frac{(1-\varepsilon_0\beta\cos\vartheta_r)^2}{(1+\varepsilon_0\beta\cos\vartheta_r)^2}, \qquad (4)$$

where ϑ_r are the refracted Cerenkov angles. It can be seen from Eq. (4) that, in the frequency range where the Cerenkov light ray makes an obtuse angle with the direction of motion of the particle,[4] more energy is emitted backward than forward. The forward radiation is a result of reflection from the back wall. It is interesting that when the radiation is emitted at Brewster's angle, for which in the given case the denominators in Eq. (4) vanish, the forward Cerenkov radiation disappears completely.

2. Let us consider the radiation in thin dielectric plates. We shall use the formula for radiation energy[2] correct for plates of arbitrary thickness. Assuming that $|\sqrt{\epsilon}|\omega d/c \ll 1$ and that $\omega d/v \ll 1$, and expanding all the exponents in Eq. (2)[2] in a series, we obtain for the case of a relativistic particle the angular distribution of radiation intensity in front of the plate in the form

$$\frac{dW_\omega(1)}{d\Omega} = \frac{e^2\omega^2d^2}{4\pi^2c^3}|\varepsilon-1|^2\frac{\sin^2\vartheta\cos^2\vartheta}{(1-\beta^2\cos^2\vartheta)^2}. \qquad (5)$$

Since the result is independent of the sign of the particle velocity, the angular distribution behind the plate is identical. The corresponding spectral density of the radiation energy is given by the formula

$$W_\omega(1) = \frac{e^2\omega^2d^2}{4\pi c^3}|\varepsilon-1|^2\left[\ln\frac{4}{1-\beta^2}-3\right]. \qquad (6)$$

It is obvious that the perturbations due to separate patches of low inhomogeneity, encountered along the particle path, are coherent. This explains why the radiation energy varies as the square of the plate thickness.*

From the results given above one can conclude that the radiation energy in a thin stack of thin plates will be proportional to the square of the number of plates. For a large separation between the plates, the coherence condition is violated, and the energy is proportional to the number of plates. In order to determine the coherence condition let us consider the angular distribution of radiation energy for the passage of a charged particle through a stick consisting of m thin plates. Omitting the calculations, the final result for a relativistic particle is

$$\begin{aligned} dW_\omega(m)/d\Omega = |1 &+ \exp[i\omega c^{-1}(l-l\beta\cos\vartheta+d)] \\ &+ \exp[2i\omega c^{-1}(l-l\beta\cos\vartheta+d)] \\ &+ \ldots + \exp[(m-1)i\omega c^{-1}(l-l\beta\cos\vartheta \\ &+ d)]|^2\, dW_\omega(1)/d\Omega, \end{aligned}$$

$$(|\sqrt{\varepsilon}|\omega dm/c \ll 1), \qquad (7)$$

where l is the distance between the plates and $dW_\omega(1)/d\Omega$ is determined from Eq. (5). The radiation energy density per unit solid angle in Eq. (5) has a maximum in the direction $\vartheta \sim \sqrt{1-\beta^2}$. All particles will radiate coherently if, in the direction $\vartheta \sim \sqrt{1-\beta^2}$, The largest exponent in Eq. (7) is much smaller than unity,

$$\omega c^{-1}[l(Mc^2/E)^2+d]m \ll 1, \qquad (8)$$

where M is the particle mass and E is its total energy. The spectral radiation energy density is proportional to m^2: $W_\omega(m) = m^2W_\omega(1)$. Under the condition

$$\omega c^{-1}[l(Mc^2/E)^2+d] \gg 1 \qquad (9)$$

the coherence condition for adjoining plates is violated and, therefore, $W_\omega(m) = mW_\omega(1)$.†

A study of Eq. (5) reveals that the logarithmic increase in the spectral energy density of the transition radiation (6) from each plate is due to the emission at all angles large compared with

---

*At small distances from the plate, the refracted Cerenkov waves are cylindrical. In the case of an isotropic dielectric plate these waves were studied by Garibyan and Chalikyan.[3] It should be taken into account that the last bracket of Eq. (7)[3] should read $(\varepsilon\sqrt{1+v^2c^{-2}(1-\varepsilon)}-1)$ instead of $(\sqrt{1+v^2c^{-2}(1-\varepsilon)}-1$. The ratio of the Cerenkov radiation energy emitted backward [Eq. (7) of reference 3] to the energy emitted forward [Eq. (8)[3]] is then identical with the expression obtained in reference 1 for an isotropic plate. It follows from Eq. (4) as a particular case for $\mu = 1$ and $\varepsilon_0 = \varepsilon_e = \varepsilon$.

*The calculations of the energy loss for a particle traversing a thin plate were carried out also by Garibyan.[5] The author calculated the work done by the force acting upon a particle, limiting himself to the term linear in the plate thickness. Since the Poynting-vector flux through a remote sphere is proportional to the square of the thickness, the estimates obtained in reference 5 should be attributed to other, non-radiative losses, i.e., ionization of the atoms in the plate.

†Garibyan[6] found the radiation field due to the passage of a charged particle through a stack of plates. His conclusions regarding the radiation energy do not follow, however, from the solution obtained.

$\vartheta \sim \sqrt{1-\beta^2}$. Since, at large angles, the coherence condition is more stringent, the above fact will lead to a lesser variation of the coherence condition with the energy of an ultra-relativistic particle.

---

[1] V. E. Pafomov, Dissertation, Phys. Inst. Acad. Sci. U.S.S.R., 1957.

[2] V. E. Pafomov, JETP **33**, 1074 (1957), Soviet Phys. JETP **6**, 829 (1958).

[3] G. M. Garibyan and G. A. Chalikyan, JETP **35**, 1282 (1958), Soviet Phys. JETP **8**, 894 (1959).

[4] V. E. Pafomov, JETP **36**, 1853 (1959), Soviet Phys. JETP **9**, 1321 (1959).

[5] G. M. Garibyan, JETP **37**, 527 (1959), Soviet Phys. JETP **10**, 372 (1960).

[6] G. M. Garibyan, JETP **35**, 1435 (1958), Soviet Phys. JETP **8**, 1003 (1959).

Translated by H. Kasha.
26

SOVIET PHYSICS JETP VOLUME 12, NUMBER 1 JANUARY, 1961

EFFECT OF PAIR CORRELATION OF NUCLEONS ON THE PROBABILITIES OF ELECTROMAGNETIC TRANSITIONS IN THE NUCLEUS

Yu. T. GRIN'

Submitted to JETP editor February 15, 1960

J. Exptl. Theoret. Phys. (U.S.S.R.) 39, 138-140 (July, 1960)

The effect is considered of the pair correlation of nucleons on the probabilities of electromagnetic transitions in deformed nuclei. It is shown that the single quasiparticle electric multipole transitions near the Fermi surface will be forbidden by a factor $\sim A^{-2/3}$ compared to single particle transitions.

It is well known that pair correlation strongly affects the distribution of nucleons near the Fermi surface and the energy spectrum of particles in the nucleus.[1,2] Therefore, the problem arises of investigating the effect of pair interaction on the electromagnetic transitions in the nucleus.

We consider an axially deformed nucleus. Then the internal state of the nucleons is characterized by the component of the total angular momentum Ω of the nucleon along the nuclear symmetry axis. We denote by $\pm\lambda$ the set of $\pm\Omega$ and the other characteristics of the state. The states $+\lambda$ and $-\lambda$ in a deformed nucleus are degenerate, and differ by the sign of the component of the total angular momentum of the nucleus along the axis along which the nucleus is elongated. As has been shown by Belyaev,[1] the wave function for a system with an odd particle in the state $+\lambda_0$ has the form

$$\Phi(+\lambda_0) = \prod_{\lambda\neq\lambda_0} (u_\lambda + v_\lambda b^{+}_{\lambda} b^{+}_{-\lambda})\, b^{+}_{\lambda_0} | \Phi_0^0 \rangle,$$

$$u_\lambda = \sqrt{{}^1/{}_2(1+\varepsilon_\lambda/E_\lambda)}, \quad v_\lambda = \sqrt{{}^1/{}_2(1-\varepsilon_\lambda/E_\lambda)}, \qquad (1)$$

where b_λ and b_λ^+ are the operators for the annihilation and the creation of a particle in the state λ, ϵ_λ is the energy of the nuclear level referred to the Fermi surface ϵ_0, and $E\lambda = \sqrt{\epsilon_\lambda^2 + \Delta^2}$. As has been shown earlier[2] the quantity Δ is determined from the difference of the mass defects by means of the formula

$$\Delta = {}^1/{}_2 |2E_0(N+1) - E_0(N+2) - E_0(N)|,$$

where $E_0(N)$ is the energy of the ground state of a system of N particles, while $|\Phi_0^0\rangle$ is the wave function of the ground state for a system of noninteracting particles.

Let the system make a transition from a state with the odd particle $+\lambda_2$ to the state with an odd particle $+\lambda_1$. These states have different values of Δ, and we shall denote this by priming u_λ and v_λ. We evaluate the matrix element for the transition between these states:

$$M_{+\lambda_2, +\lambda_1} = \langle \Phi^*(+\lambda_2), \hat{A}\Phi(+\lambda_1) \rangle, \qquad (2)$$

where $\hat{A}$ is the operator for the electromagnetic transition in the second-quantization formalism. Then we have

$$M_{+\lambda_2, +\lambda_1} = [u_{\lambda_1} u'_{\lambda_2} A_{+\lambda_2, +\lambda_1} - v_{\lambda_1} v'_{\lambda_2} A_{-\lambda_1, -\lambda_2}]$$
$$\times [(u_{\lambda_1} u'_{\lambda_1} + v_{\lambda_1} v'_{\lambda_1})(u_{\lambda_2} u'_{\lambda_2} + v_{\lambda_2} v'_{\lambda_2})]^{-1} \prod_\lambda (u_\lambda u'_\lambda + v_\lambda v'_\lambda), \qquad (3)$$

where $A_{\lambda,\lambda'}$ is the single particle matrix element for the transition between the states λ and λ'. In the present case $\Delta' - \Delta = \delta \ll \Delta$ since the maximum value of δ is given by[2] $\delta = \Delta_e - \Delta_o \sim 1/\rho_0 \sim \epsilon_0/A$, where ρ_0 is the level density at the Fermi surface, while the quantities Δ_e and Δ_o denote the values of Δ respectively for the neighboring even and odd nuclei. Therefore we have the expression $u_\lambda u'_\lambda + v_\lambda v'_\lambda = 1 - \epsilon_\lambda^2 \delta^2 / 8E_\lambda^4$. On assuming that the interval Δ contains many levels so that we can go over from summing over λ to integration we obtain

$$N = \prod_\lambda (u_\lambda u'_\lambda + v_\lambda v'_\lambda) = \exp\{-\tfrac{1}{16}\pi\rho_0\Delta(\delta/\Delta)^2\}.$$

Since $\delta_{\max}/\Delta \sim A^{-1/3}$ and $\rho_0\Delta \sim A^{1/3}$ for deformed nuclei, N differs from unity by a quantity of the order of magnitude of $A^{-1/3}$. We shall therefore, neglect the variation in the quantity Δ. Then formula (3) assumes the form

$$M_{+\lambda_2, +\lambda_1} = (u_{\lambda_2} u_{\lambda_1} \mp v_{\lambda_1} v_{\lambda_2}) A_{+\lambda_2, +\lambda_1}. \qquad (4)$$

The matrix element is $A_{-\lambda_1, -\lambda_2} = \pm A_{+\lambda_2, +\lambda_1}$ depending on the behavior of the single particle operator $\hat{A}$ under time inversion. We therefore choose in formula (4) the minus or plus sign for electric or magnetic transitions respectively.

Formula (4) means that the so called "single particle" transitions in an odd nucleus are in fact

Nucleus	Transition energy in kev	w_N/w_{exp}	w'_N/w_{exp}
Dy^{161}	74.5	47	~2.3
Np^{237}	26.4	29	~1.8
	59.6	50	~3

single quasiparticle transitions. The matrix element for such a transition will be a superposition of matrix elements for the transitions of a particle from the state $+\lambda_2$ to the state $+\lambda_1$ and of a hole from the state $-\lambda_1$ to the state $-\lambda_2$ taken with appropriate weighting factors. Thus, the pair correlation essentially alters the form of the matrix element for the transition, and consequently also the transition probability.

We consider an electric multipole transition between states close to the Fermi surface when $\epsilon_\lambda \ll \Delta$. Then (4) assumes the form

$$M_{+\lambda_2,+\lambda_1} = A_{+\lambda_2,+\lambda_1}(\varepsilon_{\lambda_1} + \varepsilon_{\lambda_2})/2\Delta. \qquad (5)$$

Since $\epsilon_\lambda \sim \epsilon_0/A$, and $\Delta \sim \epsilon_0/A^{2/3}$, the probability of this transition will be decreased by a factor of $\sim A^{-2/3}$ compared to the single particle transition.

Recently Voĭkhanskiĭ and Gnedin[3] calculated the single particle transition probabilities, using Nilsson's model. It was found that the calculated probabilities differed from the experimental ones on the average by one order of magnitude. Account of nucleon pair correlation by means of formula (4) improves the agreement between theory and experiment, at least in the case of purely electric transitions which depend on the nuclear model to a smaller extent than the magnetic ones. The results of calculations for the E1 transitions in Dy^{161} and Np^{237} are listed in the table, where w_N, w_N and w_{exp} are respectively the transition probabilities calculated according to Nilsson's model, those corrected for the pair correlation and the experimental ones.

The author expresses his gratitude to D. F. Zaretskiĭ and V. M. Strutinskiĭ for discussing these results.

---

[1] S. T. Belyaev, Kgl. Danske Videnskab, Mat.-fys. Medd. **31**, 11 (1959).

[2] A. B. Migdal, JETP **37**, 249 (1959), Soviet Phys. JETP **10**, 176 (1960), Grin', Drozdov, and Zaretskiĭ, JETP **38**, 222 (1960), Soviet Phys. JETP **11**, 162 (1960).

[3] M. E. Voĭkhanskiĭ, JETP **33**, 1004 (1957), Soviet Phys. JETP **6**, 771 (1958). Yu. N. Gnedin, Тезисы докладов на X совещании по ядерной спектроскопия (Abstracts of papers presented at the X Conference on Nuclear Spectroscopy, Moscow, 1960).

Translated by G. Volkoff.
27

SOVIET PHYSICS JETP VOLUME 12, NUMBER 1 JANUARY, 1961

THEORY OF ALPHA DECAY OF NONSPHERICAL NUCLEI

V. G. NOSOV

Submitted to JETP editor February 15, 1960

J. Exptl. Theoret. Phys. (U.S.S.R.) **39**, 141-148 (July, 1960)

A consistent theory of α decay of nonspherical nuclei is developed which is based on a suitable generalization of the quasiclassical approximation in quantum mechanics. Formulas are obtained for relative intensities of the fine structure lines of α rays, and also for the α-decay constant, and for the angular distribution of α particles emitted by oriented nuclei. A new method of measuring the quadrupole polarization of oriented nuclei is proposed.

1. INTRODUCTION

During the last 30 years the nature of the theoretical interest in the phenomenon of α decay has been greatly altered. In the early papers[1] the principal attention was devoted to the fact that the α decay process is a quantum-mechanical tunnel effect. At the present time the aspect of greatest immediate interest appears to be the use of α decay for the measurement of nuclear deformations. Indeed, the use of other methods of measuring deformations, of which the most important one is Coulomb excitation,[2] has so far turned out to be not very effective in the range $A > 220$, owing to experimental difficulties.

An essential factor in the following discussion is that the complete wave function for the parent nucleus can be represented in the form

$$\Psi = \sum_{ik} \psi_{ik}(\mathbf{r}, \omega)\, \varphi_i^{\alpha} \varphi_k, \tag{1.1}$$

where φ_i^{α} and φ_k are the wave functions for the stationary states of internal motion of the α particle and the daughter nucleus respectively. The expansion coefficients ψ_{ik} depend on the position vector $\mathbf{r}$ of the α particle relative to the center of mass of the daughter nucleus and on the Eulerian angles ω which characterize the orientation of the nonspherical daughter nucleus with respect to fixed axes. Formula (1.1) holds both inside and outside the daughter nucleus, but the qualitative behavior of the coefficients ψ_{ik} in these two regions is quite different.

In the external region due to the effect of the Coulomb barrier the functions $\psi_{ik}(\mathbf{r}, \omega)$ decay rapidly with increasing r. The decrement of this decay depends strongly on the energy of internal excitation in the state $\varphi_i^{\alpha}\varphi_k$. As a result, the only components $\psi_{ik}(\mathbf{r}, \omega)$ significant in the asymptotic region $r \to \infty$ are those corresponding to relatively small energies of internal excitation. In this case we have to take into account only the ground state $i = 0$ for the α particle, while the index k denotes several of the lowest levels of internal excitation of the nonspherical daughter nucleus. Thus, in fact, only a small fraction of the components of the total wave function shown in the sum (1.1) manifests itself in α decay. The task of the theory consists in finding these few $\psi_{0k}(\mathbf{r}, \omega)$ in the region external to the nucleus.

It should be emphasized that in this region the previously mentioned components $\psi_{0k}\varphi_0^{\alpha}\varphi_k$ are not strongly interrelated. After the emission of the α particle the internal state of the daughter nucleus φ_k can change only as a result of being affected by its Coulomb field.* An estimate shows that the probability of such a transition is negligibly small. Therefore we can write for each of the $\psi_{0k}(\mathbf{r}, \omega)$ outside the nucleus its own "single-particle" Schrödinger equation [cf. (2.3)]. It turns out to be fairly complicated, since the electrostatic interaction between the daughter nucleus and the α particle is not a central one, and the wave function ψ_{0k} depends, generally speaking, on all the five variables of the system: the three Cartesian coordinates $\mathbf{r}$ of the α particle, and the two angular variables $\nu = \cos\Theta$ and Φ, which we have previously denoted by the single letter ω. Nevertheless, the generalization we obtained for the quasiclassical method enabled us to solve this equation.† As far as we know, the quasiclassical approximation has not been previously used for the solution of partial differential equations containing so large a number of independent variables.

---

*We do not consider the case when such a change occurs as a result of the rotation of the daughter nucleus. In other words, it is assumed that in the spectrum of the nuclear energy levels the rotational bands corresponding to different internal states φ_k do not interact with each other.

†Some of the results of the present work based on this generalization of the quasiclassical approximation have been published in preliminary form without a derivation in the form

The interaction between the different configurations $\varphi_i^\alpha \varphi_k$ is extremely great inside the nucleus. This can be written as the condition $l_\alpha \ll R_0$, where l_α is the mean free path of the α particle and R_0 is the nuclear radius. Therefore, in addition to the ψ_{0k} in which we are interested, the sum (1.1) contains many other components ψ_{ik}. The normalization condition has the form

$$\sum_{ik} w_\alpha^{ik} = 1; \qquad w_\alpha^{ik} = \int d\omega \int_V |\psi_{ik}(\mathbf{r},\omega)|^2 d\mathbf{r}, \tag{1.2}$$

where w_α^{ik} are the corresponding "internal probabilities"; the integration is carried out over the volume of the daughter nucleus. The components ψ_{0k} which actually occur in α decay apparently correspond to only a very small fraction of the total internal probability:

$$w_\alpha^{0k} \ll 1. \tag{1.3}$$

Since the different components $\psi_{ik}\varphi_i^\alpha \varphi_k$ of the total wave function (1.1) are closely interrelated, there exists no single-particle Schrödinger equation for each individual $\psi_{ik}(\mathbf{r},\omega)$. However, for those few configurations $\varphi_0^\alpha \varphi_k$ which are of the greatest significance for α decay, the form of the function $\psi_{0k}(\mathbf{r},\omega)$ inside the nucleus can be established.

First of all, we have

$$\psi_{0k}(\mathbf{r},\omega) = F(\omega), \tag{1.4}$$

since as a result of the homogeneity and isotropy of nuclear matter and of the condition $l_\alpha \ll R_0$ there exist no special points singled out within the nucleus. The dependence of ψ_{0k} on the Eulerian angles ω is uniquely determined by the values of the total angular momentum of the parent nucleus Ω and of its projection M on a fixed axis, both of which remain constant in time:

$$\Omega^2\Psi = \Omega(\Omega+1)\Psi, \quad \Omega_z\Psi = M\Psi. \tag{1.5}$$

The only function that satisfies (1.4) and (1.5) has the form

$$\psi_{0k}(\mathbf{r},\omega) = \chi\psi_{rot}^{\Omega M;\,K}(\nu,\Phi), \tag{1.6}$$

where χ is a constant;

$$\psi_{rot}^{\Omega M;\,K}(\nu,\Phi) = \sqrt{(2\Omega+1)/4\pi}\, D_{KM}^{\Omega}(0,\nu,\Phi) \tag{1.7}$$

is the rotational wave function for the nonspherical nucleus, K is the projection of the angular momentum of the daughter nucleus on its symmetry axis in the state of internal motion under investigation, and $D_{KM}^{\Omega}(\alpha, \cos\beta, \gamma)$ is a generalized spherical harmonic.[5] On the nonspherical surfaces of the daughter nucleus, expression (1.6) plays the role of the boundary condition for the Schrödinger equation satisfied by the function $\psi_{0k}(\mathbf{r},\omega)$ in the external region.

It is of interest to note that condition (1.4) leads to characteristic selection rules for the α decay of nonspherical nuclei. Indeed, the initial state of the parent nucleus is also characterized by a certain value of the component of the angular momentum along the nuclear symmetry axis K_0; the corresponding rotational wave function has the form $\psi_{rot}^{\Omega M;K_0}(\nu,\Phi)$. In processes such as the formation or breakup of an α particle, which are characterized by large energies and small times, the quantum number K is conserved. On comparing with (1.6) and on taking into account the conservation of parity, we obtain

$$K = K_0, \quad \Pi = \Pi_0, \tag{1.8}$$

where Π is the parity. Precisely such selection rules were established earlier by analysis of the experimental data;[6] the so-called favored α transitions satisfying these selection rules turn out to be the most intense ones when all other conditions remain the same. The unfavored transitions, for which (1.8) is violated, are considerably less intense and we will not consider them.

2. PROBABILITY OF α DECAY

Let us obtain the wave function $\psi_{0k}(\mathbf{r},\omega)$ in the region exterior with respect to the daughter nucleus, and let us determine the probabilities of excitation of rotational levels of the daughter nucleus corresponding to its internal state φ_k. In carrying out the calculations we shall utilize two coordinate systems: a fixed system x, y, z; ν, Φ and a system tied to the nucleus ξ, η, ζ; ν, Φ, which is rotated with respect to the fixed system through the Eulerian angles Φ, Θ, 0. The corresponding Hamiltonian has the following form

$$H = -(\hbar^2/2m)\nabla^2 + H_{rot} + U,$$

$$H_{rot} = (\hbar^2/2I)[\mathbf{J}^2 - \Omega(\Omega+1)],$$

where m is the reduced mass; $\mathbf{J}^2 = \Omega(-l)^2 = \Omega^2 - 2\Omega l + l^2$ is the square of the angular momentum of the daughter nucleus, l is the orbital

---

of separate communications,[3] from which it can be seen that the problem has been completely solved analytically. Later articles have appeared[4] in which it is asserted that high-speed electronic computers are necessary to solve the Schrödinger equation describing the α decay of a nonspherical nucleus and that an analytic solution of the problem is impossible. We can not agree with such assertions.

angular momentum of the α particle, and I is the moment of inertia of the daughter nucleus corresponding to the internal state φ_k.

In the system ξ, η, ζ; ν, Φ the shape of the surface of the daughter nucleus is determined by the equation

$$R(\mu) = R_0 + \xi(\mu) = R_0\Big\{1 + \sum_n \alpha_n P_n(\mu)\Big\}, \qquad (2.1)$$

where $\mu = \cos\vartheta$. The potential energy of the electrostatic interaction U depends only on the variables r and μ; in the approximation linear in α_n we have

$$U(r, \mu) = U_b\Big\{\frac{R_0}{r} + \sum_n \frac{3\alpha_n}{2n+1}\Big(\frac{R_0}{r}\Big)^{n+1} P_n(\mu)\Big\}, \qquad (2.2)$$

where $U_b = 2Ze^2/R_0$ is the height of the Coulomb barrier and Ze is the charge of the daughter nucleus.

The form of the operators $\mathbf{\Omega}$ and $\mathbf{l}$ is well known in the system x, y, z; ν, Φ; the transition to the system ξ, η, ζ; ν, Φ can also be easily carried out.^{7} On taking into account (1.5) we obtain the Schrödinger equation

$$\begin{aligned}
&\frac{\partial^2\psi}{\partial r^2} + \frac{2}{r}\frac{\partial\psi}{\partial r} + \Big(\frac{m}{I} + \frac{1}{r^2}\Big)\Big[(1-\mu^2)\frac{\partial^2\psi}{\partial\mu^2} \\
&\quad - 2\mu\frac{\partial\psi}{\partial\mu} + \frac{1}{1-\mu^2}\frac{\partial^2\psi}{\partial\varphi^2}\Big] \\
&\quad + 2\frac{m}{I}\Big\{-\sqrt{1-\nu^2}\Big(\sqrt{1-\mu^2}\cos\varphi\frac{\partial^2\psi}{\partial\mu\partial\nu} \\
&\quad + \frac{\mu}{\sqrt{1-\mu^2}}\sin\varphi\frac{\partial^2\psi}{\partial\varphi\partial\nu}\Big) + \frac{iM}{\sqrt{1-\nu^2}}\Big(\sqrt{1-\mu^2}\sin\varphi\frac{\partial\psi}{\partial\mu} \\
&\quad - \frac{\mu}{\sqrt{1-\mu^2}}\cos\varphi\frac{\partial\psi}{\partial\varphi}\Big) \\
&\quad - \frac{i\nu}{\sqrt{1-\nu^2}}\Big[\sqrt{1-\mu^2}\sin\varphi\Big(K\frac{\partial\psi}{\partial\mu} - i\frac{\partial^2\psi}{\partial\mu\partial\varphi}\Big) \\
&\quad - \frac{\mu}{\sqrt{1-\mu^2}}\cos\varphi\Big(K\frac{\partial\psi}{\partial\varphi} - i\frac{\partial^2\psi}{\partial\varphi^2}\Big)\Big] \\
&\quad - iK\frac{\partial\psi}{\partial\varphi} - \frac{\partial^2\psi}{\partial\varphi^2}\Big\} + \frac{2m}{\hbar^2}[E - U(r, \mu)]\psi = 0. \qquad (2.3)
\end{aligned}$$

Here E is the energy of decay to the rotational level $J = \Omega$; the indices $i = 0$ and k are omitted from the wave function ψ_{0k}.

We obtain a particular solution ψ_{Jl} of equation (2.3), which describes at infinity an α particle of angular momentum l moving away from the nucleus and a daughter nucleus in a rotational state with angular momentum J. Having in mind the application of the quasiclassical approximation, we perform the substitution

$$\psi_{Jl}(r, \mu, \varphi, \nu, \Phi) = \sqrt{m/\hbar}\, Y_{Jl}^{\Omega M}(\nu, \Phi, \mu, \varphi)\, e^{\sigma(r, \mu, \varphi, \nu)} \qquad (2.4)$$

and seek σ in the form of the series $\sigma = \sigma_{-1} + \sigma_0 + \sigma_1 + \sigma_2 + \ldots$ (this corresponds in fact to an expansion in powers of the parameter $1/\kappa R_0 \ll 1$, where κ is the wave number of the α particle on the surface of the nucleus). The angular functions $Y_{Jl}^{\Omega M}$ satisfy the equations

$$\begin{aligned}
&\Omega^2 Y_{Jl}^{\Omega M} = \Omega(\Omega+1) Y_{Jl}^{\Omega M}, \quad \Omega_z Y_{Jl}^{\Omega M} = M Y_{Jl}^{\Omega M}, \\
&\mathbf{l}^2 Y_{Jl}^{\Omega M} = l(l+1) Y_{Jl}^{\Omega M}, \\
&\Omega \mathbf{l} Y_{Jl}^{\Omega M} = \frac{1}{2}[\Omega(\Omega+1) + l(l+1) - J(J+1)]\, Y_{Jl}^{\Omega M} \qquad (2.5)
\end{aligned}$$

and the normalization condition

$$\int d\omega \int Y_{Jl}^{\Omega M *} Y_{J'l'}^{\Omega' M'}\, do = \delta_{\Omega\Omega'}\delta_{MM'}\delta_{JJ'}\delta_{ll'}, \qquad (2.6)$$

where

$$d\omega = d\nu d\Phi, \quad do = d\mu d\varphi.$$

We represent each of the quasiclassical functions in the form of a series in powers of the deformations α_n:

$$\sigma_{-1} = \sigma_{-1}^{(0)} + \sigma_{-1}^{(1)} + \sigma_{-1}^{(2)} + \cdots, \quad \sigma_0 = \sigma_0^{(0)} + \sigma_0^{(1)} + \sigma_0^{(2)} + \cdots,$$
$$\sigma_1 = \sigma_1^{(0)} + \sigma_1^{(1)} + \sigma_1^{(2)} + \cdots$$

etc. On taking (2.2) into account, this yields

$$\begin{gathered}
\Big(\frac{d\sigma_{-1}^{(0)}}{dr}\Big)^2 = -k_{Jl}^2, \quad 2\frac{d\sigma_{-1}^{(0)}}{dr}\frac{\partial\sigma_{-1}^{(1)}}{\partial r} = \varkappa_b^2\sum_n \frac{3\alpha_n}{2n+1}\Big(\frac{R_0}{r}\Big)^{n+1} P_n(\mu)\cdots, \\
2\frac{d\sigma_{-1}^{(0)}}{dr}\frac{d\sigma_0^{(0)}}{dr} + \frac{d^2\sigma_{-1}^{(0)}}{dr^2} + \frac{2}{r}\frac{d\sigma_{-1}^{(0)}}{dr} = 0\ldots, \qquad (2.7)
\end{gathered}$$

where

$$\begin{gathered}
k_{Jl} = \sqrt{k_\varepsilon^2 - \varkappa_b^2 R_0/r - l(l+1)/r^2}, \quad k_\varepsilon^2 = 2m\varepsilon/\hbar^2, \\
\varepsilon \equiv \varepsilon_J = E - (\hbar^2/2I)[J(J+1) - \Omega(\Omega+1)], \\
\varkappa_b^2 = 4mZe^2/\hbar^2 R_0.
\end{gathered}$$

A solution of (2.7) satisfying the boundary condition at infinity has the form

$$\sigma_{-1}^{(0)} = i\int_{a_{Jl}}^{r} k_{Jl}\,dr, \quad \sigma_0^{(0)} = -\ln(\sqrt{-ik_{Jl}}\,r),$$

$$\sigma_{-1}^{(1)} = \frac{3}{2} i\varkappa_b^2 \sum_n \frac{\alpha_n}{2n+1} P_n(\mu) \int_r^\infty \Big(\frac{R_0}{r}\Big)^{n+1}\frac{dr}{k_{Jl}}. \qquad (2.8)$$

We do not take into account further terms in the double series for the function σ (r, μ, φ, ν) since calculations show that they are negligibly small. In accordance with (2.4), (2.6) and (2.8) the flux of α particles in the state ψ_{Jl} is normalized to unity:

$$\int d\omega \int \frac{\hbar k_\varepsilon}{m} |\psi_{Jl}(r, \mu, \varphi, \nu, \Phi)|^2 r^2\, do = 1. \qquad (2.9)$$
$$r \to \infty$$

At the turning point $r = a_{Jl}$ the wave number k_{Jl} vanishes. We can use Eqs. (2.8) in the region

$r < a_{Jl}$, if we make the substitution $k_{Jl} \to i\kappa_{Jl}$. We represent the true wave function ψ_{0k} in the form of the superposition:

$$\psi = \sum_{Jl} b_{Jl} \psi_{Jl}. \qquad (2.10)$$

At the nonspherical surface S of the daughter nucleus, i.e., for $r = R(\mu)$, we have in the required approximation

$$\sigma_{-1}^{(0)}(S) = \sigma_{-1}^{(0)}(R_0)\Big|_{\substack{l=0\\ \Delta E=0}} - \varkappa_{\Omega 0}(R_0)\,\xi(\mu) + \frac{1}{2}\gamma_E \Delta E + \frac{1}{2}\gamma_l\, l(l+1),$$

$$\sigma_{-1}^{(1)}(S) = \sigma_{-1}^{(1)}(R_0)\Big|_{\substack{l=0\\ \Delta E=0}}, \quad \sigma_0^{(0)}(S) = \sigma_0^{(0)}(R_0)\Big|_{\substack{l=0\\ \Delta E=0}}. \qquad (2.11)$$

Here we have carried out an expansion in terms of the dimensionless small parameters α_n, $l(l+1)/\kappa^2 R_0^2$ and $\Delta E/E$, where $\Delta E \equiv \Delta E_J = E - \epsilon_J = (\hbar^2/2I) \times [J(J+1) - \Omega(\Omega+1)]$ is the energy of excitation of the daughter nucleus measured from the level $J = \Omega$.

It can be easily shown that the expansion coefficients are given by

$$\gamma_E = \frac{1}{E}\left(\frac{\varkappa_b^2 R_0}{k}\tan^{-1}\frac{\varkappa}{k} + \varkappa R_0\right), \quad \gamma_l = \frac{2\varkappa}{\varkappa_b^2 R_0}, \qquad (2.12)$$

where $k \equiv k_E = \sqrt{2mE}/\hbar$, $\kappa \equiv \kappa_{\Omega_0}(R_0) = \sqrt{\kappa_b^2 - k^2}$. We substitute (2.11) into (2.4), (2.10), and the boundary condition (1.6). Taking (2.8), (2.1), and (2.6) into account we obtain, after straightforward transformations,

$$b_{Jl} = \sqrt{\frac{\hbar\varkappa R_0^2 \chi^2}{m}}\,\Gamma \exp\left(-\frac{\gamma_E}{2}\Delta E - \frac{\gamma_l}{2} l(l+1)\right) \times \int d\omega\, \psi_{rot}^{\Omega M;K} \int Y_{Jl}^{\Omega M*} \exp\left\{\sum_n \beta_n P_n(\mu)\right\} do, \qquad (2.13)$$

$$\beta_n = \left\{\varkappa R_0 - \frac{3\varkappa_b^2}{2(2n+1)}\left[\int\limits_{R_0}^{a_{\Omega 0}} \left(\frac{R_0}{r}\right)^{n+1} \frac{dr}{\varkappa_{\Omega 0}} + i\int\limits_{a_{\Omega 0}}^{\infty} \left(\frac{R_0}{r}\right)^{n+1} \frac{dr}{k_{\Omega 0}}\right]\right\}\alpha_n, \qquad (2.14)$$

$$\Gamma = \exp\left\{-2\left(\frac{\varkappa_b^2 R_0}{k}\tan^{-1}\frac{\varkappa}{k} - \varkappa R_0\right)\right\}. \qquad (2.15)$$

Here Γ is the penetrability factor for the Coulomb barrier in the case of a spherical nucleus of radius R_0.

In the laboratory system x, y, z; ν, Φ we denote the angular function Y by $\widetilde{Y}_{Jl}^{\Omega M}(\nu, \Phi, \mu, \varphi)$. Then evidently we have

$$\widetilde{Y}_{Jl}^{\Omega M} = \sum_{M'm'} C_{JM'lm'}^{\Omega M}\, \psi_{rot}^{JM',K}(\nu, \Phi)\, Y_{lm'}(\mu, \varphi), \qquad (2.16)$$

where $C_{\cdot\cdot}^{\cdot\cdot}$ are the Clebsch-Gordan coefficients and Y_{lm} are the normalized spherical harmonics.[5]

The transition to the rotating system ξ, η, ζ; ν, Φ is accomplished with the aid of the generalized spherical harmonics D^l. On taking (1.7) into account we easily obtain

$$Y_{Jl}^{\Omega M} = \sqrt{\frac{2J+1}{2\Omega+1}} \sum_m C_{JKlm}^{\Omega, K+m}\, \psi_{rot}^{\Omega M; K+m}(\nu, \Phi)\, Y_{lm}(\mu, \varphi). \qquad (2.17)$$

We substitute (2.17) into (2.13) and integrate over ω, and also over the angle φ. In accordance with (1.2) and (1.6), the constant χ is related by the equation $w_\alpha = \frac{4}{3}\pi R_0^3 \chi^2$ to the internal probability of formation of an α particle in the nucleus w_α. As can be seen from (2.10), in the case of the normalization (2.9) the probability per unit time of decay to the rotational level of angular momentum J accompanied by the emission of an α particle of angular momentum l, is equal to $W'_{Jl} = |b_{Jl}|^2$. As a result, after interchanging the indices of the Clebsch-Gordan coefficients, we finally obtain*

$$b_{Jl} = \sqrt{\frac{3\hbar\varkappa w_\alpha}{mR_0}}\,\Gamma\,(-1)^{J-\Omega} C_{\Omega K l 0}^{JK} \sqrt{B_l}\, e^{-\gamma_E \Delta E/2}\, \widetilde{X}_l,$$

$$W_{Jl} = \frac{3\hbar\varkappa w_\alpha}{mR_0}\,\Gamma\,(C_{\Omega K l 0}^{JK})^2 B_l\, e^{-\gamma_E \Delta E}\, |\widetilde{X}_l|^2, \qquad (2.18)$$

where

$$B_l = (2l+1)\, e^{-\gamma_l\, l(l+1)}, \qquad (2.19)$$

$$\widetilde{X}_l = \int\limits_0^1 \exp\left\{\sum_n \beta_n P_n(\mu)\right\} P_l(\mu)\, d\mu. \qquad (2.20)$$

Here we have utilized the fact that the shape of the daughter nucleus possesses mirror symmetry: no odd values of n appear in the right hand side of (2.1).

With the aid of (2.18) we obtain the useful relation

$$W_{J'l}/W_{Jl} \equiv w_{J'l}/w_{Jl} = (C_{\Omega K l 0}^{J'K} / C_{\Omega K l 0}^{JK})^2 \exp(-\gamma_E \Delta E_{J'J}), \qquad (2.21)$$

where $\Delta E_{J'J} = (\hbar^2/2I)[J'(J'+1) - J(J+1)]$ is the separation between the rotational levels of angular momenta J′ and J.

The total probability of excitation of a rotational level with angular momentum J is obtained by summing the second of formulas (2.18) with respect to l. We normalize the relative probability w_J by the condition $w_\Omega = 1$. As a result of this we obtain

---

*Independently of the present author and practically simultaneously with him, Fröman[8] has obtained a formula similar to (2.18), based on semi-intuitive considerations.

$$w_J = \exp(-\gamma_E \Delta E) \sum_{l=|J-\Omega|}^{J+\Omega}{}' B_l (C^{JK}_{\Omega K l 0})^2$$

$$\times |\widetilde{X}_l|^2 \Big/ \sum_{l=0}^{2\Omega}{}' B_l (C^{\Omega K}_{\Omega K l 0})^2 |\widetilde{X}_l|^2. \qquad (2.22)$$

where the prime on the summation sign indicates that the summation is taken only over even values of l.

For many purposes it is sufficient to consider only the quadrupole deformation $\xi = R_0 \alpha_2 P_2(\mu)$ which exceeds considerably the other terms in the sum (2.1). In this case the substitution $\widetilde{X}_l \rightarrow X_l$ should be performed, where

$$X_l(\beta) = \int_0^1 e^{\beta P_2(\mu)} P_l(\mu)\, d\mu,$$

$$\beta \equiv \beta_2 = \left[\frac{4}{5} \varkappa R_0 (1 - k^2 / 2\varkappa_b^2) - i2k^3 R_0 / 5\varkappa_b^2\right] \alpha_2. \qquad (2.23)$$

On summing the second of relations (2.18) over all J and l, we obtain the α-decay constant.[9] In the special case of even-even nuclei we have $\Omega = K = 0$; substitution into (2.22) and (2.18) leads to further simplifications.[3,9]

3. ANGULAR DISTRIBUTION OF α PARTICLES

The angular distribution of the α particles emitted by oriented nuclei depends on the quantum number M. In accordance with (2.10), (2.4), (2.8), and (2.16), we have in the laboratory system x, y, z; ν, Φ as $r \rightarrow \infty$

$$\psi_M = \sqrt{\frac{m}{\hbar}} \sum_{JlM'm'} b_{Jl} \exp(\sigma_{-1}^{(0)} + \sigma_0^{(0)})$$

$$\times C^{\Omega M}_{JM'lm'} \psi^{JM';K}_{rot} (\nu, \Phi)\, Y_{lm'}(\mu, \varphi). \qquad (3.1)$$

In the general case we have $\psi = \sum c_M \psi_M$. The spatial density $\int |\psi|^2 d\omega$ of the α particles breaks up into a sum of independent components corresponding to different values of J. To go over to the current density j we must multiply each of these components by the corresponding value of the velocity $\hbar k_\varepsilon / m$. The expression for the differential intensity has the form $jr^2 do$. The final averaging over the spin orientations of the parent nuclei in the initial state is achieved by the replacement $c_{M'} c^*_{M''} \rightarrow \rho_{M'M''}$, where ρ is the spin density matrix of the parent nuclei. After some straightforward transformations we obtain

$$dW = \sqrt{4\pi(2\Omega + 1)} \sum_{M'M''} \rho_{M'M''} \sum_L C^{\Omega M'}_{\Omega M'' L, M'-M''} Y_{L, M'-M''}(\mu, \varphi)$$

$$\times \sum_{Jl'l''} (-1)^{J-\Omega} \sqrt{(2l'+1)(2l''+1)}\, b^*_{Jl''} b_{Jl'}$$

$$\times \exp\{ig[l''(l''+1) - l'(l'+1)]\} C^{L0}_{l'0l''0} W(\Omega l' \Omega l''; JL) \frac{do}{4\pi}, \qquad (3.2)$$

where $g = k/\varkappa_b^2 R_0$, W(abcd; ef) are the Racah coefficients.

At not too low temperatures, when the nuclear orientation is not very pronounced, the main contribution to the anisotropy in the angular distribution is made by the term $L = 2$. If the orienting field possesses some symmetry axis, then the angular distribution becomes axially symmetric.* We restrict ourselves henceforth to the case $\Omega = K \neq 1/2$. Then from (2.18) it follows† that $b_{Jl} = (-1)^{J-K} \sqrt{w_{Jl}}$. In fact, the great majority of the emitted α particles is due to transitions to the levels $J = K$ and $J = K + 1$, with $l = 0$ and 2, while the admixture of other values of the orbital angular momentum is very small. On taking (2.21) into account and on normalizing the total probability of α decay to unity, we easily obtain

$$dw = \{1 + A_2 P_2(\mu)\} \frac{do}{4\pi},$$

$$A_2 = \sqrt{\frac{K(2K-1)}{(K+1)(2K+3)}} \frac{f_2}{1 + w_{K+1}}$$

$$\times \left\{ 2\sqrt{5} \left[\frac{(K+2)(2K-1)}{3(2K+3)\exp(-\gamma_E \Delta E)} w_{K+1} \right. \right.$$

$$\left. \times \left[1 - \frac{(K+2)(2K-1)}{3(2K+3)\exp(-\gamma_E \Delta E)} w_{K+1} \right] \right]^{1/2}$$

$$+ \frac{5}{7} w_{K+1} \frac{\sqrt{2K-1}}{\sqrt{K(K+1)(2K+3)}}$$

$$\left. \times \left[(K+6) + \frac{(K+2)(2K-3)(2K+5)}{3(2K+3)\exp(-\gamma_E \Delta E)} \right] \right\}, \qquad (3.3)$$

where ΔE is the separation between the levels $J = K + 1$ and $J = K$; f_2 is the quadrupole polarization of the parent nuclei.[10] Relations (3.3) can be utilized to measure the quadrupole polarization of nonspherical α-active nuclei by means of the angular distribution of the α particles emitted by them.

Thus, the concepts of the collective model,[11] taken together with the assumption that the mean free path of the α particle in the nucleus is small, enable us to present a complete theory of the α decay of nonspherical nuclei.

I express my gratitude to A. S. Kompaneets, Ya. A. Smorodinskiĭ, E. L. Feĭnberg, and I. S. Shapiro for discussing the results of the present work. The author also takes this opportunity to express his gratitude to P. O. Fröman for reprints of his papers.

---

*For this it is sufficient that the field should have a symmetry axis of order >2.

†Indeed, even though according to (2.23) the quantities β and X_l are complex, their imaginary part is actually negligibly small (in an analogous manner, the imaginary exponent of the exponential $\exp\{ig[l''(l''+1) - l'(l'+1)]\}$ is small for these values of the orbital angular momentum which play an important role, and we shall everywhere replace it by unity). Comparison with experiment shows that $\alpha_2 > 0$. Therefore we have $\beta, X_l > 0$.

---

[1] G. Gamow, Z. Physik. **51**, 204 (1928). E. Condon and R. Gurney, Nature **122**, 439 (1928). G. Gamow and F. Houtermans, Z. Physik **52**, 496 (1929). R. Gurney and E. Condon, Phys. Rev. **33**, 127 (1929).

[2] Alder, Bohr, Huus, Mottelson, and Winther, Revs. Modern Phys. **28**, 432 (1956).

[3] V. G. Nosov, Dokl. Akad. Nauk SSSR **112**, 414 (1957), Soviet Phys.-Doklady **2**, 48 (1957); JETP **33**, 226 (1957), Soviet Phys. JETP **6**, 176 (1958); Izv. Akad. Nauk SSSR, Ser. Fiz. **21**, 1551 (1957), Columbia Tech. Transl. p. 1541.

[4] Gol'din, Adel'son-Vel'skiĭ, Birzgal, Piliya, and Ter-Martirosyan, JETP **35**, 184 (1958), Soviet Phys. JETP **8**, 127 (1959). Gol'din, Novikova, and Ter-Martirosyan, JETP **36**, 512 (1959), Soviet Phys. JETP **9**, 356 (1959).

[5] K. Alder, Helv. Phys. Acta **25**, 251 (1952); M. E. Rose, Multipole Fields, Wiley, N.Y. 1955. A. S. Davydov, Теория атомного ядра (Theory of the Atomic Nucleus), Fizmatgiz (1958).

[6] Bohr, Fröman, and Mottelson, Kgl. Danske Videnskab. Selskab, Mat.-fys. Medd. **29**, 10 (1955).

[7] L. D. Landau and E. M. Lifshitz, Квантовая механика (Quantum Mechanics), Gostekhizdat, 1948, pp. 322-325. [Engl. Transl., Pergamon, 1958].

[8] P. Fröman, Kgl. Danske Videnskab. Selskab, Mat.-fys. Skr. **1**, No. 3 (1957).

[9] V. G. Nosov, Ядерные реакции при малых и средных энергиях (Nuclear Reactions at Low and Medium Energies), Proc. All-Union Conference, November, 1957, Publ. by Academy of Sciences, U.S.S.R., 1958, p. 589; JETP **36**, 1580 (1959), Soviet Phys. JETP **9**, 1122 (1959).

[10] G. R. Khutsishvili, Usp. Fiz. Nauk **53**, 381 (1954).

[11] A. Bohr and B. Mottelson, Kgl. Danske Videnskab. Selskab, Mat.-fys. Medd. **27**, No. 16 (1953). A. Bohr, Rotational States in Atomic Nuclei, Copenhagen (1954).

Translated by G. Volkoff
28

SOVIET PHYSICS JETP VOLUME 12, NUMBER 1 JANUARY, 1961

ON THE SINGULARITIES OF COSMOLOGICAL SOLUTIONS OF THE GRAVITATIONAL EQUATIONS. I

E. M. LIFSHITZ and I. M. KHALATNIKOV

Institute of Physics Problems, Academy of Sciences, U.S.S.R.

Submitted to JETP editor February 16, 1960

J. Exptl. Theoret. Phys. (U.S.S.R) **39**, 149-157 (July, 1960)

We formulate an analytic investigation of the general properties of the cosmological solutions of the gravitational equations near a time singularity. One particular class of solutions is found to be a generalization of the familiar solution corresponding to a homogeneous and isotropic world. A general solution is derived for the case of a centrally symmetric distribution of matter, and its extension to a broader class of solutions is presented.

THE customarily used (Friedmann) cosmological solution of Einstein's gravitational equations is based on the assumption that matter is distributed in space homogeneously and isotropically. This assumption is very farfetched mathematically, apart from the fact that its fulfillment in a real world can at best be only approximate. In this connection, the question arises of the extent to which the essential properties of the resultant solutions are connected with these specific assumptions, and primarily as to whether a time singularity exists in this solution.

A suitable way of investigating this question is to study the general properties of the solutions of the equations of gravitation near a singular point, assuming the latter to exist.

In the present communication we give two particular classes of such solutions. One is a generalization of the ordinary isotropic solution. The other is connected with the properties of the "gravitational collapse" of a centrally-symmetrical distribution of matter.

1. CHOICE OF REFERENCE FRAME

Considering the solution of the equations of gravitation near the singular point, in which the pressure p and the energy density ϵ of the matter go to infinity, it is naturally necessary to use for its equation of state the ultrarelativistic relation

$$p = \varepsilon / 3. \tag{1.1}$$

Then the energy-momentum tensor of the matter*

$$T_{ik} = (p + \varepsilon) u_i u_k + p g_{ik} = \frac{\varepsilon}{3} (4 u_i u_k + g_{ik}), \quad T_i^i = 0. \tag{1.2}$$

We impose on the reference frame the four additional conditions

$$g_{00} = -1, \qquad g_{0\alpha} = 0, \tag{1.3}$$

so that

$$ds^2 = dt^2 - dl^2, \qquad dl^2 = g_{\alpha\beta}\, dx^\alpha\, dx^\beta.$$

In such a system, the equations of gravitation ($R_i^k = T_i^k$) assume the following form (see reference 1, Sec. 92):

$$R_0^0 = \frac{1}{2} \frac{\partial}{\partial t} \varkappa_\alpha^\alpha + \frac{1}{4} \varkappa_\alpha^\beta \varkappa_\beta^\alpha = \frac{\varepsilon}{3} (4 u_0 u^0 + 1), \tag{1.4}$$

$$R_\alpha^0 = \frac{1}{2} (\varkappa_{\beta;\alpha}^\beta - \varkappa_{\alpha;\beta}^\beta) = \frac{4\varepsilon}{3} u_\alpha u^0, \tag{1.5}$$

$$R_\alpha^\beta = P_\alpha^\beta + \frac{1}{2} \frac{\partial}{\partial t} \varkappa_\alpha^\beta + \frac{1}{4} \varkappa_\gamma^\gamma \varkappa_\alpha^\beta = \frac{\varepsilon}{3} (4 u_\alpha u^\beta + \delta_\alpha^\beta). \tag{1.6}$$

Here $\kappa_{\alpha\beta}$ denotes a three-dimensional tensor with components

$$\varkappa_{\alpha\beta} = \partial g_{\alpha\beta} / \partial t, \tag{1.7}$$

and all further operations of raising and lowering the indices and covariant differentiation are carried out in three-dimensional space with a metric $g_{\alpha\beta}$; $P_{\alpha\beta}$ is a three-dimensional tensor expressed in terms of $g_{\alpha\beta}$, as is R_{ik}, which is expressed through g_{ik}. It is obvious that

$$\varkappa_\alpha^\alpha = g^{\alpha\beta} \frac{\partial g_{\alpha\beta}}{\partial t} = \frac{\partial}{\partial t} \ln(-g), \tag{1.8}$$

where g is the determinant of the tensor g_{ik}

---

*We follow the notation used in the book by Landau and Lifshitz.[1] In particular, Latin indices run through the values 0, 1, 2, and 3, while Greek indices run through the three spatial values 1, 2, and 3. The square of the interval element is written $-ds^2 = g_{ik} dx^i dx^k$, so that the matrix of g_{ik} has the signature $-+++$.

In addition, we use throughout a system of units in which the velocity of light and Einstein's gravitational constant are equal to unity.

(which differs from the determinant $|g_{\alpha\beta}|$ by the factor $g_{00} = -1$).

In the general case, the "gravitational collapse" takes place on a certain hypersurface $t = \varphi(x^\alpha)$, which is a singular surface of the solution of the gravitational equations. Since we discuss in the present communication only certain particular classes of solutions, we shall not investigate here the problem of whether there exists in general such a transformation of coordinates and time, by which this hypersurface can be converted into a "hyperplane" $t = 0$ without violating at the same time the conditions (1.3). In any case, such a transformation does exist for the solutions considered below.

The condition $t = 0$ on the singular hypersurface (together with the condition $g_{00} = -1$) fixes completely the choice of the time t. The interval element then admits of additional arbitrary transformations of the spatial coordinates, which do not involve the time.

2. GENERALIZATION OF THE ISOTROPIC SOLUTION

The solution of the equations of gravitation, corresponding to a homogeneous and isotropic distribution of matter in space, are most conveniently formulated in the "attached" reference frame, (that is, moving together with the matter, (see, for example, reference 1, Sec. 105). This system displays in explicit form the isotropy and homogeneity of the space, by virtue of which the condition $g_{0\alpha} = 0$ is automatically satisfied, and the singularity takes place in all of space at one instant of time ($t = 0$). In this solution [with the equation of state (1.1)] the metric has the form $g_{\alpha\beta} \approx a_{\alpha\beta}t$ as $t \to 0$, where $a_{\alpha\beta}$ are functions of the coordinates corresponding to a constant space curvature. The quantities $g_{\alpha\beta}$ are expanded in integral powers of t as functions of the time.

We shall show that this solution is actually a particular case of an entire class of solutions, in which

$$g_{\alpha\beta} = ta_{\alpha\beta} + t^2 b_{\alpha\beta} + \ldots, \tag{2.1}$$

where $a_{\alpha\beta}$ are arbitrary functions of the coordinates. In this case, however, the reference system that satisfied conditions (1.3) is no longer strictly attached.

The tensor inverse to (2.1) is

$$g^{\alpha\beta} = t^{-1}a^{\alpha\beta} - b^{\alpha\beta}, \tag{2.2}$$

where the tensor $a^{\alpha\beta}$ is the inverse of $a_{\alpha\beta}$, and $b^{\alpha\beta} = a^{\alpha\bar{\gamma}}a^{\beta\delta}b_{\gamma\delta}$. For the tensor $\kappa_{\alpha\beta}$ we have

$$\varkappa_{\alpha\beta} = a_{\alpha\beta} + 2tb_{\alpha\beta}, \qquad \varkappa_\alpha^\beta = t^{-1}\delta_\alpha^\beta + b_\alpha^\beta,$$

where $b_\alpha^\beta = a^{\beta\gamma}b_{\alpha\gamma}$. We shall carry out all the operations of raising the Greek indices and of covariant differentiation everywhere in this section with a time-independent metric $a_{\alpha\beta}$. Calculating the left sides of (1.4) and (1.5), accurate to two and one principal terms in $1/t$ respectively, we obtain

$$-3/4t^2 + b/2t = \tfrac{1}{3}\varepsilon(-4u_0^2 + 1), \tag{2.3}$$

$$\tfrac{1}{2}(b_{;\alpha} - b_{\alpha;\beta}^\beta) = -\tfrac{4}{3}\varepsilon u_0 u_\alpha, \tag{2.4}$$

where $b \equiv b_\alpha^\alpha$. Comparing the right halves of these equations and taking account of the identity

$$-1 = u_i u^i \approx -u_0^2 + t^{-1}u_\alpha u_\beta a^{\alpha\beta},$$

we readily see that $\epsilon \sim t^{-2}$ and $u_\alpha \sim t^2$; by virtue of the above identity we have here $u_0 - 1 \sim t^3$. We now obtain from (2.3) the first two terms of the expansion of the energy density:

$$\varepsilon = 3/4t^2 - b/2t, \tag{2.5}$$

while (2.4) yields the first term of the expansion of the velocity

$$u_\alpha = \tfrac{1}{2}t^2(b_{;\alpha} - b_{\alpha;\beta}^\beta). \tag{2.6}$$

The three dimensional Christoffel symbols, together with the tensor $P_{\alpha\beta}$, are independent of the time in the first approximation in $1/t$. $P_{\alpha\beta}$ coincides here with the expression obtained when the metric used is simply $a_{\alpha\beta}$. Taking this into account, we now find that the terms of order t^{-2} automatically cancel out in (1.6), while the terms proportional to $1/t$ yield

$$P_\alpha^\beta + \tfrac{3}{4}b_\alpha^\beta + \tfrac{5}{12}\delta_\alpha^\beta b = 0$$

(where $P_\alpha^\beta = a^{\beta\gamma}P_{\alpha\gamma}$). Hence

$$b_\alpha^\beta = -\tfrac{4}{3}P_\alpha^\beta + \tfrac{5}{18}\delta_\alpha^\beta P. \tag{2.7}$$

We see that actually the function $a_{\alpha\beta}$ remains fully arbitrary. The coefficients $b_{\alpha\beta}$ of the next term of the expansion of $g_{\alpha\beta}$ are determined by (2.7) from the specified a, and these together with expansions (2.5) and (2.6) yield the energy densities and the velocities. We note that as $t \to 0$ the energy distribution approaches homogeneity. As regards the velocity distribution (2.6), it can be transformed by taking account of the relationship

$$b_{\alpha;\beta}^\beta = \tfrac{7}{9}b_{;\alpha},$$

which is the corollary of the identity

$$P_{\alpha;\beta}^\beta - \tfrac{1}{2}P\delta_\alpha^\beta = 0,$$

which is satisfied, in turn, by any simplified curvature tensor $P_{\alpha\beta}$. We then have

$$u_\alpha = \tfrac{1}{9}t^2 b_{;\alpha}, \tag{2.8}$$

that is, in this approximation the velocity is the gradient of a certain function and its curl vanishes (a nonvanishing curl appears, however, in the next terms of the expansion).

Conditions (1.3) admit also of the possibility of arbitrary transformations of the three spatial coordinates, without involving the time. These can be used, for example, to diagonalize the tensor $a_{\alpha\beta}$. Therefore, this solution actually contains a total of three "physically different" arbitrary functions of the coordinates, specified by the initial conditions (with respect to time) of the problem.

The Friedmann solution corresponds to the particular case when $P_{\alpha}^{\beta} = \text{const} \cdot \delta_{\alpha}^{\beta}$.

It can be shown that the solution obtained is the only one in which the collapse takes place in a "quasi-isotropic" manner, by which all the components $g_{\alpha\beta}$ vanish as the same power of t.

We note also that this solution exists only in the presence of matter, that is, only in a non-empty space.

3. CENTRALLY SYMMETRICAL COLLAPSE

Proceeding now to the problem of the collapse of a centrally-symmetrical distribution, we note first that its general solution should contain only two "physically different" arbitrary functions of the radial coordinate. This number follows from the fact that the arbitrary initial centrally-symmetrical distribution of matter is specified in terms of the initial distributions of its density and radial velocity. This problem has no "degrees of freedom" corresponding to a free gravitational field, for such a field (gravitational waves) cannot have central symmetry.

We write down the centrally-symmetrical element of an interval that satisfies conditions (1.3) in the form

$$-ds^2 = -dt^2 + e^{\lambda}dr^2 + e^{\mu}(d\theta^2 + \sin^2\theta d\varphi^2), \qquad (3.1)$$

where μ and λ are functions of the time and of the radial coordinate r, and the 4-velocity of matter has only one (radial) spatial component. We shall number the coordinates $x^{1,2,3} = r, \theta, \varphi$.

A clear idea of the interrelation between different particular solutions and the general solution of the essentially-symmetrical collapse problem can be gained by considering the formal problem, with equation of state p = 0 (which, naturally, is actually inapplicable close to the instant of collapse). In this case the equations of the centrally-symmetrical field admit an exact solution (first obtained by Tolman[2]) and the character of the collapse can be readily explained by investigating this solution.

When p = 0 the reference frame can be chosen such that, simultaneously with satisfying the conditions $g_{00} = -1, g_{01} = 0$ [that is, ds^2 in the form (3.1)] the velocity u_1 of the matter vanishes, i.e., the reference frame is attached (see reference 1, Sec. 97, problems 4 and 5). Here, however, the collapse is not simultaneous in all of space. In such a reference frame, an exact solution of the equations of gravitation is given by the following formulas.

We denote

$$e^{\mu(t,r)/2} = R(t, r). \qquad (3.2)$$

Then e^{λ} is determined by the formula

$$e^{\lambda} = R / (1 + f), \qquad (3.3)$$

where f(r) is an arbitrary function, satisfying only the condition 1 + f > 0. The function R(t, r) is given in implicit form by

$$t - \Phi(r) = \sqrt{fR^2 + FR}/f - Ff^{-3/2}\sinh^{-1}\sqrt{fR/F} \text{ for } f > 0,$$

$$t - \Phi(r) = \sqrt{fR^2 + FR}/f + F(-f)^{-3/2}\arcsin\sqrt{-fR/F} \text{ for } f < 0 \qquad (3.4)$$

(the case f = 0 is obtained by going to the limit in (3.4), but does not differ qualitatively from the general case). Finally, the energy density is

$$\varepsilon = F' / R'R^2 \qquad (3.5)$$

(the prime denotes differentiation with respect to r). Here F(r) and Φ(r) are two additional arbitrary functions of r. Inasmuch as (3.1) admits of still another arbitrary transformation r → r(r′), the solution written down actually contains, as it should, not three but only two "physically different" arbitrary functions.

The instant of collapse corresponds to the hypersurface t = Φ(r). Near this hypersurface we obtain from (3.3) — (3.5)

$$e^{\mu} \equiv R^2 = \left(\frac{3}{2}\right)^{4/3} F^{2/3}(t - \Phi)^{4/3}, \quad e^{\lambda} = \left(\frac{2}{3}\right)^{2/3} \frac{\Phi'^2 F^{2/3}}{f + 1}(t - \Phi)^{-2/3},$$

$$\varepsilon = -2F' / 3F\Phi'(t - \Phi). \qquad (3.6)$$

We see that the general solution leads to a very unique character of collapse: the radial lengths (in the reference frame considered) increase without limit as t → Φ, while the peripheral distances tend to zero;* the volumes also tend to zero, while the density of matter tends accordingly to infinity.

---

*The geometry on the "plane" passing through the center is in this case the same as would occur on a conical surface of revolution which is stretched along its generatrices and at the same time compressed in all its circumferences.

The particular case $\Phi = \text{const}$ (or, what is the same, $\Phi = 0$) leads to a collapse of an entirely different nature. In this case we obtain the following limiting formulas

$$e^{\mu} = \left(\frac{3}{2}\right)^{4/3} F^{2/3} t^{4/3}, \quad e^{\lambda} = \left(\frac{2}{3}\right)^{2/3} \frac{F'^2}{4F^{4/3}(f+1)} t^{4/3}, \qquad \varepsilon = \frac{4}{3t^2}. \tag{3.7}$$

Here all the distances tend to zero in a "quasi-isotropic" manner — proportional to the same power of t, while the energy density becomes homogeneous in the limit.*

Finally, when $F = 0$ we have $R = \sqrt{f}\,(t - \Phi)$, while e^{λ} tends to a constant limit and ϵ vanishes identically. This is a fictitious case: the transformation of r and t reduces the metric to a Galilean metric in empty space.†

Let us return to the problem of collapse with an equation of state $p = \epsilon/3$. The reference system with metric (3.1) is no longer attached, but we can assume the collapse to take place in it simultaneously in all of space (the possibility of such a choice of time is proved by the fact that we obtain as a result a general solution of the problem with the required number of arbitrary functions). Equations (1.4) — (1.6), expressed in terms of the functions λ and μ, have the form

$$R_0^0 = \tfrac{1}{4}\dot{\lambda}^2 + \tfrac{1}{2}\dot{\mu}^2 + \tfrac{1}{2}\ddot{\lambda} + \ddot{\mu} = -\tfrac{1}{3}\varepsilon\,(3 + 4u_1^2 e^{-\lambda}), \tag{3.8}$$

$$R_1^0 = \dot{\mu}' - \tfrac{1}{2}\dot{\lambda}\mu' + \tfrac{1}{2}\dot{\mu}\mu' = \tfrac{4}{3}\varepsilon u_1 (1 + u_1^2 e^{-\lambda})^{1/2}, \tag{3.9}$$

$$\begin{aligned} R_1^1 = {} & \left[e^{-\lambda}\left(\tfrac{1}{2}\mu'\lambda' - \mu'' - \tfrac{1}{2}\mu'^2\right)\right] \\ & + \tfrac{1}{2}\left(\ddot{\lambda} + \dot{\lambda}\dot{\mu} + \tfrac{1}{2}\dot{\lambda}^2\right) = \tfrac{1}{3}\varepsilon\,(1 + 4u_1^2 e^{-\lambda}), \end{aligned} \tag{3.10}$$

$$\begin{aligned} R_2^2 = {} & \left[e^{-\mu} + \tfrac{1}{2}e^{-\lambda}\left(\tfrac{1}{2}\mu'\lambda' - \mu'' - \mu'^2\right)\right] \\ & + \tfrac{1}{2}\left(\ddot{\mu} + \tfrac{1}{2}\dot{\mu}\dot{\lambda} + \dot{\mu}^2\right) = \tfrac{1}{3}\varepsilon \end{aligned} \tag{3.11}$$

(the prime denotes differentiation with respect to r and the dot differentiation with respect to t; the expressions in the square brackets in (3.10) and (3.11) represent P_1^1 and P_2^2 respectively). The solutions of these equations near the singular point have, as we shall now show, the same character as when the equation of state is $p = 0$.

We seek e^{λ} and e^{μ} in the form of series in powers of $t^{2/3}$, beginning with $t^{-2/3}$ and $t^{4/3}$ respectively; λ and μ now assume the form

$$\lambda = -\tfrac{2}{3}\ln t + \lambda^{(0)} + \lambda^{(1)} t^{2/3} + \ldots,$$

$$\mu = \tfrac{4}{3}\ln t + \mu^{(0)} + \mu^{(1)} t^{2/3} + \ldots, \tag{3.12}$$

where $\lambda^{(0)}$, $\mu^{(0)}$, $\lambda^{(1)}$, and $\mu^{(1)}$ are functions of r. The energy density and the radial velocity are also expanded in powers of $t^{2/3}$; the first terms of the expansion, as verified by subsequent calculation, are

$$\varepsilon = t^{-4/3}\varepsilon^{(0)}(r), \qquad u_1 = u^{(0)}(r)\, t^{1/3}. \tag{3.13}$$

Substitution of these expressions into (3.8) and (3.11) causes the terms of order t^{-2} to disappear, while the terms of order $t^{-4/3}$ yield

$$\tfrac{1}{3}(\lambda^{(1)} - 2\mu^{(1)}) = \varepsilon^{(0)}, \quad 2\mu^{(1)} + \tfrac{2}{3}\lambda^{(1)} + 3\exp(-\mu^{(0)}) = \varepsilon^{(0)},$$

hence

$$\mu^{(1)} = -\tfrac{3}{10}[\varepsilon^{(0)} + 3\exp(-\mu^{(0)})],$$

$$\lambda^{(1)} = \tfrac{3}{5}[4\varepsilon^{(0)} - 3\exp(-\mu^{(0)})]. \tag{3.14}$$

In (3.9), the terms proportional to $1/t$ yield

$$\varepsilon^{(0)} u^{(0)} = \tfrac{3}{4}\mu^{(0)\prime}, \tag{3.15}$$

and Eq. (3.10) produces nothing new.

Thus, these three arbitrary functions [for example $\mu^{(0)}(r)$, $\lambda^{(0)}(r)$, $\epsilon^{(0)}(r)$], of which two are physically different, remain in this solution, i.e., this is the general solution of our problem.*

This general solution does not contain the quasi-isotropic collapse, which corresponds to the particular solution of the system (3.8) — (3.11) with two arbitrary functions (one of which is physically independent).† In this solution e^{λ} and e^{μ} vanish in similar fashion (proportional to t); the corresponding expansions are of the form

$$\mu = \ln t + \mu^{(0)} + \mu^{(1)} t + \ldots, \quad \lambda = \ln t + \lambda^{(0)} + \lambda^{(1)} t + \ldots,$$

$$\varepsilon = 3/4t^2 + \varepsilon^{(1)}/t + \ldots, \qquad u_1 = t^2 u^{(0)} + \ldots. \tag{3.16}$$

The functions $\lambda^{(0)}(r)$ and $\mu^{(0)}(r)$ can be specified arbitrarily, after which the following expansion coefficients are given by

$$\mu^{(1)} = \tfrac{5}{18}P_1^1 - \tfrac{7}{9}P_2^2, \qquad \lambda^{(1)} = -\tfrac{19}{18}P_1^1 + \tfrac{5}{9}P_2^2,$$

$$\varepsilon^{(1)} = -\tfrac{1}{2}(\lambda^{(1)} + 2\mu^{(1)}), \quad u^{(0)} = \tfrac{1}{9}(\lambda^{(1)\prime} + 2\mu^{(1)\prime}), \tag{3.17}$$

where P_1^1 and P_2^2 are calculated from $\exp\lambda^{(0)}$ and

---

*The gravitational collapse of a centrally-symmetrical distribution of matter with $p = 0$ was considered by Oppenheimer and Snyder.[3] However, their choice of particular solution, dictated by the choice of a homogeneous initial distribution of density of matter, corresponds to the case (3.7) and, as we see, does not reflect at all the properties of the general case.

†For this purpose it is necessary to introduce instead of t a new variable $R = \sqrt{f}\,(t - \Phi)$, after which the interval is reduced by suitable transformation $r = r(R, \tau)$ to the form $ds^2 = d\tau^2 - dR^2 - R^2(\sin^2\theta\, d\varphi^2 + d\theta^2)$.

*The boundary condition at the center requires that $\exp\mu^{(0)} \to 0$ as $r \to 0$ (the length $2\pi t^{4/3}\exp\mu^0$ of the circle with center at the origin should tend to zero as $r \to 0$).

†The fictitious solution mentioned above does not arise at all when the time is fixed by choosing the condition $t = 0$ at the instant of collapse in all of space.

$\exp\mu^{(0)}$. This solution enters as a particular case in the general quasi-isotropic solution (2.1) obtained in Sec. 2. Equations (3.17) are, naturally, exactly equivalent to (2.5), (2.7), and (2.8).

4. GENERALIZATION OF THE CENTRALLY-SYMMETRICAL SOLUTION

The solution obtained for the centrally-symmetrical problem is actually a particular case of a more general class of solutions. We shall give here this solution in its main final form, without dwelling on its construction.

We seek the solution in the form of expansions in powers of $t^{2/3}$, the first terms of which are

$$g_{11} = t^{-2/3}(a^{(0)} + a^{(1)}t^{2/3}),$$

$$g_{ab} = t^{4/3}(b^{(0)}_{ab} + b^{(1)}_{ab}t^{2/3}), \qquad g_{1a} = t^{4/3}b^{(0)}_{1a} \tag{4.1}$$

(the indices a, b, and c run here and below through the values 2 and 3). In this notation, the choice of the direction x^1 is the only one by which the lowest power of $t\,(t^{-2/3})$ enters only in g_{11}; the coordinate x^1 admits only of a transformation of the form $x'^1 = x'^1(x^1)$. The coordinates x^2 and x^3, on the other hand, admit of additional arbitrary transformations of the general form $x'^a = x'^a(x^1, x^2, x^3)$. We shall use these transformations to cause the two quantities $b^{(0)}_{1a}$ to vanish.

The corresponding distributions of the density and 4-velocity of the matter will have, in the same approximation, the following form:

$$\varepsilon = t^{-4/3}\varepsilon^{(0)}, \qquad u_1 = u^{(0)}_1 t^{1/3}, \qquad u_a = u^{(1)}_a t. \tag{4.2}$$

To check these expressions and to determine the relations between the functions introduced therein, we substitute (4.1) and (4.2) into (1.4) — (1.6), retaining those senior terms (that is, those of highest order in $1/t$), which are fully expressed in terms of the quantities in (4.1) and (4.2).

Equation (1.5) with $\alpha = 2$ and 3 yields in the first non-vanishing order

$$R^0_a = -\frac{1}{2t}\frac{\partial}{\partial x^a}\ln a^{(0)} = 0,$$

that is, $a^{(0)}$ can be a function of the coordinate x^1 only. The freedom still remaining in the choice of the latter can be used to set $a^{(0)}$ equal to unity. Then the metric assumes the form (in the accuracy employed here)

$$g_{11} = t^{-2/3}(1 + a^{(1)}t^{2/3}), \qquad g_{ab} = t^{4/3}(b^{(0)}_{ab} + t^{2/3}b^{(1)}_{ab}),$$

$$g_{1a} = 0. \tag{4.3}$$

The choice of all three coordinates is then fixed accurate to inessential transformations of the type $x'^a = x'^a(x^2, x^3)$, which involve only the coordinates x^2 and x^3.

We now obtain, after a calculation

$$R^0_0 = -\frac{1}{3t^{4/3}}(a^{(1)} - b^{(1)c}_{\;\;c}) = -\frac{\varepsilon^{(0)}}{t^{4/3}}, \tag{4.4}$$

$$R^0_1 = \frac{1}{2t}\frac{\partial}{\partial x^1}\ln b^{(0)} = \frac{4\varepsilon^{(0)}}{3t}u^{(0)}_1, \tag{4.5}$$

$$R^0_a = -\frac{1}{3t^{1/3}}\left[b^{(1)c}{}_{a;c} - b^{(1)c}{}_{c;a} + \frac{1}{2}a^{(1)}_{;a}\right] = \frac{4\varepsilon^{(0)}}{3t^{1/3}}u^{(1)}_a, \tag{4.6}$$

$$R^b_a = \frac{1}{t^{4/3}}\left[\frac{1}{2}K\delta^b_a + \frac{2}{9}b^{(1)b}_{\;\;a} + \frac{2}{9}\delta^b_a(a^{(1)} + b^{(1)c}_{\;\;c})\right] = \frac{\varepsilon^{(0)}}{3t^{4/3}}\delta^b_a \tag{4.7}$$

(the equations for R^1_1 and R^a_1 yield nothing new). All the operations of raising the indices a, b, c and covariant differentiation are carried out here in two-dimensional space (with metric $b^{(0)}_{ab}$) on the two-dimensional tensor $b^{(1)}_{ab}$ and scalar $a^{(1)}$; in this notation, the contravariant metric tensor, which is the inverse of the tensor (4.3), is

$$g^{11} = t^{2/3}(1 - a^{(1)}t^{2/3}), \quad g^{ab} = t^{-4/3}(b^{(0)ab} - t^{2/3}b^{(1)ab}), \quad g^{1a} = 0.$$

Next, K denotes a two-dimensional scalar curvature made up of b_{ab} (as is known, the two-dimensional analog K_{ab} of the tensor R_{ik} reduces to a scalar: $K^b_a = \frac{1}{2}K\delta^b_a$); $b^{(0)}$ is the determinant of the tensor $b^{(0)}_{ab}$ (the principal term in the determinant of the metric tensor g_{ik} is $-g = t^2b^{(0)}$).

From (4.4) and (4.7) we obtain

$$a^{(1)} = \frac{12}{5}\varepsilon^{(0)} - \frac{9}{10}K, \qquad b^{(1)b}_{\;\;a} = -\frac{3}{10}\delta^b_a\left(\varepsilon^{(0)} + \frac{3}{2}K\right). \tag{4.8}$$

Taking these formulas into account we obtain from (4.5) and (4.6)

$$u^{(0)}_1 = \frac{3}{8\varepsilon^{(0)}}\frac{\partial}{\partial x^1}\ln b^{(0)}, \qquad u^{(1)}_a = -\frac{3}{8}\frac{\partial}{\partial x^a}\ln\varepsilon^{(0)}. \tag{4.9}$$

Thus, the solution obtained contains four arbitrary functions of the coordinates, for example, the three quantities $b^{(0)}_{ab}$ and $\epsilon^{(0)}$. With the aid of these quantities, (4.8) and (4.9) define the first correction terms in the metric and in the distribution of the velocity of matter.

In the particular centrally-symmetrical case, the coordinates x^2 and x^3 are angular variables, while the surfaces $x^1 = \text{const}$ have a curvature K different from zero.* In the generalized solution this is not essential, and all the coordinates can have an arbitrary geometrical character (thus, the solution can be "cylindrical" or "plane").

In the absence of matter, there is naturally no centrally-symmetrical solution, since the free gravitational field, as already noted, cannot have such a symmetry. The generalized solution, on the other hand, yields a definite class of solutions for empty space, too. In this case the right halves of (4.4) — (4.7) vanish. From (4.4) and (4.7) we obtain

---

*Equations (3.14) and (3.15) correspond exactly to (4.8) and (4.9), and $a^{(1)} = \lambda^{(1)}$, $b^{(1)2}_{\;\;2} = b^{(1)3}_{\;\;3} = \mu^{(1)}$, $\varepsilon^{(0)}$ and $K = 2\exp(-\mu^{(0)})$ are functions of $x^1 = r$ only.

$$a^{(1)} = -\tfrac{9}{10}K, \qquad b^{(1)b}_{\ \ a} = -\tfrac{9}{20}K\delta^b_a, \tag{4.10}$$

after which Eq. (4.6) is identically satisfied, and we obtain, from (4.5), $b^{(0)} = f(x^2, x^3)$. This arbitrary function of the coordinates x^2 and x^3 can be set equal to unity, say, by the still permissible transformations of these coordinates [in the transformation $x^a = x^a(x'^2, x'^3)$ the determinant $b^{(0)}$ is multiplied by the square of the Jacobian $\partial(x^2, x^3)/\partial(x'^2, x'^3)$]. As a result, only two arbitrary functions remain, namely the three quantities $b^{(0)}_{ab}$, connected by the condition $b^{(0)} = 1$. We thus arrive at a class of solutions, containing two arbitrary functions of the coordinates, for empty space.

In conclusion we express our sincere gratitude to Academician L. D. Landau for continuous interest in our work and for stimulating discussions. We are also grateful to L. P. Pitaevskiĭ for discussing a number of problems.

---

[1] L. D. Landau and E. M. Lifshitz, Теория поля (Field Theory), 3d edition, Fizmatgiz, 1960.

[2] R. Tolman, Proc. Nat. Acad. Sci. **20,** 3 (1939).

[3] R. Oppenheimer and H. Snyder, Phys. Rev. **56,** 455 (1939).

Translated by J. G. Adashko
29

SOVIET PHYSICS JETP VOLUME 12, NUMBER 1 JANUARY, 1960

EXCITATION OF STANDING SPIN WAVES IN A FILM

M. I. KAGANOV

Physico-Technical Institute, Academy of Sciences, Ukrainian S.S.R.

Submitted to JETP editor February 15, 1960

J. Exptl. Theoret. Phys. (U.S.S.R.) **39**, 158-162 (July, 1960)

The surface resistance (impedance) of a metallic ferromagnetic film is calculated, with allowance for the spatial dispersion of the magnetic susceptibility. The influence of the skin effect and of the boundary conditions for the magnetic moment on the excitation curve of standing spin waves is examined.

SUCCESS has been achieved recently in observing a number of resonance peaks on the magnetic energy absorption curve of thin ferromagnetic films.[1] These peaks are correctly treated as evidence of the excitation of standing spin waves. Since the experiments were performed in a uniform magnetic field, Kittel,[2] to explain the observed phenomenon, proposed that because of large surface anisotropy energy, the magnetic moment at the surface coincides with its equilibrium value. In other words, according to Kittel the alternating part of the magnetic moment at the surface vanishes. Starting with this assumption, Kittel determined the frequencies of oscillation of the magnetic moment; these made it possible to determine from the excitation curve (the dependence of the energy absorption on the applied field) the magnitude of the exchange interaction, which enters into the spectrum of characteristic frequencies of the film.

In the present communication, the surface resistance of a ferromagnetic film is calculated. In this calculation the finite conductivity σ of the film is taken into account, and also the effect of the boundary conditions for the magnetic moment upon the character of the surface resistance (and by the same token on the excitation curve) is discussed.

The constant magnetic field H_0 is assumed to be directed along an axis of easiest magnetization, which is perpendicular to the film. (We choose this axis as z axis, with origin in the middle of the film; the thickness of the film is 2d.)

The linearized equation for determination of the alternating part of the magnetic moment $\mathbf{m}$ $(m_x, m_y, 0)$ has, under these conditions, the form

$$\left\{\omega - i\lambda\frac{H_e}{M_0} + i\lambda\alpha\frac{\partial^2}{\partial z^2} - gH_e + gM_0\alpha\frac{\partial^2}{\partial z^2}\right\} m^- = -gM_0\left(1+\frac{i\lambda}{gM_0}\right)h^-. \qquad (1)$$

Here $h^- = h_x - ih_y$, where $\mathbf{h}$ is the alternating magnetic field; $H_e = H_0 + \beta M_0$, where β is the anisotropy constant; M_0 is the equilibrium magnetic moment of unit volume; ω is the frequency of the applied field; λ is the relaxation constant in the Landau-Lifshitz[3] equation of motion of the magnetic moment $(\lambda < 0)$; α is the exchange interaction constant (in order of magnitude, α is equal to $(\Theta_c/\mu M_0)a^2$, where Θ_c is the Curie temperature, μ is twice the Bohr magneton, and a is the lattice constant); g is the gyromagnetic ratio $(g > 0)$. We mention furthermore that the field inside the film is connected with the magnetic field outside it by the relation $H_0 + 4\pi M_0 = H_{ext}$. We limit ourselves to writing down the equation for m^- and h^- alone, since the circular electromagnetic wave with right-hand polarization (h^+) does not resonate with magnetic moment rotation for any value of the magnetic field H_0. The questions that interest us hereafter will be ones connected with resonance absorption of energy.

Since we wish to take account of the skin effect, it is necessary to supplement Eq. (1) with Maxwell's equations, which after elimination of the electric field can be written*

$$\partial^2 h^-/\partial z^2 + 2ih^-\delta^{-2} + 8\pi\, im^-\delta^{-2} = 0, \qquad \delta = c/\sqrt{2\pi\sigma\omega}. \qquad (2)$$

To Eqs. (1) and (2) must be added the boundary conditions. Besides the usual electrodynamic conditions (continuity of the tangential components of the electric and magnetic field vectors), it is necessary to formulate boundary conditions for the magnetic moment. Following Kittel,[2] we shall assume that the alternating magnetic moment vanishes at the film surface, i.e.,

---

*Equation (2) was obtained on the assumption that there is a normal skin effect. This seems to be a completely justifiable assumption, since the conductivity of a film as a rule is appreciably smaller than the conductivity of the metal in bulk. Formally, the use of Eq. (2) is limited by the condition $l \ll d$, where l is the mean free path of the electrons. If this condition is not satisfied, but the opposite limiting case occurs, then evidently it is necessary to replace σ in the final formulas by $\sigma_{eff} \approx \sigma d/l$.

$$m^{-}|_{z=\pm d}=0. \tag{3}$$

We shall be interested in the excitation of magnetic moment oscillations by a symmetric field. Therefore a solution of (1) and (2) may be sought in the form of a Fourier cosine series

$$m^{-}(z)=\sum_{n=0}^{\infty} m_n \cos k_n z,$$

$$h^{-}(z)=h^{-}(d)+\sum_{n=0}^{\infty} h_n \cos k_n z, \quad k_n=(n+{}^1/_2)\pi/d. \tag{4}$$

The values of k_n are so chosen as to satisfy the boundary conditions (3).

On substituting the series (4) in (1) and (2), we easily find

$$h_n=\frac{2h^{-}(d)(-1)^n}{\pi(n+{}^1/_2)}$$

$$\times\frac{\omega-\omega_n^{(a)}(1+i\lambda/gM_0)}{[\omega-\omega_n(1+i\lambda/gM_0)](\delta^2k_n^2/2i-1)+4\pi gM_0(1+i\lambda/gM_0)}.$$

Here $\omega_n = gH_e + gM_0\alpha k_n^2 = gH_e + gM_0\alpha v_n^2/d^2$, $\omega_n^{(a)} = gB_e + gM_0\alpha v_n^2/d^2$, $v_n = k_n d$, $B_e = H_e + 4\pi M_0 = H_{ext} + \beta M_0$.

From the last expression and from (4) it is easy to determine the value of $\partial h^{-}/\partial z$ at $z = d$:

$$\left.\frac{\partial h^{-}}{\partial z}\right|_{z=d}=-\frac{2h^{-}(d)}{d}$$

$$\times\sum_{n=0}^{\infty}\frac{\omega-\omega_n^{(a)}(1+i\lambda/gM_0)}{[\omega-\omega_n(1+i\lambda/gM_0)](\delta^2k_n^2/2i-1)+4\pi gM_0(1+i\lambda/gM_0)}. \tag{5}$$

From the equation $\operatorname{curl}\mathbf{h} = (4\pi\sigma/c)\mathbf{E}$ we find that

$$E^{-}=-(ic/4\pi\sigma)\partial h^{-}/\partial z.$$

Therefore the surface impedance for waves with left-handed circular polarization is equal to

$$\zeta^{-}=-\frac{ic}{4\pi\sigma\, h^{-}(d)}\left.\frac{\partial h^{-}}{\partial z}\right|_{z=d}.$$

From this and from the expression (5) we have

$$\zeta^{-}=-\frac{2\omega d}{c\pi^2}\sum_{n=0}^{\infty}\frac{1}{(n+{}^1/_2)^2}$$

$$\times\frac{\omega-\omega_n^{(a)}(1+i\lambda/gM_0)}{[\omega-\omega_n(1+i\lambda/gM_0)](1-2i/\delta^2k_n^2)+(8\pi igM_0/\delta^2k_n^2)(1+i\lambda/gM_0)}. \tag{6}$$

Knowing the surface resistance of the film, we can determine the amount of energy absorbed by a film of area 1 cm^2 in one second. In fact, from the expression for the Poynting vector $\mathbf{W} = (c/4\pi)[\mathbf{E}\times\mathbf{h}]$ we easily find*

$$W_z=\frac{c}{32\pi}\{\operatorname{Im}\zeta^{-}|h^{-}(d)|^2-\operatorname{Im}\zeta^{+}|h^{+}(d)|^2\}.$$

From this it is clear that the power loss per unit volume of the film is

$$Q=\frac{c}{32\pi d}\{\operatorname{Im}\zeta^{-}|h^{-}(d)|^2-\operatorname{Im}\zeta^{+}|h^{+}(d)|^2\}. \tag{7}$$

By comparison of formula (7) with the usual expression for the volumetric energy loss, it is possible to determine the imaginary part of the effective magnetic susceptibility ($\mu''_{\pm}$).

The expression (6) for the surface impedance becomes considerably simpler if the conductivity of the film approaches zero (i.e., if $\delta \to \infty$):

$$\zeta^{-}=-\frac{2\omega d}{c\pi^2}\sum_{n=0}^{\infty}\frac{1}{(n+{}^1/_2)^2}\,\frac{\omega-\omega_n^{(a)}(1+i\lambda/gM_0)}{\omega-\omega_n(1+i\lambda/gM_0)}. \tag{8}$$

Neglect of spatial dispersion, i.e., of the dependence of ω_n on the "wave vector" k_n, is possible for sufficiently thick specimens, when the line width $\Delta\omega \approx |\lambda| H_e/M_0$ is considerably larger than the distance between resonance frequencies (we are of course concerned only with the first few frequencies, since on account of the factor $(n+{}^1\!/_2)^{-2}$ the intensity of the remote absorption lines, with $n \gg 1$, is extremely small):

$$2\pi^2\frac{\Theta_c}{\hbar}\frac{a}{d}(n+1)\ll|\lambda|\frac{H_e}{M_0}.$$

Thus on setting $n = 9$, we get the condition for neglect of spatial dispersion in the form

$$d\gg 20\pi^2\frac{\Theta_c/\hbar}{|\lambda|}\frac{M_0}{H_e}a. \tag{9}$$

In other words, for films whose thickness satisfies the condition (9) a single resonance maximum should be observed, at frequency

$$\omega_r=gH_e=g(H_{\mathbf{ext}}-4\pi M_0+\beta M_0).$$

Under these conditions

$$\zeta^{-}=-\frac{\omega d}{c}\,\frac{\omega-\omega_a(1+i\lambda/gM_0)}{\omega-\omega_r(1+i\lambda/gM_0)}, \quad \omega_r=gH_e, \quad \omega_a=gB_e.$$

Experiments by observation of resonance on standing spin waves are usually conducted on very thin films ($d \sim 10^{-6}$ cm). Therefore δ is always $\gg d$. By taking account of this, we can write the expression (6) in the following form:

$$\zeta^{-}\approx-\frac{2\omega d}{\pi^2 c}\sum_{n=0}^{\infty}\frac{1}{(n+{}^1/_2)^2}$$

$$\times\frac{\omega-\omega_n^{(a)}(1+i\lambda/gM_0)}{\omega-\omega_n(1+i\lambda/gM_0)+(2i/\delta^2k_n^2)(\omega_n^{(a)}-\omega)}, \tag{10}$$

---

*We note that in the absence of gyrotropy, $\zeta^{-} = i\zeta$ and $\zeta^{+} = -i\zeta$.

here we have omitted from the denominator terms containing the products $(\lambda/gM_0)(\delta k_n)^{-2}$. It is clear from the expression (10) that the skin effect increases somewhat the line width but does not shift the resonance frequency appreciably. In this connection it should be mentioned that the first few frequencies (small n) are widened more than the later ones:

$$\Delta\omega_{\text{skin}} \approx (8/\pi)(d/\delta)^2 gM_0/(n+{}^1\!/\!_2)^2. \tag{11}$$

The expression (6) and what follows are derived on the assumption that the alternating part of the magnetic moment vanishes at the film surface. If the normal derivative of the alternating part of the magnetic moment is assumed to vanish at this surface,[4] then for $\delta \to \infty$, i.e., for $\sigma \to 0$, a uniform magnetic field will excite only uniform precession. With finite conductivity, $\sigma \neq 0$, the magnetic field inside the film is nonuniform and will excite nonuniform oscillations of the magnetic moment (spin waves). By a procedure similar to the previous one, we can obtain

$$(\zeta^-)^{-1} = -\frac{\omega d}{c}\left\{\frac{\omega-\omega_0\,(1+i\lambda/gM_0)}{\omega-\omega_0^{(a)}\,(1+i\lambda/gM_0)} - \frac{2i}{\pi^2}\left(\frac{d}{\delta}\right)^2\sum_{n=1}^{\infty}\frac{1}{n^2}\right.$$
$$\left.\times\frac{\omega-\omega_n\,(1+i\lambda/gM_0)}{(2i/\delta^2k_n^2)\,[\omega-\omega_n^{(a)}\,(1+i\lambda/gM_0)]-[\omega-\omega_n\,(1+i\lambda/gM_0)]}\right\}. \tag{12}$$

Here

$$\omega_n = gH_e + gM_0\alpha k_n^2, \qquad \omega_n^{(a)} = \omega_n + 4\pi M_0, \qquad k_n = n\pi/d.$$

For $d \ll \delta$, we have

$$\zeta^- \approx -\frac{\omega d}{c}\,\frac{\omega-\omega_0^{(a)}\,(1+i\lambda/gM_0)}{\omega-\omega_0\,(1+i\lambda/gM_0)+i\,(d^2/3\delta^2)\,4\pi M_0}, \tag{13}$$

that is, the electrical conductivity leads to an additional broadening of the fundamental (uniform) oscillation

$$\Delta\omega_{\text{skin}} \approx (d^2/3\delta^2)\,4\pi M_0. \tag{14}$$

A nonuniform magnetic field can excite standing spin waves if there are more complicated boundary conditions than (3). We suppose that at the surface a linear combination of the alternating part of the moment and of its normal derivative vanishes:

$$b\,\partial\mathbf{m}/\partial z_n + \mathbf{m} = 0 \qquad (z = \pm d), \tag{15}$$

$\partial/\partial z_n$ denotes differentiation along the outward normal, and b is a constant with the dimensions of length, describing the ratio between exchange forces and anisotropy forces.

On neglecting the conductivity of the film (i.e., on supposing that $\delta \gg d$), we easily obtain an expression for the mean moment excited in the film:

$$\overline{m^-} = -2gM_0\,(1+i\lambda/gM_0)\,h^-\sum_{n=1}^{\infty}\frac{\sin^2 v_n}{v_n^2\,(1+\sin 2v_n/2v_n)}$$
$$\times\frac{1}{\omega-\omega_n\,(1+i\lambda/gM_0)}, \tag{16}$$

where the v_n's are the roots of the dispersion equation

$$\cot v = qv, \qquad q = b/d, \tag{17}$$

whose solution is easily obtained graphically. If $q = 0$, $v_n = (n - {}^1\!/\!_2)\pi$, and we have the case treated earlier [cf. formula (8)]. If $q = \infty$, only the uniform oscillation is excited ($v_1 = 0$):

$$\overline{m^-} = -\frac{gM_0\,(1+i\lambda/gM_0)}{\omega-\omega_0\,(1+i\lambda/gM_0)}\,h^-.$$

When q differs from ∞ (but is not equal to zero), all the oscillations are excited, but their amplitudes decrease with order faster than in the case $q = 0$. We give an approximate expression for $q \gg 1$:

$$\overline{m^-} \approx -gM_0\,(1+i\lambda/gM_0)h^-\left\{\frac{1}{\omega-\omega_0\,(1+i\lambda/gM_0)}\right.$$
$$\left.+\frac{2}{q^2\pi^4}\sum_{n=1}^{\infty}\frac{1}{n^4}\,\frac{1}{\omega-\omega_n\,(1+i\lambda/gM_0)}\right\}. \tag{18}$$

In this case, obviously, the amplitude of the zero-order oscillation is many times larger than of the rest. Furthermore, the amplitude of the subsequent oscillations decreases with order as n^{-4}, whereas for $q = 0$ the amplitude decreases as $(n - {}^1\!/\!_2)^{-2}$. Comparison of the formulas given with the experimental resonance curves[1] seemingly indicates that the parameter q is small ($q \ll 1$).

In closing, I wish to thank V. Bar'yakhtar for very helpful discussions.

Translated by W. F. Brown, Jr.
30

---

[1] M. H. Seavey and A. Tannenwald, Phys. Rev. Lett. **1**, 168 (1958).

[2] C. Kittel, Phys. Rev. **110**, 1295 (1958).

[3] L. Landau and E. Lifshitz, Physik. Z. Sowjetunion **8**, 153 (1935).

[4] W. S. Ament and G. T. Rado, Phys. Rev. **97**, 1558 (1955).

SOVIET PHYSICS JETP VOLUME 12, NUMBER 1 JANUARY, 1961

THE VAVILOV-CERENKOV EFFECT IN UNIAXIAL CRYSTALS

Č. MUZICAŘ*

Joint Institute for Nuclear Research

Submitted to JETP editor February 23, 1960

J. Exptl. Theoret. Phys. (U.S.S.R.) **39**, 163-170 (July, 1960)

The Vavilov-Cerenkov effect is considered for the case of an electric charge moving uniformly in an arbitrary direction relative to the optic axis of a uniaxial crystal. The shapes of the cones of normals for the ordinary and extraordinary waves are studied, and simple expressions are derived for the energy of the emitted waves.

INTRODUCTION

A general theory of the Cerenkov radiation in optically anisotropic media has been developed by Ginzburg.[1] Starting from the Maxwell equations for nonmagnetic transparent crystals, he obtained expressions for the angular distribution of the emitted energy. More detailed studies of the properties of the radiation have been made only for charged particles moving parallel or perpendicular to the optic axis in uniaxial crystals.† Quite recently Pafomov[4] has treated the more realistic case of a bounded uniaxial crystal, for which the transition radiation is superposed on the Cerenkov radiation.

Using the interference properties of the Cerenkov radiation, Frank[5,6] has investigated the conditions necessary for the occurrence of the radiation. In his Nobel lecture[5] it was shown for the first time that the direction of the light ray and the ray velocity play an important part in this connection.

In the present paper it is assumed that the crystal is transparent and has no gyrotropic properties. Its magnetic properties are given by a scalar magnetic permeability μ, and its electrical properties by the dielectric constant ϵ_{ik}, which is a symmetric tensor. In the coordinate system of the principal axes the components are positive, $\epsilon_{ii} \geq 0$.

Let a point charge move in the direction of the unit vector $\mathbf{r}$ with a speed $w = c\beta$. For the energy that it loses in the time $1/w$ we have the following formula:

$$S = \int d\omega \sum_{\lambda=1,2} S_{(\lambda)}(\omega), \tag{1}$$

where the energy per unit frequency range emitted in waves of polarization λ is

$$S_{(\lambda)}(\omega) = \frac{e^2c^2\omega}{2\pi\mu} \int d\mathbf{n} \frac{(\mathbf{e}^{(\lambda)}\mathbf{r})^2}{v^4_{(\lambda)}} \delta\left(\mathbf{rn} - \frac{v_{(\lambda)}}{c\beta}\right). \tag{2}$$

Here $d\mathbf{n}$ is an element of solid angle, $\mathbf{n}$ is the unit vector in the direction of propagation of the phase of the wave, $v_{(\lambda)} > 0$ is the speed of this propagation, and the $\mathbf{e}^{(\lambda)}$ are vectors in the direction of the electric field.

Let us introduce unit vectors $\mathbf{d}^{(\lambda)}$ directed along the electric displacement and having the following properties:

$$\mathbf{d}^{(\lambda)}\mathbf{d}^{(\nu)} = \delta_{\lambda\nu}, \quad \mathbf{nd}^{(\lambda)} = 0, \quad d_i^{(\lambda)} = \varepsilon_{ik}e_k^{(\lambda)}. \tag{3}$$

These equations, together with the condition

$$\mathbf{e}^{(1)}\mathbf{d}^{(2)} = 0 \tag{4}$$

determine the polarization vectors. The speeds of the corresponding waves are obtained from the formula

$$v^2_{(\lambda)} = c^2\mu^{-1}\mathbf{e}^{(\lambda)}\mathbf{d}^{(\lambda)}. \tag{5}$$

Since we shall be considering uniaxial crystals, we let the optic axis be along the axis x_1. For the components of dielectric-constant tensor, in diagonal form, we use the notations $\epsilon_{11} = \tau$, $\epsilon_{22} = \epsilon_{33} = \epsilon$. Let the charge move in the plane (x_1, x_2), which we shall call the principal plane. Then

$$\mathbf{r} \equiv (r_1, r_2, 0), \qquad r_1^2 + r_2^2 = 1, \qquad r_1 \geqslant 0, \qquad r_2 \geqslant 0. \tag{6}$$

We shall now investigate separately the properties of the ordinary and extraordinary waves. Instead of the indices $\lambda = 1, 2$ we introduce the notation $\lambda = o, e$.

THE ORDINARY WAVES

From Eqs. (3) — (5) we get for the polarization vector and speed of propagation of the ordinary waves

---

*Member of the Physical-Mathematical Faculty, Charles University, Prague, Czechoslovakia.

†See the review article by Bolotovskiĭ[2] and the book by Jelley.[3]

$$\mathbf{e}^{(o)} \equiv (0, n_3, -n_2)/\varepsilon\sqrt{1-n_1^2}, \qquad v_{(o)} = c/\sqrt{\varepsilon\mu}. \tag{7}$$

By using these formulas we can rewrite (2) as

$$S_{(o)}(\omega) = \frac{e^2\omega\mu}{2\pi c^2}\int d\mathbf{n}\,\frac{r_2^2 n_3^2}{1-n_1^2}\,\delta\left(\mathbf{nr} - \frac{1}{\sqrt{\varepsilon\mu}\,\beta}\right). \tag{8}$$

Here, just as in an isotropic medium, the energy will be emitted in directions that lie on a conical surface of circular cross section, with its axis parallel to the motion of the charge. The angle of emission $\Theta_{(o)}$ is given by the formula

$$\cos\Theta_{(o)} = \beta_o/\beta, \tag{9}$$

in which the quantity

$$\beta_o = (\varepsilon\mu)^{-1/2} \tag{10}$$

defines the critical speed of the charge; if $\beta < \beta_o$, emission of ordinary waves becomes impossible.*

To calculate the integral in Eq. (8), it is convenient to introduce spherical coordinates, with the polar axis along the axis of the cone of normals:†

$$n_1 = r_1\cos\vartheta - r_2\sin\vartheta\cos\varphi,$$

$$n_2 = r_2\cos\vartheta + r_1\sin\vartheta\cos\varphi, \quad n_3 = \sin\vartheta\sin\varphi. \tag{11}$$

We then get from Eq. (8)

$$S_{(o)}(\omega) = \frac{e^2\omega\mu}{2\pi c^2}\int_0^{2\pi} d\varphi\left[1-\left(\frac{\beta_o}{\beta}\right)^2\right]\frac{r_2^2\sin^2\varphi}{1-(r_1\beta_o/\beta - r_2\sqrt{1-(\beta_o/\beta)^2}\,\cos\varphi)^2}. \tag{12}$$

If we write the denominator in (12) as the product of two polynomials linear in $\cos\varphi$, the whole expression becomes the sum of two elementary integrals, and by calculating them we get the expression

$$[2-(r_1+\beta_o/\beta) - |r_1 - \beta_o/\beta|]\,\pi.$$

The sign of the difference $r_1 - \beta_o/\beta$ has an intuitive geometrical meaning, which follows from Eq. (9) and the meaning of the direction cosine r_1, namely: if $r_1 < \beta_o/\beta$, the optic axis is outside the cone of normals, and if $r_1 > \beta_o/\beta$, it is inside the cone. Thus for the cases of optic axis inside and outside the cone we have the respective formulas

$$S_{(o)}(\omega) = e^2\omega\mu c^{-2}(1-r_1), \tag{13}$$

$$S_{(o)}(\omega) = e^2\omega\mu c^{-2}(1-\beta_o/\beta). \tag{14}$$

Let us consider these expressions in more detail. If the charge moves along the optic axis ($r_1 = 1$), then (13) holds for all speeds larger than the critical, and $S_{(o)}(\omega) = 0$, as has already been shown by Ginzburg.[1] For other directions of motion of the charge, the emission increases continuously from zero for $\beta > \beta_o$, according to Eq. (14). Furthermore, if $r_1 > \beta_o$ there is a speed ($\beta = \beta_o/r_1$) at which Eq. (14) goes over continuously into Eq. (13), and for higher speeds of the charge there is no further increase of the ordinary radiation (per unit path length). If, finally, $r_1 < \beta_o$ (this means that the angle between the direction of motion of the charge and the optic axis is sufficiently large), then Eq. (14) is valid for all speeds larger than critical. In particular, for motion of the charge perpendicular to the optical axis, Eq. (14) agrees with the result previously obtained.[2]

Finally, let us examine the polarization of the ordinary waves. If the normal runs around the conical surface, then according to Eqs. (7) and (11) the positions of the vector $\mathbf{e}^{(o)}$ form a fan in the plane perpendicular to the optic axis. The axis of this fan is the perpendicular to the principal plane. The vector $\mathbf{e}^{(o)}$ reaches the extreme positions in the fan for the minimum value of $|e_3^{(o)}|$. If the optic axis is located outside the cone calculation shows that this minimum value occurs for vectors $\mathbf{e}^{(o)}$ that correspond to normals that satisfy the condition

$$r_1 - \mathbf{nr}\,n_1 = 0.$$

It is clear that these normals are the lines in which the cone touches planes passing through the optic axis. The angle 2η between these tangent planes is the vertex angle of the fan of directions, and we have for it the value given by

$$\cos\eta = r_2^{-1}\sqrt{(\beta_o/\beta)^2 - r_1^2}. \tag{15}$$

For a given speed of the charge the angle η takes its smallest value in the case of motion perpendicular to the optic axis, when it is equal to $\Theta_{(o)}$. If the direction of motion approaches the optic axis, the angle η increases, and when the cone touches the optic axis it reaches the value $\pi/2$. The directions of the polarization vector then fill an entire plane. It is clear that this is also true when the optic axis is inside the cone.

THE CONE OF NORMALS OF THE EXTRAORDINARY WAVES

In this section we are concerned with the geometrical properties of the emitted light waves. We shall return later to the question of the intensity of the radiation. For the unit vector $\mathbf{d}^{(e)}$ we get the following expression from (3) and (7):

---

*We use the indices o and e without parentheses to denote quantities associated with the critical speed.

†See Fig. 1, which illustrates the more general case of the extraordinary waves. In the present case the directions **r** and **k** are identical.

$$\mathbf{d}^{(e)} \equiv (1-n_1^2, -n_1n_2, -n_1n_3)/\sqrt{1-n_1^2}. \tag{16}$$

The vector $\mathbf{e}^{(e)}$ and the speed of propagation of the phase $v_{(e)}$ are determined from (3) and (5):

$$\mathbf{e}^{(e)} \equiv ((1-n_1^2)/\tau, -n_1n_2/\varepsilon, -n_1n_3/\varepsilon)/\sqrt{1-n_1^2}, \tag{17}$$

$$v_{(e)} = (c/\sqrt{\mu})\,[1/\tau + (1/\varepsilon - 1/\tau)n_1^2]^{1/2}. \tag{18}$$

The direction $\mathbf{s}^{(e)}$ of the extraordinary ray and the speed along the ray $u_{(e)}$ are found from (17) and (7):

$$\mathbf{s}^{(e)} \equiv (\tau n_1, \varepsilon n_2, \varepsilon n_3)/\sqrt{\varepsilon^2 + (\tau^2-\varepsilon^2)\,n_1^2}, \quad u_{(e)} = v_{(e)}/\mathbf{ns}^{(e)}. \tag{19}$$

Now we know all the quantities that determine the extraordinary waves, so that we can turn to the study of the geometrical shape of the cone of normals; its equation is determined by the argument of the δ function in Eq. (2):

$$r_1n_1 + r_2n_2 = v_{(e)}/c\beta. \tag{20}$$

Just as in the study of the ordinary waves, we introduce spherical coordinates, but postulate merely that the polar axis **k** is in the principal plane (Fig. 1). We get

$$n_1 = k_1\cos\vartheta - k_2\sin\vartheta\cos\varphi, \quad n_2 = k_2\cos\vartheta + k_1\sin\vartheta\cos\varphi,$$
$$n_3 = \sin\vartheta\sin\varphi. \tag{21}$$

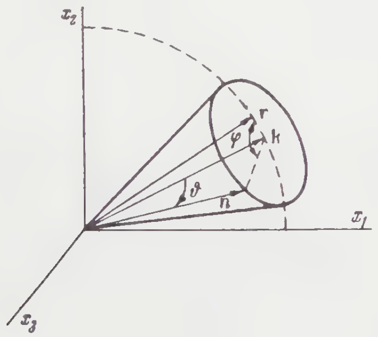

FIG. 1

Then the equation of the cone of normals takes the following form:

$$P\cos^2\vartheta + Q\sin^2\vartheta\cos^2\varphi + 2[Ak_1k_2$$
$$-r_1r_2(k_1^2-k_2^2)]\sin\vartheta\cos\vartheta\cos\varphi = R. \tag{22}$$

As a simplification we introduce the following notations

$$A = (r_1^2 - 1/\varepsilon\mu\beta^2) - (r_2^2 - 1/\tau\mu\beta^2), \quad R = 1/\tau\mu\beta^2,$$
$$P = (k_1r_1 + k_2r_2)^2 - (1/\varepsilon - 1/\tau)\,k_1^2/\mu\beta^2,$$
$$Q = (k_2r_1 - k_1r_2)^2 - (1/\varepsilon - 1/\tau)k_2^2/\mu\beta^2. \tag{23}$$

We use the indeterminacy still remaining in the choice of the direction cosines k_1 and k_2 to simplify Eq. (22). We impose the condition

$$Ak_1k_2 - r_1r_2(k_1^2-k_2^2) = 0, \tag{24}$$

which together with $k_1^2 + k_2^2 = 1$ determines k_1 and k_2:

$$k_1 = \frac{1}{\sqrt{2}}\left(1+\frac{A}{(A^2+4r_1^2r_2^2)^{1/2}}\right)^{1/2},$$
$$k_2 = \frac{1}{\sqrt{2}}\left(1-\frac{A}{(A^2+4r_1^2r_2^2)^{1/2}}\right)^{1/2}. \tag{25}$$

From Eqs. (22) and (24) we now get the following expression for the cone of the normals of the extraordinary waves:

$$\vartheta = \Theta_{(e)}(\varphi), \tag{26}$$

where we determine $\Theta_{(e)}$ from the equation

$$\cos\Theta_{(e)} = \left(\frac{R - Q\cos^2\varphi}{P - Q\cos^2\varphi}\right)^{1/2}. \tag{27}$$

From the right member of this last equation it can be seen that the cone has a symmetry axis, namely the polar axis of our spherical coordinates. In the general case the cross section of the cone will be an ellipse, as also follows from the geometrical interpretation given by Pafomov.[4,5]

The critical speed of the charge is fixed by the condition $\Theta_{(e)} = 0$. For this condition to hold, it is necessary that $P = R$, or, by Eq. (23),

$$(r_1^2 - 1/\varepsilon\mu\beta^2)\,k_1^2 + (r_2^2 - 1/\tau\mu\beta^2)\,k_2^2 + 2k_1k_2r_1r_2 = 0. \tag{28}$$

From this equation and Eq. (25) we get for the critical speed

$$\beta_e = 1/\sqrt{(\varepsilon r_1^2 + \tau r_2^2)\,\mu} \tag{29}$$

In this case the cone of normals degenerates into a line, whose direction cosines are

$$k_{1e} = \varepsilon r_1/\sqrt{\varepsilon^2r_1^2 + \tau^2r_2^2}, \qquad k_{2e} = \tau r_2/\sqrt{\varepsilon^2r_1^2 + \tau^2r_2^2}. \tag{30}$$

Finally, the speed of propagation of the phase of this critical wave is

$$v_e = \frac{c}{\sqrt{\mu}}\left(\frac{\varepsilon r_1^2 + \tau r_2^2}{\varepsilon^2r_1^2 + \tau^2r_2^2}\right)^{1/2}. \tag{31}$$

If we set in Eq. (19) $\mathbf{n} = \mathbf{k}_e$ and $v_{(e)} = v_e$, we get $\mathbf{s}^e = \mathbf{r}$ and $u_e = c\beta_e$. This result agrees with the assertion of Frank[5] that the first wave to appear is one with its ray directed along the motion of the charge. Under this condition the speed of the charge equals the ray velocity.

For particles with speeds close to the critical value, the expressions obtained for k_1, k_2, and $\cos\Theta_{(e)}$ can be simplified somewhat if we expand them in powers of $\delta = 1 - \beta_e/\beta$ and take the first two terms:

$$k_1 = k_{1e}\,[1 - 2k_{2e}^2\mu\,(\varepsilon - \tau)\,(v_e/c)^2\delta],$$

$$k_2 = k_{2e}\,[1 + 2k_{1e}^2\mu\,(\varepsilon - \tau)\,(v_e/c)^2\delta],$$

$$\cos\Theta_{(e)} = 1 - (\tau/\varepsilon)\,(v_e/v_o)^4\,[\cos^2\varphi + (v_e/v_o)^2\sin^2\varphi]^{-1}\delta. \quad (32)$$

It can be seen from (30) that in negative crystals $(\epsilon > \tau)$ the direction of propagation of the wave that appears at the critical speed is between the direction of motion of the charge and the optic axis. In positive crystals $(\epsilon < \tau)$ the normal lies outside the angle formed by the direction of motion of the charge and the optic axis. If the speed of the charge increases, then according to Eq. (32) the axis of the cone approaches the direction of motion of the charge in all crystals, but does not coincide with it even for $\beta = 1$ (except for the special cases $r_1 = 1$ and $r_1 = 0$, for which the axis of the cone and the direction of motion coincide).

The cones of the ordinary and extraordinary waves cannot intersect. They come in contract only for $\beta = \beta_o/r_1$, when they touch along the optic axis.

The polarization vectors $\mathbf{d}^{(e)}$ of the extraordinary waves are given by Eq. (16). If we use (21) and (26) to express $\mathbf{n}$, Eq. (16) gives parametric equations for the cone of polarizations. The analytic expression for the directrix of this cone is rather complicated. The use of the following estimate suffices for our further considerations.

If the optic axis is outside the cone of normals, the directions of polarization are contained in a pyramid whose faces are the following planes: 1) the tangent planes of the cone of normals that pass through the optic axis x_1; 2) planes through the axis x_3 and perpendicular to the generators of the cone of normals that lie in the principal plane (x_1, x_2) (see Fig. 2, which shows the case $r_1 = 0$. The pyramids must be continued symmetrically on the other half of the optic axis. This remark also applies to Fig. 3).

If the optic axis is inside the cone of normals, the picture changes, since there are no tangent planes passing through the optic axis. Figure 3 shows the cone of polarizations for $r_1 = 1$.

THE ENERGY OF THE EXTRAORDINARY WAVES

Let us now turn to the calculation of the energy which the charge loses in the form of extraordinary waves. On the cone of normals the following equation holds:

$$\mathbf{r}\mathbf{e}^{(e)} = \frac{r_1\varepsilon\mu\,(v_{(e)}/c)^2 - \mathbf{n}\mathbf{r}\,n_1}{\varepsilon\sqrt{1-n_1^2}} = \frac{\mathbf{n}\mathbf{r}}{\varepsilon\sqrt{1-n_1^2}}\left(r_1\left(\frac{\beta}{\beta_o}\right)^2\mathbf{n}\mathbf{r} - n_1\right).$$

If we also use the identity

$$\delta\left(\mathbf{n}\mathbf{r} - \frac{v_{(e)}}{c\beta}\right) = \frac{\mathbf{n}\mathbf{r}\,\delta\,(\cos\vartheta - \cos\Theta_{(e)})}{\sqrt{(R - Q\cos^2\varphi)\,(P - Q\cos^2\varphi)}},$$

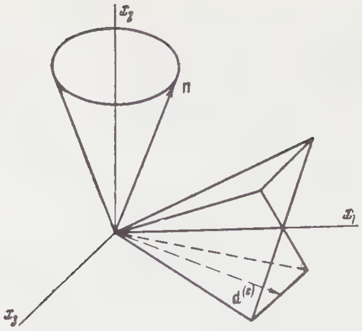

FIG. 2

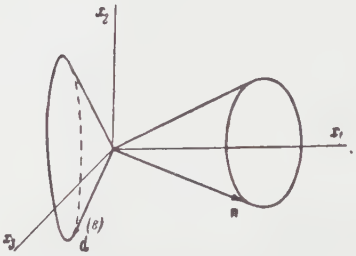

FIG. 3

then formula (2) takes the form

$$S_{(e)}(\omega) = \frac{e^2\omega\mu}{2\pi c^2}\left(\frac{\beta_o}{\beta}\right)^2\int_0^{2\pi}\frac{d\varphi}{\sqrt{(R - Q\cos^2\varphi)\,(P - Q\cos^2\varphi)}}$$
$$\times\left\{-\frac{\varepsilon}{\tau}\left(\frac{\beta_o}{\beta}\right)^2\frac{1}{\mathbf{n}\mathbf{r}} + \frac{1}{1-n_1^2}\left[\mathbf{n}\mathbf{r}\left(r_1\left(\frac{\beta}{\beta_o}\right)^2 - 1\right)\right.\right.$$
$$\left.\left. + 2n_2r_2\right]\right\}. \quad (33)$$

It will be shown in the Appendix that the value of this integral also depends essentially on the relative position of the cone of normals and the optic axis. Upon making the calculations we get (see Appendix) for the respective cases of optic axis inside and outside the cone:

$$S_{(e)}(\omega) = e^2\omega\mu c^{-2}\,(r_1 - \beta_o\beta_e/\beta^2), \quad (34)$$

$$S_{(e)}(\omega) = e^2\omega\mu c^{-2}\,(1 - \beta_e/\beta)\,\beta_o/\beta. \quad (35)$$

An examination of these formulas shows that as the speed of the charge increases beyond the critical value $c\beta_e$ the radiated energy increases continuously from zero in accordance with Eq. (35). In the region of directions of motion of the charge in which the equation $\beta = \beta_o/r_1$ can be satisfied, Eq. (35) goes over continuously into Eq. (34). For motion along the optic axis Eq. (34) holds for all speeds. In this case, and also for motion perpendicular to the optic axis, our formulas agree with results obtained previously.[2]

THE TOTAL RADIATION

Another matter of interest is the expression for the total energy radiated, $S(\omega) = S_{(o)}(\omega)$

$= S_{(e)}(\omega)$. At first, when the speed of the charge is between the critical speeds, waves of only one polarization appear. In this range of speeds the optic axis is outside the cone, and the total radiation is given either by

$$S(\omega) = e^2\omega\mu c^{-2}(1 - \beta_o/\beta), \tag{36}$$

or by

$$S(\omega) = e^2\omega\mu c^{-2}(1 - \beta_e/\beta)\,\beta_o/\beta, \tag{37}$$

depending on whether the crystal is negative or positive. For isotropic media this region is absent, since for such substances $\beta_o = \beta_e$.

For speeds at which both ordinary and extraordinary waves exist (and also always for $r_1 = 1$) the energy of the total radiation is given by the formula

$$S(\omega) = e^2\omega\mu c^{-2}(1 - \beta_o\beta_e/\beta^2), \tag{38}$$

which is independent of the relative positions of the optic axis and the cone of normals. The analogy between Eq. (38) and the well known formula for the radiation in an isotropic medium can be seen at a glance. It is curious that the formulas (36) — (38) for the total radiation involve the characteristic optical properties of the crystal and the parameters of the motion of the charge only through the quantities β_o/β and β_e/β.

CONCLUSION

The results obtained show that in spite of the complications of the structure of the electromagnetic field in an anisotropic medium, simple expressions can be given for the main properties of the Cerenkov radiation in uniaxial crystals. This is true particularly for the total radiated energy, which plays a part in a number of practical applications (counters, radiation losses in the motion of particles through matter).

For direct comparison with experiment one must take into account the influence of the surface of the crystal. The transition radiation which arises at the surface can be neglected, just as it is in the study of the radiation in isotropic media. The change of shape of the cones of normals on emergence from the crystal can be taken into account by using the law of refraction for the wave normals. The bounding surface of the crystal can affect the intensity of the radiation in a more complicated way.

In conclusion I take this opportunity to express my gratitude to Professor I. M. Frank for his interest and for helpful discussions.

APPENDIX

We write the formula (33) in the following way:

$$S_{(e)}(\omega) = (e^2\omega\mu/2\pi c^2)(\beta_o/\beta)^2(I_1 + I_2). \tag{1'}$$

The forms of the integrals I_1 and I_2 follow directly from Eq. (33). Expressing **nr** by using Eq. (21), rationalizing the denominator, and omitting terms odd in $\cos\varphi$, we get

$$I_1 = -\frac{\varepsilon}{\tau}\cdot\left(\frac{\beta_o}{\beta}\right)^2\int\limits_0^{2\pi} d\varphi\,\frac{k_1r_1 + k_2r_2}{R\,(k_1r_1 + k_2r_2)^2\sin^2\varphi - T\cos^2\varphi},$$

$$T = (k_1r_1 + k_2r_2)^2\,(Q - R)$$
$$+ (k_2r_1 - k_1r_2)^2\,(P - R) = -(\tau\mu)^{-1}(\beta_o/\beta_e)^2.$$

The integration gives the result

$$I_1 = -2\pi\beta_e/\beta_o. \tag{2'}$$

In a similar way we get for I_2 the following expressions:

$$I_2 = 2\int\limits_{-\infty}^{\infty}\frac{Uy^2 + x}{(Wy^2 - 2iDy - M)\,(Wy^2 + 2iDy - M)}\,dy$$

$$= 4\int\limits_{-\infty}^{\infty}\frac{ay + b}{Wy^2 - 2iDy - M}\,dy, \tag{3'}$$

where

$$W = P - k_1^2R,\quad D = k_1\,(P - R),$$

$$M = k_1^2\,(P - R) + k_2^2(Q - R) = r_1^2 - (\beta_o/\beta)^2,$$

$$U = W\,[(\beta/\beta_o)^2\,(k_1r_1 + k_2r_2)\,M + 2r_2k_2],$$

$$x = (\beta/\beta_o)^2\,M\,[2r_1D$$
$$- (\beta/\beta_o)^2\,(k_1r_1 + k_2r_2)\,M - 2k_2r_2\,(\beta_o/\beta)^2],$$

$$a = (UM + xW)/4MDi,\qquad b = -x/2M.$$

After integration we get

$$I_2 = \frac{4\pi i}{W}\,\frac{1}{z_2 - z_1}\,[(ib - az_1)\,\mathrm{sign}\,z_1 - (ib - az_2)\,\mathrm{sign}\,z_2],$$

where iz_1 and iz_2 are the roots of the denominator in Eq. (3'):

$$z_{1,2} = W^{-1}(D \pm k_2r_2\beta_o/\beta).$$

The root z_1 is positive. The sign of z_2 depends on the relative position of the optic axis and the cone of normals, since $z_2 = 0$ for $\beta = \beta_o/r_1$. We have finally

$$I_2 = 2\pi r_1(\beta/\beta_o)^2,\quad I_2 = 2\pi\beta/\beta_o, \tag{4'}$$

for $r_1 > \beta_o/\beta$ and $r_1 < \beta_o/\beta$, respectively. The formulas (34) and (35) follow directly from Eqs. (1'), (2'), and (4').

[1] V. L. Ginzburg, JETP **10**, 601, 608 (1940).

[2] B. M. Bolotovskiĭ, Usp. Fiz. Nauk **62**, 201 (1957).

[3] J. V. Jelley, Cerenkov Radiation and its Applications, Pergamon Press, London, 1958.

[4] V. E. Pafomov, JETP **36**, 1853 (1959), Soviet Phys. JETP **9**, 1321 (1959); Dissertation, Phys. Inst. Acad. Sci. 1957.

[5] I. M. Frank, Usp. Fiz. Nauk **68**, 387 (1959).

[6] I. M. Frank, JETP **38**, 1751 (1960), Soviet Phys. **11**, (1960).

Translated by W. H. Furry
31

SOVIET PHYSICS JETP VOLUME 12, NUMBER 1 JANUARY, 1961

ON THE THEORY OF RADIATIVE PROCESSES IN PIECEWISE HOMOGENEOUS MEDIA

F. F. TERNOVSKIĬ

Moscow State University

Submitted to JETP editor February 25, 1960

J. Exptl. Theoret. Phys. (U.S.S.R.) 39, 171-180 (July, 1960)

The radiation emitted by an electron passing from vacuum into a semi-infinite medium is studied with account of multiple scattering and polarization of the medium. The probabilities for bremsstrahlung and pair production by γ quantra are computed for plates of finite thickness.

. INTRODUCTION

Landau and Pomeranchuk[1] and Migdal[2-4] have shown that radiative processes in a medium become much less intence at higher energies than is called for by the usual theory.[5] This is caused by the fact that the great longitudinal distances become important to these processes at high energies, and this in turn makes these processes sensitive to multiple scattering.

Ter Mikaelyan has shown[6] that the polarization of the medium must be accounted for in an analysis of the softest quanta.

The results cited, however, pertain to effects in infinite media. Since the radiation field is produced under different conditions near the boundaries, radiation should occur as a particle goes from one medium to another.

A distinction should be made between two types of transition radiation. One is connected with the realignment of the particle field, due to polarization of the medium. It occurs at all energies and all particle rest masses, and causes radiation of electromagnetic waves of frequency not higher than optical in a direction opposite to that of the motion, while the forward-radiation spectrum contains frequencies up to $\omega = \omega_0/\sqrt{1-\beta^2}$, where $\omega_0^2 = 4\pi n Z e^2/m$ and $v = \beta c$ is the velocity of the particle.[7,8]

The transition radiation of the second type is connected with the effect of multiple scattering. It therefore arises only at sufficiently high energy and can be observed in practice only in the case of electrons or positrons. The angular distribution has a sharp maximum along the direction of motion, and at sufficiently large energies the spectrum can contain frequencies on the order of $mc^2/\hbar\sqrt{1-\beta^2}$.

The classical theory of the transition radiation of the second kind was given by Gol'dman.[9]

The present paper contains a simultaneous quantum analysis of the transition radiations of both kinds. The formulas obtained are valid at frequencies considerably higher than optical, so that the backward transition radiation is completely neglected in the calculations.

2. RADIATION OCCURRING UPON TRANSITION OF AN ELECTRON FROM VACUUM INTO A SEMI-INFINITE MEDIUM

Let a fast ($p_0 \gg 1$)* electron move along the z axis through the boundary of a semi-infinite medium filling the space $z > 0$.

Assumed that when $t = 0$ the state of the electron is described by a wave packet $\psi^{\lambda_0}_{p_0}$ with an average momentum p_0. The wave function of the initial state can be written in the form

$$\Psi_0 = e^{-iH_0 t}\psi^{\lambda_0}_{\mathbf{p}_0}, \quad t \leqslant 0; \qquad \Psi_0 = e^{-iHt}\psi^{\lambda_0}_{\mathbf{p}_0}, \quad t \geqslant 0;$$

$$H = H_0 + \sum_n V(\mathbf{r} - \mathbf{r}_n), \tag{1}$$

where H is the Hamiltonian of the electron and includes all the scatterers. In the following calculations, however, we shall put $\psi^{\lambda_0}_{\mathbf{p}_0} = u^{\lambda_0}_{\mathbf{p}_0} \times \exp(i\mathbf{p}_0 \cdot \mathbf{r})$ ($u^{\lambda_0}_{\mathbf{p}_0}$ is the unit bispinor amplitude, and the normalization volume is chosen equal to unity), since allowance for the small indeterminacy in the momentum of the incident electron would lead only to an averaging of the integral cross section over a narrow interval of momentum values in the vicinity of p_0.

Analogously, the wave function of the final state is written

---

*We use a system of units in which $\hbar = m = c = 1$.

$$\Psi_s = e^{-iH_0 t}\psi_{\mathbf{p}_s}^{\lambda_s}, \quad t \leqslant 0; \qquad \Psi_s = e^{-iHt}\psi_{\mathbf{p}_s}^{\lambda_s}, \quad t \geqslant 0. \tag{2}$$

The probability of emission of a quantum with a wave vector **k** is determined by the square of the modulus of the matrix element

$$M = ie\sqrt{2\pi/k}\int(\Psi_s^* \boldsymbol{\alpha}\boldsymbol{\varepsilon}_\nu \Psi_0)\, e^{-i\omega t + i\mathbf{k}\mathbf{r}}\, dt\, d\mathbf{r}, \tag{3}$$

where $\boldsymbol{\epsilon}_\nu$ is the polarization vector and ω is the quantum energy. In vacuum $\omega = \mathrm{k}$, but on entering the medium the interaction with the electrons of the medium changes the energy of the quantum to $\mathrm{k}/\sqrt{\epsilon}$ (ϵ is the dielectric constant of the medium). We must therefore put in (3) $\omega = \mathrm{k}$ when $\mathrm{t} < 0$ and $\omega = \mathrm{k}/\sqrt{\epsilon}$ when $\mathrm{t} > 0$. It can be shown (see Appendix) that such a procedure is valid when $|1 - \sqrt{\epsilon}| \ll 1$ and takes correct account of the transition radiation forward.

Substituting in (3) the expressions (1) and (2) for Ψ_0 and Ψ_S, we obtain

$$M = ie\sqrt{\frac{2\pi}{k}}\Big[(\boldsymbol{\alpha}\varepsilon_\nu)^{\lambda_s\lambda_0}_{\mathbf{p}_0-\mathbf{k},\,\mathbf{p}_0}(k + \varepsilon_{\mathbf{p}_0-\mathbf{k}} - \varepsilon_{\mathbf{p}_0})^{-1}\,\delta_{\mathbf{p}_S,\,\mathbf{p}_0-\mathbf{k}}$$

$$+ i\sum_{\mathbf{p}}\int_0^\infty e^{i\omega t}\, dt\, (e^{iHt})_{\mathbf{p}_S,\,\mathbf{p}-\mathbf{k}}(e^{-iHt})_{\mathbf{p}\mathbf{p}_0}(\boldsymbol{\alpha}\varepsilon_\nu)^{\lambda_0\lambda_s}_{\mathbf{p}-\mathbf{k},\,\mathfrak{v}}\Big] \equiv A + B.$$

The probability of emission of a quantum is determined by the square of the modulus of the matrix element, averaged over the positions of the scatterers and over the spins of the initial state, and summed over the polarizations of the quantum and the final states of the electron. The Migdal method[4] is used to average over the positions of the scatterers. Denoting by the symbol $<\ldots>$ the totality of the indicated operations, we obtain

$$\langle|A|^2\rangle = \frac{2\pi e^2}{k}\,\frac{\Lambda(\mathbf{p}_0, \mathbf{p}_0 + \mathbf{k}/2)}{(\varepsilon_{\mathbf{p}_0-\mathbf{k}} + k - \varepsilon_{\mathbf{p}_0})^2},$$

$$\langle A^* B\rangle = \frac{2\pi e^2}{k}\, i\int_0^\infty dt e^{i\omega t}\int\frac{d\mathbf{p}}{(2\pi)^3}\,\frac{\Lambda(\mathbf{p}_0, \mathbf{p})\, f_{\mathbf{k}}(\mathbf{p}_0, \mathbf{p}, t)}{\varepsilon_{\mathbf{p}_0-\mathbf{k}} + k - \varepsilon_{\mathbf{p}_0}},$$

$$\langle|B|^2\rangle = 4\pi e^2 k^{-1}\,\mathrm{Re}\int_0^\infty dt\int_0^\infty d\tau e^{i\omega\tau}$$

$$\times\int\frac{d\mathbf{p}}{(2\pi)^3}\frac{d\mathbf{p}_1}{(2\pi)^3}\,\Lambda(\mathbf{p}_1, \mathbf{p})\, f_0(\mathbf{p}_0, \mathbf{p}_1, t)\, f_{\mathbf{k}}(\mathbf{p}_1, \mathbf{p}, \tau);$$

$$\Lambda(\mathbf{p}, \mathbf{p}') = \frac{1}{2}\sum_{\substack{\lambda_s,\,\lambda_0,\,\nu\\ \varepsilon^{\lambda_0}>0,\,\varepsilon^{\lambda_s}>0}}(\boldsymbol{\alpha}\varepsilon_\nu)^{\lambda_0\lambda_s}_{\mathbf{p},\,\mathbf{p}-\mathbf{k}}(\boldsymbol{\alpha}\varepsilon_\nu)^{\lambda_s\lambda_0}_{\mathbf{p}'-\mathbf{k}/2,\,\mathbf{p}'+\mathbf{k}/2}, \tag{4}$$

where the summation over **p** and $\mathbf{p}_1$ is replaced by integration. The function $\mathrm{f}_\mathbf{k}$ introduced by Migdal obeys the same equation as the averaged density matrix (see references 3 and 4).

The probability of emission of a quantum with energy in the interval k, k + dk is given by

$$W(p_0, k)\, dk = dk\int\langle|M|^2\rangle\frac{k^2}{(2\pi)^3}\, d\boldsymbol{\vartheta}, \tag{5}$$

where $\boldsymbol{\vartheta} = \mathbf{k}/\mathrm{k} - \mathbf{p}_0/\mathrm{p}_0$. The subsequent transformations of (4) and (5) and the calculation of Λ follow Migdal's procedure. As a result we obtain

$$W(p_0, k) = \lim_{T\to\infty}\frac{e^2 k g^2}{2(2\pi)^2 p_0^2}\,\mathrm{Re}\Big\{\int\frac{K_1 + K_2\eta^2}{a^2(1 + g^2\eta^2)^2}\, d\eta$$

$$+ 2i\int_0^\infty d\tau e^{i\omega\tau}\int\frac{[K_1 + K_2\eta\eta_0]\, v(\eta, \tau)}{a(1 + g^2\eta_0^2)}\, d\eta\, d\eta_0$$

$$+ 2\int_0^T dt\int_0^\infty d\tau e^{i\omega\tau}\int[K_1 + K_2\eta\eta_0]\, v(\eta, \tau)\, d\eta\, d\eta_0\Big\},$$

$$g = p_0 - k/2, \qquad a = k/2\, p_0(p_0 - k),$$

$$K_1 = k^2/p_0^2(p_0 - k)^2, \qquad K_2 = [p_0^2 + (p_0 - k)^2]\, g^2/p_0^2(p_0 - k)^2. \tag{6}$$

The function v is connected with $\mathrm{f}_\mathbf{k}$ by

$$f_\mathbf{k}(\mathbf{p}_0, \mathbf{p}, t)\, d\mathbf{p}/(2\pi)^3 \approx \delta(p - g)\, dp v(\eta, t)\, d\eta,$$

where $\boldsymbol{\eta} = \mathbf{p}_\perp/\mathrm{g}$, $\boldsymbol{\eta}_0 = \mathbf{p}_{0\perp}/\mathrm{g}$, and the index $\perp$ denotes the projection of the vector on the plane perpendicular to **k**. The equation for the function $\mathrm{w} = \mathrm{v}e^{i\omega t}$ has the form

$$\frac{\partial w}{\partial t} = ia(1 + \delta + g^2\eta^2)w + \int p(\eta' - \eta)\,[w(\eta') - w(\eta)]\, d\eta', \tag{7}$$

$$\delta = 2p_0(p_0 - k)(1/\sqrt{\varepsilon} - 1), \qquad p(\theta) = 4nZ^2 e^4/g^2[\theta^2 + \theta_1^2]^2,$$

$$\theta_1 = Z^{1/3}/137\, g, \tag{8}$$

with

$$w(\eta, \tau)\,|_{\tau=0} = \delta(\eta - \eta_0). \tag{9}$$

As shown by Gol'dman,[9] it is necessary to separate the finite part, which pertains to the radiation at the boundary, from the last term in (6), which is formally infinite as $\mathrm{T} \to \infty$. We finally obtain

$$W(p_0, k) = \lim_{T\to\infty}(MT + N), \tag{10}$$

where

$$M(p_0, k) = \frac{e^2 k g^2}{(2\pi)^2 p_0^2}\,\mathrm{Re}\int_0^\infty d\tau\int[K_1 + K_2\eta\eta_0]\, w(\eta, \tau)\, d\eta\, d\eta_0 \tag{11}$$

is the known expression obtained by Migdal[4] for the probability of bremsstrahlung on a unit path in an infinite medium, and

$$N(p_0, k) = \frac{e^2 k g^2}{2(2\pi)^2 p_0^2}\,\mathrm{Re}\Big\{\int\frac{[K_1 + K_2\eta_0^2]}{a^2(1 + g^2\eta_0^2)^2}\, d\eta_0$$

$$+ 2i\int_0^\infty dt\int\frac{[K_1 + K_2\eta\eta_0]\, w(\eta, t)}{a(1 + g^2\eta_0^2)}\, d\eta\, d\eta_0$$

$$- \int_0^\infty \mathrm{i\,dt}\int[K_1 + K_2\eta\eta_0]\, w(\eta, t)\, d\eta\, d\eta_0\Big\} \tag{12}$$

is the radiation-probability increment due to the effect of the boundary.

Going over in (7) to the approximate Fokker-Planck expression, we obtain

$$\partial w/\partial t = ia(1+\delta+g^2\eta^2)w + q(\partial^2 w/\partial\eta_1^2 + \partial^2 w/\partial\eta_2^2), \quad (13)$$

$$q = 2\pi n Z^2 e^4 g^{-2}\ln(\theta_2/\theta_1) = B/g^2. \quad (14)$$

The choice of the angle θ_2 will be made later [see (17)].

Equation (13) has the same form with the equation for the Fourier component of the classical distribution function, and the two are identical when $k \ll p_0$. A solution satisfying the initial condition (9) was obtained for this equation by Gol'dman; its form, in our notation is

$$w(\eta, t) = \frac{\lambda}{\pi\sinh\gamma t}\exp[ia(1+\delta)t - \lambda(\eta^2+\eta_0^2)\coth\gamma t$$

$$+2\lambda\eta\eta_0\cosh\gamma t],$$

$$\gamma = 4q\lambda, \quad \lambda = [-ikg^2/8p_0(p_0-k)B]^{1/2}. \quad (15)$$

Substituting (15) in (12) we ultimately obtain, after simple but rather cumbersome transformations,

$$N(p_0, k) = \frac{e^2}{2\pi k}\left\{\frac{k^2}{p_0^2}\left[1 - 2\,\mathrm{Re}\,\sigma\int_0^\infty \frac{dz}{1+z}\right.\right.$$

$$\times\int_0^\infty \frac{\exp\{-\sigma(1+\delta)x - \sigma z\tanh x\}}{\cosh x}dx$$

$$\left.+\mathrm{Re}\,\sigma\int_0^\infty \frac{x\exp\{-\sigma(1+\delta)x\}}{\sinh x}dx\right]$$

$$+\frac{p_0^2+(p_0-k)^2}{p_0^2}\left[2\,\mathrm{Re}\,\sigma(1+\delta)\int_0^\infty\frac{dz}{1+z}\right.$$

$$\times\int_0^\infty \exp\{-\sigma(1+\delta)x - \sigma z\tanh x\}dx$$

$$+\mathrm{Re}\int_0^\infty\left(\coth x - \frac{1}{x}\right)[1-\sigma(1+\delta)x]$$

$$\left.\left.\times\exp\{-\sigma(1+\delta)x\}dx - 2 - \ln(1+\delta)\right]\right\},$$

$$\sigma = 2(1-i)s, \quad s = {}^1/_8\sqrt{k/p_0(p_0-k)B}. \quad (16)$$

In (16), z is the square of the angle of emission of the quantum, measured in units of g^{-2}. The values $x \sim 1/s(1+\delta)$ and $z \sim 1+\delta$, become important when $s(1+\delta) \gg 1$ while $x \sim 1$ and $z \sim 1/s$ become important when $s(1+\delta) \ll 1$.

From this we obtain

$$\eta \sim \sqrt{z}/g = \min\{1/g\sqrt{s}, \sqrt{1+\delta}/g\},$$

so that we must put in (14)

$$\theta_2 \sim \min\{1/g\sqrt{s}, \sqrt{1+\delta}/g\}. \quad (17)$$

When $k \ll p_0$ and $\delta = 0$, (16) leads to the Gol'dman formula.[9]

When $s \gg 1$, (16) assumes the form

$$N = \frac{e^2}{2\pi k}\left\{\frac{k^2}{p_0^2}\left[1+\frac{1}{1+\delta} - \frac{2}{\delta}\ln(1+\delta)\right]\right.$$

$$\left.+2\frac{p_0^2+(p_0-k)^2}{p_0^2}\left[\frac{1+\delta/2}{\delta}\ln(1+\delta) - 1\right]\right\}, \quad (18)$$

If, furthermore, $k \ll p_0$, we obtain from (18)

$$N = \frac{2e^2}{\pi k}\left[\frac{1+\delta/2}{\delta}\ln(1+\delta) - 1\right]. \quad (19)$$

Equation (19) can be obtained from Garibyan's exact formula for $|1-\sqrt{\epsilon}| \ll 1$. It gives the frequency distribution of the transition radiation due to polarization of the medium. The quantum corrections to (19), as seen from (18), are quite small.

When $s < 1$, two cases must be distinguished, $s\delta > 1$ and $s\delta < 1$. In the former case (18) and (19) remain in force, but if $s\delta \ll 1$, we obtain from (16)

$$N = \frac{e^2}{2\pi k}\left\{\frac{k^2}{p_0^2} + 2\frac{p_0^2+(p_0-k)^2}{p_0^2}\ln\frac{\varkappa}{\sqrt{s}}\right\}, \quad \varkappa \sim 1. \quad (20)$$

The inequalities $s\delta < 1$ and $s < 1$ do not contradict each other only when $p_0 > p_1 = \omega_0/8B$ (in ordinary units $p_1 \sim 0.1$ Bev for lead, ~ 3 Bev for aluminum).

If $p_0 < p_1$ the probability of transition radiation is determined by (19) for all values of k, so that we obtain for the integral losses Garibyan's result

$$\Delta E_1 = \int_0^{p_0} Nk\,dk = \frac{1}{3}e^2\omega_0 p_0. \quad (21)$$

If, however, $p_0 > p_1$, then (19) remains in force when $k \ll \omega_1 = (1/4)(\omega_0^4 p_0^2/B)^{1/3}$, and when $k \gg \omega_1$ the transition radiation probability is given by (20). In this case the radiation spectrum will include the frequencies $k \lesssim p_1/(1+s_0^2)$, where $s_0 = (1/8)\sqrt{1/Bp_0}$, and if $s_0 \ll 1$ the integral losses reach a value

$$\Delta E_2 = e^2\pi^{-1}p_0\ln(\varkappa/s_0), \quad \varkappa \sim 1,$$

which exceeds ΔE_1 by a factor 10^5.

3. RADIATION OCCURRING UPON PASSAGE THROUGH A PLATE

If many collisions take place during the time of passage through a plate, the quantum kinetic equation as developed by Migdal,[4] can be used, as before, to describe the behavior of the electron inside the plate. The wave functions chosen for the initial and final states are

	$t<0$	$0<t<\tau$	$\tau<t$
Ψ_0	$e^{-iH_0 t}\psi_{\mathbf{p}_0}^{\lambda_0}$	$e^{-iHt}\psi_{\mathbf{p}_0}^{\lambda_0}$	$e^{-iH_0(t-\tau)}e^{-iH\tau}\psi_{\mathbf{p}_0}^{\lambda_0}$
Ψ_s	$e^{-iH_0 t}e^{iH\tau}\psi_{\mathbf{p}_s}^{\lambda_s}$	$e^{-iH(t-\tau)}\psi_{\mathbf{p}_s}^{\lambda_s}$	$e^{-iH_0 t}\psi_{\mathbf{p}_s}^{\lambda_s}$

After transformations analogous to those given in Sec. 2, the expression for the probability of emission of a quantum with energy in the interval k, k + dk is reduced to the form

$$W(p_0, k, \tau) = \frac{e^2kg^2}{(2\pi)^2 p_0^2} \operatorname{Re}\left\{\int \frac{[K_1 + K_2\eta_0^2]}{a^2(1+g^2\eta_0^2)^2} d\eta_0 - \int \frac{[K_1 + K_2\eta\eta_0]\, w(\eta, \tau)}{a^2(1+g^2\eta_0^2)(1+g^2\eta^2)} d\eta\, d\eta_0 + 2i\int_0^\tau dt \int \frac{[K_1 + K_2\eta\eta_0]\, w(\eta, \tau)}{a(1+g^2\eta_0^2)} d\eta\, d\eta_0 + \int_0^\tau dt \int_0^t dt' \int [K_1 + K_2\eta\eta_0]\, w(\eta, \tau)\, d\eta\, d\eta_0\right\}. \tag{22}$$

In the energy region where the effect of polarization of the medium can be completely neglected (i.e., when $\delta \ll 1$), the expression (22) can be represented in a more illustrative form

$$w(p_0, k, \tau) = e^2g^2(2\pi^2k)^{-1}\left\{\tau\int\left[\frac{k^2}{p_0^2}A^2(\eta, \eta_0) + \frac{p_0^2 + (p_0 - k)^2}{p_0^2}\mathbf{B}^2(\eta, \eta_0)\right] p(\eta - \eta_0)\, d\eta\, d\eta_0 - 2\operatorname{Re}\int_0^\tau dt \int_0^t dt' \int\left[\frac{k^2}{p_0^2}A(\eta_0', \eta_0)\,A(\eta, \eta') + \frac{p_0^2 + (p_0 - k)^2}{p_0^2}\mathbf{B}(\eta_0', \eta_0)\,\mathbf{B}(\eta, \eta')\right] \times d\eta_0' p(\eta'_0 - \eta_0) d\eta_0 w(\eta, t') d\eta p(\eta' - \eta) d\eta'\right\},$$

$$A(\eta, \eta') = 1/(1 + g^2\eta^2) - 1/(1 + g^2\eta'^2),$$

$$\mathbf{B}(\eta, \eta') = g\eta/(1 + g^2\eta^2) - g\eta'/(1 + g^2\eta'^2). \tag{23}$$

The term in (23) linear in τ coincides with the ordinary Bethe-Heitler expression for the bremsstrahlung probability. Upon integration over the angles, this term is found to be

$$W_{\mathrm{BH}}(p_0, k, \tau) = (\tau/3kL)\{k^2/p_0^2 + 2[p_0^2 + (p_0 - k)^2]/p_0^2\}, \tag{24}$$

where L is the unit radiation length. The second term in (23) describes the contribution of the interference of radiations from different parts of the trajectory. It is proportional to τ^2 when $\tau \to 0$, and, as will be seen below, becomes much smaller than the first term when $\tau < \tau_0 = L/2\pi \cdot 137$, so that in a plate of thickness $\tau \ll \tau_0$, the bremsstrahlung probability is determined by the Bethe-Heitler theory for all values of the particle and quantum energies.

As $\tau \to \infty$, the function $w(\eta, \tau)$ tends to zero, and therefore the second term in (22) tends to zero while the third tends to a finite limit and the fourth can be represented in the form

$$\tau\int_0^\infty dt \int [K_1 + K_2\eta\eta_0] w\, d\eta\, d\eta_0 - \int_0^\infty t\,dt \int [K_1 + K_2\eta\eta_0] w\, d\eta\, d\eta_0 + \ldots,$$

where the terms which vanish as $\tau \to \infty$ have been discarded.

Thus, as $\tau \to \infty$, we have

$$W(p_0, k, \tau) = M\tau + 2N, \tag{25}$$

where N is given by (12), (16), and (18)—(20) and M is given by (11). Substituting in (11) the expression (15) for $w(\eta, \tau)$, we obtain the Migdal formulas*

$$M(p_0, k) = \frac{2e^2B}{3\pi k}\left\{\frac{k^2}{p_0^2}\frac{G[(1+\delta)s]}{(1+\delta)^2} + 2\frac{p_0^2 + (p_0 - k)^2}{p_0^2}\frac{\Phi[s(1+\delta)]}{(1+\delta)}\right\}; \tag{26}$$

$$\Phi(s) = 12s^2\left[\int_0^\infty \coth\frac{x}{2} e^{-sx} \sin sx\, dx - \frac{\pi}{2}\right],$$

$$G(s) = 24s^2\left[\frac{\pi}{2} - \int_0^\infty \cosh\frac{x}{2} e^{-sx} \sin sx\, dx\right]. \tag{27}$$

When $s \ll 1$, we obtain from this $\Phi(s) \approx 6s$, $G(s) \approx 12\pi s^2$, and when $s > 1$ $G(s) \approx \Phi(s) \approx 1$.

In order to estimate the smallest plate thickness for which (25) is valid, we note that, according to (15), W vanishes (or becomes rapidly oscillating) when

$$t \gg \min\{t_k, t_\delta\},$$

$$t_\delta \sim 1/a(1+\delta), \quad t_k \sim 1/|\gamma| = \sqrt{p_0(p_0 - k)/2kB}\,.$$

Since $t_k/t_\delta \sim s(1 + \delta)$, Eq. (25) becomes applicable when $s(1 + \delta) \gg 1$ if $t \gg t_\delta$, and when $s(1 + \delta) \ll 1$ if $t \gg t_k$.

Let now $t < \min\{t_k, t_\delta\}$ and $\delta > 1$, and let us assume that the bremsstrahlung intensity is small compared with the intensity of transition radiation. We can then put approximately in (22)

$$w(\eta, \tau) \approx \delta(\eta - \eta_0) \exp\{ia(1 + \delta + g^2\eta^2)\tau\},$$

after which we obtain

$$W(p_0, k, \tau) = 2e^2\delta^2(\pi k)^{-1} \times \int_0^\infty \frac{\{k^2/p_0^2 + [p_0^2 + (p_0 - k)^2]z/p_0^2\}[1 - \cos a\tau(1 + \delta + z)]\, z\,dz}{(1+z)^2(1+\delta+z)^2}. \tag{28}$$

If $a(1 + \delta)\tau \approx t/t_\delta \sim 1$ and $\delta \gtrsim 1$, the expression (28) is found to be much greater than (24) when $t \sim t_\delta$, thus justifying our assumption. On the other hand, if $t \ll t_\delta$, then the contribution of the transition radiation may become much smaller than the contribution of the bremsstrahlung.

---

*The expression for G(s) is misprinted in the Migdal article (reference 4).

Let us show that if the condition $t \ll \max\{t_k, t_\delta\}$ is satisfied, we can replace the function w in (22) and (23) by the function w_0, which is obtained from w when $a = 0$. For this purpose we seek a solution of (7) in the form $w = w_1 \times \exp\{iat(1 + \delta + g^2\eta^2)\}$. For the function w_1 we obtain

$$\frac{\partial w_1}{\partial t} = \int p(\eta' - \eta)\left[w_1(\eta') \exp\left\{\frac{i}{2} ag^2(\eta'^2 - \eta^2)\tau\right\} - w_1(\eta)\right] d\eta'.$$

In order of magnitude, $\eta^2 \sim \eta'^2 = q\tau$, the mean square of the angle of multiple scattering along the path τ. From this we obtain

$$ag^2\eta^2\tau \sim ag^2\eta'^2\tau \sim (\tau/t_k)^2 \ll 1,$$

which proves our statement. The function w_0 satisfies the equation

$$\frac{\partial w_0}{\partial t} = \int p(\eta' - \eta)[w_0(\eta', t) - w_0(\eta, t)]\, d\eta', \tag{29}$$

and the initial condition (9), and is normalized in accordance with

$$\int w_0(\eta, \tau)\, d\eta = 1. \tag{30}$$

Putting $w = w_0$ in (23) and using (29), (30), and (9) we obtain

$$W(p_0, k, \tau) = \frac{e^2g^2}{2\pi^2 k} \int \left[\frac{k^2}{p_0^2} A^2(\eta, \eta_0) + \frac{p_0^2 + (p_0 - k)^2}{p_0^2} B^2(\eta, \eta_0)\right] p(\eta - \eta_0)\, d\eta\, d\eta_0. \tag{31}$$

The corrections to this formula are proportional to $(\tau/t_k)^2$ and $(\tau/t_\delta)^2$.

The function $w_0(\eta, \tau)$ depends only on $|\eta - \eta_0|$, viz.: $w_0(\eta, \tau) \equiv w_0(|\eta - \eta_0|, \tau)$. Introducing new variables

$$x = g(\eta - \eta_0)/2, \quad y = g(\eta + \eta_0)/2$$

and carrying out partial integration over the angles, we obtain

$$W(p_0, k, \tau) = \frac{8e^2}{kg^2} \int_0^\infty \left[\frac{k^2}{p_0^2} \varphi(x) + \frac{p_0^2 + (p_0 - k)^2}{p_0^2} \psi(x)\right] w_0\left(\frac{2x}{g}, \tau\right) x\, dx, \tag{32}$$

$$\varphi(x) = 1 - \frac{1}{x\sqrt{1 + x^2}} \sinh^{-1} x, \quad \psi(x) = \frac{2x^2 + 1}{x\sqrt{1 + x^2}} \sinh^{-1} x - 1. \tag{33}$$

As is well known,[10,11] an exact solution of (29) has the structure

$$\frac{1}{g^2} w_0\left(\frac{2x}{g}, \tau\right) = \begin{cases} \exp\{-x^2/B_1\tau\}/4B\tau, & x^2 \ll B_1\tau \\ nZ^2e^4\tau/4x^4, & x^2 \gg B_1\tau \end{cases}, \tag{34}$$

where $B_1 = 2\pi n Z^2 e^4 \ln(\sqrt{B_1\tau} \cdot 137 Z^{-1/3})$.

Since the functions φ and ψ behave differently when $x < 1/2$ and $x > 1/2$, we obtain different expressions for $W(p_0, k, \tau)$ when τ is greater than or less than $1/4\, B_1$. Let first $4B_1\tau \ll 1$; then the main contribution to the integral (32) will be made by the values $x \lesssim 1/2$, so that we can put $\varphi(x) \approx 2x^2/3$ and $\psi(x) \approx 4x^2/3$, obtaining

$$W(p_0, k, \tau) = \frac{16e^2}{3k}\left[\frac{k^2}{p_0^2} + 2\frac{p_0^2 + (p_0 - k)^2}{p_0^2}\right] \frac{1}{g^2} \int_0^\kappa x^3 w_0\left(\frac{2x}{g}, \tau\right) dx,$$

where $\kappa \sim 1$. From this we obtain with the aid of (34) an expression which coincides with (24) when $\kappa = 1.4$. Thus, when $\tau \ll \tau_0 \equiv 1/4\, B_1$ and at all values of the parameter s, the bremsstrahlung probability is determined by the Bethe-Heitler theory.

As regards the transition radiation, it is negligibly small in plates of any thickness when $\delta \ll 1$, but if $\delta \gtrsim 1$, then $\tau_\delta \approx k/\omega_p^2$ and the inequality $\tau_\delta > \tau_0$ satisfied when $k < 137/Z \ln(190 Z^{-1/3})$. If $t_\delta \ll \tau_0$, on the other hand, (24) will be valid when $\tau \ll t_\delta$, (28) when $\tau \sim t_\delta$, and (25) when $\tau \gg t_\delta$.

Let now $\tau_0 \ll \tau \ll \max\{t_\delta, t_k\}$. In this case the important values in the integral (32) will be $x \gtrsim 1$, where $\varphi(x) \approx 1$ and $\psi(x) \sim \ln 4x^2$, so that we obtain

$$W(p_0, k, \tau) \approx \frac{e^2}{\pi k}\left[\frac{k^2}{p_0^2} + \frac{p_0^2 + (p_0 - k)^2}{p_0^2} \ln\frac{\tau}{\tau_0}\right], \tag{35}$$

and only the order of magnitude of the numerical factor under the logarithm is known. If $s(1 + \delta) \ll 1$, then $t_k \ll t_\delta$, and on putting $t \sim t_k$ in (35) we see that (25) and (35) yield results that coincide within the limits of accuracy with which they have been obtained. If $s(1 + \delta) \gg 1$, then $t_\delta \ll t_k$ and (35) remains valid only in the region $\tau \ll t_\delta$. When $\tau \sim t_\delta$, formula (28) holds, while formula (25) applies when $\tau \gg t_\delta$.

Thus, if $\delta \ll 1$ the probability of bremsstrahlung can be represented in the form

$$W(p_0, k, \tau) = \frac{e^2}{6\pi k}\left[\frac{k^2}{p_0^2} G(s, \tau) + 2\frac{p_0^2 + (p_0 - k)^2}{p_0^2} \Phi(s, \tau)\right]. \tag{36}$$

When $s > 1$ we have $G(s, \tau) \approx \Phi(s, \tau) \approx \tau/\tau_0$, and when $s < 1$ the values of the functions G and Φ are as listed in the table.

The length of the interval τ_0, expressed in centimeters, is given by

$$\tau_0 = L / 2\pi \cdot 137\, \xi(s, \tau),$$

where L is the radiation-length unit, and the val-

	$\tau \ll \tau_0$	$\tau_0 \ll \tau \ll t_k$	$t_k \ll \tau$
Φ	τ/τ_0	$3 \ln (\tau/\tau_0)$	$(\tau/\tau_0)\, \Phi (s) + 3 \ln (1/s)$
G	τ/τ_0	6	$(\tau/\tau_0)\, G (s) + 6$
ξ	1	$\min \left\{2, \dfrac{\ln (190\, Z^{1/3} \sqrt{\tau/\tau_0})}{\ln 190\, Z^{1/3}}\right\}$	$\min \left\{2, \dfrac{\ln (190\, Z^{-1/3}\, s^{-1/2})}{\ln 190\, Z^{-1/3}}\right\}$

ues of the function $\xi(s, \tau)$ are listed in the table. For the parameter s we obtain

$$s = 1.37 \cdot 10^3\, [kL/p_0\, (p_0 - k)\, \xi\, (s, \tau)]^{1/2},$$

in which k and p_0 are measured in units of mc^2 and L is in centimeters. The interval $t_k = \tau_0/s$.

In order for the theory developed here to be valid it is essential that the probability of emission of more than one quantum during the passage through the plate be negligible.

4. PAIR PRODUCTION BY A QUANTUM IN A PLATE OF FINITE THICKNESS

We denote by $\widetilde{W}(k, q, \tau)$ the probability of production of a pair with an electron energy in the interval q, q + dq by a quantum of energy k in a plate of thickness τ.

An expression for W can be obtained by replacing $p_0 - k$ by $k - q$ and p_0 by q in (36), multiplying the result by the factor q^2/k^2, which takes the change in the statistical weight into account.

As a result we obtain

$$\widetilde{W}(k, q, \tau) = \frac{e^2}{6\pi k}\left\{G(\tilde{s}, \tau) + 2\,\frac{q^2 + (k-q)^2}{k^2}\,\Phi(\tilde{s}, \tau)\right\},$$

$$\tilde{s} = 1.37 \cdot 10^3\, [kL \,/\, q\, (k - q)\, \xi\, (\tilde{s}, \tau)]^{1/2}, \qquad (37)$$

and the functions G, Φ and ξ are listed in the table, in which the parameter s must now be replaced by $\tilde{s}$. In order for expression (37) to be valid it is essential that the condition $\widetilde{W} \ll 1$ be satisfied.

The author is most grateful to Prof. A. B. Migdal for suggesting the problem and for discussions, to V. D. Vaks for help in the earlier stages of the investigation, and to I. I. Gol'dman for an opportunity to read his paper[9] prior to publication.

APPENDIX

METHOD OF ACCOUNTING FOR THE POLARIZATION OF THE MEDIUM

We have seen that the method used above to calculate the polarization of the medium yields, in the limiting case when $k \gg \omega_p$, a result which is almost exact.[8] In order to explain the limits of the validity of this method, we present here an independent derivation.

Inasmuch as the polarization of the medium leads to the emission of quanta of energy much lower than the energy of the electron, we shall use the classical theory.

We denote by $\mathbf{A}_{01}$ and $\mathbf{A}_{02}$ the solutions of the equations

$$\Delta \mathbf{A}_{01} + k^2 \mathbf{A}_{01} = -4\pi e \int_{-\infty}^{\infty} \mathbf{v}\,(t)\, e^{ikt}\, \delta\, (\mathbf{r} - \mathbf{r}\,(t))\, dt,$$

$$\Delta \mathbf{A}_{02} + k^2 \varepsilon \mathbf{A}_{02} = -4\pi e \int_{-\infty}^{\infty} \mathbf{v}\,(t)\, e^{ikt}\, \delta\, (\mathbf{r} - \mathbf{r}\,(t))\, dt, \qquad (A1)$$

where $\mathbf{v}(t)$ is the velocity and $\mathbf{r}(t)$ is the radius vector of the particle at the instant t. When $t < 0$ we have $\mathbf{v} = \mathbf{v}_0$ and $\mathbf{r} = \mathbf{v}_0 t$. When $t > 0$ the particle is scattered. To take into account the influence of the boundary, we put

$$\mathbf{A} = \begin{cases} \mathbf{A}_{10} + \mathbf{A}_1', & z < 0 \\ \mathbf{A}_{20} + \mathbf{A}_2', & z > 0 \end{cases},$$

where $\mathbf{A}_1'$ and $\mathbf{A}_2'$ obey the homogeneous equations.

An elementary analysis of the boundary conditions in the plane $z = 0$ shows that $\mathbf{A}_2' = \mathbf{A}_{10} - \mathbf{A}_{20}$, accurate to terms proportional to $1 - v_0^2$ and $1 - \epsilon$, while $\mathbf{A}_1' \sim (1 - \epsilon)\mathbf{A}_{10}$. Thus, if the conditions $1 - v_0^2 \ll 1$ and $1 - \epsilon \ll 1$ are satisfied, we have

$$\mathbf{A}_2' \big|_{z=0} = (\mathbf{A}_{10} - \mathbf{A}_{20}) \big|_{z=0}. \qquad (A2)$$

With the aid of the Huygens principle we can obtain the form of $\mathbf{A}_2'$ when $z > 0$. As $r \to \infty$ we obtain for $\mathbf{A}_2'$

$$\mathbf{A}_2' \approx \frac{\tilde{k} e \exp (i\tilde{k}r)}{2\pi i r} \int_{z=0} \mathbf{A}_2\,(\boldsymbol{\rho}, 0) \exp (-i\tilde{\mathbf{k}}\boldsymbol{\rho})\, d\boldsymbol{\rho}, \qquad (A3)$$

where $\tilde{\mathbf{k}} = \sqrt{\epsilon} k \mathbf{r}/r$, and $\boldsymbol{\rho}$ is the radius vector in the plane $z = 0$.

With the aid of (A1) and (A2) we obtain, after simple transformations,

$$\mathbf{A}_2' = \frac{e \varepsilon v}{2\pi i k}\, \frac{\exp (i\tilde{k}r)}{r} \left\{\frac{\mathbf{v}_0}{1 - v_0^2 + \varepsilon v_0^2 \sin^2\theta} - \frac{\mathbf{v}_0}{1 - \varepsilon v_0^2 \cos^2\theta}\right\}. \qquad (A4)$$

In the derivation of this formula we made use of the fact that the greatest contribution to the values of $\mathbf{A}_{10k}$ and $\mathbf{A}_{20k}$ in the plane $z = 0$ is made by the negative values of t, during which the particle moves in a straight line.

Next, as $r \to \infty$ we have

$$\mathbf{A}_{20} \approx \frac{e}{2\pi ik}\frac{\exp(i\tilde{k}r)}{r}\left\{\frac{\mathbf{v}_0}{1-\sqrt{\varepsilon}\,v_0\cos\theta} + ik\int_0^{\infty}\exp[ikt - i\tilde{\mathbf{k}}\mathbf{r}(t)]\,\mathbf{v}(t)\,dt\right\}. \qquad \text{(A5)}$$

Adding (A4) and (A5) we see that if the conditions $1 - v^2 \ll 1$ and $1 - \epsilon \ll 1$ are satisfied, the first term in (A5) cancels the second term (A4) over a significant range of radiation angles, and therefore, in accordance with the assumption made in Sec. 2, the Fourier component of the radiation field can be represented in the form

$$\mathbf{A}_k(r) \approx \frac{e}{2\pi}\frac{\exp(ikr)}{r}\int_{-\infty}^{\infty}\exp[i\omega t - i\mathbf{k}\mathbf{r}(t)]\,\mathbf{v}(t)\,dt, \qquad \text{(A6)}$$

where we must put in the integration $\omega = k$ when $t < 0$ and $\omega = k/\sqrt{\epsilon}$ when $t > 0$.

[1] L. D. Landau and I. Ya. Pomeranchuk, Dokl. Akad. Nauk SSSR **92**, 537, 735 (1953).

[2] A. B. Migdal, ibid. **96**, 49 (1954).

[3] A. B. Migdal, ibid. **105**, 77, 237 (1955).

[4] A. B. Migdal, JETP **32**, 633 (1957), Soviet Phys. JETP **5**, 527 (1957).

[5] H. A. Bethe and W. Heitler, Proc. Roy. Soc. **A146**, 83 (1934).

[6] M. L. Ter-Mikaelyan, Dokl. Akad. Nauk SSSR **94**, 1033 (1954).

[7] V. L. Ginzburg and I. M. Frank, JETP **16**, 15 (1946).

[8] G. M. Garibyan, JETP **37**, 527 (1959), Soviet Phys. JETP **10**, 372 (1960).

[9] I. I. Gol'dman, JETP **38**, 1866 (1960), Soviet Phys. JETP **11**, 1342 (1960)

[10] A. S. Kompaneets, JETP **15**, 235 (1945).

[11] H. A. Bethe, Phys. Rev. **89**, 1256 (1955).

Translated by J. G. Adashko
32

SOVIET PHYSICS JETP VOLUME 12, NUMBER 1 JANUARY, 1961

ON THE INSTABILITY OF A PLASMA WITH AN ANISOTROPIC DISTRIBUTION OF VELOCITIES IN A MAGNETIC FIELD

R. Z. SAGDEEV and V. D. SHAFRANOV

Submitted to JETP editor February 25, 1960

J. Exptl. Theoret. Phys. (U.S.S.R.) **39**, 181-184 (July, 1960)

It is shown that a plasma situated in a uniform magnetic field is unstable even in the case of a weak temperature anistropy $|T_\perp - T_\parallel|/T_\perp \ll 1$. The instability is due to the charges in the "tail" of the velocity distribution which come into cyclotron resonance with the perturbing wave.

In this article we investigate the instability of a homogeneous plasma with ions (or electrons) having a non-Maxwellian velocity distribution. There exist two causes which lead to the instability of such a plasma: 1) the presence of a "beam" and 2) the anisotropy of "temperatures" parallel and perpendicular to the static magnetic field. In this article we investigate the instability due to the "temperature" anisotropy.

It has been shown earlier[1,2] in the "drift" approximation that in the case of a sufficiently strong anisotropy of the "temperatures" of the ions (or the electrons), an instability of convective type $\mathrm{Re}(\omega) \neq 0$ can occur. The so-called "drift" approximation utilized in these papers is valid only when the Larmor radii of all the particles are considerably smaller than the wavelengths of the perturbations, and the Larmor frequencies are correspondingly much higher than the oscillation frequencies.

In going over to higher frequencies we shall see that an instability of the type of "oscillation with hunting", $\mathrm{Re}(\omega) \neq 0$, will arise. However, it should be noted that even in the case of low frequency plasma oscillations the "tail" of the velocity distribution will generally speaking contain such particles for which the "drift" approximation will not be applicable as a result of the Doppler effect, and these particles cause the oscillations to build up even in the event of a small departure from an isotropic velocity distribution*.

We can easily obtain the dispersion equation for the plasma oscillations if we know the expression for the components of the tensor $\epsilon_{\alpha\beta}(\omega, \mathbf{k})$.

The general expression for the tensor $\epsilon_{\alpha\beta}(\omega, \mathbf{k})$ in the case of an anisotropic velocity distribution has been given in references 3 and 4. We take the unperturbed distribution function for the particles to be of the form

$$f(\mathbf{p})\,d\mathbf{p} = f(\varepsilon_\perp, \varepsilon_\parallel)\,d\mathbf{p}, \qquad \varepsilon_\perp = p_\perp^2/2m, \qquad \varepsilon_\parallel = p_\parallel^2/2m$$

($\epsilon_\perp$ and $\epsilon_\parallel$ are the energies of motion perpendicular and parallel to a line of force of the magnetic field). In this case the components of the tensor $\epsilon_{\alpha\beta}$ have the following form [the z axis is directed along the magnetic field, the time dependence is taken to be of the form $\exp(-i\omega t)$, $\mathbf{k} = \{k_x, 0, k_z\}$]:

$$\varepsilon_{xx} = 1 + \sum \frac{m\omega_0^2}{\omega} \int d\mathbf{p} \sum_{n=-\infty}^{\infty} \left(-i\pi\delta_+ F_1 + \frac{1}{\omega} F_2\right) \frac{n^2\omega_H^2}{k_x^2} J_n^2,$$

$$\varepsilon_{xy} = -\varepsilon_{yx}$$

$$= -i \sum \frac{m\omega_0^2}{\omega} \int d\mathbf{p} \sum_{n=-\infty}^{\infty} \left(-i\pi\delta_+ F_1 + \frac{1}{\omega} F_2\right) \frac{n\omega_H v_\perp}{k_x} J_n J_n',$$

$$\varepsilon_{yy} = 1 + \sum \frac{m\omega_0^2}{\omega} \int d\mathbf{p} \sum_{n=-\infty}^{\infty} \left(-i\pi\delta_+ F_1 + \frac{1}{\omega} F_2\right) v_\perp^2 J_n'^2,$$

$$\varepsilon_{xz} = \varepsilon_{zx}$$

$$= \sum \frac{m\omega_0^2}{\omega} \int d\mathbf{p} \sum_{n=-\infty}^{\infty} [-i\pi(\omega - n\omega_H)\delta_+ - 1] F_1 \frac{n\omega_H}{k_x k_z} J_n^2,$$

$$\varepsilon_{yz} = -\varepsilon_{zy} = i \sum \frac{m\omega_0^2}{\omega} \int d\mathbf{p}$$

$$\times \sum_{n=-\infty}^{\infty} [-i\pi(\omega - n\omega_H)\delta_+ - 1] F_1 \frac{v_\perp}{k_z} J_n J_n',$$

$$\varepsilon_{zz} = 1 + \sum \frac{m\omega_0^2}{\omega} \int d\mathbf{p}$$

$$\times \sum_{n=-\infty}^{\infty} [-i\pi(\omega - n\omega_H)\delta_+ - 1] F_1 \frac{\omega - n\omega_H}{k_z^2} J_n^2. \tag{1}$$

Here J_n is the Bessel function,

---

*After his trip to Harwell, M. A. Leontovich quoted Mittelman as saying that M. Rosenbluth had investigated the instability of a plasma with a weak temperature anisotropy. Unfortunately we have no further details as to Rosenbluth's formulation of his problem.

$$\delta_+ = \delta_+(\omega - n\omega_H - k_z v_z), \quad \delta_+(x) = i/\pi x + \delta(x),$$
$$\omega_0^2 = 4\pi n_0 e^2/m, \quad J_n = J_n(k_x v_\perp/\omega_H),$$
$$F_1 = \frac{\partial f}{\partial \varepsilon_\parallel} + \frac{n\omega_H}{\omega}\left(\frac{\partial f}{\partial \varepsilon_\perp} - \frac{\partial f}{\partial \varepsilon_\parallel}\right), \quad F_2 = \frac{\partial f}{\partial \varepsilon_\perp} - \frac{\partial f}{\partial \varepsilon_\parallel}. \qquad (2)$$

The first summation in (1) is taken over the kinds of charges. It may be seen that the sign of the anti-hermitian part of $\epsilon_{\alpha\beta}$ depends on F_1. In the case of an isotropic distribution function $F_1 = \partial f/\partial \epsilon_\parallel < 0$. This corresponds to damping of the oscillations.

The presence of an anisotropy in the distribution may lead to a change in the sign of the anti-hermitian part of $\epsilon_{\alpha\beta}$. It is obvious that this can occur when

$$\omega < n\omega_H\left(1 - \frac{\partial f/\partial \varepsilon_\perp}{\partial f/\partial \varepsilon_\parallel}\right) \qquad \left(n > 0, \quad \left|\frac{\partial f}{\partial \varepsilon_\perp}\right| < \left|\frac{\partial f}{\partial \varepsilon_\parallel}\right|\right),$$
$$\omega < |n|\,\omega_H\left(\frac{\partial f/\partial \varepsilon_\perp}{\partial f/\partial \varepsilon_\parallel} - 1\right) \qquad \left(n < 0, \quad \left|\frac{\partial f}{\partial \varepsilon_\perp}\right| > \left|\frac{\partial f}{\partial \varepsilon_\parallel}\right|\right). \quad (3)$$

Since the possible instability is associated with cyclotron resonance ($n \neq 0$) it is useful to investigate the simplest case in which this resonance appears — a wave propagated parallel to the field, $k_x = k_y = 0$, $k_z = k$. In this case the dispersion relation for the two types of circularly polarized waves has the form

$$N^2 = 1 + \sum \omega_0^2 \int d\mathbf{p} \left\{\varepsilon_\perp \left[-i\pi\delta_+(\omega \pm \omega_H - k_z v_z)\right] \times \left[\frac{\partial f}{\partial \varepsilon_\parallel} \mp \frac{\omega_H}{\omega}\left(\frac{\partial f}{\partial \varepsilon_\perp} - \frac{\partial f}{\partial \varepsilon_\parallel}\right)\right] + \frac{1}{\omega}\left(\frac{\partial f}{\partial \varepsilon_\perp} - \frac{\partial f}{\partial \varepsilon_\parallel}\right)\right\}. \qquad (4)$$

We consider first the case of ion oscillations. For the sake of simplicity we restrict ourselves to the case $kv_\parallel \ll \omega$, which corresponds to the condition $8\pi p_\parallel \ll H^2$ ($p_\parallel = n_0\epsilon_\parallel$). According to (3), in the case of a weak temperature anisotropy the instability may occur when $\omega \ll \omega_{Hi}$. In this case, neglecting the thermal corrections to the hermitian part of $\epsilon_{\alpha\beta}$, we obtain

$$N^2 = \frac{k^2c^2}{\omega^2} = \frac{c^2}{c_H^2} - i\pi\frac{\omega_0^2}{\omega} \times \int d\mathbf{p} \left\{\varepsilon_\perp \left[\frac{\partial f}{\partial \varepsilon_\parallel} \pm \frac{\omega_H}{\omega}\left(\frac{\partial f}{\partial \varepsilon_\perp} - \frac{\partial f}{\partial \varepsilon_\parallel}\right)\right]\delta(\omega \mp \omega_H - k_z v_z)\right\}.$$

In the case of $\mathrm{Re}(\omega) \gg \mathrm{Im}(\omega)$ we have

$$\omega^2 = k^2 c_H^2 + i\pi\frac{\omega_0^2 k c_H^2}{c^2} \times \int d\mathbf{p} \left\{\varepsilon_\perp \left[\frac{\partial f}{\partial \varepsilon_\parallel} \pm \frac{\omega_H}{\omega}\left(\frac{\partial f}{\partial \varepsilon_\perp} - \frac{\partial f}{\partial \varepsilon_\parallel}\right)\right]\delta(\omega \mp \omega_H - k_z v_z)\right\}. \qquad (5)$$

When the integrand in expression (5) is positive the imaginary part of ω is positive, and in the case when the time dependence is given by $\exp(-i\omega t)$ this leads to building up of oscillations. If we take for f the "Maxwellian" distribution function

$$f = \frac{m}{2\pi T_\perp}\left(\frac{m}{2\pi T_\parallel}\right)^{1/2} \exp\left\{-\frac{\varepsilon_\perp}{T_\perp} - \frac{\varepsilon_\parallel}{T_\parallel}\right\},$$

then the maximum increment occurs when

$$k = \frac{\omega_{Hi}}{c_H}\left|1 - \frac{T_\perp}{T_\parallel}\right|\left[1 - \frac{T_\parallel}{Mc_H^2}\left(1 - \frac{T_\perp}{T_\parallel}\right)^2\right].$$

The corresponding frequency is given by

$$\omega = \omega_{Hi}\frac{|T_\perp - T_\parallel|}{T_\perp} + i\omega_{0i}\frac{T_\perp}{\sqrt{2T_\parallel Mc^2}}\exp\left\{-\frac{H^2}{8\pi n T_\parallel}\frac{T_\parallel^2}{(T_\perp - T_\parallel)^2}\right\}. \qquad (6)$$

For $T_\perp > T_\parallel$ that wave builds up, for which the electric vector rotates in the direction of rotation of the ions. For $T_\perp < T_\parallel$ the wave of opposite polarization is built up.

In the case of electron oscillation with $\omega < \omega_{He}$, only the so-called extraordinary wave exists, in which the electric vector rotates in the direction of rotation of the electrons. The instability in this case occurs only for one sign of the anisotropy $T_\perp > T_\parallel$. For $kv_\parallel \ll \omega$ and $\omega_{0e}^2 \gg \omega_{He}^2$, the dispersion equation for the electron oscillations has the form

$$\frac{k^2c^2}{\omega^2} = \frac{\omega_{0e}^2}{\omega\omega_{He}} + i\sqrt{\pi}\,\frac{\omega_{0e}^2}{\omega k v_\parallel}\exp\left(-\frac{\omega_{He}^2}{k^2 v_\parallel^2}\right)\left\{\frac{T_\perp}{T_\parallel} + \frac{\omega_{He}}{\omega}\left(1 - \frac{T_\perp}{T_\parallel}\right)\right\}.$$

Just as in the case of the ion oscillations, we obtain for waves having the greatest build-up rate:

$$\omega = \omega_{He}\frac{T_\perp - T_\parallel}{T_\perp} + i\frac{\sqrt{\pi}}{4}\omega_{0e}\left(\frac{T_\perp - T_\parallel}{T_\perp}\right)^{3/2}\frac{T_\perp}{T_\parallel}\left(\frac{2T_\parallel}{mc^2}\right)^{1/2} \times \exp\left\{-\frac{H^2}{8\pi n T_\parallel}\frac{T_\perp}{T_\perp - T_\parallel}\right\}. \qquad (7)$$

As follows from the expressions just given, the rate of build up of the waves is determined by those ions (or electrons) contained in the velocity distribution, in whose rest frame the frequency of the wave is equal to their cyclotron frequency as a result of the Doppler effect. Such particles can effectively exchange energy with the wave. The bal-

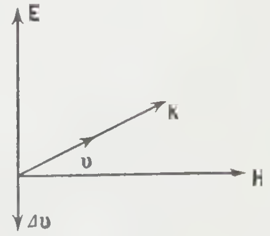

ance between absorption and emission of energy by the particles is determined by the change in the distribution function, which is proportional to the quantity

$$\{\mathbf{E} + c^{-1}[\mathbf{v} \times \mathbf{H}]\}\partial f/\partial \mathbf{p}.$$

On taking account of $\mathbf{H} = c\omega^{-1}[\mathbf{k} \times \mathbf{E}]$, this expression takes the form $(k_\perp = 0,\ E_\| = 0)$

$$-E_\perp v_\perp \{\partial f/\partial \varepsilon_\perp - k_z v_z \omega^{-1}(\partial f/\partial \varepsilon_\perp - \partial f/\partial \varepsilon_\|)\}, \qquad (8)$$

where, as before, $\epsilon_\perp$ and $\epsilon_\|$ are the transverse and the longitudinal kinetic energies.

The first term in this expression corresponds to that fraction of the particles whose velocities have been increased in the direction of the electric field $E_\perp$, while the second term corresponds to that fraction of the particles whose longitudinal velocities have been altered by the magnetic field. When $k_z v_z > 0$, this change in velocity is obviously directed opposite to the electric field (see diagram). In this case the particles are retarded and give up their energy to the wave. The last term corresponds to that fraction of the particles whose transverse velocities have been altered by the magnetic field of the wave. Its sign is opposite to that of the second term, so that in the case of an isotropic velocity distribution the last two terms compensate for each other.

The conditions of resonance with the electric field are satisfied by particles of velocity v_z, determined from $\omega - n\omega_H - k_z v_z = 0$. For $n < 0$ we have $k_z v_z > 0$, and the instability is caused by particles whose longitudinal velocities have been altered by the magnetic field of the wave; for $n > 0$, when $k_z v_z < 0$ the building up of the wave is due to particles whose transverse velocity has been altered by the magnetic field of the wave.

We note that the instability which we have investigated will not occur for arbitrarily small anisotropy. For any velocity distribution there exists a limiting velocity v_{lim} (which is in any case smaller than the velocity of light). We then obtain from the resonance condition $\omega - \omega_H - k_z v_{lim} = 0$, for the limiting velocity v_{lim}, the minimum frequency $\omega_{min} = \omega_H(1 + v_{lim}/c_H)^{-1}$ In accordance with (6) the instability will occur when $|\Delta T|/T > (1 + v_{lim}/c_H)^{-1}$.

The authors are grateful to academician M. A. Leontovich and to B. B. Kadomtsev for useful discussions of the results of this work.

---

[1] A. A. Vedenov and R. Z. Sagdeev, Collection Физика плазмы и проблема управляемых термоядерных реакций (Plasma Physics and the Problem of Controlled Thermonuclear Reactions), Acad. Sci. U.S.S.R., 1958, vol. 3, p. 278.

[2] L. I. Rudakov and R. Z. Sagdeev, ibid. vol 3, p. 268.

[3] V. D. Shafranov, ibid. vol. 4, p. 416.

[4] R. Z. Sagdeev and V. D. Shafranov, Papers presented by Soviet Scientists at the 2nd Geneva Conference on the Peaceful Uses of Atomic Energy, 1958, Publ. by Glavatom, paper No. 2215.

Translated by G. Volkoff.
33

SOVIET PHYSICS JETP VOLUME 12, NUMBER 1 JANUARY, 1961

THE MICROSCOPIC THEORY OF THE FERMI LIQUID

V. I. KARPMAN

Minsk Pedagogical Institute

Submitted to JETP editor February 26, 1960

J. Exptl. Theoret. Phys. (U.S.S.R.) **39**, 185-188 (July, 1960)

A connection is established between the Fermi excitation energies as defined by the Landau theory of the Fermi liquid and by the many-particle quantum theory at zero temperature.

At the present time a number of papers[1-4] discuss the microscopic derivation of the fundamental premises of Landau's general theory of the Fermi liquid.[5] Landau[3] obtained a most essential result by establishing the exact microscopic meaning of the function $f(\mathbf{p}, \mathbf{p}')$, which plays a fundamental part in the theory of the Fermi liquid and determines the variation of the quasi-particle energies ϵ_p under infinitesimal changes in their distribution functions $n(p)$

$$\delta\varepsilon_p = \mathrm{Sp}_\sigma \int f(\mathbf{p}, \mathbf{p}')\, \delta n(\mathbf{p}')\, d\tau'. \tag{1}$$

As regards the quasi-particle energy, the following must be kept in mind. In the theory of the Fermi liquid, ϵ_p is defined as the variational derivative of the total energy of the system with respect to the distribution function $n(p)$

$$\varepsilon_p = \delta E / \delta n(p). \tag{2}$$

On the other hand, in the general many-particle quantum theory, it has been shown[6,7] that the energies and attenuations of the Fermi excitations of the system (quasi-particles or holes), for momenta close to the boundary, are determined by the poles of the one-particle Green's function in the momentum representation

$$G(p, \varepsilon) = [\varepsilon_p^0 - \varepsilon - \Sigma(p, \varepsilon)]^{-1},$$

$$\varepsilon_p^0 = p^2/2m, \tag{3}$$

along the lower half-plane (for quasi-particles) or the upper half-plane (for holes). From this we obtain the following equations for the energy ϵ_p and the attenuation Γ_p of a quasi-particle:

$$\varepsilon_p^0 - \varepsilon_p - \Sigma_0(p, \varepsilon) = 0; \tag{4}$$

$$\Gamma_p = \Sigma_1(p, \varepsilon_p) \,/\, [1 + (\partial\Sigma_0 / \partial\varepsilon)_{\varepsilon=\varepsilon_p}], \tag{4a}$$

where $\Sigma_0 = \mathrm{Re}\Sigma$, $\Sigma_1 = \mathrm{Im}\Sigma$, and Σ is the compact part of the self energy of the particle. Obviously, it is to be expected that the quantity ϵ_p, defined by the relation (2), should agree with the root of Eq. (4). The aim of the present communication is to prove this statement.

We shall make some preliminary observations. It has been shown[6,8] that the imaginary part of the Green's function, and therefore also the attenuation, change sign at $\epsilon = \mu$, where $\mu = \partial E/\partial N$ is the chemical potential of the system. To supplement this theorem, which is completely general in character, we shall make the assumption that the imaginary part of the self energy is continuous at $\epsilon = \mu$, i.e.,

$$\lim_{\varepsilon \to \mu} \Sigma_1(p, \varepsilon) = 0 \tag{5}$$

[we note that this assumption serves as the basis for the derivation of (4) and (4a)].

Let us now consider the equation $\epsilon_p = \mu$ (relative to p), which, according to (4), can also be written in the form

$$\varepsilon_p^0 - \mu - \Sigma(p, \mu) = 0. \tag{6}$$

The root (p_0) of this equation is the limiting momentum for the quasi-particles $\epsilon(p_0) = \mu$.

Using an expansion in powers of the interaction constant, Hugenholtz and van Hove[9] (see also reference 7) showed that p_0 coincides with the limiting Fermi momentum for an ideal gas:

$$p_0 = (3\pi^2 N)^{1/3} \quad (\hbar = 1), \tag{7}$$

where N is the number of particles in the system, whose volume is taken to be unity. This theorem may prove to be incorrect under conditions in which perturbation theory is inapplicable. For instance, for systems displaying superconductivity, Eq. (6) has in general no real solution*.[10] In our work it has been assumed that perturbation theory is applicable. We also assume that the forces acting between particles are paired.

---

*In this connection we note that it follows from Landau's results, obtained without the aid of perturbation theory (see footnote 3 of reference 4), that if (6) has a real root, it coincides with (7).

Let us now undertake the quantum-mechanical determination of $\delta E/\delta n(p)$ (we assume that $T = 0$), starting from the assumptions given above. In doing so we shall use, in a definite manner, the idea used by Klein and Prange[7] for the proof of the cited theorem of Hugenholtz and van Hove.

Let us consider any diagram which makes a contribution to the total energy of the system, for example one of those in the figure. The dotted lines correspond to the expression

$$iu(k) = i\int U(x) \exp(ikx)\, d^4x, \quad U(x) = v(\mathbf{x})\, \delta(x_0),$$

where $v(\mathbf{x})$ is the potential of the interaction between the particles, the vertex corresponds to a delta function expressing the law of conservation of the 4-momentum, and the full line corresponds to the Green's function of the non-interacting particles

$$G_0(\mathbf{p}, \varepsilon) = (\varepsilon_p^0 - \varepsilon - i\delta)^{-1},$$

$$\delta \to +0 \ \text{for}\ p > p_0; \quad \delta \to -0 \ \text{for}\ p < p_0. \tag{8}$$

To obtain the energy of the system as a functional of the occupation numbers of the quasi-particles, we express (8) in the form

$$G(p, \varepsilon) = P\frac{1}{\varepsilon_p^0 - \varepsilon} + i\pi(1 - 2n(p))\,\delta(\varepsilon_p^0 - \varepsilon), \tag{9}$$

where $n(p)$ are the occupation numbers of the non-interacting particles at $T = 0$

$$n(p) = \begin{cases} 1 & (p < p_0) \\ 0 & (p > p_0) \end{cases}. \tag{10}$$

In what follows it is important that the occupation numbers of the non-interacting particles coincide with the occupation numbers of the quasi-particles in the ground state and in states differing infinitesimally from the ground state.

The expression for the total energy will have the form

$$E = E_0 - S(\Omega), \tag{11}$$

where E_0 is the energy of the non-interacting fermions, which can be expressed in the form

$$E_0 = \int \varepsilon_p^0 n(p)\, d^3p; \quad d^3p = dp_x\, dp_y\, dp_z / (2\pi)^3, \tag{12}$$

and $S(\Omega)$ is the sum of the contributions of all the corrected diagrams. The quantity Ω corresponding to an n-th order diagram has the following form:

$$\Omega = \alpha(-1)^l(-i)^n \int d^4k_1 \ldots \int d^4k_n \int d^4q_1 \ldots \int d^4q_{2n} \prod_{j=1}^{2n-1} \delta_j$$
$$\times\, u(k_1) \ldots u(k_n)\, G_0(q_1) \ldots G_0(q_{2n}), \tag{13}$$

where $d^4q = dq_x\, dq_y\, dq_z\, dq_0/(2\pi)^4$, l is the number of closed loops, δ_j is the delta function located at one of the vertices, and the factor α can take on one of the two values 1 or ½ (see below).

Each of the Green's functions $G_0(q) = G_0(\mathbf{q}, q_0)$ in (13) depends on the occupation numbers $n(\mathbf{q})$. Hence Ω is a functional of $n(\mathbf{q})$. Upon evaluating $\delta\Omega/\delta n(\mathbf{q})$ we obtain 2n terms, some one of the functions $G_0(q_i)$ being varied in each term. In the remaining quantities, $n(\mathbf{q})$ is equal to its value at $T = 0$ [see Eq. 10)]. Thus, each of the 2n components has the form

$$-i\frac{\delta}{\delta n(\mathbf{p})}\int G_0(\mathbf{q}, q_0)\, \Sigma_R^{(i)}(\mathbf{q}, q_0)\, d^4q, \quad i = 1, \ldots, 2n, \tag{14}$$

where in performing the variation it is only the function G_0 which need be assumed to depend on $n(\mathbf{q})$. Substituting into this the expression for G_0 from (9) and performing the variation, we obtain instead of (14),

$$-\int \Sigma_R^{(i)}(\mathbf{p}, \varepsilon)\, \delta(\varepsilon - \varepsilon_p^0)\, d\varepsilon = -\Sigma_R^{(i)}(\mathbf{p}, \varepsilon_p^0). \tag{15}$$

The function $\Sigma_R^{(i)}(\mathbf{p}, \epsilon)$, from its definition contained in (14), is represented by a diagram obtained by eliminating one of the full lines in the total energy diagram (see the figure). Consequently $\Sigma_R^{(i)}$ corresponds to one of the diagrams of particle self energy (generally speaking, a non-compact one).

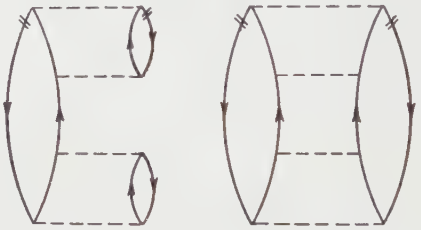
a b

We now observe that in some of the total-energy diagrams it is possible to obtain one and the same self-energy diagram by eliminating either of two different lines (see b in the figure). This effect is compensated by the factor α in (13), which, as Klein and Prange have shown[7] is equal to ½ for such diagrams, and to unity in the remaining cases. Finally, it can be stated that variation of $S(\Omega)$ yields the totality of all possible self-energy diagrams for the particles, each diagram being counted only once, i.e.,

$$\delta S(\Omega) / \delta n_p = -\Sigma_R(p, \varepsilon_p^0), \tag{16}$$

where the index R indicates that non-compact as well as compact diagrams enter into (16). In view of (11), (12), and (16) we obtain

$$\delta E/\delta n(p) = \varepsilon_p^0 - \Sigma_R(p, \varepsilon_p^0). \tag{17}$$

For Σ_R we may write the expansion

$$\Sigma_R(p, \varepsilon) = \Sigma + \Sigma G_0 \Sigma + \Sigma G_0 \Sigma G_0 \Sigma + \ldots, \tag{18}$$

where $\Sigma(p, \epsilon)$ is the compact portion of the self energy of the particle. The right-hand side of (18) has a singularity at $\epsilon = \epsilon^0_p$. Nevertheless, the quantity $\Sigma_R(p, \epsilon^0_p)$ can be assigned a definite value by following the method described in the appendix to Klein and Prange's paper.[7]

Let us first put $p = p_0$. In this case the imaginary part of the self energy (and consequently the attenuation) is equal to zero. It follows from (15) that when $\epsilon = \epsilon^0_{p_0}$, $\Sigma_R(p_0, \epsilon)$ must be taken to mean*

$$\lim_{\varepsilon \to \varepsilon^0_{p_0}} \Sigma_R(p_0, \varepsilon) = \int \Sigma_R(p_0, \varepsilon)\, \delta(\varepsilon - \varepsilon^0_{p_0})\, d\varepsilon. \qquad (19)$$

As shown in the appendix to reference 7, it follows from (18) and (19) that

$$\Sigma_R(p_0, \varepsilon^0_{p_0}) = \Sigma(p_0, \varepsilon_{p_0}), \qquad (20)$$

where ϵ_{p_0} is the energy of a quasi-particle with a momentum equal to the limiting momentum p_0. Consequently,

$$\delta E / \delta n(p_0) = \varepsilon_{p_0}, \qquad (21)$$

where ϵ_{p_0} satisfies Eq. (4), q.e.d.

Turning to the case $p \neq p_0$, we note that here the attenuation is not equal to zero. The concept of quasi-particle energy is meaningful only when the attenuation, and therefore also the imaginary part of the self energy, are sufficiently small and can be neglected. According to our assumption of the continuity of $\operatorname{Im} \Sigma$ at $\epsilon \sim \mu$, this will be the case if p is sufficiently close to p_0. Neglecting the imaginary part of Σ for these values of p, and repeating the considerations which led to (20) and (21), we obtain

$$\delta E / \delta n(p) \approx \varepsilon_p,$$

where ϵ_p satisfies Eq. (4), and p is sufficiently close to p_0. When $p = p_0$ this equation becomes exact.

The author expresses sincere thanks to E. S. Fradkin, L. P. Gor'kov, and D. A. Kirzhnits for valuable discussions and critical comments.

---

[1] A. A. Abrikosov and I. M. Khalatnikov, JETP **33**, 1154 (1957), Soviet Phys. JETP **6**, 888 (1958).

[2] V. M. Galitskiĭ, JETP **34**, 151 (1958), Soviet Phys. JETP **7**, 104 (1958).

[3] L. D. Landau, JETP **35**, 97 (1958), Soviet Phys. JETP **8**, 70 (1959).

[4] L. P. Pitaevskiĭ, JETP **37**, 1794 (1959), Soviet Phys. JETP **10**, 1267 (1960).

[5] L. D. Landau, JETP **30**, 1058 (1956) and **32**, 59 (1957), Soviet Phys. JETP **3**, 920 (1956) and **5**, 101 (1957).

[6] V. M. Galitskiĭ and A. B. Migdal, JETP **34**, 139 (1958), Soviet Phys. JETP **7**, 91 (1958).

[7] A. Klein and R. Prange, Phys. Rev. **112**, 994 (1958), Probl. Sovr. Fiz. **3**, 66 (1959).

[8] L. D. Landau, JETP **34**, 262 (1958), Soviet Phys. JETP **7**, 182 (1958).

[9] N. M. Hugenholtz and L. van Hove, Physica **24**, 363 (1958).

[10] L. P. Gor'kov, JETP **34**, 735 (1958), Soviet Phys. JETP **7**, 505 (1957).

Translated by D. C. West
34

---

*In view of the singularity of $\Sigma_R(p_0, \varepsilon)$ at $\varepsilon = \varepsilon^0_{p_0}$, formula (19) is by no means a trivial consequence of the definition of the δ-function.

SOVIET PHYSICS JETP VOLUME 12, NUMBER 1 JANUARY, 1961

ELECTRONIC LEVELS OF ATOMS OF SUPER-HEAVY ELEMENTS

V. V. VORONKOV and N. N. KOLESNIKOV

Moscow State University

Submitted to JETP editor February 28, 1960

J. Exptl. Theoret. Phys. (U.S.S.R.) **39**, 189-191 (July, 1960)

On the basis of the Dirac equation, the behavior of electronic ns-levels in the field of a nucleus of finite size with $Z > 137$ is investigated in the neighborhood of $\epsilon \sim -m$ and $\epsilon \sim +m$. The critical values $Z = Z_{cr}$ are found, the existence of quasilevels for $\epsilon \sim -m$ and $Z > Z_{cr}$ is shown and an interpretation of them is given.

1. The question of the properties of electronic levels of super-heavy nuclei has taken on renewed interest recently in connection with the obtaining of new transuranic elements. In order to estimate the position of electronic ns levels, we shall for simplicity choose the potential of a nucleus with charge Ze in the form $V = -\alpha Z/r$ for $r > r_0$ and $V = -\alpha Z/r_0$ for $r < r_0$, where r_0 is the nuclear radius. From the conditions for matching the solutions of the Dirac equation at $r = r_0$, we then find, for $Z > 137$ and $mr_0 \ll 1$ (m is the electron mass), the following equation for determining the level energy ϵ:

$$\varphi_0 + \varphi_\varepsilon = -n\pi, \tag{1}$$

where on the left the part depending on ϵ is equal to

$$\varphi_\varepsilon = \arg\Gamma\left(ig - \frac{\gamma\varepsilon}{\lambda}\right) + g\ln\frac{\lambda}{m} + \tan^{-1}\frac{g}{(1+\gamma/W)},$$

and

$$\varphi_0 = g\ln 2mr_0 - \arg\Gamma(1+2ig) - \tan^{-1}\frac{g}{\gamma}\tan\gamma.$$

Here

$$\gamma = \alpha Z, \quad g = \sqrt{\gamma^2 - 1}, \quad \lambda = \sqrt{m^2 - \varepsilon^2}, \quad W = (m+\varepsilon)/\lambda.$$

Equation (1) coincides with the corresponding equation of the paper by Pomeranchuk and Smorodinskiĭ[1] if the following correction is made in the latter: $\zeta(\gamma) = \gamma\cot\gamma - 1$ should be replaced by $(1 - \gamma\cot\gamma)^{-1}$. For $\epsilon = -m$ and $n = 1$, we find from (1) the equation for the determination of Z_{cr}:

$$g\ln 2mr_0\gamma = \arg\Gamma(1+2ig) + \tan^{-1}\frac{g}{\gamma}\tan\gamma - n\pi. \tag{2}$$

Z_{cr} has a weak dependence on r_0 and is equal to 178 for $r_0 = 12 \times 10^{-13}$ cm and 172 for $r_0 = 8 \times 10^{-13}$ cm (instead of the values 200 and 175 of reference 1). For nuclei on the β-stability curve[2] extrapolated to the region of super-heavy nuclei and for $r_0 = 1.2 \times 10^{-13}A^{1/3}$ cm, we find $Z_{cr} = 174$.

2. We now consider the character of the discrete levels near the limit of the continuous spectrum: $\epsilon = m$ ($Z > 137$). Noting that for $\epsilon \to +m$, $\lambda \to 0$, and using the asymptotic formula for $\arg\Gamma(ig - \gamma\epsilon/\lambda)$ for $\gamma\epsilon/\lambda \to \infty$, we find from (1)

$$\tan^{-1}\frac{\tanh\pi g}{\tan\pi N} = -\pi n + \psi_0 - g\ln 2mr_0,$$

$$\varepsilon = m/\sqrt{1+\gamma^2/N^2},$$

$$\psi_0 = \arg\Gamma(1+2ig) + \tan^{-1}\frac{g}{\gamma}\tan\gamma - g\ln\gamma - \tan^{-1}g, \tag{3}$$

where $N = \gamma\epsilon/\lambda$ has the significance of an "effective" principal quantum number. Furthermore, we find from (3),

$$N = n + \frac{1}{\pi}\tan^{-1}\frac{\tanh\pi g}{\tan(\psi_0 - g\ln 2mr_0)}, \tag{4}$$

whereas for a pure Coulomb field for $Z < 137$ we have $N = n + \sqrt{1-\gamma^2}$.[3] As r_0 is decreased the levels are pushed downward. From (3) it follows that the rate at which the levels with principal quantum number N are pushed is characterized by the derivative

$$dN/dr_0 = g(\tan^2\pi g\cos^2\pi N + \sin^2\pi N)/r_0\pi\tanh\pi g,$$

which is a minimum for $N = n$ [so that $(\pi r_0/g) \times dN/dr_0 = \tanh\pi g$], i.e. when the spectrum of the cut-off Coulomb field in the region $\epsilon \sim m$ and $Z > 137$ coincides with the spectrum of the Coulomb field for $Z = 137$. dN/dr_0 is a maximum for $N = n + 1/2$ [then $(\pi r_0/g)\,dN/dr_0 = (\tanh\pi g)^{-1}$], i.e. when the spectrum differs most from the spectrum of the pure Coulomb field for $Z = 137$. This effect is especially important for Z only slightly exceeding 137.

3. Let us now illustrate on the example of a potential well of radius r_0 the appearance of quasilevels in the region $\epsilon < -m$ after the pushing of the lowest discrete level to $-m$. For $U = U_{cr} + \Delta$

(U is the well depth, U_{cr} corresponds to Z_{cr}, $\Delta > 0$ and small), the lowest discrete level disappears. Matching the external (e) and internal (i) solutions of the Dirac equation[3] for $\epsilon = -m - w$ ($w > 0$ and small):

$$G_i = \sin kr, \quad G_e = A \sin (pr + \alpha),$$

$$F_i = \frac{p}{U}\left(\cos kr - \frac{\sin kr}{kr}\right),$$

$$F_e = -\frac{Ap}{w}\left(\cos (pr + \alpha) - \frac{\sin (pr + \alpha)}{pr}\right),$$

$$k = \sqrt{(\varepsilon + U)^2 - m^2}, \quad p = \sqrt{\varepsilon^2 - m^2},$$

we get

$$\cot \beta = (1/pr_0)(1 - \pi w/U\delta), \quad \beta = \alpha + pr_0,$$

$$\delta = (r_0^2/\pi)(U_{cr} - m)(\Delta - w).$$

In this case $G_e \ll F_e$ so that G_e and G_i can be disregarded in what follows. The ratio of the amplitude F_e to F_i, which is equal to $2mU_{cr}\delta/\pi\rho \sin \beta$, is anomalously small for $\beta \sim \pi/2$, i.e. for

$$w = \Delta (mr_0^2 U_{cr} + \pi^2) / (mr_0^2 U_{cr} + 2\pi^2). \qquad (5)$$

This indicates the possible existence in this energy region of a quasistationary state — a quasilevel.

In fact, solving the Dirac equation with the condition of outgoing waves at infinity $\sim e^{ipr}/r$ and $\epsilon = -m - w - i\Gamma$, we find formula (5) for w, and a level width

$$\Gamma = w^{3/2} (\sqrt{2m}\pi^2 r_0^2) / (2\pi^2 + mr_0^2 U_{cr}). \qquad (6)$$

One can give an interpretation of the behavior of the electron-positron system starting from the second-quantized Hamiltonian of the system. For $U < U_{cr}$ the state Φ^0, in which the lower continuum is filled, is finite and neutral, just as for $U = 0$.

The state Φ', in which the lowest discrete level ϵ, (with degeneracy η_1) is also filled, has a charge $-\eta_1 e$ and is finite in the neighborhood of $U = U_{cr}$, since for $U = U_{cr}$ the gap separating Φ' from the continuous spectrum of states with the same charge is finite (this gap is $\epsilon_2 - \epsilon_1$ where ϵ_2 is the next level after ϵ_1). But then for $U > U_{cr}$ all the neutral states are infinite, since they are obtained from Φ' by the application of η_1 annihilation operators corresponding to the lower continuum. Since as shown above there are quasilevels in the lower continuum, this corresponds to a quasi-stationary state Φ^{*0} which decays with emission of η_1 positrons with a lifetime $1/2\Gamma$.

The authors thank Prof. D. D. Ivanenko for discussion of the results.

---

[1] I. M. Pomeranchuk and Ya. A. Smorodinskiĭ, J. of Phys. U.S.S.R 9, 97 (1945).

[2] N. N. Kolesnikov, JETP 30, 889 (1956), Soviet Phys. JETP 3, 844 (1957).

[3] A. I. Akhiezer and V. B. Berestetskiĭ, Квантовая электродинамика (Quantum Electrodynamics), Fizmatgiz, (1959).

Translated by M. Hamermesh
35

SOVIET PHYSICS JETP VOLUME 12, NUMBER 1 JANUARY, 1961

RAMAN SCATTERING OF LIGHT NEAR SECOND-ORDER PHASE-TRANSITION POINTS

V. I. GINZBURG and A. P. LEVANYUK

P. N. Lebedev Physics Institute, Academy of Sciences, U.S.S.R.

Submitted to JETP editor March 5, 1960

J. Exptl. Theoret. Phys. (U.S.S.R.) **39**, 192-196 (August, 1960)

The spectral composition of light scattered in crystals near second-order phase-transition points is studied (quartz, ferroelectrics). It is shown that the "critical opalescence" which appears in such cases when the critical Curie point is approached is closely related to the Raman scattering of light.

NEAR second-order phase-transition points there appear, as is well known, fluctuations of the parameters η_i, characteristic of the given transition (for instance, in the case of ferroelectrics the η_i are usually the components of the vector of the spontaneous electrical polarization P_i). Inasmuch as changes of these parameters lead, generally speaking, to changes of the index of refraction, an increase in the intensity of the scattered light should also be observed near transition points. In the event of the transition being near the critical Curie point, the phenomenon will have the character of a "critical opalescence" in a solid. This effect indicated in reference 1, and considered in more detail in references 2, 3, and 4, has been experimentally observed[5,6] in the $\alpha \rightleftarrows \beta$ transition in quartz ($T_c = 573°C$). However, in all the above references the problem of the fluctuation kinetics, and thereby also of the spectral constitution of the scattered light, were not investigated, although, as will be shown below, this aspect of the phenomenon is also of great interest.

The scattering at an angle θ to the incident light is due to the Fourier component $\Delta\epsilon_{\mathbf{q}}$ of the fluctuations of $\Delta\epsilon \equiv \Delta n^2$ with a wave vector $q = (4\pi/\lambda_0)\sin(\theta/2)$. The medium will be considered here for simplicity optically isotropic (cf. references 2 and 3 for a generalization to the anisotropic case); $n(\lambda_0)$ is the index of refraction, and $\lambda_0 = 2\pi c/\omega_0$ is the wavelength of the light in vacuo. If the phase transition is characterized by one parameter η, as in the case of quartz, then

$$\Delta\varepsilon = a\,(\Delta\eta^2 - \overline{\Delta\eta^2}), \quad \Delta\varepsilon_{\mathbf{q}} = a\,\{2\eta_0 A_{\mathbf{q}} + \sum_{\mathbf{k}} A_{\mathbf{k}} A_{\mathbf{k}-\mathbf{q}}\},$$

where $\eta = \Sigma A_{\mathbf{k}} \exp(i\mathbf{k}\cdot\mathbf{r})$, and $\eta_0(T)$ is the equilibrium value of η. As a result, with statistical averaging,

$$\overline{|\Delta\varepsilon_{\mathbf{q}}|^2} = \overline{|\Delta\varepsilon_{\mathbf{q}}|_1^2} + \overline{|\Delta\varepsilon_{\mathbf{q}}|_2^2},$$

where the main first term is proportional to $\overline{|A_{\mathbf{q}}|^2}$, and the second term is proportional to the sum $\Sigma\,\overline{|A_{\mathbf{k}}|^2}\;\overline{|A_{\mathbf{k}-\mathbf{q}}|^2}$ (cf. reference 2). Thus the spectrum of the main part of the scattering I_1 is determined by the propagation velocity and the damping of the wave $\eta_{\mathbf{q}}(\mathbf{r}) = A_{\mathbf{q}} \exp(i\mathbf{q}\cdot\mathbf{r})$. As the parameter η in quartz we can choose the displacement of the mean position of the silicon atom in α quartz compared with its position in β quartz. Since the nonequilibrium change of η corresponds to a mutual displacement of various sublattices, this displacement will vary with the frequency of the optical vibration of the crystal $\Omega_i(q)$.

At the transition point $\eta_0 = 0$, that is, there is no elastic force (see below), and the frequency of the vibration $\Omega_i(0)$ becomes zero; here $\Omega_i(0) \approx \Omega_i(q)$, since $q \ll q_{\max} = \pi/d \sim 10^8$ ($d \sim 3\times10^{-8}$ is the lattice constant). Unfortunately we cannot uniquely state the corresponding frequency Ω_i at room temperature. In α quartz the lattice symmetry does not change for lines with frequencies $\tilde{\nu}_i = \Omega_i/2\pi c$ equal to 207, 356, 466, and 1082 cm^{-1} (reference 7); the 466-cm^{-1} line was also observed in β quartz.[8] The frequency of at least one of the remaining three lines should become zero at the transition point. It is known that the frequencies $\tilde{\nu}_i$ decrease with increasing temperature;[9] the $\tilde{\nu}_i = 207$ cm^{-1} line is shifted and broadened particularly strongly. In addition, Landsberg and Mandel'shtam have already shown[8] that this line is lacking in β quartz. This is completely understandable, since this vibration is asymmetrical in β quartz, and is consequently inactive in first-order Raman scattering. The 356- and 1082-cm^{-1} lines should also be lacking in β quartz.

As $T \to T_c$, the line corresponding to the vibration with vanishing frequency approaches the undisplaced line and its intensity I_1 is in fact determined by the formulas given in references 1 and 2. If the frequencies of two of the aforementioned

207-, 356-, and 1082-cm^{-1} lines do not become zero, then the intensity of these lines in α quartz should tend to zero as $T \to T_c$. From the experiments of Yakovlev and Velichkina[5,6] it follows that the depolarization of the scattering in the immediate neighborhood of the transition point is considerably smaller than for $T < T_c$. This becomes understandable in the light of what has been said; for $T \approx T_c$ the basic contribution to the scattering is due to the line with $\Omega_i(0) \approx 0$, and the depolarization of this line is zero (in contrast, the depolarization of the Rayleigh scattering amounts to 12–13% at room temperature and apparently still increases with increasing temperature).

Therefore, what has actually been considered in the previous investigations[1-6] is Raman light scattering which has the character of critical opalescence at the $\alpha \rightleftarrows \beta$ transition in quartz. The scattering by the $\overline{|\Delta\epsilon_{\mathbf{q}}|_2^2}$ fluctuations, with an intensity I_2 (cf. reference 2), is the second-order Raman scattering, which has a broad spectrum not very weak only very near the transition point, but present also above it. The reason why higher-order scattering is not taken into account in reference 2 is because the relation $\Delta\epsilon = a(\Delta\eta^2 - \overline{\Delta\eta^2})$, which does not contain higher powers of $\Delta\eta^2$, is used.

There is likewise no first-order Raman scattering in ferroelectrics of the $BaTiO_3$ type above the transition point (we are referring to the vibration of Ba relative to the TiO_3 group, due to the appearance of polarization along the cube axes). The picture is therefore analogous to that in quartz. True, the difference consists in the fact that in a free $BaTiO_3$ crystal the transition to the tetragonal phase is a first-order transition near the critical Curie point. Therefore, although the frequency $\Omega_i(0)$ at the transition point is anomalously small, it is not zero. Disregarding this point[10] for simplicity, we can approximately write down the dielectric constant for frequencies near Ω_i in the form[10,11]

$$T > T_c:\ \varepsilon \approx 2\pi/\left(\alpha - \mu\,\Omega^2 + ig\,\Omega\right), \qquad \Omega_i^2(0) = \alpha/\mu,$$
$$T < T_c:\ \varepsilon_z \approx 2\pi/\left(-2\alpha - \mu\,\Omega^2 + ig\,\Omega\right), \qquad \Omega_i^2(0) = 2|\alpha|/\mu, \tag{1}$$

where $\alpha = \alpha'(T_c)(T_c - T)$ is the coefficient in the expansion of the thermodynamic potential in terms of the polarization

$$\Phi = \Phi_0 + \alpha P^2 + \frac{\beta}{2}P^4 + \ldots;$$

the connection of μ and g with the atomic constants is indicated in references 10 and 11. The dependence of Ω_i^2 on q was neglected. When $T < T_c$, the polarization in (1) is taken to be directed along the z axis. The value of $\epsilon_x = \epsilon_y$ differs from ϵ_z, i.e., a splitting of the characteristic frequencies takes place. The corresponding expressions for first- and second-order transitions are given in reference 10. We also note that here we do not differentiate between the adiabatic and isothermal coefficients α. These differences are, generally speaking, not large; for not too low a frequency Ω the adiabatic values appear in (1). Inasmuch as the constant electric field and the elastic stresses affect the properties of ferroelectrics in the region of a transition considerably, the same can also be said about the effect of these factors on the vanishing frequencies $\Omega_i(0)$.

When account is taken of the field equations, the transverse optical vibrations in a crystal, due to the change in the polarization, turn out to be, as is known, simply "normal" electromagnetic waves in the given medium; the index of refraction here is $n(\Omega) = \sqrt{\epsilon(\Omega)}$. Furthermore, $q^2 = (\Omega/c^2\epsilon(\Omega)$, and with sufficiently small absorption $(g \to 0)$ we obtain from (1)

$$\Omega^2 = \Omega_i^2(0)\,/\,(1 + 2\pi/\mu c^2 q^2).$$

For visible light $q \sim 10^5$[$\lambda_0 \sim 5000$ A, $\theta \sim \pi/2$, $n(\lambda_0) \sim 1$]; at the same time in $BaTiO_3$ $\mu \sim 10^{-27}$ (reference 10). Therefore, the frequency of the light-scattering electromagnetic waves is, with great precision,* $\Omega = \Omega_i(0)$. In other words, these transverse optical vibrations in a crystal can practically be considered purely mechanical; indeed this is usually done in studying Raman scattering. For ferroelectrics that exhibit piezoelectric effects also outside the ferroelectric region (Rochelle salt, KH_2PO_4, etc), the first-order Raman scattering does not disappear even in the more symmetric phase. The intensity of such scattering was calculated by Krivoglaz and Rybak;[3] it increases on approaching the transition point from either side (at the same time the frequency Ω_i for a second-order transition also tends to zero as $T \to T_c$).

We shall now take into account the attenuation of the light-scattering waves, which leads to a broadening of the lines. The scattered light field

---

*In taking account of the dependence of Φ on the gradient of P, i.e., of the dependence of Ω_i on q, a term δq^2 is added in the denominator of expressions (1) for ε. Therefore

$$\Omega^2 = \Omega_i^2\,(1 + \delta q^2/\mu\Omega_i^2)/(1 + 2\pi/\mu c^2 q^2),$$

where $\delta \sim d^2 \sim 3 \times 10^{-16}$ (cf. reference 10). Hence $\delta q^2/\mu\Omega_i^2 = \delta q^2/\alpha \sim 3 \times 10^{-2}$ for $\alpha \sim 10^{-4}$, and we can assume, just as when the term δ is not taken into account, that $\Omega = \Omega_i(0)$.

is in a first approximation proportional to

$$\Delta\varepsilon_q e^{i\omega_0 t} = 2a\eta_0 A_q e^{i\omega_0 t}$$

(ω_0 is the frequency of the incident light) and its spectrum is determined by the Fourier components

$$G_\omega = \frac{1}{2\pi}\int_{-\infty}^{+\infty} A_q(t)\, e^{i(\omega_0-\omega)t}\, dt = A_\Omega,$$

where

$$\Omega = \omega - \omega_0, \quad A_\Omega = \frac{1}{2\pi}\int_{-\infty}^{+\infty} A_q(t)\, e^{-i\Omega t} dt.$$

Furthermore, to a first approximation we can assume

$$\ddot{A}_q + \gamma\dot{A}_q + \Omega_i(0)\, A_q = f,$$

where $\gamma = g/\mu$ [cf. (1)], and f is the generalized random force due to thermal motion. Hence

$$A_\Omega = f_\Omega / (\Omega_i^2 - \Omega^2 + i\gamma\Omega)$$

and the scattering intensity $I(\Omega)$ is proportional to $\overline{|A_\Omega|^2}$ and equal to

$$I(\Omega) = \frac{(\gamma\Omega_i^2/\pi)I_1}{(\Omega_i^2 - \Omega^2)^2 + \gamma^2\Omega^2}, \quad I_1 = \int_{-\infty}^{+\infty} I(\Omega)\, d\Omega, \qquad (2)$$

where I_1 has been calculated in reference 2.

If the red and violet satellites do not overlap, i.e., $\Omega_i \gg \gamma$, then for each satellite

$$I_c(\Omega) = \frac{\gamma I_1/4\pi}{(\Omega - \Omega_i)^2 + \gamma^2/4}$$

(I_1 is the total intensity of both satellites; in the classical approximation considered the intensities of these satellites are equal).

According to (2), it is obvious that

$$I(0) = \gamma I_1/\pi\Omega_i^2, \quad I(\Omega_i) = I_1/\pi\gamma.$$

Therefore, for $\Omega_i > \gamma$ but at the same time $\Omega_i \sim \gamma$, the satellites essentially overlap; when $\Omega_i < \gamma$ the function $I(\Omega)$ has a maximum only when $\Omega = 0$. It is interesting that the intensity for this maximum, $I(0) = \gamma I_1/\pi\Omega_i^2$, is strongly temperature dependent. Thus, for second-order transitions far from the critical Curie point I_1 depends weakly on T (cf. reference 2) and

$$\Omega_i^2 = -2\alpha/\mu = 2\alpha'(T_k)(T_k - T).$$

With regard to the coefficient $\gamma = g/\mu$, we note that it apparently should not have any singularities at the transition point. In ferroelectrics γ increases with increasing electric conductivity. In the absence of conductivity γ is determined by the relation of the given vibration with all the remaining vibrations, i.e., by the anharmonicity. In either case one can expect an increase of γ (more precisely of $g = \mu\gamma$) with increasing temperature. Experimentally γ can be determined, for example, by measuring the electrical losses [cf. (1)], or from the additional relaxation absorption of elastic (sound) waves in the crystal (cf. reference 6). In the latter case it is usually assumed that $\Omega_i = 0$ near T_c and the equation

$$\dot{\eta} = -\frac{1}{2g}\frac{\partial\Phi}{\partial\eta} = -\frac{1}{2g}\left(\frac{\partial^2\Phi}{\partial\eta^2}\right)_0(\eta - \eta_0) = -\frac{1}{\tau}(\eta - \eta_0),$$

is employed, from which

$$\dot{A}_q \quad A_q/\tau \quad 0,$$

where

$$\tau = g/\alpha = g/\alpha'(T_k)(T - T_{.}) \text{ for } T > T_k,$$
$$\tau = g/2\alpha'(T_k)(T_k - T) \quad \text{for } T < T_k.$$

The relaxation absorption of sound takes place only for $T < T_c$ when $\eta_0 \neq 0$; measuring τ and $\alpha'(T_c)$ one can obviously find g for $T \approx T_c$. From here we can then find γ, if the value $\Omega_i^2(0) = 2|\alpha|/\mu$ is known [cf. (1)].

The Raman lines which we are discussing are connected in ferroelectrics with the fluctuations of the polarization, i.e., they are also known to be active in the "infrared" absorption (in $BaTiO_3$ the frequency corresponding to the vibrations of Ba relative to the TiO_3 group becomes zero). However, when the transition is approached the frequencies Ω_i are in the difficultly accessible millimeter or submillimeter portions of the spectrum. Therefore the method of Raman scattering can here too compete with and complement the measurements on the absorption and reflection of electromagnetic waves (Raman scattering has already been observed in some ferroelectrics,[12] but not for all lines and outside the transition region).

Besides, the study of the spectrum and of the intensity of the scattered light near second-order transition points close to the critical Curie point* is also most interesting in other respects, as is clear from what has already been said in earlier papers.[1-6]

---

*A related effect is, for instance, neutron scattering in ferro- and antiferroelectric substances near the Curie point (cf. references 13 and 1). We note that the existence of analogous phenomena also appears possible in macromolecules and polymer chains and structures (when the structure is changed, say the chain is lengthened, and also when the temperature is increased, some characteristic frequencies may become anomalously small; this may lead to a strong increase in the scattering intensity).

[1] V. L. Ginzburg, Dokl. Akad. Nauk SSSR **105**, 240 (1955).

[2] V. L. Ginzburg and A. P. Levanyuk, J. Phys. Chem. Solids **6**, 51 (1958), Coll. in memoriam G. S. Landsberg, Acad. of Sci. Press, 1959, p. 104.

[3] M. A. Krivoglaz and S. A. Rybak, JETP **33**, 139 (1957), Soviet Phys. JETP **6**, 107 (1958).

[4] A. P. Levanyuk, JETP **36**, 810 (1959), Soviet Phys. JETP **9**, 571 (1959).

[5] Yakovlev, Velichkina, and Mikheeva, Кристаллография (Cristallography) **1**, 123 (1956), Dokl. Akad. Nauk SSSR **107**, 675 (1956), Soviet Phys.-Doklady **1**, 215 (1956).

[6] I. A. Yakovlev and T. S. Velichkina, Usp. Fiz. Nauk **63**, 411 (1957).

[7] B. D. Saksena, Proc. Indian Acad. Sci. **A12**, 93 (1940).

[8] G. S. Landsberg and L. I. Mandel'shtam, Z. Physik **58**, 250 (1929).

[9] P. K. Narayanaswamy, Proc. Indian Acad. Sci. **A26**, 521 (1947).

[10] V. L. Ginzburg, Физ. тв. тела (Solid State), in press.

[11] V. L. Ginzburg, JETP **19**, 36 (1949), Usp. Fiz. Nauk **38**, 490 (1949).

[12] Baryshanskaya, Landsberg, and Motulevich, Izv. Akad. Nauk SSSR, Ser. Fiz. **12**, 573 (1948).

[13] L. Van Hove, Phys. Rev. **95**, 1374 (1954).

Translated by Z. Barnea
36

SOVIET PHYSICS JETP VOLUME 12, NUMBER 1 JANUARY, 1961

A DIAGRAM TECHNIQUE FOR EVALUATING TRANSPORT QUANTITIES

O. V. KONSTANTINOV and V. I. PEREL'

Leningrad Physico-Technical Institute

Submitted to JETP editor March 18, 1960

J. Exptl. Theoret. Phys. (U.S.S.R.) **39**, 197-208 (July, 1960)

We have developed a diagram technique to evaluate the single-electron density matrix. Quantum mechanics is used to obtain a transport equation which takes into account the inhomogeneity of an external electrical field and the self-consistent electron field.

IT is well known that the evaluation of transport quantities requires the summation of an infinite number of terms of a perturbation-theory series, however small the coupling constant. It must therefore always lead to the formulation and solution of some kind of integral equation. Boltzmann's classical transport equation is an example of such an equation.

Many papers[1-5] have been devoted to the derivation of a transport equation. In some of them[1] the problem is studied using classical mechanics. In the papers by Kohn and Luttinger[3] and van Hove,[4] which are based upon quantum theory, there is no diagram technique. The technique proposed by Montroll and Ward[5] and by Prigogine and Ono[6] does not use the convenient second quantization formalism and is thus complicated (in reference 6 three-dimensional diagrams are even used). Also, if there is no simple and convenient diagram technique, it is extremely difficult to apply it in those cases where the classical Boltzmann equation is inapplicable (for instance, the problem of plasma kinetics or the polaron). In a paper by Abrikosov, Gor'kov, and Dzyaloshinskiĭ[7] a simple diagram technique was proposed which enabled one in principle to evaluate transport coefficients directly. However, the straightforward evaluation of transport coefficients, even in the case where the transport equation is valid, is a difficult problem. Also, the authors of the cited paper did not derive a transport equation, and its derivation by means of their technique is difficult. We must note that the idea of analytical continuation, proposed in reference 7 and used with success by Larkin,[8] turns out to be extremely helpful for evaluating the internal block diagrams obtained in the present paper. We restrict ourselves here to a derivation of a generalized transport equation and we show that it turns into the usual transport equation when the latter is valid. In a subsequent paper we shall obtain a transport equation for a plasma on the basis of the technique developed here.

1. THE SINGLE ELECTRON DENSITY MATRIX IN AN EXTERNAL ELECTROMAGNETIC FIELD

We consider a system of electrons and some other particles interacting with them (phonons or impurity centers). We assume that in the initial state, $t \to -\infty$, the system was in contact with a thermostat and could be described by a density matrix

$$F_0 = Z^{-1}\exp(-\beta H'), \quad Z = \mathrm{Sp}\exp(-\beta H'),$$

$$\beta = (kT)^{-1}, \quad H' = H - \mu\hat{N},$$

where μ is the chemical potential and $\hat{N}$ the operator of the total number of electrons. At $t \to -\infty$ an adiabatically increasing weak electromagnetic field is applied to the system and at the same time the contact with the thermostat is broken. The time variation of the density matrix F of the system is determined by the equation

$$i\hbar\partial F/\partial t = [(H + H_t), F],$$

$$H_t = \int \rho(\mathbf{x})\, U(\mathbf{x}, t)\, d\mathbf{x} - \frac{1}{c}\int J_\mu(\mathbf{x})\, A_\mu(\mathbf{x}, t)\, d\mathbf{x},$$

where $\rho(\mathbf{x})$ is the charge density operator, $J_\mu(\mathbf{x})$ the current density operator of the system, and $U(\mathbf{x}, t)$ and $A_\mu(\mathbf{x}, t)$ are respectively the scalar and vector potentials of the weak electromagnetic field.

In the approximation which is linear in the field, the solution of the equation for the density matrix can be written in the form $F = F_0 + F_t$, where

$$F_t = \int_{-\infty}^{0} d\tau \int d\mathbf{x} E_\mu(\mathbf{x}, t+\tau) \int_0^\beta d\lambda\, J_\mu(\mathbf{x}, \tau + i\hbar\lambda)\, F_0$$

$$+ \frac{1}{c}\int d\mathbf{x}\, A_\mu(\mathbf{x}, t) \int_0^\beta d\lambda J_\mu(\mathbf{x}, i\hbar\lambda)\, F_0. \qquad (1)$$

To derive this formula we used the relation div $\mathbf{J}(\mathbf{x}) = \dot{\rho}(\mathbf{x})$ and the identity[9]

$$[F_0, L] = i\hbar \int_0^\beta d\lambda \dot{L}(i\hbar\lambda) F_0,$$

where

$$L(t) = \exp(-H't/i\hbar) L \exp(H't/i\hbar),$$

$$\dot{L} = (i\hbar)^{-1}[L, H'].$$

The average value $\overline{B}$ of a quantity B can be evaluated using the formula

$$\overline{B} = \mathrm{Sp}\, F_0 B_0 + \mathrm{Sp}\, F_t B_0 + \mathrm{Sp} F_0 B_t, \quad B = B_0 + B_t,$$

where B_t is the correction to the operator B, necessitated by the perturbing vector potential in the approximation which is linear in the field. If, for instance, B is the current density operator, we have

$$B_t = -(e^2/mc)\, \mathbf{A}(\mathbf{x}, t)\, \Psi^+(\mathbf{x}) \Psi(\mathbf{x}),$$

where $\Psi(\mathbf{x})$ is the operator of the quantized wave function. Using Eq. (1) we can write $\overline{B}$ in the form

$$\overline{B} = \mathrm{Sp}\, F_0 B_0 + \overline{B}^{(1)} + \overline{B}^{(2)},$$

$$\overline{B}^{(1)} = \int_{-\infty}^{0} d\tau \int d\mathbf{x} E_\mu(\mathbf{x}, t+\tau) \int_0^\beta d\lambda\, \mathrm{Sp}\{F_0 B_0 J_\mu(\mathbf{x}, \tau + i\hbar\lambda)\},$$

$$\overline{B}^{(2)} = \frac{1}{c} \int d\mathbf{x} A_\mu(\mathbf{x}, t) \int_0^\beta d\lambda\, \mathrm{Sp}\{F_0 B_0 J_\mu(\mathbf{x}, i\hbar\lambda)\} + \mathrm{Sp}\, F_0 B_t. \tag{2}$$

Although the quantity $\overline{B}^{(2)}$ contains the vector potential, we can show that it is gauge invariant. We can verify that this quantity owes its existence purely to the magnetization current. Indeed, if $E_\mu = 0$ the total change in the average value of B is due to $\overline{B}^{(2)}$. Also, $\overline{B}^{(2)}$ does not contain a time retardation relative to the vector potential. $\overline{B}^{(2)}$ is thus that value of $\overline{B}$ which would have been obtained if the magnetic field were constant and if there were no electrical field. Then, of course, only the magnetization current would exist in the system. We have studied earlier[10] the properties and the physical meaning of $\overline{B}^{(2)}$ for the case where B is the current density operator. In the present paper we shall not be interested any further in the quantity $\overline{B}^{(2)}$.

Let us consider the quantity $\overline{B}^{(1)}$ in more detail.

Bearing in mind that in the second quantization representation

$$B_0 = \int \Psi^+(\mathbf{x})\, b_0 \Psi(\mathbf{x})\, d\mathbf{x} = \sum_{nn'} (b_0)_{nn'} a_n^+ a_{n'}.$$

(where b_0 is a single-electron operator and the n are the quantum numbers of the set of single-electron states) we get

$$\overline{B}^{(1)} = \sum_{nn'} (b_0)_{nn'} f_{nn'}^{(1)}(t). \tag{3a}$$

Here

$$f_{nn'}^{(1)}(t) = \int_{-\infty}^{0} d\tau \int d\mathbf{x} E_\mu(\mathbf{x}, t+\tau) \int_0^\beta d\lambda\, \mathrm{Sp}\{F_0 a_n^+ a_{n'} J_\mu(\mathbf{x}, \tau + i\hbar\lambda)\}. \tag{3b}$$

We can call the quantity $f_{nn'}^{(1)}(t)$ the correction to the single-electron density matrix.

Let

$$E_\mu(\mathbf{x}, t) = E_\mu(\varkappa, s) \exp(i\varkappa\mathbf{x} + st), \quad s = -i\omega + \nu,$$

where ω is the frequency of the field and ν the adiabatic parameter, which we shall let tend to zero in the final formulae. If we write the operator $J_\mu(\mathbf{x}, \tau + i\hbar\lambda)$ in the second-quantization representation, Eq. (3b) becomes

$$f_{nn'}^{(1)}(t) = E_\mu(\varkappa, s)\, e^{st} \sum_{mm'} G_{mn}^{m'n'}(s, \beta) \int e^{i\varkappa\mathbf{x}} j_\mu(\mathbf{x})_{mm'} d\mathbf{x}, \tag{4b}$$

$$G_{mn}^{m'n'}(s, \beta) = \int_{-\infty}^{0} e^{s\tau} d\tau \int_0^\beta d\lambda\, \mathrm{Sp}\Big\{F_0 \exp\Big[\frac{H'}{i\hbar}(\tau + i\hbar\lambda)\Big] a_n^+ a_{n'} \times \exp\Big[-\frac{H'}{i\hbar}(\tau + i\hbar\lambda)\Big] a_m^+ a_{m'}\Big\}. \tag{4a}$$

Let $H = H_0 + V$, then

$$\exp\Big[\frac{H_0'}{i\hbar}(z_1 - z_2)\Big] = \exp\Big(\frac{H_0' z_1}{i\hbar}\Big)\Big[T_c \exp\Big(\frac{1}{i\hbar}\int_{z_2}^{z_1} V_z dz\Big)\Big] \exp\Big(-\frac{H_0' z_2}{i\hbar}\Big),$$

$$V_z = \exp\Big(-\frac{H_0' z}{i\hbar}\Big) V \exp\Big(\frac{H_0' z}{i\hbar}\Big).$$

z_1 and z_2 are here complex numbers and the integration is along an arbitrary contour C in the complex plane from z_2 to z_1. The T_c sign indicates an ordering of the operators along this contour in such a way that points on the contour which lie nearer to z_2 along the contour are assumed to be earlier. Using this formula we can write the exponents in Eq. (4b) in the following form

$$F_0 \exp\Big[\frac{H'}{i\hbar}(\tau + i\hbar\lambda)\Big] = Z^{-1} \exp\Big\{\frac{H'}{i\hbar}[(\tau - i\hbar\beta) - (-i\hbar\lambda)]\Big\}$$

$$= Z^{-1} \exp\Big[\frac{H_0'}{i\hbar}(\tau - i\hbar\beta)\Big] \exp\Big[\frac{1}{i\hbar}\int_{-i\hbar\lambda}^{\tau - i\hbar\beta} V_z dz\Big] \exp(\lambda H'_0),$$

$$\exp\Big[-\frac{H'}{i\hbar}(\tau + i\hbar\lambda)\Big] = \exp(-H_0'\lambda) \exp\Big[\frac{1}{i\hbar}\int_{\tau}^{-i\hbar\lambda} V_z dz\Big] \exp\Big(-\frac{H_0'\tau}{i\hbar}\Big).$$

Substituting these expressions into Eq. (4b) we write $G_{mn}^{m'n'}$ in a form which is convenient for a series expansion in the coupling constant:

$$G_{mn}^{m'n'}(s, \beta) = \int_{-\infty}^{0} e^{s\tau} d\tau G_{mn}^{m'n'}(\tau, \beta), \qquad (5a)$$

$$G_{mn}^{m'n'}(\tau, \beta)$$
$$= \int_{0}^{\beta} d\lambda \, \mathrm{Sp}\left\{e^{-\beta H_0} T_c \exp\left[\frac{1}{i\hbar}\int_C V_z dz\right](a_n^+ a_{n'})_{-i\hbar\lambda}(a_m^+ a_{m'})_\tau\right\} Z^{-1}. \qquad (5b)$$

The integration in the exponent is over the contour C shown in Fig. 1. The sign T_c orders the operators along the same contour.

$G_{mn}^{m'n'}$ is thus some kind of temperature-dependent Green function with the peculiar feature that the S-matrix contains an integral over a contour in the complex "time" plane.

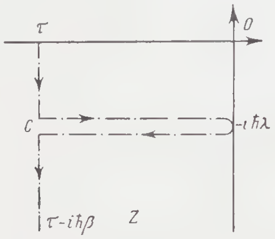

FIG. 1

2. A DIAGRAM TECHNIQUE TO EVALUATE THE FUNCTION $G_{mn}^{m'n}$

1. Let V_{ph} be the electron-phonon interaction operator

$$V_{ph} = \sum_{f, q \neq 0} (c_q b_q a_f^+ a_{f-q} + c_q^* b_q^+ a_f^+ a_{f+q}),$$

where b_q^+ and b_q are the creation and annihilation operators of the phonons. We have taken for the set of single-electron states plane waves, and **f** is the electron and **q** the phonon wave vector. After expanding the exponent in Eq. (5b) in a series, we get the usual Feynman expansion for the function $G_{kp}^{k'p'}(\tau, \beta)$. It occurs as a sum of terms, in which every term corresponds to a diagram. All points of the diagram lie on the contour C. Each point is the start of one and the end of another electron line and either the start (phonon emission) or the end (absorption) of a phonon line. The points τ and $-i\hbar\lambda$ are excepted, and we call them the terminal points.

No phonon lines go to them. The line **k'** ends and the line **k** starts at the terminal point τ. The line **p'** ends and the line **p** starts at the terminal point $-i\hbar\lambda$.

To each electron line going from the point z_2 to the point z_1 there corresponds a factor

$$g_\alpha(z_1, z_2) = \mathrm{Sp}\{e^{-\beta H_0'} T_c (a_\alpha)_{z_1} (a_\alpha^+)_{z_2}\} Z_0^{-1}$$
$$= \exp\frac{\varepsilon_\alpha'(z_1 - z_2)}{i\hbar}\begin{cases}(1 - n_\alpha) & \text{if } z_2 \text{ is earlier than } z_1 \\ -n_\alpha & \text{if } z_2 \text{ is later than } z_1\end{cases}$$

(here $\epsilon_\alpha' = \epsilon_\alpha - \mu$), and to a phonon line a factor

$$d_q(z_1, z_2) = |c_q|^2 \mathrm{Sp}\{e^{-\beta H_0'} T_c (b_q)_{z_1} (b_q^+)_{z_2}\} Z_0^{-1}$$
$$= |c_q|^2 \exp[-i\omega_q(z_1 - z_2)]$$
$$\times \begin{cases}(1 + m_q) & \text{if } z_2 \text{ is earlier than} \\ m_q & \text{if } z_2 \text{ is later than } z_1\end{cases}$$

where ϵ_α is the electron energy, ω_q the phonon frequency, and

$$Z_0 = \mathrm{Sp}\exp[-\beta(H_0 - \mu N)],$$

$$n_\alpha = [\exp\beta(\varepsilon_\alpha - \mu) + 1]^{-1}, \qquad m_q = [\exp\beta\hbar\omega_q - 1]^{-1}.$$

To each point (except the terminal points) there corresponds a factor $dz/i\hbar$. For each z one must integrate along the contour C. Moreover, λ is integrated from 0 to β.

Unconnected diagrams, similar to vacuum loops, need not be taken into account as they are cancelled by diagrams from the expansion of Z.

We need $G_{kp}^{k'p'}(s, \beta)$ to evaluate the single-particle density matrix [see Eq. (5a)]. It is in fact more convenient to evaluate the function*

$$G_{kp}^{k'p'}(s, \sigma) = \int_0^\beta e^{-\beta\sigma} G_{kp}^{k'p'}(s, \beta) d\beta.$$

We do not consider β, which enters into n_α and m_q, as an integration variable.

We proceed now to justify the rules for evaluating $G_{kp}^{k'p'}(s, \beta)$. These rules will be formulated later on. The integration over τ and β is easily performed if each Feynman diagram is broken up into a sum of diagrams with different relative arrangements of points. As an example we give in Fig. 2 some modified diagrams of second order,† which must be considered to be different and which originate from the same Feynman diagram. The horizontal sections of the "time" contour are pulled apart for the sake of convenience. Owing to this modification, the order of the integrals in each diagram containing n points on the horizontal and r points on the vertical sections of the contour C is of the form

$$\int_{-\infty}^{0} e^{s\tau} d\tau \int_0^\tau dt_1 \ldots \int_0^{t_{n-1}} dt_n \int_0^\infty e^{-\beta\sigma} d\beta \int_0^\beta d\gamma_1 \ldots$$
$$\times \int_0^{\gamma_m} d\lambda \int_0^\lambda d\gamma_{m+1} \ldots \int_0^{\gamma_{r-1}} d\gamma_r.$$

---

*V. V. Tolmachev has drawn our attention to the fact that C. Bloch[11] has used essentially a similar method to evaluate the partition function.

†We do not for the present turn our attention to the thin intersecting straight lines.

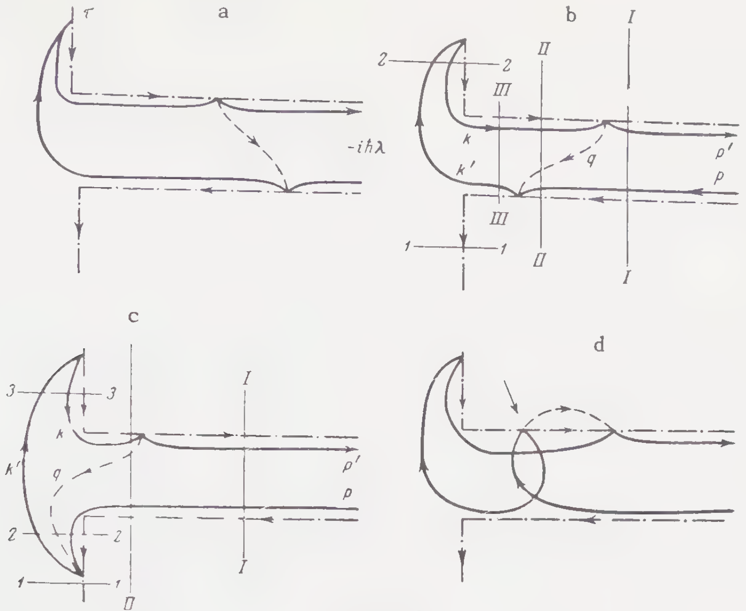

FIG. 2

Here $t_1, \ldots, t_n$ are the real parts of the complex “time” points on the horizontal sections of the contour C (the imaginary part of the “time” is for all these points equal to $-\hbar\lambda$). The quantities $-\hbar\gamma_1, \ldots, -\hbar\gamma_m$ are the imaginary parts of the “time” points on the upper vertical section of the contour C; and $-\hbar\gamma_{m+1}, \ldots, -\hbar\gamma_r$ the imaginary parts of the “time” points on the lower vertical section of the contour C (the real part of the times is for all these points equal to τ).

The time dependent exponents contained in g_α and $d_{\mathbf{q}}$ are best referred to the points. Each point z (including the terminal points) will then correspond to a factor $\exp(i\Omega_{AB}z)$, where $\hbar\Omega_{AB} = E_A - E_B$, with E_A the energy of the line starting at the point z and E_B the energy of the line ending at the point z. For a point on the horizontal section we have $z = t - i\hbar\lambda$. We set the factor $\exp(i\Omega_{AB}t)$ along a suitable differential dt, and the factor $\exp(\hbar\lambda\Omega_{AB})$ along $d\lambda$. For points on the vertical sections we have $z = \tau - i\hbar\gamma$. We set the exponent $\exp(\hbar\Omega_{AB}\gamma)$ along the differential $d\gamma$ and the factor $\exp(i\Omega_{AB}\tau)$ along $d\tau$. After this, all integrals can easily be evaluated by consecutive integrations by part. As a result we get the following rules for writing down the expression corresponding to the modified diagram for the function $G_{\mathbf{kp}}^{\mathbf{k'p'}}(s, \sigma)$.

1) A line going from an earlier point on the contour to a later point will be called a regular line. To each regular line there corresponds a factor $1 - n_\alpha$ for the electrons and $|c_{\mathbf{q}}|^2(1 + m_{\mathbf{q}})$ for the phonons. For an irregular line we have respectively n_α and $m_{\mathbf{q}}|c_{\mathbf{q}}|^2$.

2) To each point on the upper horizontal section of the contour there corresponds a factor $(i\hbar)^{-1}$, on the lower section a factor $(-i\hbar)^{-1}$, and on the vertical sections (-1); momentum is conserved at each point.

3) We imagine a vertical line taking up consecutively the positions I, II, . . . in the intervals between the points on the horizontal section as is shown, for example, in Figs. 2b and 2c.

To each interval there corresponds a factor $(s + i\omega_{MN})^{-1}$ where $\hbar\omega_{MN} = E_M - E_N$, with E_M the total energy of the lines entering the interval on the right of the intersecting line and E_N the total energy of the lines leaving this region. For instance, in Fig. 2c the intersection I corresponds to a factor $(s + i\omega_{\mathbf{p'p}})^{-1}$ and the intersection II to a factor $[s + i(\omega_{\mathbf{kp}} - \omega_{\mathbf{q}})]^{-1}$ where $\omega_{\mathbf{kp}} = (\epsilon_{\mathbf{k}} - \epsilon_{\mathbf{p}})/\hbar$.

Similarly we imagine a horizontal line taking up consecutively the positions 1, 2, . . . between the points on the vertical axis (see Figs. 2b and 2c). To each vertical interval there corresponds a factor $(\sigma + \hbar\omega_{MN})^{-1}$, where E_M is the total energy of the lines entering the region below the intersecting line and E_N the energy of the lines coming from that region. For instance, in Fig. 2c the intersection 1 corresponds to a factor σ^{-1} and the intersection 2 to a factor $[\sigma + \hbar(\omega_{\mathbf{pk'}} + \omega_{\mathbf{q}})]^{-1}$.

4) Each diagram is multiplied by $(-1)^M$, where M is the number of mutual intersections of electron lines. One must draw here the electron line to the point “in the same sense” as the time axis (see in Fig. 2d the point indicated by an arrow).

We give as an example the expression corresponding to the diagram 2b:

$$[(1-n_{\mathbf{p}'})(1-n_{\mathbf{p}})(1+m_{\mathbf{q}})]\frac{(-1)}{(i\hbar)^2}\frac{(c_{\mathbf{q}})^2}{s+i\omega_{\mathbf{p}'\mathbf{p}}}\frac{n_{\mathbf{k}'}(1-n_{\mathbf{k}})}{s+i(\omega_{\mathbf{kp}}-\omega_{\mathbf{q}})}$$
$$\times\frac{1}{\sigma}\frac{1}{\sigma+\hbar\omega_{\mathbf{kk}'}}\frac{1}{s+i\omega_{\mathbf{kk}'}}\delta_{\mathbf{k},\,\mathbf{p}'+\mathbf{q}}\delta_{\mathbf{k}',\,\mathbf{p}+\mathbf{q}}. \tag{6}$$

Summation over $\mathbf{q}$ is implied.

Let us consider some properties of the modified diagrams.

If we transfer one point from the lower horizontal axis to the upper one (or the other way round) without changing its coordinates in the complex plane, only the regularity of the lines joining it from the right is changed. Also, the sign of the expression may change. Examples of diagrams obtained from one another by the transfer of a point are the diagrams of Figs. 2b and 2d (the transferred point is indicated by an arrow). It is convenient to consider such diagrams together, transferring the points mentally. For instance, the sum of all diagrams obtained from 2b by a transfer of points differs from (6) only in that now the square brackets contain

$$\{(1-n_{\mathbf{p}})(1+m_{\mathbf{q}})+n_{\mathbf{p}}m_{\mathbf{q}}\}(1-n_{\mathbf{p}}+n_{\mathbf{p}})=1+m_{\mathbf{q}}-n_{\mathbf{p}}.$$

When all lines from a point on the horizontal axis go to the left (right-hand return) the transfer of a point changes only the sign of the diagram (the sign changes because when such a point is transferred the parity of the number of intersections is not changed, but the upper point becomes the lower one and vice versa). We can therefore in general neglect diagrams with a right-hand return. An example is shown in Fig. 3. The arrow indicates the right-hand return.

2. The presence of an interelectronic interaction

$$V_e=\frac{1}{2}\sum_{\mathbf{q}\neq\mathbf{q}',\,\mathbf{ff}'}u_{\mathbf{q}-\mathbf{q}'}a_{\mathbf{q}}^{+}a_{\mathbf{q}'}a_{\mathbf{f}}^{+}a_{\mathbf{f}'}\delta_{\mathbf{q}+\mathbf{f},\,\mathbf{q}'+\mathbf{f}'}$$

only leads to the occurrence in the diagrams of points where four electron lines meet. Such a point can conveniently be indicated in the way shown in Fig. 4.

It will correspond to a factor $u_{\mathbf{q}-\mathbf{q}'}$ (apart from those mentioned in the preceding subsection).

3. Let the perturbation V contain the operator for the interaction of the electrons with heavy impurities

$$V_n=\sum_{\mathbf{q}\neq\mathbf{q}'}v_{\mathbf{q}-\mathbf{q}'}a_{\mathbf{q}}^{+}a_{\mathbf{q}'}\sum_{\nu}\exp[-i(\mathbf{q}-\mathbf{q}')\mathbf{r}_{\nu}],$$

where $\mathbf{r}_\nu$ is the coordinate of the ν-th impurity center. In that case averaging over all $\mathbf{r}_\nu$ is implied in the operation Sp{exp(−βH′) . . .}. The changes introduced in this case into the diagram technique are confined to the following ones:

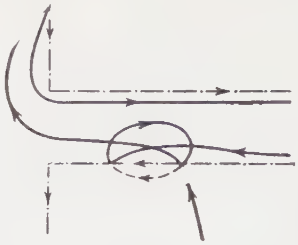

FIG. 3

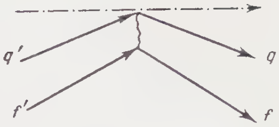

FIG. 4

a) Impurity points appear along the contour C.

b) Such a point gives rise to a factor $v_{\mathbf{q}-\mathbf{q}'}$ (apart from these mentioned in subsection 1).

c) The loose ends of the impurity lines are tied up in bundles in such a way that there are at least two lines going to each knot* (examples can be seen in Figs. 5a and 5b). To each bundle there corresponds a factor N: the total number of impurity centers. There are no factors corresponding to an impurity line as it does not carry any energy (in contradistinction to the phonon line). They need therefore not be taken into account when ω_{MN} is calculated for each intersection and when the right-hand return is determined. For instance, in Fig. 5b there is a right-hand return. In each bundle the sum of the momenta of the electron lines entering into all the points corresponding to the bundle is equal to the sum of the momenta of the lines leaving these points.

We note in conclusion that we can directly draw the diagrams for the single-particle density matrix $f_{\mathbf{pp}'}$. They will differ from the diagrams described in the foregoing only by the fact that the terminal point τ will now correspond to a factor

$$E_{\mu}(\varkappa,\,s)\,e^{st}\,\frac{e\hbar}{2m}(\mathbf{k}+\mathbf{k}')\,\delta_{\mathbf{k}',\,\mathbf{k}-\varkappa}$$

[see Eq. (4a)] and that one sums over $\mathbf{k}$ and $\mathbf{k}'$.

To emphasize the difference between the diagrams for $f_{\mathbf{pp}'}$ and for $G_{\mathbf{kp}}^{\mathbf{k}'\mathbf{p}'}$, we shall draw the diagrams for $f_{\mathbf{pp}'}$ in a way which is similar to the diagrams for the vertex part in electro-dynamics,

---

*The bundling of the impurity lines can be elucidated as follows. We consider, for instance, the term of fourth order in the interaction. It contains the quantity

$$\Big\langle\sum_{\nu_1\nu_2\nu_3\nu_4}\exp[-i(\mathbf{q}_1-\mathbf{q}_1')\,\mathbf{r}_{\nu_3}]\cdot\,.\,.\,\exp[-i(\mathbf{q}_4-\mathbf{q}_4')\,\mathbf{r}_{\nu_4}]\Big\rangle$$

(the angular brackets indicate the averaging over the positions of the impurity centers). In this sum there will be a term for which $\nu_1=\nu_2=\nu_3=\nu_4$. To this term there corresponds a diagram with one bundle, where all four impurity lines are tied together. Furthermore, there will be one for which $\nu_1=\nu_2$, $\nu_3=\nu_4$. To this term there corresponds a diagram with two bundles with two lines going to each of them. There will clearly be altogether three such diagrams. There are no diagrams where the bundle contains only one line (for instance, $\nu_1=\nu_2=\nu_3\neq\nu_4$) as there is no term with $\mathbf{q}=\mathbf{q}'$ in the expression for V_n.

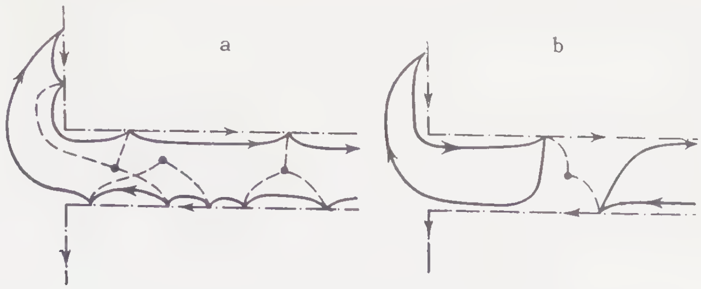

FIG. 5

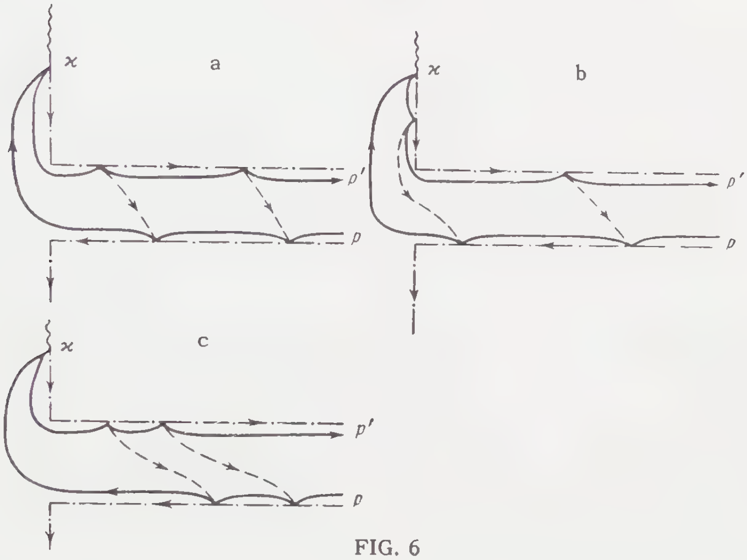

FIG. 6

with a "photon" wavy line included at the terminal point τ (see Fig. 6).

3. THE TRANSPORT EQUATION

Let us classify the modified diagrams. We call an intersection (vertical or horizontal) which cuts only two electron lines and nothing else a free intersection. That part of a diagram which is bounded by two vertical free intersections and which does not contain free intersections in the intervals between its points we call a horizontal irreducible part. A vertical irreducible part is defined in a similar way. A part of a diagram which contains points both on the vertical and on the horizontal segments which can not be cut by a free intersection is called an angular part. For instance, in Fig. 5a there is one horizontal irreducible part and an angular part.

In the case where the frequency ω and the wave vector κ of the electrical field tend to zero, there occurs an important singularity in the perturbation-theory series. The factors corresponding to the vertical free intersections increase without bound. Therefore the number of terms cannot be kept finite in an expansion in any interaction parameter, however small. In that case we must compare with one another only those diagrams which contain the same number of vertical free intersections (and hence the same number of horizontal irreducible parts). For instance, we can neglect the diagram 2c compared with a free line, but we can not neglect diagrams 2a, 2b, and 2d. In exactly the same way, we can neglect diagrams 6b and 6c compared to 2a, but not diagram 6a. If the frequency and the wave vector of the electrical field are thus sufficiently small it is necessary to sum an infinite number of terms. This summation leads to an exact integral equation for $f_{pp'}$ which is depicted in Fig. 7 (the first diagram is equal to the sum of the next two):

$$f_{pp'}(s,\ \sigma) = r_{pp'}(s,\ \sigma)(s + i\omega_{p'p})^{-1} + f_{qq'} W^{qp'}_{q'p}(s)(s + i\omega_{p'p})^{-1} \tag{7}$$

(summation over q is implied). $r_{pp'}(s, \sigma)$ is here the sum of all diagrams which do not contain horizontal irreducible parts without the last free intersection on the right; $W^{qp'}_{q'p}$ is the sum of all possible horizontal irreducible parts. The term corresponding to each irreducible part includes the factors from all points occurring in it, from all intersections (except the last, free ones), and from all lines except the two last ones on the left.

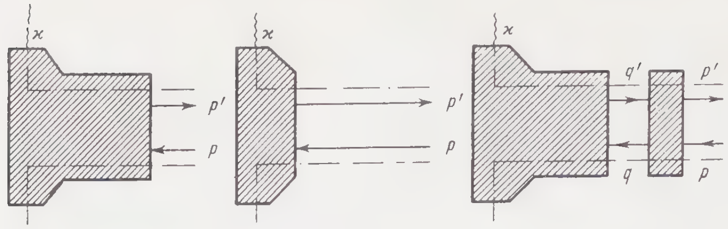

FIG. 7

Because of the conservation of momentum we have $\mathbf{p}' = \mathbf{p} + \kappa$, $\mathbf{q}' = \mathbf{q} + \kappa$. For simplicity denoting $W^{\mathbf{q},\mathbf{p}+\kappa}_{\mathbf{q}+\kappa,\mathbf{p}}$ by $W_{\mathbf{qp}}$ we can write Eq. (7) in the form

$$(s + i\omega_{\mathbf{p}+\varkappa,\, \mathbf{p}}) f_{\mathbf{p},\, \mathbf{p}+\varkappa} = r_{\mathbf{p},\, \mathbf{p}+\varkappa}(s,\ \beta) + \sum_{\mathbf{q}} f_{\mathbf{q},\, \mathbf{q}+\varkappa} W_{\mathbf{qp}}(s),$$

$$r_{\mathbf{pp}'}(s,\beta) = (2\pi i)^{-1} \int\limits_{-i\infty+a}^{i\infty+a} r_{\mathbf{pp}'}(s,\ \sigma)\, e^{\beta\sigma} d\sigma. \qquad (8)$$

This equation is a generalized transport equation. It is important to note that the quantities W and r occurring in it do not contain free intersections.

If we take into account that the distribution function is

$$f_{\mathbf{p}}(x) = \int e^{i\varkappa\mathbf{x}} f_{\mathbf{p}-\varkappa/2,\ \mathbf{p}+\varkappa/2}\, d\varkappa,$$

the meaning of the different terms in Eq. (8) becomes clear: the term on the left hand side corresponds to the expression $\partial f_{\mathbf{p}}/\partial t + v_{\mathbf{p}} \nabla_{\mathbf{x}} f_{\mathbf{p}}$ when $\kappa \ll p$, the first term on the right hand side describes the change in $f_{\mathbf{p}}(x,\ t)$ under the action of the electrical field, and the second one the influence of collisions (it will become clear in the following that the second term also includes the self-consistent field).

As examples we shall consider the interaction of electrons with phonons and with impurities.

1. Interaction with phonons. We shall assume that the interaction is weak. We can then restrict ourselves to second order diagrams when evaluating W. Typical diagrams are given in Fig. 8. We shall for simplicity assume that the wave length of the electrical field is much larger than the electron de Broglie wave length and that $\hbar\omega \ll kT$ ($s = -i\omega - \nu$). Diagrams of the type 8b give them a contribution to W equal to

$$W^{(\mathrm{b})}_{\mathbf{qp}} = 2\pi\hbar^{-2} |c_{\mathbf{p}-\mathbf{q}}|^2 [(1 + m_{\mathbf{q}-\mathbf{p}} - n_{\mathbf{p}})\, \delta(\omega_{\mathbf{pq}} + \omega_{\mathbf{p}-\mathbf{q}})$$

$$+ (m_{\mathbf{p}-\mathbf{q}} + n_{\mathbf{p}})\, \delta(\omega_{\mathbf{pq}} - \omega_{\mathbf{p}-\mathbf{q}})].$$

The contribution of diagrams of type 8a is equal to

$$W^{(\mathrm{a})}_{\mathbf{qp}} = -\delta_{\mathbf{pq}} \sum_{\mathbf{r}} W^{(6)}_{\mathbf{pr}}.$$

If we restrict ourselves to diagrams such as 8a and 8b, the second term on the right hand side of (8) takes on the usual form of the collision term in the transport equation, where diagrams of type 8b correspond to an electron entering a state **p**, and diagrams of type 8a to an electron leaving this state. Diagrams of type 8a give a contribution

$$W^{(\mathrm{c})}_{\mathbf{qp}} = -\frac{|c_{\varkappa}|^2}{\hbar^2} \frac{2\omega_{\varkappa}}{\omega^2_{\varkappa} - \omega^2}\, i(\varkappa \mathbf{v}_p) \frac{\partial n_{\mathbf{p}}}{\partial \varepsilon_{\mathbf{p}}}, \qquad v_{\mathbf{p}} = \frac{1}{\hbar} \frac{\partial \varepsilon_{\mathbf{p}}}{\partial \mathbf{p}}.$$

The corresponding term in the transport equation (8) describes the influence of the self-consistent field created by the electrons through the phonons. The potential energy for the interaction between two electrons has the Fourier components

$$G_{\varkappa\omega} = -\hbar^2 |c_{\varkappa}|^2 2\omega_{\varkappa} / (\omega^2_{\varkappa} - \omega^2).$$

We must note that a study of the actual value of this potential requires that the direct Coulomb interaction between the electrons is taken into account at the same time.

The diagram of lowest order in the interaction is for the quantity r a free line. If $\kappa \ll p$, we have then

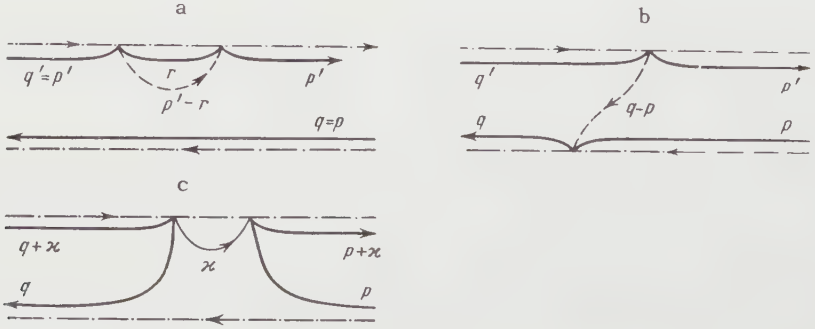

FIG. 8

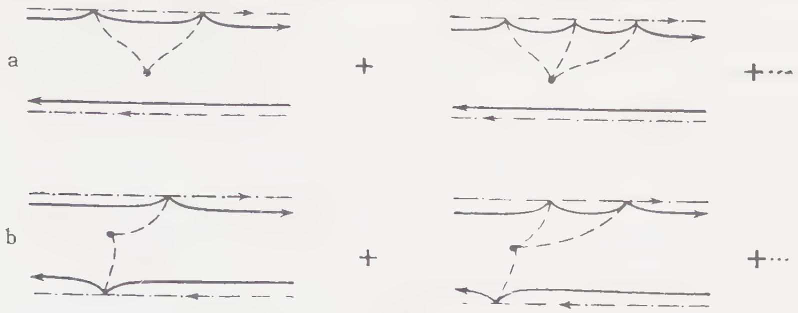

FIG. 9

$$r_{\mathbf{p},\mathbf{p}+\varkappa} = -e\mathbf{E}(\varkappa, s)\,e^{st}\,\mathrm{v}_{\mathbf{p}}\,dn_{\mathbf{p}}/d\varepsilon_{\mathbf{p}},$$

which corresponds to the field term in the transport equation.

2. Interaction with neutral impurities. We shall assume the impurity concentration to be small. We can therefore restrict ourselves to diagrams with one bundle when evaluating W. Typical diagrams are given in Fig. 9. As before we shall assume $\kappa \rightarrow 0$ and $s \rightarrow 0$. After transferring each point we find that each line occurring in W will correspond to a factor 1. One can verify that the sum of diagrams 9b, $W^{(b)}$, is the exact probability that an electron through scattering at an impurity center makes a transition from a state **q** into a state **p** per unit time (the first term of this sum is the first Born approximation). The sum of diagrams of type 9a gives

$$W_{\mathbf{qp}}^{(a)} = -\delta_{\mathbf{qp}} \sum_{r} W_{\mathbf{pr}}^{(b)}.$$

The second term on the right hand side of (8) takes thus the usual form of the collision term, linearized in the field. The diagram of the self-consisent field type is in this case equal to zero (right hand return).

If we restrict ourselves for the quantity r to the zeroth approximation in the impurity concentration we obtain the usual transport equation.

The authors are grateful to L. É. Gurevich and Yu. A. Firsov for helpful discussions.

---

[1] N. N. Bogolyubov, Проблемы динамической теории в статистической физике (Problems in the Dynamical Theory in Statistical Physics) Gostekhizdat, 1946.

[2] I. Prigogine and R. Balescu, Physica **25**, 281, 302 (1959).

[3] W. Kohn and J. M. Luttinger, Phys. Rev. **108**, 590 (1957), J. M. Luttinger and W. Kohn, Phys. Rev. **109**, 1892 (1958).

[4] L. Van Hove, Physica **21**, 517, 901 (1955), **22**, 343 (1956).

[5] E. W. Montroll and J. C. Ward, Physica **25**, 423 (1959).

[6] I. Prigogine and S. Ono, Physica **25**, 171 (1959).

[7] Abrikosov, Gor'kov, and Dzyaloshinskiĭ, JETP **36**, 900 (1959), Soviet Phys. JETP **9**, 636 (1959).

[8] A. I. Larkin, JETP **37**, 264 (1959), Soviet Phys. JETP **10**, 186 (1960).

[9] R. Kubo, J. Phys. Soc. Japan **12**, 570 (1957).

[10] O. V. Konstantinov and V. I. Perel', JETP **37**, 786 (1959), Soviet Phys. JETP **10**, 560 (1960).

[11] C. Bloch and C. De Dominicis, Nucl. Phys. **7**, 459 (1958), **10**, 181, 509 (1959).

Translated by D. ter Haar
37

Letters to the Editor

CONCERNING THE PAPER "EVALUATION OF PHASE INTEGRALS IN THE COVARIANT FORMULATION OF THE THEORY OF MULTIPLE PRODUCTION OF PARTICLES" BY L. G. YAKOVLEV

G. I. KOPYLOV

Submitted to JETP editor December 4, 1959

J. Exptl. Theoret. Phys. (U.S.S.R.) **39**, 209 (July, 1960)

THE paper by Yakovlev[1] contains basically a proposal to utilize the simple integral (12), over the multidimensional region defined by Eq. (16) and Fig. 1, for the phase volume evaluation. We shall show that the integral (12) is incorrect and that it is impossible to regard (16) as representing the limits of integration.

Deriving Eq. (12) from (11), the author integrates over the directions of the particle momenta after fixing their magnitudes. While doing so, he assumes the possibility of having arbitrary angles between the momentum which is being integrated and the vector sum of those not yet integrated. However, when one of the momenta is close enough to the limiting value, the angles mentioned above cannot differ very much from 180°. In the case of similar (and many other) states there exists a limiting angle which is a function of the chosen momentum values. In the presence of such a limiting angle [cf. reference 2, Eq. (17)] the limits of integration become variable, and one cannot derive Eq. (12).

Further, it is easy to show that the portions of the region of integration (16) close to the vertices of the hexagon in Fig. 1 of reference 1 do not correspond to physical states of a system consisting of three zero-rest-mass particles. In the region close to the right lower vertex, particle 3 should come almost to rest and simultaneously move at almost the limiting velocity. It is equally true that when $n > 3$ (16) does not represent the region of integration but a polyhedron circumscribed around it. The author errs here by accepting the necessary conditions imposed on the energy (16) as necessary and sufficient. If the sufficient conditions are also taken into account, the region of integration is not bounded by planes but by some very complicated curved surfaces (plotted roughly in Fig. 1 of reference 3 and given analytically by Eq. (2.13) of the same paper). The character of these surfaces does not permit simple integrations as those attempted by Yakovlev.

It follows from the above that the simplicity of the method for evaluation of covariant weights was achieved by means of an incorrect extension of the region of integration to nonphysical states, i.e., to impossible values of angles and energy. Inaccurate are, in particular, Eqs. (12), (13), and (17) to (19), and the estimate of the applicability of the correct formula (9) is questionable.

---

[1] L. G. Yakovlev, JETP **37**, 1041 (1959), Soviet Phys. JETP **10**, 741 (1960).

[2] Yu. N. Blagoveshchenskiĭ and G. I. Kopylov, Preprint R-213, Joint Institute for Nuclear Research (U.S.S.R.) (1958).

[3] G. I. Kopylov, JETP **35**, 1426 (1958), Soviet Phys. JETP **8**, 996 (1959).

Translated by M. Todorovich
38

SIGNS OF CONSTANTS OF STRONG INTERACTIONS

I. Yu. KOBZAREV and L. B. OKUN'

Submitted to JETP editor April 6, 1960

J. Exptl. Theoret. Phys. (U.S.S.R.) **39**, 210 (July, 1960)

STRONG interactions of known elementary particles are characterized by eight vertices

$$N N\pi,\ \Lambda\Sigma\pi,\ \Sigma\Sigma\pi,\ \Xi\Xi\pi,\ N\Lambda K,\ N\Sigma K,\ \Xi\Lambda K,\ \Xi\Sigma K, \qquad (1)$$

to each of which corresponds a respective coupling constant. The only one known for the present is the NNπ-interaction constant. The determination of the remaining seven constants represents one of the basic tasks of high energy physics. A fundamental characteristic of a vertex is not only the absolute magnitude of the coupling constant but also its sign. The knowledge of the signs of the constants is of special importance in inquiries into various symmetry properties characterizing strong interactions.

It is obvious that the absolute sign of a particular constant does not have physical meaning, since it can always be associated with the field of one of the particles entering the vertex. Only a product of signs of vertices whose aggregate contains any particle an even number of times has physical meaning. One sees easily that from the eight vertices (1) one can choose independently only four products, e.g.,

$$a : (\Sigma\Sigma\pi)(NN\pi),\quad b : (\Sigma\Sigma\pi)(\Xi\Xi\pi),$$
$$c : (\Sigma\Lambda\pi)(\Sigma\Sigma\pi)(\Sigma NK)(\Lambda NK),\quad d : (\Sigma\Lambda\pi)(\Sigma\Sigma\pi)(\Sigma\Xi K)(\Lambda\Xi K). \qquad (2)$$

Here $(\Sigma\Sigma\pi), \ldots$ denotes the sign of the $\Sigma\Sigma\pi, \ldots$ vertex. Further products of vertex signs having a physical significance can be obtained from (2) by multiplying again among themselves a, b, c, and d.

As a consequence of (2), one can choose arbitrarily the signs of four vertices, while the signs of the remaining four can be determined experimentally. It is, for instance, convenient to choose as arbitrary the signs of the four vertices containing the Σ hyperon. The signs of $a : (\Sigma\Sigma\pi)(NN\pi)$ and $ab : (\Xi\Xi\pi)(NN\pi)$ (and consequently of $b : (\Sigma\Sigma\pi)(\Xi\Xi\pi)$ can be fixed by investigating the scattering of the Σ and Ξ hyperons by nucleons. At the same time, one has to determine (e.g., using the interference with the Coulomb scattering) the sign of the single-meson (polar) scattering amplitude (see Fig. 1). The signs of c and d are much harder to fix, because they require the determination of the sign of a more complex amplitude.

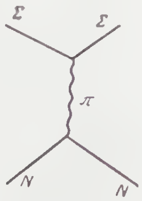

FIG. 1

Let us show how to find out which amplitudes correspond to a particular product of signs of constants.

Let us examine, for example, the product $ac : (\Sigma\Lambda\pi)(NN\pi)\cdot(\Sigma NK)(\Lambda NK)$. We compare it to the closed diagram in Fig. 2. The Feynman diagram of the amplitudes in question may now be obtained by cutting two arbitrary lines in Fig. 2. If the figure is cut at points x and y, we obtain a diagram corresponding to the two-meson amplitude of the Σ-hyperon scattering by a nucleon, shown in Fig. 3.

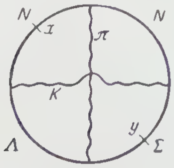

FIG. 2

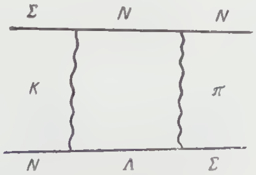

FIG. 3

The authors are grateful to B. L. Ioffe and I. Ya. Pomeranchuk for their helpful discussion.

Translated by M. Todorovich
39

ELECTROMAGNETIC RADIATION FROM ELECTRON DIFFUSION

G. A. ASKAR'YAN

P. N. Lebedev Physics Institute, Academy of Sciences, U.S.S.R.

Submitted to JETP editor, February 18, 1960

J. Exptl. Theoret. Phys. (U.S.S.R.) **39**, 211-212 (July, 1960)

We shall study the emission of electromagnetic radiation in the multiple elastic scattering of electrons formed in a medium by some ionizing agent (e.g., an ionizing particle).

We assume that the molecules of the medium have a small probability of electron capture and that a number of free electrons are formed which rapidly multiply and lose energy so fast that they soon have insufficient energy to excite the molecules in the medium. Subsequently the collisions become elastic, and in each strong scattering event an electron loses only a small part of its energy: $\Delta\epsilon \approx \epsilon m/M$, where ϵ is the kinetic energy of the diffusing electrons and m/M is the ratio of the electron mass to the molecules of the medium. The reciprocal gives the number of collisions necessary for the electron to dissipate its energy.

If the average time between collisions exceeds the periods of the wavelengths that are of interest, then radiation pulses will have time to form in each collision, and the energy radiated will be comparable with that radiated in an instantaneous stop: $\Delta\epsilon_r \sim r_0\epsilon\Delta\omega/c$ (see, e.g., reference 1) where $r_0 = e^2/mc^2$ is the classic electron radius, c the velocity of light, and $\Delta\omega$ the width of the spectrum detected.

However, the necessary condition between the frequency of collisions and the wave frequency is not always fulfilled, especially in condensed media. For example, for a mean free path $l_s \simeq 3 \times 10^{-8}$ cm and an electron velocity $v = 3 \times 10^8$ cm/sec, the collision frequency is $v/l_s \gtrsim 10^{16}$, which exceeds the frequency of light oscillations by almost an order of magnitude. Therefore, for waves to be effectively generated by these electrons, the diffusion process must be extended in time, i.e., the free path must somehow be increased. This can be done by reducing the density of the medium, i.e., by passing from condensed media to compressed gases. In this connection it is interesting to investigate the pressure dependence of the radiation intensity from the drifting electrons (sharp variation when $l_s \sim v/\omega$).

We wish to evaluate the number of quanta radiated by an electron during elastic collisions in a medium in which the conditions for radiation-pulse formation have been fulfilled for every scattering event; i.e., $l_s \gtrsim v/\omega$. When moderated, each electron radiates a number of quanta

$$\nu \approx \frac{r_0}{c} \varepsilon \frac{\Delta\omega}{\hbar\omega} \frac{M}{m} .$$

Assuming that $\Delta\omega/\omega \simeq 0.5$ and that the electron energy is $\epsilon \simeq 10$ ev and $M/m \approx 10^5$ (these last figures being characteristic for argon, for example), we obtain $\nu \simeq 10^{-2}$ quanta per drifting electron. The number of these drifting electrons formed by a single-charge relativistic particle per unit mass of track is $n_e \approx 10^4$ electrons/g, so that $\nu n_e \approx 10^2$ quanta/g; i.e., the radiation from the diffusing electrons comprises a significant part of the radiation of luminescence (on the order of one percent of the quantum yield of a good luminophor). Incidentally, in places where ionization and excitation are concentrated (e.g., along the tracks of secondary electrons or of other heavily-ionizing particles) there may be an additional energy transfer from the excited atoms to the drifting electrons because of collisions of the second kind.

The radiation discussed here, unlike luminescence radiation, has a continuous spectral distribution, i.e., it also exists in regions of the spectrum where there is little or no luminescence radiation. The emission time of this radiation, $\tau \sim l_s M/vm$, has nothing in common with the lifetime of the excited atoms and may be very much shorter than this lifetime. All this, and the sensitivity of the diffusion radiation to the addition of impurities that absorb free electrons and to variation in the density of the medium and other peculiarities, facilitates its differentiation even in regions of the spectrum where luminescence radiation is stronger.

Incidentally, the total radiated energy from each strong elastic scattering event can constitute a significant portion (on the order of one percent) of the energy transferred to the molecule.

The difference between the radiation effect discussed here and true luminescence should be apparent also when there are superimposed strong electric fields capable of compensating for the reduction of the energy of the drifting electrons in low-density media; thereby causing a sharp increase in scattering events and in the number of radiated quanta.

In some media, e.g., in inert elements, a sharp decrease occurs in the scattering cross section for an electron energy ~ 1 ev (the so-called Ramsauer effect). In crossing this energy range, the conditions for pulse formation for infrared frequencies may be fulfilled even in condensed media.

The discussed specific radiation processes can be used, for example, to analyze the stages and dynamics of electron behavior; to generate waves less than a millimeter long by exposing a substance to a beam of light, to a stream of ionizing particles, or to x rays from a powerful x-ray tube; to sort out the conditions needed for increasing the fast portion of the radiation created by a recorded particle, and for other practical applications.

---

[1] L. D. Landau and E. M. Lifshitz, Теория поля, Gostekhizdat (1948) p. 208. see English translation, L. Landau and E. Lifshitz, The Classical Theory of Fields, (Addison-Wesley Press, Cambridge, Mass., 1951) p. 197.

Translated by A. Skumanich
40

OSCILLATOR DEPENDENCE OF THE SURFACE RESISTANCE OF A METAL ON A WEAK MAGNETIC FIELD

M. S. KHAĬKIN

Institute for Physics Problems, Academy of Sciences, U.S.S.R.

Submitted to JETP editor April 30, 1960

J. Exptl. Theoret. Phys. (U.S.S.R.) **39**, 212-214 (July, 1960)

THEORETICAL investigation of the dependence of surface resistance of a metal on a constant magnetic field applied to it leads to the conclusion that the surface resistance in a weak field must change monotonically with increasing field.[1,2] Measurements were carried out[3] which are in full agreement with these calculations. However, as shown by experiments some results of which are given in this letter, the dependence of the surface resistance of a metal on the magnetic field in regions of weak fields is not at all monotonic.

Measurements were carried out at a frequency of 9400 Mcs by the method of frequency modulation[4] on single crystals of tin of very high purity, with less than 6×10^{-5} per cent impurities (reference 5, tin No. 6). Tin, cadmium, and indium were also tested, with impurities $\sim 2 \times 10^{-3}$ per cent.

The single crystals were grown from the melt in a glass mold in the plates with dimensions $13 \times 6 \times 1$ mm. Such a plate serves as a strip-type resonator one-half wavelength long; the high-frequency currents flow along the plate.

A series of experiments were carried out with a single crystal prepared from very pure tin, with a tetragonal axis parallel to the middle dimension and the binary axes parallel to the other two dimensions. A record of the dependence of the field of the logarithmic derivative of the reactive surface impedance with respect to the field, $\xi = X^{-1}\,\partial X/\partial H$ is given in Fig. 1, where the constant field H is parallel to the high frequency magnetic field H_ω, i.e., it lies in the plane of the specimen perpendicular to its length. Rotation of H in the plane of the specimen leads to a decrease in the amplitude of oscillations of $\xi(H)$ and to their shift to higher fields. The oscillations die out as the field approaches $H \perp H_\omega$. The absolute values of the field H_n for which $\xi(H_n) = 0$, where n is an ordering number, increase as $H_n(0)/H_n(\alpha) = \cos\alpha$ when H is rotated by an angle α from the direction of H_ω. An arbitrary position of the vector H in the plane $\perp H_\omega$ does not give oscillations of $\xi(H)$; slanting of the direction of H outside of this plane makes it possible to observe the oscillations. It follows from this that the oscillations of ξ on a given specimen are brought about by the projection of H in the direction H_ω.

It is difficult to establish the law of periodicity of the observed oscillations because of their small number. However, the first four values of H_n (Figs. 1 and 2) satisfy the relation $H_{n+1}/H_n = 1.6 \pm 0.1$. A similar relation for four values of H_n obtained with cadmium yields $H_{n+1}/H_n = 2.1 \pm 0.2$. The same effect is also noted in indium. It should be noted that the periodicity of the oscillations is not a function of H^{-1}. Upon increase in the field $H \parallel H_\omega$ above 5 oe, a monotonic decrease is obtained for the quantity ξ which changes sign at $H \sim 20$ oe, and at $H \gtrsim 40$ oe begins to undergo oscillations which are periodic functions of H^{-1}, evidently corresponding to cyclotron resonance.[4]

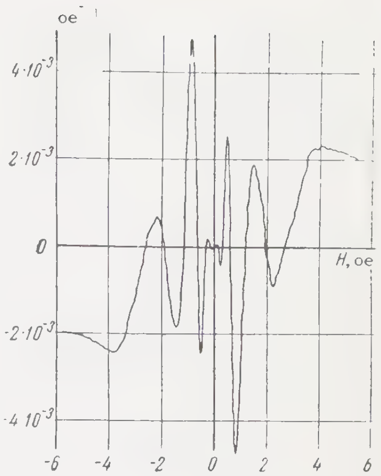

FIG. 1. Dependence of $\xi(H)$ for monocrystalline tin, obtained in a slow increase of the field from −6 to +6 oe. The noise in the recording is evident; the symmetry of the curve makes it possible to judge the reproducibility of the results of the experiment.

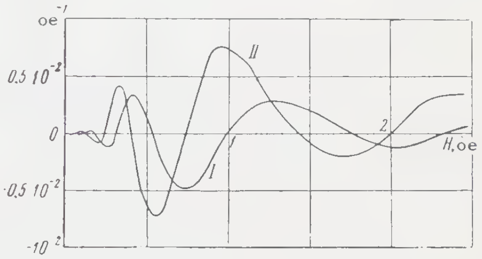

FIG. 2. Curve I is the function $\xi(H)$ and curve II is the dependence of $\xi(H) = 0.9R^{-1}\partial R/\partial H$ on H. The curves were obtained by the analysis of recordings similar to those of Fig. 1 (as the sum and difference of two experimental recordings).

Figure 2 shows the results of experiments for $H \parallel H_\omega$ on the field dependence of the logarithmic derivative of the reactive and active surface impedances with respect to the field. These experiments were carried out on a single crystal of tin. Within the accuracy of the experiment, curve II is proportional to the derivative of curve I with respect to the field.

The curves we have described were obtained at a specimen temperature of 3.8° K; heating to 4.2° K approximately halves the amplitude of the oscillations and increases somewhat the values of H_n. The oscillations disappear at ~ 10° K or somewhat higher. The transition of the specimen to the superconducting state leads to the vanishing of the effect. If the temperature of the specimen is a little less than critical, so that the critical magnetic field H_c is $\sim 1-3$ oe, then oscillations are not observed in the superconducting state of the specimen $(H < H_c)$, but in the normal state they are the same as for 3.8° K.

The amplitude of the high frequency field H_ω in the resonator amounts to ~ 0.1 oe, i.e., of the same order of magnitude as H. However, decrease of H_ω by a factor of 10 has no effect on the observed phenomenon. The fact that the amplitude of H_ω changes from zero up to the maximum along the specimen, which is a strip of resonant length, also speaks in favor of the absence of a dependence of the effect on H_ω.

The observed effect is anisotropic. Both the location and the amplitude of the oscillations are different in specimens with other crystallographic orientations, but the general character of the phenomenon is preserved: some oscillations of $\xi(H)$ are observed in the region $H < 5$ oe, changing to a monotonic variation upon increase in H. The oscillations have a much smaller amplitude in less pure specimens. The effect is completely absent in controlled experiments with specimens made from polycrystalline copper of technical purity.

The physical reasons for the new phenomenon just described are still not clear. There is a basis for assuming that the oscillations of the surface impedance take place as the result of quantum oscillations of the magnetic susceptibility of the metal. In particular, the connection of this phenomenon with the magnetic properties of a metal is shown by the character of its dependence on the direction of the constant magnetic field. It is possible that the phenomenon described is related to the de Haas — van Alphen effect. However, it differs qualitatively from the latter by highly characteristic features: the oscillations of ξ are nonperiodic as functions of H^{-1}, their periods are very small in absolute value and large in relative value. Strictly, the entire resemblance between these two effects is limited to the non-monotonic dependence of the magnetic susceptibility of the metal on the field.

It should be noted that the non-monotonic dependence of the surface impedance of the metal on the weak magnetic field is not only never observed experimentally, but also there do not exist theoretical calculations which would make it possible to predict or explain the nonlinear dependence of the surface impedance of the metal on the weak magnetic field, so strongly marked in the newly discovered phenomenon. The latter circumstance makes the further study of this phenomenon especially interesting.

The author is grateful to P. L. Kapitza and A. I. Shal'nikov for attention and interest in the research and to G. S. Chernyshev for technical assistance.

---

[1] M. Ya. Azbel' and É. A. Kaner, JETP **32**, 896 (1957), Soviet Phys. JETP **5**, 730 (1957).

[2] É. A. Kaner and M. Ya. Azbel', JETP **33**, 1461 (1957), Soviet Phys. JETP **6**, 1126 (1958).

[3] P. A. Bezuglyĭ and A. A. Galkin, JETP **34**, 237 (1958), Soviet Phys. JETP **7**, 164 (1958).

[4] M. S. Khaĭkin, JETP **37**, 1473 (1959), Soviet Phys. JETP **10**, 1044 (1960).

[5] V. B. Zernov and Yu. V. Sharvin, JETP **36**, 1038 (1959), Soviet Phys. JETP **9**, 737 (1959).

Translated by R. T. Beyer
41

PROPERTIES OF THE AXIAL VECTOR INTERACTION AND THE DECAY $\Sigma \to \Lambda + e + \nu$

L. B. OKUN'

Submitted to JETP editor May 6, 1960

J. Exptl. Theoret. Phys. (U.S.S.R.) **39**, 214-216 (July, 1960)

FEYNMAN, Gell-Mann, and Levy[1] have shown recently that, if one postulates

$$\partial_\alpha j_\alpha = G f m^2 \pi, \qquad (1)$$

for the divergence of the axial vector describing the strangeness conserving current j, the relation*

$$f = \sqrt{2}\, M G_A / gG \qquad (2)$$

follows without any further assumptions.

Here π is the operator of the π meson field, g is the coupling constant for the strong interaction of the π mesons with the nucleons ($g^2/4\pi \approx 14$), $G = 10^{-5} M^{-2}$ is the universal constant of the weak interaction, G_A is the axial vector coupling constant of β decay ($G_A \approx 1.25\, G$), and the lifetime of the π meson, τ, is given in terms of f in the following fashion (see, for example, the author's review article[2]):

$$1/\tau = (G^2/8\pi) f^2 m^2 \mu^2 (1 - \mu^2/m^2)^2, \qquad (3)$$

M, m, and μ are the mass of the nucleon, the π meson, and the μ meson, respectively. It follows from the comparison of formula (3) with experiment that $f \approx m$. This implies that relation (2) is satisfied with an accuracy of about 15%.

The condition (1), which was first considered by Polkinghorne,[4] requires very special assumptions about the form of both the strong and weak interactions.[1,4-6]† It is therefore desirable to derive other consequences, besides relation (2), from the hypothesis (1).

The aim of this letter is to show that the hypothesis (1) can be verified in an independent fashion by measuring the as yet unknown $\Sigma\Lambda\pi$ interaction constant and the probability of the as yet unobserved decay

$$\Sigma^{\pm} \rightarrow \Lambda^{0} + e^{\pm} \pm \nu. \tag{4}$$

The axial vector part of the amplitude of the decay (4) has the form (see, for example, reference 2)

$$\langle \Lambda | j_{\alpha} | \Sigma \rangle = \bar{u}_{\Lambda} [A\gamma_{\alpha} + Bk_{\alpha} + C(\gamma_{\alpha}\hat{k} - \hat{k}\gamma_{\alpha})] O u_{\Sigma}, \tag{5}$$

where k is the summed four-momentum of the leptons, A, B, and C are functions of k^2, and the operator O is equal to γ_5 if the parities of Σ and Λ are identical ($P_{\Sigma\Lambda} = +1$), and equal to 1 if $P_{\Sigma\Lambda} = -1$. Using condition (1) we easily obtain

$$k_{\alpha} \langle \Lambda | j_{\alpha} | \Sigma \rangle = Gfm^2 \langle \Lambda | \pi | \Sigma \rangle = Gfm^2 \Gamma(k^2) D(k^2) \bar{u}_{\Lambda} O u_{\Sigma}. \tag{6}$$

Here the vertex part $\Gamma(k^2) = h\gamma(k^2)$, where h is the $\Sigma\Lambda\pi$ interaction constant, and $D(k^2) = (k^2 - m^2)^{-1}$ is the Green's function for the π meson, where $\gamma(m^2) = d(m^2) = 1$. Since the nearest singularities of $A(k^2)$, $\gamma(k^2)$, and $d(k^2)$ lie at $k^2 = 9m^2$, it may be expected that A, γ, and d change slowly in the interval $-m^2 \leq k^2 \leq m^2$.‡

Multiplying (5) by k_{α} and using (6), we find

$$Gfm^2\Gamma(k^2) D(k^2) = A(M_{\Sigma} \pm M_{\Lambda}) + Bk^2 \tag{7}$$

(the upper sign corresponds to $P_{\Sigma\Lambda} = +1$, the lower sign to $P_{\Sigma\Lambda} = -1$). Considering equation (7) at the point $k^2 = m^2$, we obtain

$$B(k^2) \approx Gfh / (k^2 - m^2). \tag{8}$$

If we look at (7) at the point $k^2 = 0$, we find

$$f \approx A(M_{\Sigma} \pm M_{\Lambda}) / Gh. \tag{9}$$

Relation (8) is not a specific consequence of the hypothesis (1); it should hold in any arbitrary theory if one assumes, as we essentially did, that the one-meson pole graph gives the most important contribution to $B(k^2)$ (the effective pseudoscalar) in the region $-m^2 \lesssim k^2 \lesssim m^2$.

Relation (9), which is the analog of (2), is a specific consequence of hypothesis (1). For its verification one must know the values of h and A.

By virtue of the conservation law for the vector current, the contribution of the vector interaction to the decay (4) is very small.[7,2,8] Therefore it is just the value of A (with an accuracy up to terms proportional to k in the amplitude) which determines the probability of the decay (4):

$$\begin{aligned} w_{\Sigma\Lambda} &\approx 3A^2\Delta^5 / 60\pi^3, \quad \text{if} \quad P_{\Sigma\Lambda} = +1, \\ w_{\Sigma\Lambda} &\approx A^2\Delta^5 / 60\pi^3 \quad \text{if} \quad P_{\Sigma\Lambda} = -1, \end{aligned} \tag{10}$$

where $\Delta = M_{\Sigma} - M_{\Lambda}$, and $\hbar = c = 1$ as in all the preceding equations. The value of the $\Sigma\Lambda\pi$ interaction constant h, on the other hand, might, for example, be obtained from an analysis of processes of the type

$$\Lambda(\Sigma) + N \rightarrow \Sigma(\Lambda) + N.$$

---

*Relation (2) was first obtained by Goldberger and Treiman[3] with the help of dispersion theory techniques and a number of unjustified assumptions.

†We note that within the framework of the Sakata model relation (1) could serve as a definition of what is called the π meson field in the usual form of the weak interaction.

‡We note that the physical region of values of k^2 in the decay (4) lies within the limits $0 \leqslant k^2 \leqslant (M_{\Sigma} - M_{\Lambda})^2$.

[1] Feynman, Gell-Mann, and Levy, preprint.

[2] L. Okun', Usp. Fiz. Nauk **68**, 449 (1959); Ann. Rev. Nucl. Sic. **9**, 61 (1959).

[3] M. Goldberger and S. Treiman, Phys. Rev. **111**, 354 (1958) and **110**, 1178 (1958).

[4] J. C. Polkinghorne, Nuovo cimento **8**, 179 and 781 (1958).

[5] R. E. Norton and W. K. R. Watson, Phys. Rev. **110**, 996 (1958).

[6] R. F. Swayer, Phys. Rev. **116**, 231 (1959).

[7] Belov, Mingalev, and Shekhter, JETP **38**, 541 (1960), Soviet Phys. JETP **11**, 392 (1960).

[8] N. Cabibo and R. Gatto, Nuovo cimento **15**, 159 (1960).

Translated by R. Lipperheide
42

THE PROBLEM OF THE FORM OF THE SPECTRUM OF ELEMENTARY EXCITATIONS OF LIQUID HELIUM II

L. P. PITAEVSKIĬ

Institute of Terrestrial Magnetism, Ionosphere and Radio Wave Propagation, Academy of Sciences, U.S.S.R.

Submitted to JETP editor May 11, 1960

J. Exptl. Theoret. Phys. (U.S.S.R.) **39**, 216-217 (July, 1960)

IN a recently published preliminary communication by Henshaw, Woods, and Brockhouse,[1] data are given on the behavior of the energy spectrum of liquid helium II in the region of energies $\epsilon \approx 2\Delta$

= 17.3° K, obtained by investigation of the inelastic scattering of neutrons. In this case it was shown that the function $\epsilon(p)$ in this region has a negative second derivative, i.e., that the spectrum begins to "bend." In the opinion of the authors of the communication, this suggests the presence of a second maximum in the function $\epsilon(p)$.

The purpose of the present note is to turn attention to the fact that this phenomenon actually has another explanation. That is, we have shown[2] that the curve of the energy spectrum of liquid helium II generally cannot rise above the energy $\epsilon = 2\Delta$. This is connected with the fact that an elementary excitation with energy $\epsilon \geq 2\Delta$ can divide into two excitations with energy $\epsilon = \Delta$. At the energy $\epsilon = 2\Delta$ the curve $\epsilon(p)$ reaches a maximum and breaks off, so that this point is the end point of the spectrum. Close to it the spectrum has the form

$$\varepsilon(p) = 2\Delta - \alpha \exp[-a/(p_c - p)], \tag{1}$$

where p_c is the momentum for which the energy is equal to 2Δ while α and a are certain constants. Thus the complete curve of the spectrum of elementary excitations of liquid helium II has, qualitatively, the form shown in the drawing. However, it should be noted that, until experimental data become available, theoretical prediction of the behavior of the curve $\epsilon(p)$ was not completely unique, inasmuch as the possibility was not excluded that the velocity of the excitation at some point with $\epsilon < 2\Delta$ would not equal the velocity of sound.* In this case the curve $\epsilon(p)$ would be gradually washed out because of radiation of phonons, not achieving the value 2Δ. The data obtained in reference 1 precisely show that this is not the case, i.e., that the spectrum without damping achieves the energy 2Δ where it must terminate.

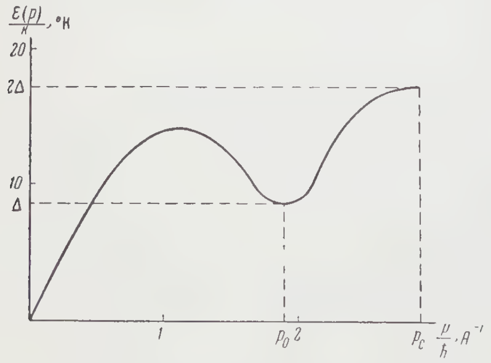

We also note that the probability of the creation of a single excitation with energy ϵ by a neutron vanishes as $\epsilon \to 2\Delta$ according to the law

$$w = A\frac{(2\Delta - \varepsilon)}{a}\ln^2\frac{\alpha}{2\Delta - \varepsilon}. \tag{2}$$

This is in qualitative agreement with the fact that, for the maximum energy obtained in reference 1, $\epsilon = 17.1$° K, the probability of the creation of an excitation amounts to 6 per cent of the probability of the creation of an excitation with $\epsilon = \Delta$.

---

*We do not mention another method of termination of the spectrum described in reference 2, inasmuch as it is extremely improbable in helium.

---

[1] Henshaw, Woods, and Brockhouse, Bull. Am. Phys. Soc. **5**, 12, C3 (1960).

[2] L. P. Pitaevskiĭ, JETP **36**, 1168 (1959), Soviet Phys. JETP **9**, 830 (1959).

Translated by R. T. Beyer
43

NEGATIVE ABSORPTION IN METAL VAPORS

S. G. RAUTIAN and I. I. SOBEL'MAN

P. N. Lebedev Physics Institute, Academy of Sciences of the U.S.S.R.

Submitted to JETP editor May 12, 1960

J. Exptl. Theoret. Phys. (U.S.S.R.) **39**, 217-219 (July, 1960)

SCHAWLOW and Townes[1] have considered the use of negative absorption for the amplification and generation of radiation in the optical region of the spectrum. As an example they have considered potassium vapor, excited by ultraviolet light from a potassium lamp. However, the intensity of the exciting light proved to be insufficient, and this behavior is typical for metals. The use of a different source cannot be a universal method, since there exist at most 2 or 3 coinciding pairs of lines from different elements suitable for the purpose in view. There is therefore a limited outlook for the direct optical excitation of metal vapors. It seems possible to circumvent this difficulty by working with a mixture of two gases, in which a resonance level of one gas is close to an excited level of the other. Under these conditions we can expect an intense optical excitation of the first gas and an effective population of the neighboring level in the other, thanks to resonance transfer of the excitation energy. It is this effect, in fact, which leads to an intense sensitization of fluorescence.[2,3]

As an example, let us consider a mixture of sodium and mercury vapors, irradiated by Hg resonance radiation, $\lambda = 2537$ A. The displacements ΔE of a number of Na levels from the Hg 6^3P_1 resonance level, and their radiation widths A, are given in the table. Using the data of reference 4 on the intensity of sensitized fluorescence, and knowing the transition probabilities, it is easy to ascertain that the levels 9^2S and 8^2P are populated approximately in the ratio 1 : 5, while their populations exceed those of the other s and p levels by at least one order of magnitude.

Levels	E, cm^{-1}	ΔE, cm^{-1}	A $\times 10^{-6}$, sec^{-1}
10^2S	39983.0	573	—
9^2S	39574.5	162	1.5
8^2S	38968.3	—444	2.4
7^2S	38011.7	—1400	3.8
9^2P	39794.3	382	—
8^2P	39298.8	—113	0.25
7^2P	38540.8	—871	0.45
8^2D	39728.1	316	—
7^2D	39200.4	—212	3.1
6^2D	38387.1	—1025	5.2

Let us calculate N_{8p}, the absolute concentration of sodium on the 8^2P level. An estimate of the effective cross section σ for the transfer of excitation in the case of exact resonance ($\Delta E = 0$) gives $\sigma \approx 3 \times 10^{-14}$ cm^2. If $E \neq 0$, but $\sqrt{\sigma}\,\Delta E/vh \sim 1$, as in our case, then the cross section diminishes, but not by more than an order of magnitude. Hence we can take as the lower limit $\sigma = 3 \times 10^{-15}$ cm^2. An estimate of the probability of quenching collisions and of the transfer of excitation energy from Na to Hg shows that, for a partial concentration of 10^{14} to 10^{15} cm^{-3}, which is convenient for a number of reasons of an experimental nature, these processes can be neglected. Under these circumstances

$$N_{\varepsilon p} = \frac{\sigma v N_{\mathrm{Na}}}{p} \frac{b N_{\mathrm{Hg}}}{A} = \frac{\sigma v N_{\mathrm{Na}}}{A_{8p}} \frac{3\lambda^3}{8\pi c} \frac{\mathscr{E}}{h\delta\nu} N_{\mathrm{Hg}},$$

where N_{Na} and N_{Hg} are the total concentrations of Na and Hg, A_{8p} and A are the radiation widths of the Na 8^2P and the Hg 6^3P_1 levels, b is the excitation probability of Hg, v is the relative velocity, $\mathscr{E}$ is the intensity of illumination, and $\delta\nu$ is the line width of the excitation. Bactericidal and other similar low-pressure mercury lamps permit one to obtain[9] $\mathscr{E} \sim 10^{-12}$ w/cm^2 when $\delta\nu \lesssim 1$ cm^{-1}. When $N_{Na} = 5 \times 10^{14}$, $N_{Hg} = 2 \times 10^{14}$, and $T = 600°$K we have $N_{8p} = 3 \times 10^9$ cm^{-3}.

As has already been mentioned, the n^2S and n^2D levels lie below 8^2P, and are considerably less populated. Therefore the absorption coefficients k for the transitions n^2S-8^2P and n^2D-8^2P are negative. This means that the stimulated emission exceeds the absorption. Under the given conditions, the line widths are determined by the Doppler effect $\delta\nu = \delta\nu_D$, and in that case, as is well known,

$$|k| = 2\sqrt{\pi \ln 2}\,(e^2/mc) f N_{8p} / \delta\nu_D,$$

where f is the oscillator strength for a transition from the 8^2P level. The most convenient transitions are 8^2S-8^2P ($\lambda = 30.2\,\mu$; $f = 1.1$) and 7^2S-8^2P ($\lambda = 7.77\,\mu$; $f = 0.037$). In the first case $|k| = 2$, and in the second $|k| = 0.02$. Both these values of $|k|$ are large enough to be used in the proposed system for the purpose of amplifying and generating infrared radiation.* The transitions n^2P-9^2S can also be used.

The high values of N_{8p} and $|k|$ have arisen as a result of the high density of the resonance radiation (see reference 1, where the excitation of non-resonant radiation is considered). Note also that we have not considered the effect of "imprisonment" of radiation in the above treatment. Since $\sigma v N_{Na}/A \sim 10^{-2}$, the quenching of the mercury resonance fluorescence is not important, and this effect leads to an increase in N_{8p}.

The authors express their thanks to P. A. Bazhulin for discussions of the work.

---

*The Na level scheme which we have considered above shows that the corresponding frequencies will not be absorbed because of transitions from the 8^2P level to higher levels.

---

[1] A. L. Schawlow and C. H. Townes, Phys. Rev. **112**, 1940 (1958).

[2] A. C. G. Mitchell and M. W. Zemansky, Resonance Radiation and Excited Atoms, Macmillan, N.Y., 1934.

[3] P. Pringsheim, Fluorescence and Phosphorescence, Interscience, N.Y., 1949.

[4] H. Beutler and B. Josephy, Z. Physik **53**, 747 (1929).

[5] A. N. Filippov and V. K. Prokof'ev, Z. Physik **56**, 458 (1929).

[6] D. R. Bates and A. Damgaard, Phil. Trans. Roy. Soc. London **242**, 101 (1949).

[7] Anderson, Busko, Grinberg, and Saulgozha, Вестник ЛГУ (Bull. Leningrad State Univ.) No. 4, 27 (1956).

[8] Dronov, Sviridov, and Sobolev, Оптика и спектроскопия (Optics and Spectroscopy) **5**, 490 (1958).

[9] Справочная книга по светотехнике (Handbook of Light Techniques) Vol. 1, Chap. V, U.S.S.R. Acad. Sci., 1956.

Translated by D. C. West
44

BEHAVIOR OF THE TOTAL CROSS SECTION FOR THE PHOTOPRODUCTION OF π MESONS AT HIGH ENERGIES

E. D. ZHIZHIN

Submitted to JETP editor May 20, 1960

J. Exptl. Theoret. Phys. (U.S.S.R.) **39**, 219-220 (July, 1960)

We shall consider the process of collision of a photon with a nucleon for very high incident photon energies $\omega \gg m$, where ω is the photon energy in the c.m. system and m is the mass of the nucleon. At such energies, processes involving the production of two or more π mesons, as well as processes involving the production of heavier mesons, etc., are already possible.

In order to obtain some information on the behavior of the total cross section for the photoproduction of π mesons at high energies, we shall estimate the contribution to this cross section from peripheral interactions. The condition for a collision to be peripheral is $l \gg \omega/\mu$,[1] where μ is the mass of the π meson, and l is the orbital angular momentum. For such large l the basic contribution to the amplitude is made by terms corresponding to a diagram with one virtual meson (see figure). Making use of the results of reference 2 [see formula (6)], we obtain the following expression for the amplitude of the photoproduction of π mesons with an orbital angular momentum l and parity $(-1)^{l+1}$:

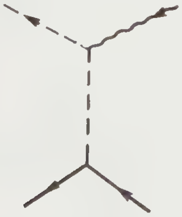

$$|a^{(1)}_{l\pm\frac{1}{2},l,M}| = (eg\pi\mu^2/2\omega^3)\sqrt{\omega/2\mu}\exp(-\mu l/\omega). \qquad (1)$$

Here $g^2 = 0.08(2m/\mu)^2$; $e^2 = 1/137$; $M = \pm 3/2$ and $\pm 1/2$ are the projections of the total angular momentum on the z axis (the z axis is chosen in the direction of the incident photon momentum).

The total cross section of the process can be written in the form $\sigma = \sigma_0 + \sigma_1$. Here σ_0 contains the contribution from the nonperipheral part of the π-meson photoproduction process, σ_1 is the peripheral part of the cross section. Only one-meson amplitudes with orbital angular momenta $l > \omega/\mu$ contribute to it.

The cross section σ_1 is written in the following way:

$$\sigma_1 = \sum_j \sum_{l=\omega/\mu}^{\infty} \sum_{M=-3/2}^{3/2} |a^{(1)}_{jlM}|^2. \qquad (2)$$

Performing the summation, we obtain

$$\sigma_1 = e^2g^2\pi^2\mu^2/15\omega^4.$$

This expression corresponds to small scattering angles $\theta \lesssim \mu/\omega$. Since $\sigma_0 > 0$, then

$$\sigma > e^2g^2\pi^2\mu^2/15\omega^4. \qquad (3)$$

Hence the total cross section for the π meson photoproduction process at high energies cannot drop more rapidly than ω_{lab}^{-2}, where ω_{lab} is the photon energy in the laboratory system. This conclusion is evidently not in agreement with the results obtained from the statistical-hydrodynamical theory of multiple production of particles,[3,4] which predicts that the total cross section of the process at high energies should drop exponentially with an increase in energy: $\sigma \sim \exp(-kE^{1/4})$.

In conclusion, I wish to express my graitude to I. Ya. Pomeranchuk for suggesting the problem and for helpful comments.

---

[1] L. B. Okun' and I. Ya. Pomeranchuk, JETP **36**, 300 (1959), Soviet Phys. JETP **9**, 207 (1959).

[2] V. B. Berestetskiĭ and E. D. Zhizhin, JETP **39**, 418 (1960), Soviet Phys. JETP **11**, in press.

[3] E. Fermi, Progr. Theoret. Phys. (Kyoto) **5**, 570 (1950); Phys. Rev. **81**, 683 (1951).

[4] L. D. Landau, Izv. Akad. Nauk SSSR, Ser. Fiz. **17**, 51 (1953).

Translated by E. Marquit
45

HYPERFINE STRUCTURE OF GAMMA RAYS PRODUCED BY QUADRUPOLE INTERACTION IN A CRYSTAL LATTICE

N. N. DELYAGIN, V. S. SHPINEL', V. A. BRYUKHANOV, and B. ZVENGLINSKIĬ

Institute for Nuclear Physics, Moscow State University

Submitted to JETP editor May 25, 1960

J. Exptl. Theoret. Phys. (U.S.S.R.) **39**, 220-222 (July, 1960)

As was recently shown in the experiments of Mössbauer,[1,2] emission (or absorption) of γ rays by nuclei bound in a crystal lattice can occur without energy loss to nuclear recoil. The most interesting result was obtained by Mössbauer with a moving source.[2] If the source is given a velocity v with respect to the absorber, the energy of the radiated quanta is changed because of the Doppler effect by the amount Ev/c; the shift of the radiated line with respect to the absorption line results in a corresponding change in the effective cross section for resonance absorption. This makes it possible to measure directly the shape of the resonance line, whose half-width (for a thin absorber) is equal to twice the natural width of the level.[2,3] Recently, by a similar method, the hyperfine structure of the excited state at 14 kev in Fe^{57} was studied. This hyperfine structure is the result of the interaction of the magnetic moment of the nucleus with the internal magnetic field of the domains in iron.[4]

Alikhanov and Lyubimov observed[5] the resonance absorption of the 23.8 kev γ quanta of Sn^{119} and noted the influence of an external magnetic field on the size of the effect. In the present work we have investigated the hyperfine structure of the 23.8-kev excited state of Sn^{119} resulting from the interaction of the quadrupole moment of the nucleus in its excited state with the internal electric field in the tin crystal.

The measurements were carried out with a source of Sn^{119m} (metallic tin), which was set in motion with respect to the absorber. Unlike the equipments previously described,[2-4] where the source was given a definite fixed velocity, in our experiment the velocity of the source varied linearly in time within definite limits. The law of motion of the source, which was at liquid nitrogen temperature, was determined by a rotating cam of definite profile. The limits of variation of the source velocity are determined by the angular speed of rotation of the cam. The x rays of tin (26 kev) were almost completely absorbed by a characteristic filter — a plate of palladium 0.06 mm thick. The γ quanta passing through the absorber (which was also at liquid nitrogen temperature) were recorded by a NaI(Tl) crystal 2 mm thick. The pulses from a single channel pulse analyzer entered a circuit which modulated the height of the pulses according to a linear law synchronously with the change in velocity of the source. The modulated pulses were recorded in an AI-100 hundred-channel pulse-height analyzer, each channel of which thus recorded a definite value of the source velocity. Such an arrangement enabled us to measure simultaneously the entire absorption spectrum (i.e., the dependence of the absorption on the source velocity over the whole selected velocity interval from $-v_{max}$ to $+v_{max}$). The measurements were made with absorbers containing Sn^{119} in two different compounds: metallic tin and an alloy of $SnNb_3$.

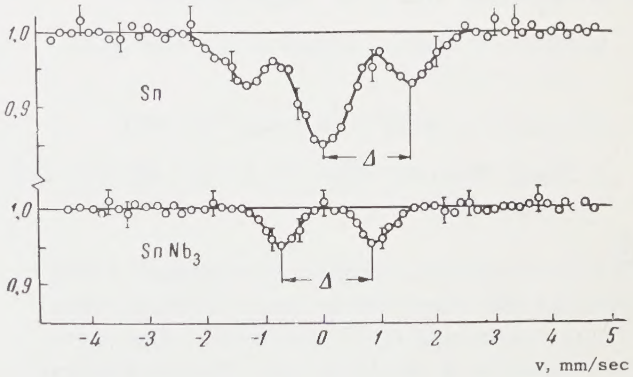

The dependence of the resonance absorption on source velocity for the case of an absorber of tin 20 mg/cm² in thickness is shown in the upper part of the figure (the ordinates give the transmission in relative units). Three absorption maxima are observed whose peaks correspond to source velocities of 0 and ±1.46 mm/sec. This result can be explained as the presence of a hyperfine structure of the 23.8-kev level of Sn^{119}, caused by interaction of the quadrupole moment Q of the nucleus in the excited state with the electric field in the tin crystal. The ground state of Sn^{119}, which has a spin $\frac{1}{2}$, cannot have such a hyperfine structure; the excited state (spin $\frac{3}{2}$) splits into two levels corresponding to absolute values of spin projection equal to $\frac{1}{2}$ and $\frac{3}{2}$. Since the splittings in the source and absorber are the same, at zero velocity of the source the radiated line and the absorption line coincide, which corresponds to the central absorption maximum. The maxima at velocities of ±1.46 mm/

sec correspond to overlap of one of the two lines in the spectrum of the radiator with one of the components of the hyperfine structure in the spectrum of the absorber.

Such an interpretation of the result is confirmed by measurements with an absorber in the form of an alloy $SnNb_3$ (30 mg/cm^2), the results of which are shown in the lower part of the figure. The $SnNb_3$ crystal has a crystal lattice similar to the lattice of β tungsten, which is very close to cubic;[6] this gives grounds for assuming the absence of hyperfine structure of the 23.8-kev level of Sn^{119} in such a crystal. At zero source velocity there is no resonance absorption, since the unsplit absorption line in $SnNb_3$ does not coincide with the split line of the source. For source velocities of ± 0.73 mm/sec an overlap occurs of one of the components of the hyperfine structure of the radiated line with the line of the absorber, which corresponds to the two absorption maxima in the figure. The separation $\Delta = (eQ/2)\,\partial^2V/\partial z^2$ between the components of the hyperfine structure of the 23.8-kev level was equal to $(1.15 \pm 0.25) \times 10^{-7}$ ev. The size of the quadrupole moment of the 23.8 kev level cannot be determined since we do not know the electric field gradient in the tin crystal.

---

[1] R. L. Mössbauer, Z. Physik **151**, 124 (1958).

[2] R. L. Mössbauer, Z. Naturforsch. **14a**, 211 (1959).

[3] Lee, Meyer-Schutzmeister, Schiffer, and Vincent, Phys. Rev. Lett. **3**, 223 (1959).

[4] Hanna, Heberle, Littlejohn, Perlow, Preston, and Vincent, Phys. Rev. Lett. **4**, 177 (1960).

[5] A. I. Alikhanov and V. A. Lyubimov, Report to the Tenth Annual Conference on Nuclear Spectroscopy, Moscow, 1960.

[6] A. F. Wells, Structural Inorganic Chemistry, (Russ. transl.) IIL, 1948, p. 629.

Translated by M. Hamermesh
46

ELECTRON PARAMAGNETIC RESONANCE OF VANADIUM IN RUTILE

G. M. ZVEREV and A. M. PROKHOROV

Institute of Nuclear Physics, Moscow State University

Submitted to JETP editor May 28, 1960

J. Exptl. Theoret. Phys. (U.S.S.R.) **39**, 222-223 (July, 1960)

AN electronic paramagnetic resonance (EPR) spectrum was observed in single-crystal rutile (TiO_2), containing 0.01% vanadium. The spectrum consists of two lines with characteristic hyperfine structure, corresponding to the isotope V^{51} with nuclear spin $\frac{7}{2}$.

Each line (group of eight hfs components) belongs to its own system of non-equivalent vanadium ions, which are isomorphic substitutions for the Ti^{4+} ions in the crystal lattice of rutile.

The crystallography of rutile was described in detail by Grant.[1] A unit cell contains two titanium ions differing in the placement of the six neighboring oxygen ions, which produce an electric field of rhombic symmetry. When the crystal is rotated 90° about the tetragonal axis, one system of non-equivalent ions goes into the other. Accordingly, when the crystal is rotated about a tetragonal axis oriented perpendicular to the direction of the external magnetic field, the overall appearance of the vanadium spectrum is repeated every 90°. A similar picture is observed also for Cr^3 ions introduced into rutile.[2]

The EPR spectrum of vanadium can be set in correspondence with the following spin Hamiltonian ($S = \frac{1}{2}$; $I = \frac{7}{2}$):

$$\mathscr{H} = g_x\beta H_x\hat{S}_x + g_y\,\beta H_y\hat{S}_y + g_z\beta H_z\hat{S}_z + A_x\hat{I}_x\hat{S}_x + A_y\hat{I}_y\hat{S}_y + A_z\hat{I}_z\hat{S}_z,$$

where $\hat{S}$ and $\hat{I}$ are the electron and nuclear spin operators, g is the anisotropic factor of spectroscopic splitting, A is the hfs constant, and β is the Bohr magneton. The axes are chosen as follows: the z axis coincides with the tetragonal axis, while the x and y axes are parallel to the [110] and [1$\bar{1}$0] directions for one system of non-equivalent ions; the x and y axes are interchanged for the second system.

The constants of the Hamiltonian, determined at T = 77° K and 9800 Mcs, are:

$$g_x = 1.955 \pm 0.001, \qquad A_x = 14.15 \pm 0{,}07,$$
$$g_y = 1.913 \pm 0.001 \qquad A_y = 3.09 \pm 0{,}03,$$
$$g_z = 1.912 \pm 0.001, \qquad A_z = 4.41 \pm 0{,}03.$$

The values of A are given in units of 10^{-3} cm^{-1}.

Experiments carried out at 37,500 Mcs at T = 77° K have shown that the constants of the Hamiltonian are independent of the frequency, while measurements at T = 4.2°K (ν = 9800 Mcs) have shown that they do not change noticeably with the temperature.

No vanadium EPR ions were observed in rutile at room temperature. When the sample is cooled to approximately 135°K, broad lines appear, which gradually narrow down with further decrease in temperature. At T = 90°K the lines reach a width of 3.5 oe. There is no further reduction in the width of the line. This width is probably due to the spin-spin interaction of the paramagnetic ions of vanadium. This is also confirmed by the shape of the line, which corresponds exactly to the Lorentz curve. A line of this shape is expected for magnetically-dilute systems with a concentration of paramagnetic ions less than 1%.[3]

The continuous saturation method was used to measure the spin-lattice relaxation times of the vanadium ion in rutile: $\tau_1 = 2 \times 10^{-1}$ sec at T = 4.2° and $\tau_1 = 6 \times 10^{-6}$ sec at T = 90°.

Line broadening was observed at T = 90°K upon saturation, thus confirming again the assumed nature of the observed line width.

The totality of the experimental facts gives grounds for assuming that the vanadium enters the rutile lattice in the form of the ion V^{4+}.

We note that the broadening of the V^{4+} line when heating to temperature above 90°K cannot be due to spin-lattice interaction, since the measurement of τ_1 by the saturation method yields an order of 10^{-6} sec at these temperatures. More detailed investigations of this effect are now in progress.

The authors are grateful to R. P. Bashuk and A. S. Bebchuk for furnishing the samples of rutile with vanadium.

---

[1] F. A. Grant, Revs. Modern Phys. **31**, 646 (1959).

[2] Gerritsen, Harrison, Lewis, and Wittke, Phys. Rev. Lett. **2**, 153 (1959).

[3] C. Kittel and E. Abrahams, Phys. Rev. **90**, 238 (1953).

Translated by J. G. Adashko
47